MONITORING OF HIGH VOLTAGE OIL-IMPREGNATED TRANSFORMER INSULATION

July 2006

AUTHOR:
RIFFAT HASSAN KHAWAJA

SUPERVISOR:
DR. T. R. BLACKBURN

A thesis submitted in fulfillment of the requirements for the degree of
Doctor of Philosophy

Faculty of Engineering

School of Electrical Engineering
and Telecommunications

THE UNIVERSITY OF NEW SOUTH WALES

Abstract

Power transformers are the most expensive and indispensable components of a transmission system. Insulation failure in transformers can cause long term interruption to the power supply and loss of revenue so their long term operational condition is thus a major concern for supply utility asset managers. The monitoring of transformers can give an early picture of the changes that are caused by electrical, thermal, environmental and mechanical stresses before failure occurs. Power transformer insulation within an oil-impregnated insulation consists of organic materials including mineral oil, cellulose paper and pressboard layers. These organic materials deteriorate inexorably over the lifetime of the transformer and their insulating properties become impaired due to chemical change. A major cause of deterioration of the cellulose paper is by excess operating temperature of the transformer coupled with moisture in the insulation.

The presence of moisture, coupled with high operating temperature in the insulation reduces the dielectric strength of the cellulose paper, the pressboard and the transformer oil. The presence of moisture and oxygen especially at high temperature in transformers deteriorates the transformer insulation by decreasing its dielectric strength. Excessive moisture in the paper insulation causes partial discharge (PD) activity within the cellulose structure and this causes degradation to occur at an increased rate. Increased temperature further accelerates chemical change thus reducing insulation lifetime. In addition to normal temperature operation, transformers are often subject to sudden thermal overload and the effect of this on the insulation has not been fully investigated. The rate of degradation will be dependent on the moisture level and the temperature.

The aim of condition monitoring of insulation is to monitor degradation to assess the condition of the insulation. Modern practice for assessment of transformer insulation condition is also to use partial discharge monitoring methods for identification of any degradation. The availability of sophisticated digital signal processing has promoted the use of partial discharge to a stage where it is now possible to use PD patterns to identify particular types of faults. However to enable this to be done requires a substantial program of laboratory investigation of PD behaviour in typical configurations and typical service operation. PDs are important because they will be generated if insulation is degraded and they will also cause such degradation. They are a main cause of long-term degradation in insulation. Detecting partial discharge during overloading establishes not only insulation quality but also can detect change or trends in the insulation quality as it deteriorates.

This thesis report and gives analysis of a number of different experimental investigations aimed at a detailed quantification of the partial discharge patterns in an oil-impregnated transformer insulation. These include the details of partial discharge patterns together with inception and extinction data at different temperatures and with different levels of moisture contamination of oil and paper. Further, they include results of thermal generation of gas bubbles and the associated temperature levels, moisture levels and PD pattern characteristics. Finally, they include the effects of aged and new transformer oil on PD patterns and also the effects of simultaneous voltage and thermal stress on PD behaviour and the effects of high temperature on moisture level in the insulation and the effect on PD patterns due to aging.

Results of PD activity over a range of temperatures with and without bubble formation indicated that there may be significant impact on the validity of interpretation of PD levels obtained in either separate source or in on-line PD tests of transformers. The result of these experimental work and conclusions can be used in analysing PD data obtained using both offline and preferably on-line measurement, particularly in oil-impregnated power transformers. It was found that the use of the PD statistical parameters of skewness and kurtosis gave a better indication of temperature effects on insulation than did the simple PD magnitude and number. Use of such parameters would be more useful in practice to determine the condition of insulation in transformers subjected to overloads and with moisture present.

Certificate Of Originality

I hereby declare that this submission is my own work and to the best of my knowledge it contains no matter previously published or written by another person, nor material which to a substantial extent has been accepted for the award of any other degree or diploma at UNSW or any other educational institution, except where due acknowledgement is made in the thesis. Any contribution made to the research by others, with whom I have worked at UNSW or elsewhere, is explicitly acknowledged in the thesis.

I also declare that the intellectual content of this thesis is the product of my own work, except to the extent that assistance from others in the project's design and conception or in style, presentation and linguistic expression is acknowledged.

Copyright and DAI Statement

'I hereby grant the University of New South Wales or its agents the right to archive and to make available my thesis or dissertation in whole or part in the University libraries in all forms of media, now or here after known, subject to the provisions of the Copyright Act 1968. I retain all proprietary rights, such as patent rights. I also retain the right to use in future works (such as articles or books) all or part of this thesis or dissertation.

I also authorise University Microfilms to use the 350 word abstract of my thesis in Dissertation Abstracts International (this is applicable to doctoral thesis only).

I have either used no substantial portions of copyright material in my thesis or I have obtained permission to use copyright material; where permission has not been granted I have applied/will apply for a partial restriction of the digital copy of my thesis or dissertation.'

Signature: ____________ Date: 25/3/09

Authenticity Statement

'I certify that the Library deposit digital copy is a direct equivalent of the final officially approved version of my thesis. No emendation of content has occurred and if there are any minor variations in formatting, they are the result of the conversion to digital format.'

Signature: ____________ Date: 25/3/09

Acknowledgements

The completion of this thesis report was made possible by the co-operation of numerous individuals. I would like to take this opportunity to express my greatest appreciation for their valuable contributions.

First and foremost, I would like to show my deepest thanks to my supervisor, Associate Professor Trevor R. Blackburn for his valuable guidance and advice throughout the completion of this report.

I gratefully acknowledge the support and suggestions of Adjunct Professor Ron E. James, Senior Lecturer Dr. B. T. Phung and Professor E. S. Kim (Hoseo University Korea). Thanks must go to my fellow colleagues Wayan G. Ariastina, Yen H. Lu and Chew H. Tan for our joint efforts in some experiments.

My thanks to both School of Electrical Engineering and Telecommunications for providing academic facilities and the Faculty of Engineering for a scholarship.

I would also like to thank my family members and friends for the love and support they provided throughout especially my wife Afsheen Farooq and my son Haris Hassan Khawaja.

Finally and most important my sincere thanks to my creator "Almighty Allah" who gave me ability and strength to complete this thesis.

RIFFAT HASSAN KHAWAJA

Monitoring Of High Voltage Oil-Impregnated Transformer Insulation

APPENDIX A	AUTHOR'S PUBLICATIONS
APPENDIX B	SOFTWARE DESIGN OF THE CDA3 SYSTEM
APPENDIX C	POLARISATION AND DEPOLARISATION CURRENT (PDC) RESULTS (STEEL TANK)
APPENDIX D	POLARISATION AND DEPOLARISATION CURRENT (PDC) RESULTS (GLASS CELL)
APPENDIX E	RECOVERY VOLTAGE MEASUREMENT (RVM) MANUAL

Table of Contents

List of Figures

List of Figures

List of Figures

List of Figures

List of Figures

List of Tables

Chapter 1

Introduction

1.1 Introduction

Power transformers are perhaps the most important and expensive component of an electrical supply system. The capital cost of a power transformer is the single largest capital investment in substations and the economic penalties incurred by transformer failure and the resulting outage cost is considerable. As society relies more and more on electricity, demands for highly reliable power system equipment are increasing. A sudden failure of a power transformer instantly and vividly affects not only the electrical power system but also the many different spheres of human life. In fact it can bring today's modern human life to a virtual standstill by way of affecting almost everything from traffic signals on roads to manufacturing industries. Other elements of prime concern are safety, an enormous capital cost, and potential environmental damage such as fire and oil spillage. Even under normal operating conditions, transformers degrade and have a finite operating lifetime that is very difficult to predict. As such it becomes imperative to constantly monitor the condition of power transformers to prevent a sudden and an unfortunate condition involving insulation breakdown. The reliable operation of the large electrical power transformer depends on the integrity of its insulation, and insulation failure is one of the major causes of such equipment outages [1-3].

The insulation within the standard power transformer consists primarily of organic dielectric materials; including mineral oil and cellulose-based materials such as oil impregnated paper and pressboard. The paper derives its required tensile strength from its fibrous nature, which results from its filamentary and linear molecular chain structure. Loss of the tensile strength of the paper and the resulting brittleness are considered to indicate the end of useful life of the insulation. The rate of loss of tensile strength is temperature-dependant because of the chemical scission of the bonds, which hold the molecular chains together. These organic materials will deteriorate over the operating lifetime of the transformer and their insulating properties will also deteriorate as a result.

Paper in particular may deteriorate rapidly if the operating temperature is excessive, if there is excessive oxygen in the oil or if significant moisture is present in the oil/paper system. The ingress of moisture, combined with high temperature, into the paper insulation reduces the dielectric strength of both the oil-impregnated cellulose materials and the transformer oil itself. As most transformer failures occur in the insulation, condition monitoring (preferably continuous and on-line) of a transformer insulation is required to provide an early indication of any degradation that may be caused by abnormal electrical, thermal, mechanical and environment stresses which may occur during operation of a transformer [4-7].

Power consumption continues to increase at the rate of approximately 2% per year and installation of new transformers is declining [8]. This problem causes overloading of aged transformers in operation and therefore causes degradation. Transformer insulation problems that derive from degradation processes and those induced by operating conditions may exceed the design capability of the transformer and cause its failure. These problems may take many years to develop into more serious problems or failure. However, in some cases undesirable consequences can be created quite suddenly. Deterioration processes related to ageing are accelerated by electrical, thermal, environmental and mechanical stresses. Increasing temperature, interaction with oxygen, moisture, and other contaminants all contribute to insulation degradation. The deterioration is particularly exaggerated in the presence of some catalysts. Characteristics of the deterioration processes include sludge accumulation, weakened mechanical strength of insulation material such as paper-wrapped conductor, shrinkage of materials that provide mechanical support, and improper alignment of tap changer mechanisms.

Moisture is a major deteriorating element for paper and oil insulation and even relatively low levels of moisture will accelerate the ageing of such insulation materials, particularly the paper, over many years of operation [198]. During extreme thermal transients (thermal shocks) that may occur during some extreme loading cycles, high moisture content in the paper can result in the generation of water vapour bubbles. These bubbles can cause a serious short term reduction in the dielectric strength of the insulating liquid, perhaps resulting in a dielectric failure. In a power transformer oil-impregnated insulation, gas filled cavities or voids are formed in the solid insulation during manufacture, installation or operation. When the electric stress in the void exceeds the breakdown strength of gas within the void, partial discharges occur [9-14]. The behaviour of these bubbles and their impact on insulation integrity and the way in which they are generated by thermal shocks are not well understood. This thesis work attempts, in part, top investigate the behaviour of such operation and to estimate its effect on insulation efficacy.

Partial discharges (PD) can be generated by moisture in oil and paper and are a major source of insulation failure in transformers. They occur in the insulation system and may have different characteristics and locations in the transformer insulation structure. The power transformer has a significantly more complex insulation structure than other types of power devices. Since partial discharges could occur at any place where the insulation becomes defective, and PD measurements can only be made at a limited number of measuring points (e.g. the transformer terminal), knowledge about the modes of propagation and characteristics of PD pulses becomes very important, if we are to correctly interpret the impact on insulation denoted by the measured PD signals. PD activity in the insulation will gradually degrade and erode the insulation, eventually leading to its breakdown. Thus, the detection, measurement and location of such discharges in equipment are of significant importance [15-17]. To this end the partial discharge activity in insulation has been used to determine the impact of moisture on the transformer insulation.

The price of premature and unanticipated collapse of a power transformer can be very substantial, both in economic terms and in outage terms. There is not only the refurbishment or replacement cost but also possible costs associated with environmental clean-up, loss of revenue and deterioration in the quality of power delivery. Monitoring of the transformer insulation helps to decrease the transformer life cycle cost and increases availability and reliability. Early detection and accurate diagnosis of incipient insulation failure mechanism in the insulation can greatly improve asset management.

In addition to PD analysis, there are a number of diagnostic methods available that can provide some reliable information of the ageing process and the condition of the transformer insulation. The degree of polymerisation (DP) test, dissolved gas analysis (DGA) including furan (HPLC) analysis, recovery voltage measurement (RVM), polarisation and depolarisation current (PDC) and the dielectric dissipation factor (DDF) test are some of the more common and often-used nowadays for insulation testing of transformers [18-25]. However all of the above-named diagnostics give an integrated or global assessment of the accumulated deterioration of the insulation rather than an instantaneous and localised evaluation of its current condition. Also most of these are not able to be done on-line, but require equipment outages for the tests.

Partial discharge (PD) measurements of insulation however do provide the required instantaneous and time-resolved assessment of the insulation condition. In addition, they can be adapted easily to on-line application. PD monitoring using a Computerised Digital Analyser (for example the CDA3 which is used in these thesis investigations) is thus one of the more important tools available for the maintenance engineer to assess the condition of transformer insulation [26-27]. This thesis describes in detail the investigations of such PD activity as applied to determination of insulation ageing from the effects of moisture, particularly when accompanied by thermal shock during operation.

The focus of chapters 2, 3 and 4 of this thesis give a detailed survey of transformer's oil, paper and pressboard insulation and factors causing partial discharges and ageing in oil-impregnated insulation. Following this chapters 5 and 6 provide the results of investigations of the effects of high temperature and moisture on partial discharges in oil-impregnated insulation. Next, chapter 7 gives the results of an experimental investigation of the effect of high temperature and moisture using recovery voltage measurements. Chapter 8 provides the conclusions of this study and recommendations for further study. The appendixes include author's publications, software design of CDA3 system, polarisation and depolarisation current test results and recovery voltage measurement method used.

In summary, the main aim of this study is to investigate and analyse the PD behaviour in oil-impregnated transformer insulation systems subjected to electrical, thermal and environmental stress so that the most expensive component of the power system can be monitored to avoid catastrophic failure. Laboratory models of transformer-type oil-impregnated insulation were used to investigate the behaviour of the insulation under different operating conditions. The first model consists of the insulation enclosed in a steel tank to simulate the actual operating condition of a power transformer. Another set-up incorporating a glass cell has also been used in the study for comparing the results. The models were operated for extended periods at elevated temperatures with different level of moisture contents to simulate over-temperature conditions such as those that may occur during substantial overloading of a transformer. Recovery Voltage Measurements (RVM) [28] have also been used to find the moisture condition of the insulation at different temperatures.

Apart from other significant results and conclusions, the main finding of this work, is that moisture in paper insulation wrapped around transformer winding conductors is more dangerous than moisture in the oil in terms of PD activity. Therefore the current indicators are that drying of paper insulation under controlled conditions without damaging considerably the mechanical strength (degree of polymerisation value) of paper can avoid or limit power transformer failures. As a result such information can save significant revenue, improve reliability of supply, avoid major environmental damage and improve personal safety. The outcome of this study could be used to help analyse PD data obtained using off-line or on-line measurement, particularly in power transformers.

Chapter 2

The Transformer and its Insulation

2.1 Basics of Transformer Insulation

Power transformers are one of the most important components in electric power transmission and distribution systems because they allow economical power transmission with high efficiency and low series voltage drop. The development in 1885 by William Stanley of a commercially practical transformer allowed the distribution of AC electrical energy over long distances without the large energy losses that would be associated with the distribution using DC. Subsequently this has made AC power systems more attractive options than DC power systems [29].

Power transformers are very expensive and form a high percentage of the total investment in a power system. The majority of power transformers have been in service for many years experiencing a wide variation of electrical, thermal, mechanical and environmental stresses that can affect the transformer lifetime. Extending transformer life as much as possible is not only economically valuable, but can also prevent loss of revenue when there are power outages. Therefore their reliable and efficient operation for many years is of basic importance for electric supply utility asset managers [30-32].

Most transformers have a very complex electrical insulation system employing both solid and liquid insulation. The most common form is a mineral oil-impregnated cellulosic insulation system. The insulated winding is then insulated from the core by synthetic-resin-bounded paper and by pressboard. The pressboard insulation also provides insulation between the high voltage and low voltage windings. The oil impregnates the paper insulation and provides high quality insulation. The transformer oil is used for a cooling function by transferring heat from the windings and core to the heat exchanger [29].

2.1.1 Transformer Components with Insulation

2.1.1.1 The Oil-filled Bushing

The bushing consists of a central conductor surrounded by capacitor graded insulation, which is usually of oil-impregnated paper. The bushing insulation in a large transformer is required to provide insulation between the HV conductor and the earthed metal tank. Bushings are a significant cause of transformer failures. The paper is susceptible to ingress of moisture through the seals and this can cause problems with the graded insulation layers of the bushing, particularly at the ends of the grading foil layers [29].

2.1.1.2 Tap Changer

An automatic on-load tap changer (OLTC) is provided in large transformers to adjust the secondary output voltage as required to maintain load voltage. The tap changer is installed within the same transformer tank as the windings or within a separate chamber [32]. The insulation material in the tap-changer is primarily oil but cellulosic materials are also used as structural insulation components. The on load tap changer not equipped with switching contacts in vacuum chambers, when operating on load, generates an arc and this can cause gas generation that can be then dissolved in the oil and can then affect the whole insulation structure. Moisture in the OLTC oil is also a significant problem. The arcing during operation may cause distortion of contact interfaces which can then generate high contact resistance and further problems with the oil.

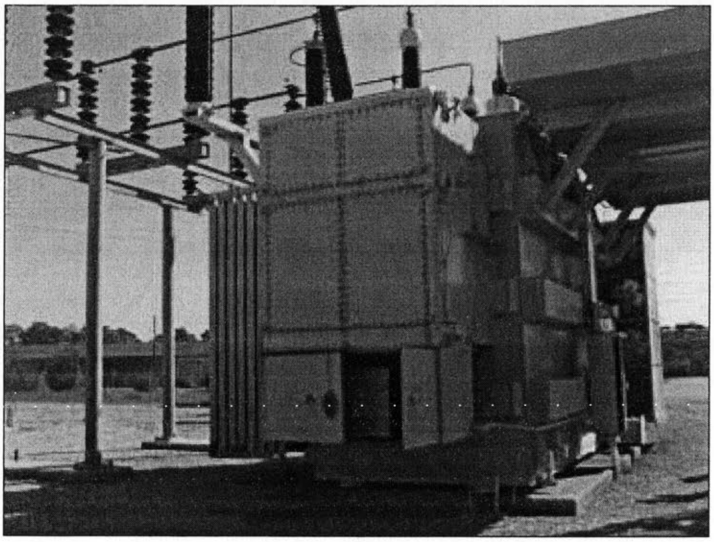

Figure 2-1: Power Transformer in Substation [34]

2.1.2 Transformer Windings

A standard power or distribution transformer consists of two windings. The primary winding is connected to the supply system voltage and the load is connected to the secondary winding [31]. The windings are usually constructed from paper insulated copper or aluminium conductor strip, but in some distribution transformers the secondary may be in a sheet form. The edges of the conductor strip are radiused in order to assist in paper covering and to avoid high electric fields. The two windings are both placed on a common magnetic core, with the HV winding on the outer. The winding paper insulation is oil-impregnated and is thus subject to any problems with the oil, including moisture effects. The paper has a high capacity to absorb and retain moisture and, while the moisture level in the paper is dependent on the moisture level in the oil, the relationship is complex and is not easy to predict because of its very high temperature dependence [198]. Once in the paper however, the moisture is very difficult to remove and is a prime cause of paper insulation deterioration.

The winding insulation is arguably the most stressed insulation in the whole transformer. It will deteriorate with temperature rise over time and when the cellulose in the paper breaks down it will generate moisture as a by-product. Thus it is not necessary to have moisture ingress from the outside. It can be generated internally and this is a major problem. Recently, commercial vegetable oils have been developed for transformer use which have claims to reducing the moisture-related degradation of paper in the transformer [199] however such oils are not yet widely used and thus the effect of moisture on mineral-oil impregnated paper is still the main issue.

2.1.3 Insulation

All parts of the transformer which operate at different voltage require electrical insulation between them. Within a winding the insulation must be arranged not only to provide sufficient dielectric strength to prevent breakdown under any conditions likely to be met in service but also must be spaced to allow adequate circulation of the cooling medium so that no part of the winding becomes excessively hot above hot spot [36].

The transformer insulation is usually divided into two categories: *major* and *minor* insulation. **Major insulation** includes the insulation between the windings, insulation between the windings and core, insulation between winding and earthed tank and insulation between core laminations. **Minor insulation** is the insulation between the individual adjacent turns of a winding. The difference is in the voltage and thus the electrical stress levels that the two insulation types are subject to, with major insulation having full phase voltage across it and minor insulation only some small fraction of total voltage across it.

The life of a transformer is determined by the life of its insulation which, apart from mechanical damage, is mostly dependent on the temperature and moisture content at which it is operated [32].

There are basically two types of insulation materials used in large transformers. The type of insulation used is determined by the usage and requirements of the transformer. Most power transformers used in the world are mineral oil-filled. The solid insulation of the oil filled transformer is mainly paper wound around the winding turns and this is then impregnated with the mineral oil. The purpose of the oil is to provide insulation in its own right and also to impregnate the paper and other cellulosic materials to exclude air and to strengthen their insulation level. The oil serves another useful function as convective heat transfer agent and cooling medium in transformers. Mineral oil has a flash point of 170°C [29] and is combustible and can cause a significant fire hazard. As a result of such fire hazards with mineral oil, transformers which are used in buildings are of the dry type, with no oil or, alternatively, use a synthetic oil with a high flash point, such as silicone oil.

Dry type transformers are larger in size and are more costly but have higher temperature ratings. In dry type transformers the insulation used is usually cellulose paper or synthetic paper such as Nomex and the winding is insulated by varnish in the exposed winding dry types. The other style of dry type transformer is the cast-resin type. In this type, the windings are encased in a solid epoxy resin casting around the structure.

In this thesis only mineral oil-impregnated paper transformers have been studied.

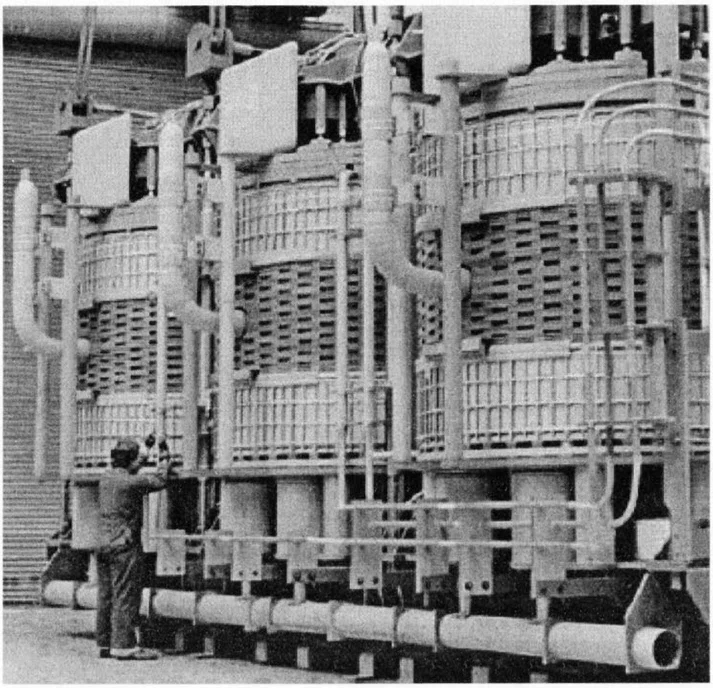

Figure 2-2: Power Transformer Solid Insulation [34]

2.2 Insulation Basics

The function of the insulation in the transformer is to isolate parts at different voltage potential from one another. The voltage stresses arising in a transformer must be known for the initial design of the insulation system. The magnitude of these stresses depends on the voltages across the transformer terminals in service. The stresses on the insulation within the windings can be determined from the design terminal voltage and from knowledge of the voltage distribution in the transformer structure [37].

Such an insulation system needs to be designed to withstand a number of conditions while in service and to last for a reasonable period of time, as it is the insulation system that usually determines the ultimate life of the transformer. The insulation system must be designed to withstand normal operating voltage as well as over voltages produced by lightning and switching transients. The frequency spectrum of variations of switching impulse voltages extends up to tens of kilohertz and that those of the lightning impulse voltage up to several hundred kilohertz [38].

The insulation system must be mechanically strong enough to withstand the forces experienced during switching operation or during through-faults and it must be able to dissipate the ohmic and dielectric heat losses generated efficiently during normal operation, short term and long term overloads and through-faults. The insulating materials of optimum dielectric strength properties that have been used in large high voltage power transformers are oil-impregnated cellulose based products, primarily paper and pressboard [39].

In the bushings, which are used for leading out the high voltage ends of the transformer windings from the tank, oil-impregnated paper or resin bonded or resin impregnated paper are also employed as insulation in the inside of the porcelain or composite material bushing housing. In the internal insulation where high mechanical strength is required phenolic resin-based paper insulation or pressboard are employed [32].

Modern power transformers have insulation systems which are a combination of solid and liquid materials. Synthetic solid and liquid materials are becoming more widespread especially in areas where their low flammability is an advantage. In large power transformers, no kind of insulation has so far succeeded in superseding the oil-impregnated paper and oil-impregnated pressboard insulation. The insulation system of a transformer also comprises materials such as porcelain, wood, fibres, resin etc. [29].

The overall insulation system and its deterioration determine the life and the condition of the transformer. The deterioration process of most insulating materials is caused by the influence of temperature, moisture and gas generation from oil and paper breakdown [3]. Over the years a range of different types of insulation materials have been used in transformers apart from the common ones listed above. The more common materials are briefly discussed below, although they are not all a matter of interest insofar as the thesis work described here is concerned. Only the oil and cellulosic materials are of interest here.

2.2.1 Gases

Air is used in dry-type transformers as an insulant, although it is not the primary insulation material. SF_6 gas has much better insulating properties than air and also much better thermal transfer characteristics and is now being used as the primary insulation in large power transformers where there may be a potential fire hazard from oil transformers (such as in buildings) and where dry type transformers are too small in rating.

2.2.2 Liquids

Mineral oil is extensively used in power transformers and originates from petroleum-based mineral oil which is purified to a suitable grade for insulation use. It is extensively used in power transformers mainly because of its easy availability, low cost and inherent properties as an excellent dielectric and cooling medium. Mineral oil and its deterioration will be discussed in detail later.

As mineral oil is combustible and has a flash point of 170°C [29], synthetic oils such as silicone oil and polychlorinated biphenyl (PCB) were developed for transformer use. PCB is an extremely good insulator with non-flammable nature, but is toxic by nature and is banned from use in electrical equipment. Silicone oil is much more expensive than mineral oil and is currently used only in special application such as locations where flammability is a problem.

A major and increasing problem with mineral oils is their disposal. They are not easily bio-degradable and thus in recent years fully biodegradable oils such as vegetable oil, coconut oil and soybean oil have been investigated to overcome the environmental disposal problems with mineral oil and silicones. Two commercial bio-degradable oils are now available from ABB and Cooper Power Systems.

2.2.3 Solids

It is essential in electrical equipment to have solid structural insulation materials. The mechanical and electrical strength of such materials are the most critical factors. Cellulose-based materials such as pressboard and synthetic resin bonded paper have been the oldest and widely used insulating materials for structural insulation purposes. When impregnated with oil, paper provides a very good insulation and materials such as pressboard (compacted cellulose material) has very good structural and mechanical strength capabilities.

Cellulose is the basic form of paper and similar naturally occurring materials such as cotton. It is a natural substance formed from the basic glucose molecule. The molecular formula is $(C_6H_{10}O_5)_n$ with typically about 1200 glucose rings making up a cellulose chain [36]. Most cellulose material used in electrical apparatus is manufactured from wood using the Kraft process. The mechanical and thermal properties of the paper material are very dependant on the number of glucose molecules in the basic chain. As the paper ages the number of glucose rings in the chain decreases. The applications of cellulose material in transformers are quite prominent as their relative cheapness is a major attraction.

Porcelain has been used by the electrical industry for quite some time in transformers. Its good flashover characteristics and resistance to ageing are well known. It is used widely in transformer bushings because of its ability to withstand atmospheric conditions. Composite polymer materials are increasingly being used for bushings to replace porcelain. They are primarily glass fibre with an outer surface casing of silicone resin (although ethylene propylene diene monomer [EPDM]) is also commonly used.

Some other solid insulation materials such as resins and laminates are also discussed briefly below.

2.2.3.1 Resins

Resins initially had a drawback because of their susceptibility to damage from partial discharges (PDs) and the difference in expansion coefficients between some resins and conductors, which led to some problems of cavitation that promoted such discharges. However improved manufacturing techniques e.g. addition of silica flour to epoxy resin have resulted in the reduction of these drawbacks to some extent.

2.2.3.2 Laminates

A most important example in this category includes paper and cloth layers bonded together by resins. Special plywood (fully or partially impregnated with resins), higher quality materials of glass fibre layers impregnated with silicone, polyester and other resins are also used. The choice of material when used for external purposes is decided by the electrical tracking properties and its capacity to withstand atmospheric extremities, moisture and dirt.

2.2.4 Liquid Impregnated System

At higher voltages, liquid-impregnated systems have a substantial dominance over other types of insulants, particularly for extra high voltage transformers. However the moisture content, the impregnant material losses at operating stresses, and the PDs are of critical importance in this form of insulation. Research and development activities are in progress to minimise the impact of these factors and develop optimum liquid impregnated system.

2.3 Transformer Insulation

The life of a transformer depends very much upon the life of its insulation [40]. Thus the degradation mechanisms of transformer insulation are an important determinant of the transformer insulation condition. There is consequently a very significant level of research into the ageing mechanisms of transformers and how these will affect the transformer operation and how its condition can be assessed from such knowledge. In particular there is a need to understand better the impact of sudden thermal shock and its effect on transformer insulation particularly when there is moisture present. Sudden thermal shock will arise from short circuit effects and will potentially form gas bubbles in the oil and the presence of moisture will be a major factor is such bubble formation and in the long term effect on the insulation. When over-voltage is applied to such oil-impregnated insulation the gas bubbles can generate PDs and these discharges can then continue at the operating voltage [37].

As the dielectric strength is affected by so many factors, it is useful for the design engineer to appreciate those factors and mechanisms, such as the above, which can cause insulation failure so that by appropriate design, manufacture and testing they can ensure that the more deleterious conditions do not occur in installed insulation. In badly designed or degraded materials dielectric losses may exceed the rate of heat dissipation at relatively low stress and thus cause cumulative long term heating and thermal breakdown. In better quality materials, breakdown is usually caused in air or oil around the electrode [37].

The electric strength of insulation in electrical equipment is very much dependent on the configuration, the electrical properties of the insulation medium and any contamination present and these factors thus affect the long term behaviour of equipment insulation. In particular, they will determine the inception level of partial discharges (PDs). Partial discharge activity is an important indicator of insulation degradation and is a useful precursor of full electrical breakdown of the insulation [35]. For this reason partial discharge monitoring has been used in this study to determine the deterioration processes of impregnated paper insulation under thermal shock and moisture contamination conditions.

The partial discharge inception stress and PD magnitude in oil-impregnated paper transformer insulation is determined and affected by several factors, including the thickness of the paper and presence of metal foils, such as in bushings, the relative permittivities of paper and oil impregnant, the completeness of impregnation and the degree of dryness of the paper. With well-dried paper the discharge inception stress can be very high, but the presence of moisture can greatly reduce the stress at which gas liberation and thus discharges occur. The discharges in oil impregnated insulation can start due to the presence of cavities in the insulation or can be initiated by moisture concentrations. The discharge magnitude in cavities depends on the location, size, and shape of the cavities. Electrical discharges can also occur in a high voltage region due to disturbance of the moisture equilibrium, causing low PD inception voltage and higher PD intensity [33, 41-42].

Both paper and oil will absorb moisture in the transformer, and their dielectric strength deteriorates with increasing level of moisture content [43]. Moisture may come from external sources such as leaks which can allow some atmospheric gases into contact with the oil, or internal sources such as the degradation of the cellulose chains. One product of the cellulose chain break-up is moisture. High levels of moisture in the paper can lead to accelerated ageing of the solid insulation and formation of gas bubbles in the oil. As the transformer heats up on load, water held in the paper will migrate into the oil. As the transformer cools down again, the moisture in the oil migrates more slowly back into the paper thus resulting in some excess moisture remaining in the oil for a period of time.

The dielectric properties of the oil and the cellulose-based materials (paper and pressboard) within the power transformer are strongly influenced by operating temperature, moisture and general ageing [5]. The ageing degradation rate depends on the thermal, oxidative, electrical and mechanical conditions of the insulation materials inside the transformer. Most of the solid insulation material used is made from basic cellulose without any binder. Transformer paper is used for wrapping the conductors of the winding to provide basic inter-turn insulation and insulation from earth. The pressboard is built up to be thicker than paper layers and is used to mechanically support the winding discs and to separate the high and low voltage windings. Transformer oil filled within the transformer tank provides dielectric strength, cooling and protects the paper. The windings are cooled by circulation of the transformer oil through the windings.

It is very important for the solid insulation to be dry and fully oil-impregnated. The presence of moisture will reduce the dielectric strength and can cause low PD inception voltage and higher PD intensity, thus accelerating the degradation of the insulation material [44-45]. The disturbance in the moisture equilibrium can also lead to breakdown of the insulation. In oil-impregnated transformer insulation, the quality of the insulation depends heavily on the properties of insulating materials.

Figure 2-3 below (taken from [198]) shows the complex relationship between oil and paper moisture content and temperature. It can be seen from the curves that at the very high temperatures used in the experiments of this investigation (140°C) the moisture level in the paper will be very low and quite high in the oil. Thus operation at very high temperatures will dry the paper out and change their PD activity characteristics. It is this effect that is under investigation in this work.

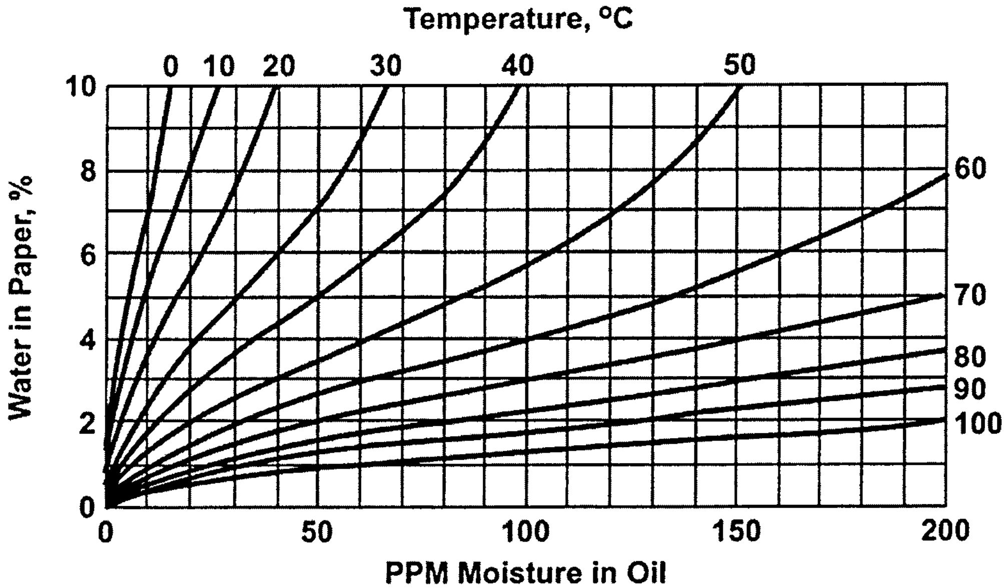

Figure 2-3: Moisture Equilibrium Levels in Oil-impregnated paper
(From Oommen and Prevost [198])

2.4 Structural Insulating Material

Oil-impregnated cellulose insulation is still the preferred basic insulation material in transformers because of its ability to withstand the extreme electrical and mechanical stresses that can occur in service. Cellulose based structural materials are mechanically strong, light weight, easily available and relatively cheap. They can be manufactured in the required sizes and thickness needed for different applications. Thick pressboard or wood is used between turns of the windings to provide ducts, through which cooling oil can flow. Pressboard cylinders are used to insulate the windings from the metal core. The impregnating mineral oil displaces air bubbles in the material improving the electrical strength and cooling ability of the insulation system [39].

Cooling is required to dissipate the heat generated in the winding resistance and in the core from magnetic field losses. Excessive temperature rise in the core and windings promotes increased degradation of the insulating materials and thus must be controlled. The transformer windings have ducts to allow oil circulation for cooling. Oil circulation is achieved either by natural or forced convection [32].

Ultimately, temperature rise limitation is the major problem for transformer operation. The lifetime of the solid insulation depends on the operating conditions and thus on the temperature. Temperature will also affect the moisture content and to reduce the insulation ageing, it is therefore helpful to limit or remove the influences that cause adverse effects, particularly the moisture that may diffuse slowly inside the transformer during service or be generated by paper degradation in the windings. Even small amounts of moisture can reduce the electric strength of the insulant. Moreover the cellulose insulation absorbs water out of the liquid leading to an accelerated ageing rate [46-47].

2.4.1 Insulating Oil Properties

The chemical structure of oil is very complex, being made up of hydrocarbon and non-hydrocarbon molecules and some other impurities. The hydrocarbon compounds consist of paraffinic, naphthenic and aromatic types. The non-hydrocarbon compounds consist of acids, esters, alcohols and ketones. The chemical make up of the oil and the impurities can have a major impact on oil properties such as oxidation behaviour and dielectric strength [33, 48]. The general molecular structures of the hydrocarbons are shown in Figure 2-4.

Transformer oil is a complex organic compound which oxidises and decays over time. The products of oxidation and decomposition lead to damage of the insulating paper of a transformer and degradation of the oil. Oxidation is a very common cause of oil degradation and the main products of oxidation process are acids, water, carbon dioxide, carbon monoxide and solid constituents, and the degradation process of the oil molecules is promoted by dissolved metals in the oil that can act as catalysts [49].

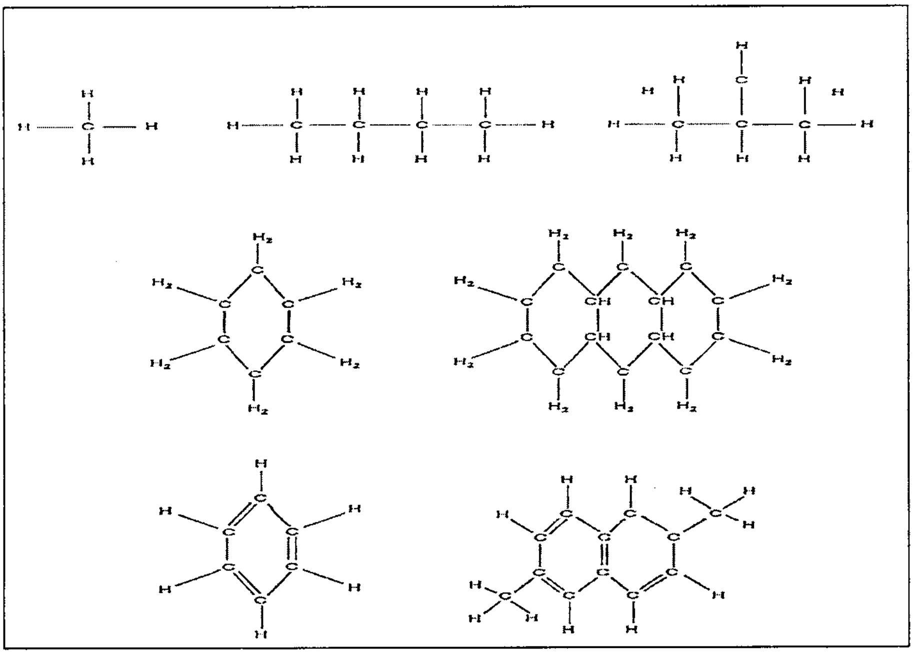

Figure 2-4. Molecular Structures of Hydrocarbons

Top are paraffins (left is Methane, middle is Normal Butane, Right is Isobutane), Middle are Naphthenes (Left is Cyclohexane and Right is 3-Ring Homologue) and Bottom are Aromatics (Left is benzene and Right is Double Ring Aromatic)

Water is the major contaminant in transformer oil and affects the dielectric properties of oil, particularly as the temperature increases the solubility of the oil. Water can exist in oil in the dissolved state, tightly bound to oil molecules, and also in the free state when the moisture in the oil exceeds its saturation value. Elevated temperature in oil enhances the rate of oxidation and solubility of the oil and hence the amount of water in the oil also increases [50]. The moisture in the transformer reduces the insulation strength by decreasing the dielectric strength of the transformer insulation system. When the transformer warms up, moisture migrates from the solid insulation into the fluid. The rate of migration is dependent on the conductor temperature and the rate of change of the conductor temperature. As the transformer cools, the moisture returns to the solid insulation at the slower rate.

Although the most important property of insulating oil is its dielectric strength, the flash point, pour point and kinematic viscosity are also important properties. These physical properties of oil are typically determined by conducting tests on new oil after the distillation process. The key oil properties usually recorded are colour and appearance, density, specific gravity, viscosity, pour point, flash point, interfacial tension, neutralisation number/total acidity, water content, electric strength, gassing tendency, dielectric dissipation factor, breakdown voltage, specific resistance and sludge content. The most important of these are discussed below.

2.4.1.1 Colour and Appearance

Colour and appearance can be used during both acceptance and qualification tests to indicate substandard oil [33]. A high colour number may be an indication of oil deterioration or contamination. Besides colour, the appearance of the oil may show cloudiness or sediments which may indicate the presence of free water, insoluble sludge, particles etc.

2.4.1.2 Specific Gravity

Specific gravity is very important in extreme cold weather when there is a concern about water in oil freezing and rising to float on top of the oil in a power transformer.

2.4.1.3 Viscosity

Low viscosity of transformer oil is an absolute essential in order to ensure the proper circulation and unrestricted flow in the transformer in order to dissipate the heat. An increase in viscosity will depend on the oil constitution. Increase of temperature decreases the viscosity increasing rate of convective flow. Low viscosity of oil assists initial penetration of oil into ducts and promotes circulation through the winding to overcome local overheating. Ageing and oxidation of the oil tend to increase the viscosity [51].

2.4.1.4 Flash Point

Flash point of oil is the minimum temperature at which it gives enough vapour to form a flammable mixture with air under standard test conditions. Flash point is affected by the impurities in the oil. For example, volatile combustible products when present in oil reduce the flash point of oil. Also prolonged exposure of the oil to high temperature under fault conditions may produce sufficient quantities of low molecular weight hydrocarbons to cause a lowering of the flash point of the oil. Therefore it is desirable for fewer hazards that the oil should have very high flash point [53].

2.4.1.5 Interfacial Tension (IFT)

Interfacial tension is defined as the strength of the film separating two immiscible fluids. The IFT level between water and oil gives a determination of whether the oil has been subjected to an ageing process. IFT is determined by soluble polar contaminants and other products of deterioration. The IFT characteristic changes rather quickly during the early stages of ageing but levels off when the deterioration is still only moderate. Good new oil exhibits a high IFT. Oil oxidation contaminants lower the IFT because the contaminants have a high affinity to water and the oil molecules. IFT can be used to indicate when all chemical stabilizer has been used up so more can be added. IFT is a sensitive parameter used for screening the new oil exposed in transport to soaps, acids, varnishes and solvents [53]. IFT is a valuable monitor of transformer oil condition.

2.4.1.6 Neutralisation Number/Total Acidity

The neutralisation number is a measure of the amount of acidic contaminants in oil. Acidity of oil slowly increases with ageing of transformer oil. The oxidation of oil produces acids, which are harmful to the solid insulation. Acids can also cause rusting of iron in the presence of moisture. Increase in acidity is less predominant in paraffinic oil and interfacial tension is considered a more important way to monitor the oxidation status of paraffinic oil [33].

2.4.1.7 Water Content

Water content is one of the most important chemical tests as the presence of water in oil insulation is highly undesirable due to its adverse affects on the dielectric properties. Solubility of water in oil increases with increase in temperature. When the oil in service oxidises, acids are formed that also increase water solubility of oil. Acids coupled with water further decompose oil forming more acids and water. Consequently the rate of deterioration of oil can increase very rapidly. The water present in a transformer is distributed between paper and oil with the paper having a much higher % water content because of the potential of the fibrous structure of cellulose to absorb large quantities of moisture. As the temperature of a transformer increases, the paper releases water thus increasing the water content of the oil. The temperature of oil at the time of sampling is thus very important for analysis based on water content [54].

Water present in the transformer oil mostly originates from the atmosphere. At comparatively low water contents water remains in very small droplets forming an oil-water solution and does not alter the appearance of the oil. Dissolved water may or may not affect the electrical properties of the oil. The very small droplets of free moisture cannot sink to the bottom of the transformer because of the interfacial surface tension and the oil viscosity. Above a certain water content all the water cannot remain in solution and free water may then be seen in the form of cloudiness or water droplets. At still higher water content, water may be deposited on horizontal surfaces and on the transformer bottom. Free water invariably results in decreased electrical strength and electrical resistivity and an increased dielectric dissipation factor (DDF) [55].

2.4.1.8 Dielectric Strength

Dielectric strength is the measure of the ability of the oil to withstand electric stress without failure. The dielectric strength is an important property of oil in order to provide adequate insulation between the windings. The dielectric strength is strongly dependent on the amount of free water content and on the level of contamination or conducting particles in the insulating oil. The dielectric strength of hydrocarbon gas-filled oil is lower than that of oil free of dissolved gas. The reduction in the dielectric strength can lead to breakdown of the transformer insulation.

2.4.1.9 Gassing Tendency

Gassing tendency is the measure of the amount of gas that can be dissolved in oil. The gases are formed and become dissolved in the transformer oil during the normal deterioration of aging or due to the presence of the faults. The solubility of gases in mineral oils is strongly dependent on the partial pressure of the gas above the oil surface at a given pressure. This also depends on temperature but reliance on temperature is small [33, 37]. This is an important quantity in terms of sudden thermal shock and its effects on the oil, potentially in bubble formation.

2.4.1.10 Dielectric Dissipation Factor (DDF)

Dielectric dissipation factor (DDF) [loss angle or Tangent Delta (Tanδ)] is a very important monitor of overall insulation quality. It is a non-destructive AC voltage test. DDF has characteristic values for the quality of the oil as a dielectric. Good oil should have a DDF less than 0.005 at 90°C. A high DDF is an indication of the presence of contaminants [56].

Since oil will age in service, change in DDF value serves as an indication for the change of the electrical properties of oil and the solid insulation. The values of DDF are strongly dependent on temperature. There is generally a relationship between DDF and resistivity at elevated temperature as both are affected by same contaminants. A decrease in resistivity is coupled with an increase in DDF [53]. The temperature dependence of DDF must be taken into account when performing such tests and in drawing conclusions from the tests, particularly when trend analysis is being performed.

2.4.1.11 Sludge Content

Sludge is the final product of oil oxidation. It increases the viscosity of the oil and this can reduce the cooling efficiency. Once sludge formation has started in transformer it is deposited on the paper insulation and closes its pores to oil impregnation. With time the layer of sludge becomes hardened and obstructs the passage of oil to the windings and thus effectively reduces the cooling process. If electrical resistivity, IFT and acidity values rise to near the limit levels it is important to monitor the sludge content in oil regularly [53].

The principle characteristics of oil can be divided into mechanical, physical and electrical groupings. Mechanical properties include changes in volume with temperature and pressure. Physical change includes the chemical structure of the oil that include acidity and oxidation, and gas absorption. Electrical properties include the dielectric strength of oil, the DDF and resistivity.

The dielectric strength of transformer oil is affected by the moisture content and the presence of fibrous and similar impurities. One requirement of oil quality is that it must primarily be resistant to PD activity. PD activity will cause gas generation which will degrade the oil. In addition, good quality oil must show very good cooling characteristics. It must have low viscosity, a solidification temperature as low as possible, and no tendency to form sludge during operation [58].

The presence of oxygen in transformer oil causes chemical degradation. Hydrocarbons in the oil are oxidised when oxygen is present. The rate of oxidation depends on the oxygen level, temperature, moisture and other parameters. Hydrocarbons are oxidised to alcohols, aldehydes, ketones and finally acids. These oxidation products are polar in nature and will have an effect on the interfacial tension of the oil.

The decrease of interfacial tension (IFT) means acid level increases and the transformer oil ages as shown in figure below.

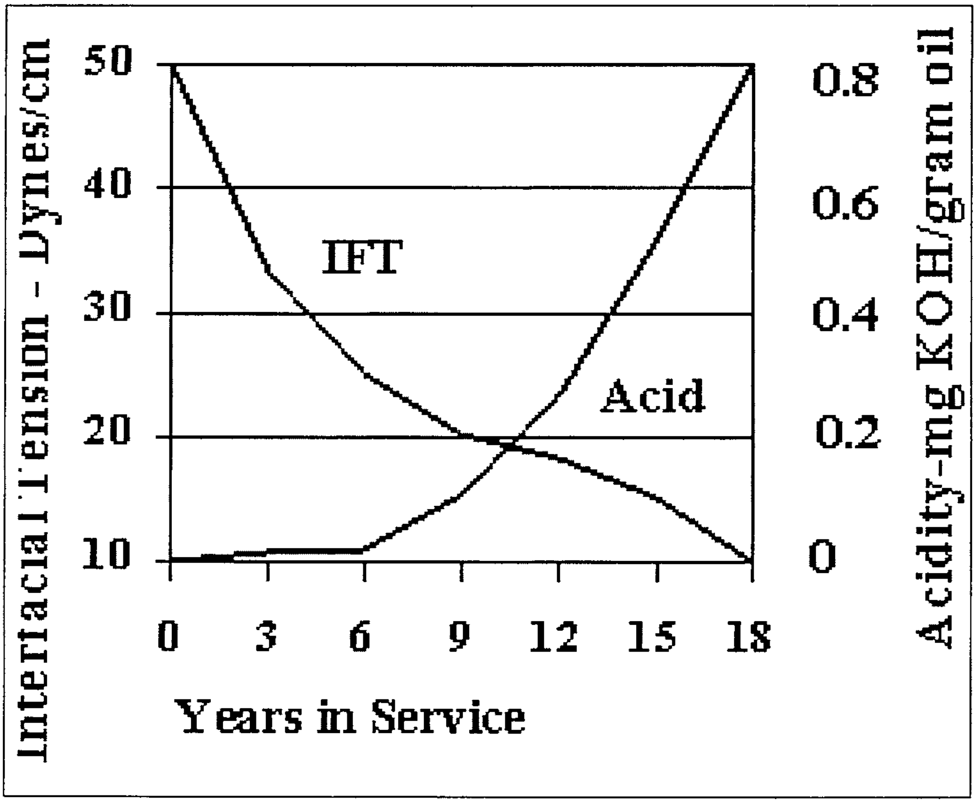

Figure 2-5 Interfacial Tension and acidity variation with service age [42]

Mineral oil is somewhat hydrophobic and the amount of moisture that can dissolve in oil is very small. The solubility of water in oil is dependent on temperature [33]. It is commonly accepted that water that is fully dissolved in the oil has a minimal effect on the breakdown voltage. On the other hand, free water (droplets) in oil significantly lowers the dielectric strength of the oil. Cellulose insulation is hydrophilic so the bulk of moisture that ends up in a transformer migrates into the cellulose insulation. Once the moisture is absorbed by the cellulose it is strongly held due to hydrogen bond formation. It is nevertheless true that some moisture exchange will occur between these two phases, oil and paper, as the temperature changes.

The development of electrical breakdown in liquid dielectrics, including mineral oil, is complex and there is no consistent theory explaining all of the processes leading to breakdown in oil [57, 59]. Some theories try to implement a similar mechanism as that which occurs in avalanche breakdown in gases. Other approaches focus on phenomena occurring due to contamination in the oil volume and liquid, highlighting the role of contaminant particles (also including liquid and gaseous contaminants). Academic studies explain the mechanisms of breakdown in liquids as being variations of electronic (with development of electron avalanche, leaders, and streamers), ionic (utilising the ion conduction in contaminated liquid), suspended particles (which polarise in the field and concentrate, resulting in breakdown), gaseous (where presence of gas bubbles decrease local strength) and electro-convection effects (involving dynamics of space charge in liquid) [57 – 59].

As there is no single consistent theory explaining complete breakdown or ageing of oil due to the complex chemistry of mineral oils there is no single test method that can exactly tell the conditions existing within an operating transformer. Thus regular monitoring of various parameters and maintaining oil quality are essential in ensuring the reliable operation of oil-filled transformer.

To ensure that oil is of adequate quality it must possess certain essential properties mainly: high electric strength to withstand the electric stresses imposed in service, sufficiently low viscosity so that its ability to circulate and transfer heat is not impaired and proper oxidation resistance to ensure long life in service.

It is necessary that the oil be tested and if necessary treated and brought to purity degree that corresponds to the operating stresses. Clearly, equipment failure can be avoided if the condition of the oil in a functioning unit is monitored and based on the results, remedial action is taken [60- 63].

2.4.2 Insulating Paper

Paper used for transformer winding insulation is made from wood pulp by the Kraft process. It contains about 90% cellulose, 6-7% lignin and the rest is pentosans [36]. The natural moisture content of such paper is 4-5% by weight and the insulation on the windings is dried to a moisture level of less than 0.5%. The dehydrated paper is impregnated with insulating oil, which increases its dielectric strength [36, 39]. The typical cellulose structure is shown in Figure 2-6. It consists of chains of glucose molecules linked together by the so-called glycosidic bond comprising the oxygen link shown.

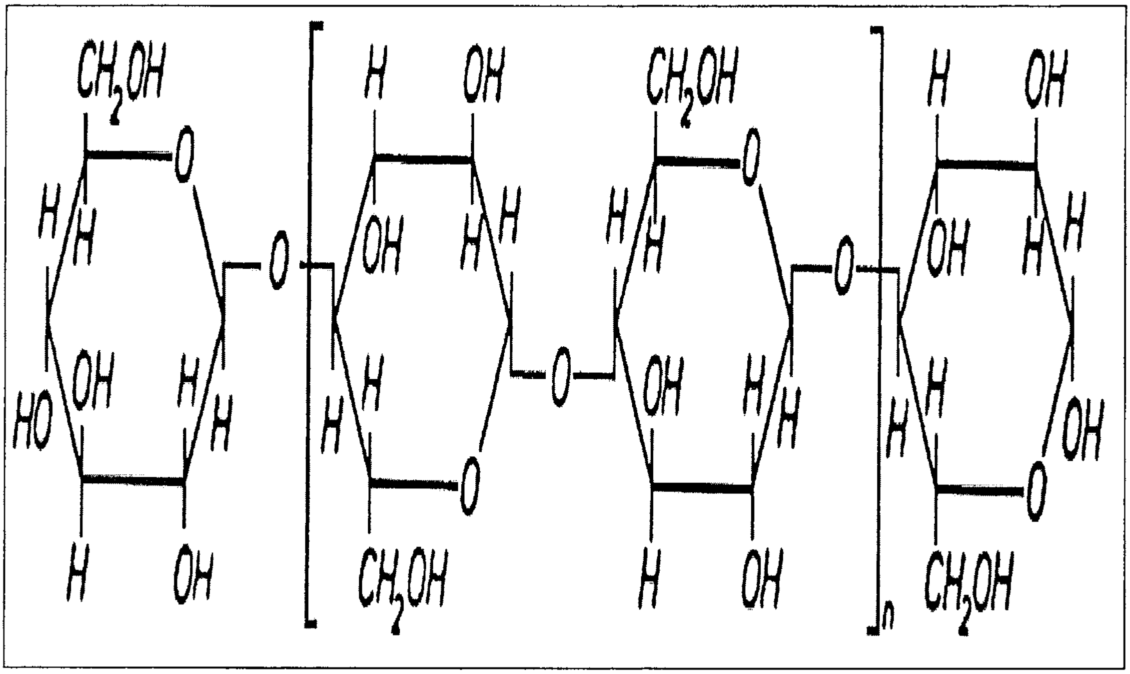

Figure 2-6. Typical Cellulose Structure [36]

Cellulose paper is thus a natural polymer of glucose. The strength of the cellulose paper is significantly dependent on the degree of polymerisation (DP) of the cellulose polymer. The DP of the paper is effectively the number of coupled glucose molecules in the basic cellulose chain. The average DP is monotonically related to the breaking (tensile) strength of the paper: the lower the DP value the lower the breaking strength. Cellulose degradation due to ageing in transformers causes the chains to break up and results in smaller numbers of glucose molecules in the chains. This reduces the average DP value and causes loss of mechanical strength, leading to tearing, brittleness and defibrillation. In contrast, the dielectric strength is not greatly affected [64]. However the loss of mechanical strength and the brittleness makes the paper unsuitable as an insulant if the number of glucose molecules in the chains becomes too low.

After manufacture, the average DP value of new paper is between 1000 and 1300. Drying the paper in the transformer decreases this and ageing in service due to operational heating decreases it further. At an average DP level from 950 to 500, the strength of the paper is almost constant but, in the range 500-200, it decreases in direct proportion to the average DP value. An average DP value lower than 200 makes cellulose paper very brittle and it is then considered to have insufficient strength for HV insulation applications [65-66] and is then quite unsuitable for use as a dielectric material in transformers.

Degradation of cellulose in electrical insulating paper occurs via complex sequences of low temperature chemical reactions, which are not yet completely understood. The processes involve molecular chain scission (de-polymerisation) and the release of breakdown products such as hydrogen, short-chain hydrocarbons, carbon monoxide, carbon dioxide and water. The carbon oxides and moisture dissolve in the oil, where their concentrations can be used to forecast transformer condition. Degradation of the paper also releases larger molecules in the furan group. The gas 2-furfuraldehyde (2-furfural or simply 2FAL) is the major furan gas and can be detected in the oil and can be used to give a more precise indication of the condition of paper [22, 66-67]. Although the precise relationship between DP and 2FAL is not able to be determined analytically, there are a number of empirical relationships that have been established and which have been used to provide useful indication of paper degradation in transformers [198].

Degradation of the paper generally involves one of the following mechanisms: (i) hydrolytic (moisture) degradation, (ii) oxidative (oxygen) degradation and (iii) thermal degradation [68]. The moisture present in the paper, besides accelerating the ageing process also increases the loss factor (tanδ), this increase of tanδ may be so high that thermal instability is caused and breakdown can occur [56]. Any oxygen that may enter the transformer from external sources will be dissolved in the oil and will act directly on the paper to accelerate its ageing. This occurs because the oxidation can weaken the glucosidic bonds and lead to de-polymerisation which reduces the DP number and ages the paper.

Sudden temperature rise (thermal shock) can cause rapid evolution of moisture from the insulation causing potential failure [64]. High temperature of the oil and paper can lead to premature destruction of the transformer, because the high temperature will increase the rate of oxidation and also increase the solubility of moisture in the oil and thus lead to an increase of moisture level in the paper. In a transformer the total water content is distributed between the paper and the oil in a ratio that is predominately in favour of the paper because of its ability to absorb large quantities of moisture [68-69]. At high temperatures bubble formation will occur, and free water formation and static charge relaxation at the various interfaces are the associated detrimental effects that result from the moisture movement [70].

2.4.3 Insulating Pressboard

Pressboard material is made up of sulphate cellulose, a very high-grade insulating material. Pressboard is produced by compressing several paper layers (made from pine wood) while in a wet condition, without any cementing or bonding material to attain high mechanical strength. The addition of bonding agents has proved deleterious in every way from the electrical aspect. The thinner the individual paper layers the better is the quality of the resulting pressboard. The quality of cellulose and water used in the manufacturing process is very important in achieving a quality pressboard [39, 55, 71].

In high voltage power transformers, pressboard has acquired an important role as structural sheet barriers used in the main oil gap, while pressboard spacers called chocks are used to separate the winding discs or layers from one another. Insulating cylinders and moulded pieces are also made up of pressboard [72].

The dielectric properties of pressboard mostly depend on the temperature and on the amount of water contained in the cellulose layers. In order for pressboard to have high dielectric strength and minimum moisture, it is important to monitor the moisture content of the pressboard. Cellulose paper and pressboard have a comparatively low thermal withstand capability and during any operation involving overloading, water is generated that can accelerate ageing, disturb the moisture balance that can result in breakdown and also cause lowering of the PD inception voltage and can also result in a higher PD intensity [71, 73].

Excessive moisture in pressboard, when their molecules are subjected to the high electric field inside a transformer, become polarised and if contained inside bubbles formed by the thermal overload, will distort the bubble. The result is elongation of the bubble along the electric field lines. Eventually, the molecules break through the interfacial tension of the bubble and tiny water globules escape and race in opposite directions along the field lines, forming a long bridge that can causes PD activity or even transformer insulation failure. The presence of water in pressboard around the transformer winding can thus cause much greater problems compared to those arising from water in the oil. Water in the transformer's solid insulation causes its insulating properties to deteriorate quickly [55, 74].

The phenomena of PDs due to high temperature and moisture contents in pressboard are considered dangerous for the satisfactory performance of the insulation system. The continuing deterioration in pressboard insulation due to PD activity can lead to premature failure of the system. Therefore, it is necessary to understand the PD phenomena in such cases in order to understand the degradation processes and thus provide useful design data to assist in the proper design, manufacture and maintenance of high voltage transformer [41, 73].

All that has been said in relation to insulation paper in previous sections will mostly applies to pressboard material as well, so all steps should be taken to protect pressboard from the damaging effects of moisture and temperature in order to avoid insulation failure resulting in breakdown [55].

2.4.4 Oil-Paper Insulation

The oil-paper insulation combination has been of enormous importance to electrical equipment from the very beginning of electrical engineering development. It is still a predominant and most important form of electrical insulation in the modern high voltage transformer insulation, due to its superior insulation properties and low cost. The properties of oil-paper insulation depend on the properties of both paper and oil, and also the technology of the preparation of each and of the impregnation procedure. The electric strength of paper impregnated with oil in combination is much greater than that of the oil or paper individually [58].

In the process of preparing good oil-paper insulation, the condensed and absorbed water from the paper is removed and all of the capillaries in the cellulose structure are filled (impregnated) with good quality oil. This is done with the use of a combination of elevated temperature and high vacuum. The dielectric strength of the oil-paper combination depends primarily on how well the impregnation of paper with oil is performed. Unless the paper is perfectly oil-impregnated there will be voids of air or other gases present as impurities that can cause partial discharge activity [75].

The strength of the oil-paper insulation can be reduced by the combined effect of temperature, moisture and gases. Small changes in temperature significantly increase the moisture absorption capability of the oil water content but only increases that of the paper slightly. The effect of moisture content is most significant during transformer overload conditions. The presence of air and other gases in the oil-paper insulation cause harmful effects to the insulation system [48] in such situations. To achieve good oil-paper insulation system, the transformer has to be maintained virtually free of moisture for its entire life. It is much more difficult to extract moisture out of oil-impregnated paper once it has been allowed to penetrate significantly into the paper [75].

To summarise, the insulating material used in oil transformers must have good electrical properties, good mechanical properties and good thermal stability. The electrical properties are required not only to withstand the rated power frequency voltage but also lightning and switching impulse voltages. Good mechanical properties required include mechanical strength and an ability to withstand the very high electromagnetic forces that occur during overloads and short circuit through-faults and also during fabrication and handling during the manufacture phase. Insulating materials must also have good thermal stability to maintain both the electrical and mechanical properties at the highest level during the life of the transformer.

2.5 Drying of Paper and Pressboard

High moisture contents in cellulose insulation can cause partial discharge. It thus needs to be dried very effectively. Cellulose with high moisture content is dried in three stages, during the first stage, the insulation is still so wet that all pores and capillaries are filled with water and its whole surface is covered with a cohesive water film. As soon as the surface is dry, the water diffuses into the cellulose, since the moisture content does not reduce uniformly throughout all layers. Instead drying is carried out, one layer at a time, towards the interior of the cellulose, with the process not being totally clear-cut due to inhomogeneous composition and hydroscopic properties. Below a certain moisture content however, the attractive absorption forces of water and cellulose molecules are so great that considerable energy is required to overcome them [75].

During the drying process the moisture must first be transferred from the liquid to vapour phase: this process can be accelerated by reducing the pressure. Energy in the form of heat is also needed to transform moisture to vapour and to overcome secondary bonds. This heat must be transmitted to the cellulose by heat conduction, radiation or condensation. Satisfactory drying as well as complete impregnation of the cellulose by oil is possible only when proper drying and impregnation techniques are employed [34].

In some cases, a transformer may be in such a bad condition that it should not be disturbed in any way (for example the paper may be very brittle). Typically, such units are very old, very badly sludged and are usually near failure and therefore attempting to dry the insulation might accelerate failure. Most transformer manufacturers and many large users of transformer, such as electric utility companies, recommend that a transformer be removed from service and kept de-energised throughout the oil reclamation process. This practice eliminates the possibility of failure during reclamation in the event of an air bubble, sludge, or foreign matter getting into wrong places [76].

2.6 Transformer Insulation Testing/Checking Methods

Recently, there has been a very significant growing interest in the condition assessment of transformer insulation [63]. Primarily this is due to the increasingly aged population of transformer in the older utilities around the world. A large percentage of existing power transformer within these electric utilities are approaching the end of their design life. Many of these transformers appear to be operating satisfactorily. However, insulation degradation continues to be a major concern for these aged transformers and much work is being devoted to developing improved techniques to assess the condition of aged transformers. In particular there has been very considerable development of the use of dielectric spectroscopy and its derivative techniques (Recovery Voltage, Polarization De-polarization Current etc.) for monitoring of moisture content in particular [200].

A variety of electrical, mechanical and chemical techniques are available for insulation testing of a power transformer. For estimating its effective insulation condition, most of the techniques have been in use for many years. These include methods such as (i) measurement of insulation resistance (IR), (ii) dielectric loss factor (DDF), (iii) partial discharges (PD's), (iv) interfacial polarisation (IP) using anomalous IR and frequency dispersion of capacitance, (v) oil quality, moisture content, (vi) dissolved gas analysis (DGA), (vii) degree of polymerisation (DP) of cellulosic paper and pressboard, and (viii) tensile strength of paper and pressboard. Other methods are relatively new, having been applied and implemented in more sophisticated ways over the last 10 years or so.

These include (i) high performance liquid chromatography (HPLC) furan analysis, (ii) interfacial polarisation spectra (IPS) using return voltage measurements (RVM) and (iii) polarisation and depolarisation current (PDC) [79-80].

To assess the overall condition of a transformer, several testing techniques are used and some newer ones are still under investigation. The traditional routine tests used over the years include:

(i) transformer ratio measurement,
(ii) winding impedance,
(iii) short circuit impedance and loss,
(iv) excitation impedance,
(v) dielectric dissipation loss factor and capacitance

as well as applied and induced potential tests. These tests usually give information on faults in windings, winding conductor and joint problems, winding deformation, oil moisture and contamination, and dielectric problems.

Special tests include:

(i) PD measurement,
(ii) frequency response analysis,
(iii) vibration analysis,
(iv) infrared examination,
(v) recovery voltage measurement,
(vi) polarisation and depolarisation current and
(vii) DP measurement.

These tests detect problems such as local PD activity, winding looseness and displacement, slack winding and mechanical faults, connection hot spots, moisture in paper and ageing of paper as well as insulation degradation [29, 77-78].

The operating life of a transformer is affected by the integrity of its insulation. It is very important to test the insulation from time to time, in order to have an idea of its quality and strength. The techniques used most often to assess the integrity of power transformer insulation are as follows:

1. Power-Frequency Voltage Test
2. Lightning Impulse Test
3. Switching Impulse Test
4. Insulating Oil Checking
5. Insulation Resistance
6. Analysis of Gases Dissolved in Oil (DGA)
7. High Performance Liquid Chromatography (HPLC)
8. Short Circuit Reactance/Low Voltage Impulse Testing
9. Insulation Power Factor (Tanδ)
10. Recovery Voltage Measurement (RVM)
11. Polarisation and Depolarisation Current (PDC)
12. Partial Discharges (PD's) Location and Measurement

The different methods used for the insulation testing/checking of the transformer are briefly reviewed in the following.

2.6.1 Power-Frequency Voltage Test

The power-frequency voltage test is the traditional way of checking transformer insulation. Its purpose is to verify the dielectric strength of major insulation between individual windings, between windings and the earth parts, and of the insulation within individual windings. On windings with uniform insulation the test is performed in two parts. The dielectric strength of insulation is checked by a separate-source, power-frequency voltage withstand test and that of the insulation within the windings by the induced over voltage withstand test [29].

2.6.2 Lightning Impulse Test

The lightning impulse test (1/50 μsec voltage waveform) is performed to check the dielectric strength of transformer insulation against overvoltages of atmospheric origin. This test is applied as a routine test on a transformer of higher voltage rating. The existence of a fault can be recognised without any difficulty on the basis of waveform plotted during the tests, but not so the location of the defect. Testing experience can however indicate the kind of defect, e.g. whether it is a fault involving a few turns of a winding, or a breakdown between discs or layers or a fault within the tap changer, or an earth fault [31].

Accurate location of the fault, e.g. in the case of a turn to turn fault, as to which part of a winding (its beginning, middle or end) is not possible with any reliability. Such information is usually available only after dismantling the transformer and it remains difficult to pinpoint the defect even then, as an insignificant puncture occurring under the effect of the impulse voltage barely leaves any trace in the winding. By applying further pulses the damage can be made more extensive and the defect can be located more easily [31].

Conclusions concerning the test results can be drawn on the basis of the test impulse waveform. The waveform recorded during a chopped wave impulse test may be useful for fault detection purposes. If the required accuracy cannot be attained, the result of the chopped wave test should be assessed by the waveform of the subsequent full wave test [31].

2.6.3 Switching Impulse Test

The aim of the switching impulse test is to confirm the dielectric strength of transformers against switching surges. The lightning impulse voltage phenomena are of such short duration that no saturation of the transformer core can take place. In the case of switching surges, the role of such saturation becomes considerable. Thus, both the lightning impulse and the switching impulse may be considered as voltage surges bringing about unidirectional changes of flux. The duration of a switching impulse is sufficiently long to permit the flux to reach saturation level in the iron core. The detection of a breakdown occurring in the course of a switching impulse test is much simpler than in the case of lightning impulse test [30].

Any minor defect of the winding, e.g. a turn to turn fault, causes a very obvious change in the switching surge impedance of the transformer and gives rise to large distortion not only in the wave shape of the neutral current but also in that of the terminal voltage. When a switching impulse test is performed, it is sufficient to investigate the waveform for the voltage applied to the transformer and provide a reliable evidence of any breakdown that may have occurred within the transformer [30].

2.6.4 Insulating Oil Checking

The testing of oil samples drawn from transformer in service does not permit any reliable conclusion about the condition of oil-impregnated paper insulation in the transformer. However such tests represent the simplest and most practical means of detecting the presence of contaminants in the oil that may be harmful to the electrical safety of the transformer [81]. The standard testing method with commercial test cells checks breakdown voltage and the DDF of the oil.

2.6.5 Insulation Resistance

The insulation resistance is a basic quantity indicating the general well-being of a (primarily solid) insulation system. It is also a useful measure of the contamination of the insulation, particularly by the moisture. The method is based on measurement of the current flowing through a dielectric following the application of a direct current (dc) voltage. The most common instrument used is the "Megger" [37] high resistance meter. Insulation resistance is most useful for solids. It is of no use for gases and of very limited use for liquids.

Although the measurement of direct current as an indication of the condition of insulation in equipment has its limitation (e.g. ac conditions are not represented correctly, low resistance paths in series with good insulation are not easily detectable and parallel path effects cannot be eliminated within structures), this simple test has been developed by the industry as a valuable assessment tool [80].

The test is actually based on determination of the variation in current following the application of voltage. This variation is determined by the polarization response of the material and this is a function of the dielectric condition. The current can be modelled as comprising three separate components, which are (i) the true capacitance charging current, (ii) the dielectric absorption current, and (iii) the true ohmic conduction or leakage current [80].

The tests generally used with the IR meter are;

1. Short-Time or Spot Reading test
2. Time-Resistance test
3. Step-Voltage test

2.6.5.1 Short-Time or Spot Reading test

The test is known as the spot-reading test because the actual test is applied for a short period of time, usually sixty seconds. The readings obtained by this method indicate a point on a curve of increasing resistance. The value of resistance value obtained can be used to show a trend in insulation condition [37]. This is the traditional test that gives the direct insulation resistance (IR) reading.

2.6.5.2 Time Resistance Test

The time-resistance test is based on the dielectric absorption effect of good insulation compared to that of insulation which is contaminated by moisture for example. The insulation resistance value of good insulation is expected to increase with time until reaching a final steady state value. The readings are carried out for ten minutes and the variation with time is recorded. The readings of insulation resistance will increase with time if the insulation is good because of the absorption charge affect, which takes longer to complete than the capacitance charging effect. If the insulation resistance remains the same for the time span, then the chances are that the insulation is contaminated by moisture [37]. The advantage of this method is that the condition of insulation can be shown directly without reference to previous tests. This method has also the advantage that it is largely independent of temperature and size of equipment under test.

The extensions of time resistance test include the dielectric absorption ratio and the polarisation index of solid insulation materials [37].

2.6.5.2.1 Dielectric Absorption Ratio

The dielectric absorption ratio is the ratio of the resistance reading at sixty seconds to the resistance reading at thirty seconds. The table below shows the different dielectric absorption ratio values and their general corresponding insulation condition.

Dielectric Absorption Ratio	***Insulation Condition***
Less than 1	Unsatisfactory
1.0 - 1.25	Dubious
1.4 - 1.6	Good
1.6 onward	Very Good

Table 2-1 Dielectric Absorption Ratio and Insulation Condition [82]

2.6.5.2.2 Polarisation Index Ratio

The polarisation index (PI) is the ratio of the resistance reading at ten minutes to the resistance reading at one minute. The value obtained by this ratio gives a good indication of the presence of moisture in the insulation in general, although it is limited in its assessment value for aged insulation. Table 2-2 below indicates polarisation index values and their general corresponding insulation condition. The results obtained from insulation resistance tests indicate localised flaws, moisture ingress and end-winding contamination when performed on motors.

Polarisation Index Ratio	***Insulation Condition***
0 – 1	Unsatisfactory
1 – 2	Dubious
2 – 4	Good
4 onward	Very Good

Table 2-2 Polarisation Index Ratio [82]

2.6.5.3 Step Voltage Test

The step voltage test is performed on solid insulation initially at one level of applied voltage followed then by step increases (usually about 1000 volts per step) at higher applied voltages. The duration of the test is sixty seconds, with preferably voltage steps of 1000 V or if only two are used this may be for example 1kV and 5kV. If the reading obtained at the higher voltage is significantly less than that at the lower voltage then the weakness is revealed at the higher voltage. If the reduction in resistance between the result at a lower voltage and that at the higher voltage is around twenty five percent this indicates an unacceptable level of moisture contamination [82].

2.6.6 Analysis of Gases Dissolved in Oil (DGA)

DGA is universally accepted as the method of choice to detect incipient thermal and electrical faults. DGA methodology and applicability have evolved significantly since its development. Under the effect of electric and thermal stresses, the degradation of organic insulation materials produces many gases. The kind, the amount and the proportions of these gases depend partly on the material damaged, partly on the nature of the phenomena responsible for this damage and on the level of energy they involved in action. The gases formed are also collected in a Buchholz relay which does not respond to all forms of breakdown at early stages [29, 83].

All gases generated by insulation decomposition are soluble in transformer oil to some degree and are able to be recovered by applying vacuum for chemical analysis of their species and quantity. Transformer faults which consist of overheating faults, arcing faults, discharge faults and faults involving cellulose will generate varying levels of dissolved gases and thus determination of the gas species and quantity can give information as to the fault type. Overheating faults produce ethylene, methane and acetylene. Hydrogen, acetylene, methane, ethane and ethylene are produced as a result of arcing faults. Methane, hydrogen, carbon monoxide, ethane, ethylene and acetylene are products of discharge faults. Faults involving cellulose degradation produce carbon monoxide and carbon dioxide. Hydrogen and carbon monoxide are the first fault gases to form as an evolving transformer fault initiates, therefore they are defined as two key fault gases, they represent an early warning for both oil and cellulose type dielectric failure modes [84-86].

The information supplied by analysing gases dissolved in oil provides assistance to the monitoring and maintenance of transformer and information can be very valuable in preventive measurement program. Also advance warning of a developing fault allows for convenient scheduling of repairs. The experience gained from the past has shown that the DGA is a powerful and sophisticated technique, successfully applied to transformers for many years. Refinements of the method are still needed to increase the usefulness of dissolved gas analysis (DGA). However, sole reliance on this method cannot provide complete protection against all types of evolving type faults [70, 87].

2.6.7 High Performance Liquid Chromatography (HPLC)

The condition of the paper insulation is much harder to detect by direct means because the paper is wrapped around the HV conductor and thus access is difficult. Paper cannot be sampled without taking the equipment out of service. Further, the more easily accessible sections of the paper for sampling are likely to be those located in lower temperature regions of the transformer and are thus likely to be less degraded than paper which is located closer to the hot spot and which has thus suffered most deterioration.

In DGA the carbon monoxide and carbon dioxide dissolved in the oil results from deterioration of both the mineral oil and the paper and are difficult to separate and use as a diagnostic tool. However the cellulose degradation generates a variety of furan compounds which also dissolve in the impregnating mineral oil and these provide a very sensitive monitor if paper degradation. Their detection in oil requires a more sensitive analysis of the oil using High Performance Liquid Chromatography (HPLC) techniques rather than the simpler gas chromatography method used in standard DGA. The HPLC technique has been developed to enable detection of the furan concentrations in the oil. The concentration of one of these, 2-furaldehyde or 2FAL, has been associated directly with the reduction of the DP of the paper. The benefit of using furan levels, instead of the carbon oxide levels, is that the furans are degradation products specific to the paper. Oil degradation will not produce furans. Furan analysis has been in use for condition monitoring on routine basis for a number of years [88].

The empirical equations below are the more common versions which relate DP number of aged paper to furan level (F = 2-FAL)) measured in the oil [198]:

$DP = [1.51 - \log_{10}(F)]/0.0035$ [Chendong equation]

$DP = [1.17 - \log_{10}(F)]/0.00288$ [Scholnik equation]

$DP = 800/[(0.186.F) + 1]$ [Pahlavanpour equation]

$DP = 7100/[8.88 + F]$ [DePablo equation]

2.6.8 Short Circuit Reactance/Low Voltage Impulse Testing

A short-circuit reactance and low voltage testing methods are expected to reveal permanent deformations of the windings in transformers that have been subjected to heavy fault current. These methods are indirectly a means of detecting possible consequent insulation weakness [29]. The main form is the modern Frequency Response analysis Test (FRA) [201] which is now almost a mandatory test to be performed after a transformer suffers a through fault.

2.6.9 Insulation Dielectric Dissipation Factor (DDF or Tanδ)

The insulation dielectric dissipation factor is also known by other names such as dielectric loss, loss angle, insulation power factor and tangent delta (tanδ). The dielectric loss in any insulation system is the power dissipated by the insulation when an ac voltage is applied and the polar materials of the insulation attempt to follow the changes in applied field orientation. Insulation DDF is an important property which provides vital information on the general well being of the overall insulation structure. AC bridge techniques are commonly used for measuring the DDF and capacitance. Although the DDF is the more useful parameter the capacitance can also provide useful information, for example in a capacitor graded bushing any short circuiting of layers may show up as a change of bushing capacitance.

All electrical insulation materials apart from the gases have a measurable quantity of dielectric loss, regardless of their condition. Normal ageing of an insulating material will cause the dielectric loss to increase. In addition, contamination of insulation by moisture or chemical substances may cause losses to be higher than normal. Partial discharge activity will also increase DDF. The dielectric loss is thus a sensitive measure of the electrical losses in the insulation. Low values of dielectric loss are usually required as proof of the quality of the insulation. Increases in the value of dielectric loss over time are taken as a sign of deterioration of the insulation condition. Dielectric loss is one of the best indicators of the quality of a specimen of insulation, as its value changes with increase and decrease of moisture contents in the insulation [56]. It is particularly useful if the DDF is measured versus voltage to about 1.2 per unit as it will exhibit a "tip-up" at higher voltages that is a sensitive indicator of condition. DDF is also very sensitive to the measurement temperature and this must be considered and adjusted for if trends of DDF over time are being used to analyse condition.

In modern tests of paper insulation for moisture the polarization de-polarization test (PDC) provides DDF in the frequency domain over the range DC up to about 2 MHz and this frequency domain representation is found to be a more useful indication of insulation condition than the purely 50 Hz version [202].

2.6.10 Recovery Voltage Measurement (RVM)

The Recovery voltage measurement is a very useful technique in evaluating the condition of oil-paper insulation, as RVM can be used to determine the aging characteristics of dielectrics and is very sensitive to moisture [91].

The aging process can be determined by using various parameters of recovery voltage measurement as the properties of the dielectric changes when the degradation in insulation occurs.

RVM is a method that obtains the response of a dielectric by measuring the return voltage of the dielectric system to evaluate the condition of the insulation with respect to moisture content and ageing.

During the RVM test the specimen is charged to a specified DC voltage, held at that voltage for a specified time, then discharged through a low impedance for a specified time and then the DC voltage that returns under the open circuit conditions is recorded over time and the maximum value of return voltage is recorded as a function of charging time [91]. This is the “Return Voltage” and its magnitude and variation over time is an important guide to the insulation condition.

Three characteristic parameters of the return voltage variation with time can be defined which are useful in terms of insulation condition. These are: (i) the maximum value of the return voltage, (ii) the time at which the maximum is reached and (iii) the initial slope of the return voltage versus time curve.

By plotting the peak return voltage as a function of charging time, the “Polarisation Spectrum” of the insulation can be obtained. The time of the maximum in that polarisation spectrum is called the domain time constant and this will tend to change significantly with insulation condition or with moisture content.

The technique measures the dielectric polarisation in oil-paper insulation and impurities such as moisture, ageing products etc. tend to collect at the interfaces between the components of the insulation and increase the electrical conductance at the interface. The increased conductivity in turn enhances interfacial polarisation in the composite dielectric.

If the condition of the oil-paper insulation is homogeneous and if the distribution of the temperature, moisture, and ageing by products in the insulation is uniform then the resulting curves have one dominant time constant because the dominant time constant and the intensity of elementary polarisation have uniform values [44, 84].

2.6.11 Polarisation and Depolarisation Current Method (PDC)

The polarisation and depolarisation current measurement is a useful technique for assessing the condition of the insulation materials in transformers, as well as in other solid insulation materials. When dielectric materials are exposed to an electric field, it becomes polarized.

The PDC method is, to a degree, an extension of the RVM technique in that it uses the same method but does not open circuit the insulation after the depolarization sequence starts.

The PDC measurement applies DC voltage across the test sample for a long time (~ 10,000 sec.). During the charging time, the time variation of the polarisation current arising due to the conductivity of the insulation material is measured. Then the test sample is short circuited after removing the applied voltage. The depolarisation current as a function of time is then measured for a similarly long period.

The polarisation and de-polarisation currents are strongly influenced by moisture content of the insulation materials and therefore the PDC measurement technique can be used to examine the condition of both insulation paper and transformer oil in the transformers. This technique gives general information about the state of insulation and is useful in estimating presence of moisture and in tracking development of ageing phenomena [86].

2.6.12 Partial Discharges (PD's) Location And Measurement

Power transformer failures caused by the breakdown of the insulation materials are normally caused as a consequence of the gradual and cumulative damaging effects of partial discharges on the insulation materials over prolonged periods (perhaps years).

The PDs are localised ionisation of small high field regions in the insulation oil and paper in transformers. They occur particularly where there are interfaces of insulation with differences in dielectric permittivity (e.g. gases and solids) and this will result in high electrical stress and when the electrical stress is too high the PDs may occur at the interface of the insulation materials or in gas filled cavities within the dielectric.

Failure of the dielectric insulation inside transformers is often preceded by PD activity. A significant increase either in the PD level or in the rate of increase of PD level can provide an early indication that changes are evolved inside the transformer. PD activity in oil will produce hydrogen dissolved in the oil, whereas the generation of acetylene is more closely associated with higher level PDs where sparking occurs.

PD sources most commonly encountered are surface tracking in the insulation, voids in solid insulation, metallic particles, and gas bubbles generated due to some fault condition [89-90]. Detection of these PDs can provide a clear warning about the existence of incipient faults in insulation.

PDs can be measured electrically, by galvanic coupling to the PD currents or by radiative coupling to the electromagnetic radiation, or by acoustic methods, where the ultrasonic pressure pulses associated with the PD activity are monitored.

Acoustic methods of detecting PDs may allow location by triangulation. The interpretation of detected PD activity signals is not straight forward. Although PDs can indicate clearly insulation degradation, there is as yet no available detailed quantitative correlation of the remaining life of a transformer to PD activity level [41].

Traditionally PD monitoring measures discharge current pulses that arise from changes in the external circuit caused by charge redistribution in the insulation. This method does not allow direct correlation of the PD current pulse signals with insulation condition [37, 41]. However modern PD methods now allow direct recording of the high frequency individual PD current waveforms and these true current waveforms provide a better correlation with insulation condition and trending [203].

Evaluation of the results of PD measurement is a complicated problem. The value of measured apparent charge in itself is not always a suitable or incontrovertible means for judging PD risks. Such a conclusion may be drawn by analysis of discharge current pulses and from location of the defect. If the PDs detected are only slightly higher than the specified limits, but are considered to be dangerous, or if they have a very high intensity, the insulation should be taken off line and some action or repair taken [37].

2.7 Condition Monitoring of Transformer

The insulation condition assessment of a power transformer is the most important aspect of its maintenance and is required to ensure the continuous operation. Continuous insulation condition monitoring can provide an early indication of any insulation degradation. The insulation breakdown can also be a risk to personnel. Thus, insulation condition monitoring is required to monitor the insulation integrity.

Monitoring means essentially sensor development, data acquisition, data collection and development of methods for analysis of data. Diagnostic interpretation is the step following monitoring and involves interpretation of offline and on line measured data. Monitoring is the basis for diagnostics but, without diagnostics and some ability to evaluate the data, the measured data is of limited value [92-93].

The cost of acquiring, replacement, transportation, installation and repair of power transformer are among the highest on the power system. Many power transformers around the world are functioning beyond their design life and the degradation of the insulation material may cause the transformers to be unreliable. The high cost of a new transformer and good condition of most of the transformers are the main reasons that explain why these old transformers are still in use. Hence, in order to extend the life of the transformers, a regular condition assessment is required to test its reliability. By doing so, transformers might be able to operate past their design life [1, 94].

Condition monitoring of power transformers has attracted considerable attention for many years. The early indication of incipient faults in transformers can provide economic benefits that have a measurable effect in the results required to meet the formidable challenges facing the electric utilities. To detect incipient faults various methods are used which have made possible an early warning system and fault location to ensure a smooth and safe operation of a power transformer [95-96].

In summary, continuous monitoring of the condition of transformer insulation can, reduce the maintenance/repair cost, lower the probability of destructive failures, provide means of quality control, improve the safety of personnel and reliability of supply, limit the severity of any damage incurred, identify the root cause of failures, provide the transformer operating life estimation and also enable asset managers to make decisions wisely.

Chapter 3

Ageing of Oil, Paper and Pressboard Insulation

3.1 Ageing Phenomena in Paper

Oil, paper and pressboard have been used as insulating materials in power transformers for over a century. Despite apparent weaknesses of these materials they are effective insulators, especially when used in combination. Even in ideal conditions, oil and paper will degrade, or age, as their useful service life is finite. The actual processes involved depend on the operating conditions of the equipment, but the rate of ageing is normally primarily a function of temperature and moisture.

Oil and paper both will age rapidly at high temperature and moisture acts as a catalyst for the ageing of oil. There are also other catalysts present in the transformer that are responsible for oil ageing; the most predominant is oxygen. The principle mechanism of oil ageing is oxidation, which results in acids and other polar compounds being formed. These oxidation products will have a harmful effect on the paper degradation processes.

Thermal degradation of paper insulation will take place in a transformer at the normal operating temperature [83]. This degradation is accelerated at higher temperatures, especially if the unit overheats or develops hot spots. As a result, the useful life of the transformer may be significantly reduced due to change in the degree of polymerization (DP) of the cellulose material (paper and pressboard). Although damaged or degraded paper may have acceptable electrical properties. Its mechanical properties might be sufficiently weakened so that it is no longer able to withstand mechanical vibration due to marked decrease in DP values [97].

There are several techniques that can be used to assess the condition of insulating oil and paper. The use of a combination of these diagnostic tests allows the insulation to be monitored for degradation changes over time, whether the changes are due to dielectric, thermal, mechanical or chemical effects.

The advantages of knowing how quickly the oil and paper is ageing are that it permits the oil to be used for as long as possible and then replacing or reclaiming it before it can cause permanent damage to the transformer. Sampling of paper from the transformer windings is not as simple as for oil. The difficulty in accessing paper quality especially at locations subject to hot spot temperatures is another challenge. The replacement of paper insulation is also very time consuming and costly [83].

The transformer oil always contains some (small amounts) water absorbed in it when it is received from the manufacturer. Further moisture ingress can occur from the atmosphere during normal service life if the transformer is not well sealed. Water cannot be removed completely from transformer oil and there always remains some water in the oil. This water migrates into the paper insulation. Once the water reaches the body of the paper, it migrates under the influence of any non-uniform electric field towards the high field region at the source of the non-uniformity [97-98]. In addition the decomposition process of the paper will generate moisture as a by-product.

The degradation of oil-impregnated paper is assessed through the measurement of its electrical and mechanical strength. The mechanical strength of cellulose insulating material is measured either by its tensile strength or its DP value as described in chapter 2. Generally, the insulating paper may be considered to have its life expended once the tensile strength is reduced to approximately half of the initial (new) value. With the tensile strength dropped to half of the initial value, the DP of the paper will have also dropped.

New transformer paper has a DP value of around 1000-1300. After the manufacturing process, the DP comes down to about 1000. It de-polymerises over the life of the transformer and as the insulation DP reaches below 200, the paper is no longer considered useful. Any appreciable decrease in the tensile strength will be indicated by the DP and this can thus be used to indicate the paper condition and any degradation of the paper that has occurred. The presence of water in oil/paper insulated transformer will degrade the paper and the degradation will be enhanced if the water contains some ions [97, 99].

The service reliability of the power transformer largely depends upon the condition of the oil-paper insulation. The gradual deterioration of oil purity during its ageing process has an important impact upon the internal insulation of the transformer. High temperature with moisture and oxygen increase the oxidation rate of the transformer oil, reducing the bonding strength between the molecules of the cellulose materials. The long molecular chains of the cellulose break down more rapidly in such conditions causing the formation of water, carbon monoxide and small amount of methane [36].

The chemical reactions also transform the completely separated molecules into other substances such as sludge and acids. These cleavage products cause further chemical reactions and deterioration of the cellulose materials [39]. The damage done to the winding becomes obvious when the improvements in dielectric properties are measured after the replacement of aged oil with new oil.

The decay products that progressively damage the initial properties of oil-paper insulation in power transformers are mostly the outcome of chemical reactions under the impact of electrical and thermal stress. Therefore the ageing of oil-paper insulation is the result of complex physical and chemical processes [98].

The internal transformer construction consists of a laminated iron core, windings with paper insulation and structural solid insulation (pressboard) components providing separation, mechanical support and barriers in a metal tank filled with liquid insulation. The paper and pressboard provide mechanical and dielectric strength. The transformer oil protects the paper insulation, acts as an insulation medium, and also provides means to monitor transformer condition and operation. The insulation system is the most important part of a transformer to maintain since damage to the solid cellulose based insulation is irreversible [99].

Transformer oil dissolves more moisture at higher temperatures than at lower temperatures and the greater the extent of the refining operation, the less is the solubility of water. If the oil and water combination is cooled, then water droplets can precipitate out. The water phasing out of solution will be absorbed by the insulation, attacked by the decay products in the oil or end up as free water at the bottom of the tank. The moisture will divide between the paper and the oil in a definite ratio ensuring a state of equilibrium at any given temperature [83].

Oxidation of oil produces some water as a degradation product, together with acids, sludge and other polar compounds. Sludge formation is a dangerous stage of the deterioration process. The acid formed in the process of oxidation attacks the cellulose fibres and metals, forming an acidic sludge on the insulation and different parts of the transformer. Sludge appears faster in overloaded transformers, increasing the viscosity of the oil and reducing its cooling ability. It is also partially conductive, absorbs moisture and act as a heat insulator. Sludge deposits on the core and windings can increase the transformer operating temperature and it is considered one of the prime causes of premature mechanical failures of a transformer [99]. Once sludge is absorbed in the cellulose, the DP and tensile strength start to decline. At the same time the formation of furanic compounds, which are derivatives of aromatic compounds and are products of the degradation process of the cellulose insulating materials, accelerates and the cellulose insulation deteriorates further.

Design engineers expect a transformer to last for over thirty years under ideal conditions. Owing to its age a transformer in an electric utility needs special attention, as the power transformer is the most expensive item of equipment in the power system. As a result of economic condition in power industry in the last few years, the life management and estimation of the remaining service life of power transformer has fortunately gained more attention. To manage the transformer asset better and to provide investigations in this important area of the effects of temperature shock and moisture on transformer insulation we have to understand the present state knowledge of oil-paper insulation as well as the transformer history and its operating conditions over the lifetime [100].

The ingress of moisture coupled with high operating temperature ages and reduces the dielectric strength of the cellulose insulation and transformer oil. In addition the voltage stress caused by impulse transients and power frequency overvoltages decrease the dielectric strength of the transformer insulation and also cause mechanical deterioration. Furthermore system short circuits, inrush current, vibration, thermally generated expansion forces will also reduce the dielectric strength of the insulation.

Excessive moisture in the insulation system causes PD activity and tracking and electrical treeing effects within the moisture soaked cellulose insulation. As a consequence, there is a significant reduction in their dielectric strength that reduces the ability of these materials to withstand high electrical field stress [101]. Electrical failure due to bubble formation can also occur at high temperatures when there is a sudden thermal shock.

The degree of polymerisation (DP) is closely related to the quality of the degraded components generated upon degradation of the insulation paper. These include carbon oxides and, particularly, furans. A power transformer therefore may have an ageing degradation level which can be monitored by sampling the quantities of these components contained in oil [101-103].

There are many diagnostic parameters indicative of the ageing process. Periodic or continuous measurement and assessment of these parameters and constant comparison of these parameters with new insulation characteristics can provide reliable information on the ageing process. The decision relating to operating life of the equipment in service must be taken using information from monitoring and from ageing characteristics of the materials used.

The tool required to monitor the performance of the transformer, the current insulation condition, and to predict remaining life is condition monitoring. This can help in preventing catastrophic failure, unsafe operation and unnecessary maintenance [3].

3.2 Ageing Effects

Ageing effects can include the effects of electrical, thermal, mechanical and environmental stresses on insulation over sustained periods of service. The ageing factors produce ageing mechanisms that can eventually lead to failure. When ageing is dominated by one ageing factor, this is referred to as single factor ageing. Multi-factor ageing occurs when more than one ageing factor substantially affects the performance of the electrical insulation system [3].

The ageing of cellulose materials in the transformer is affected by the water, oxygen and temperature. The hydroscopic nature of the cellulose encourages water molecules to accumulate between the cellulose chains and thus promote degradation of the cellulose during the ageing of the oil. The moisture present at the beginning of the ageing process, as well as the water formed by the reaction of the cellulose and of the oil causes additional decomposition of the chain molecules. The water continuously causes fresh molecular cleavage and thus has the negative property of constantly accelerating the ageing process of the cellulose.

The process of ageing of cellulose/oil due to the presence of water and oxygen can be determined from the change in the material properties and from the formation of reaction products. The primary connection between deterioration in the material properties and the formation of ageing products is the DP. DP is one of the most informative parameter to assess the ageing of the cellulose [39].

Transformer ageing includes contributions from the following factors:

1. Thermal Stress Ageing
2. Electrical Stress Ageing
3. Ageing Caused by Chemical Changes
4. Environmental Ageing
5 Mechanical Ageing.
6. Ageing of Cellulose (Paper/Pressboard)
7. Ageing of Transformer Oil

3.2.1 Thermal Stress Ageing

Thermal ageing involves the progress of chemical and physical changes as a consequence of accelerated chemical degradation reactions with the acceleration caused by increased thermal activity at higher temperatures. It also involves the thermo-mechanical effects caused by forces due to thermal expansion and contraction. The rate of thermal ageing and the ageing caused by thermo-mechanical effects, as far as chemical reactions are concerned, are thus very much influenced by the operating temperature [39].

The maximum operating temperature that can be attained by any particular transformer without reducing its design life is determined by standard levels given for the conductor hot spot operating temperature, which is usually taken as a maximum permissible level of 98°C. This is specified in Standards such as AS 2222 [204]. The rate of thermal degradation of conductor insulation increases rapidly when its hot spot operating temperature rating is exceeded. The prolonged thermal stress causes harmful effects in the transformer insulation, particularly solid insulation [3]. This has brought about the classification of various materials as per the performance that is expected from various insulating materials at specified temperatures.

Dakin in 1940 developed a theory for quantifying electrical insulation ageing based on chemical reaction rate theory. He formulated the following equation for relating the lifetime (L) of insulation to its operating temperature:

$$L = A \exp. (B / T) \text{ or}$$

$$\ln (L) = \ln A + (B / T)$$

Where, A and B are constants determined by the activation energy and T is the absolute temperature [3]. This theory of the thermal behaviour and lifetime of organic electrical insulation is now widely taken as the basis for operational ageing of transformers. It should be noted that it is applicable only for organic insulation, not inorganic materials such as mica.

3.2.2 Electrical Stress Ageing

The electric field strength applied to the insulation influences electrical ageing. An empirical result obtained by work of many investigators has led to the establishment of a Life vs. Voltage (stress) relationship [80].

$$L = K\,(1 / V^{n})\ \text{years}$$

Where K is a constant, n is the inverse slope of lifeline on a log - log graph and V is applied voltage. The value of 'n' is usually between 9 and 20 but can be smaller [80].

3.2.3 Ageing Caused by Chemical Changes

In the power transformer many by-products are formed within the insulation while the insulation is deteriorating. The by-products of this deterioration process are used to analyse the changes occurring in the insulation. The important compounds are the furans. Furan analysis is a very powerful technique for estimating life of insulation [83].

3.2.4 Environmental Ageing

Environmental ageing involves chemical reaction processes mentioned under thermal ageing but with the addition of environmental contaminants. The presence of oxygen and moisture ingress together with high temperature further accelerates the ageing process of the insulating materials. Environmental factors may also influence in various ways the kind and degree of degradation caused by other stresses to which an electrical insulation system is exposed. Other important factors are the redistribution of stresses caused by the environmental contaminants on electrical behaviour [105].

3.2.5 Mechanical Ageing

There are various mechanical forces that can occur inside an operating transformer, and if the paper cannot withstand these forces, it will not be able to successfully insulate the conductors. Mechanical ageing is strongly influenced by the rate of occurrence of repetitive mechanical stresses and the magnitude of non-repetitive stress [106]. Such forces may include through-fault winding stresses (hoop stress and compression stress).

3.2.6 Ageing Of Cellulose (Paper / Pressboard)

The paper used in transformer insulation is made from the Kraft process and has a matted brown appearance. The thickness of paper used varies and several layers are wrapped around each conductor to insulate each turn from the next.

The Kraft process was developed by the German chemist, Carl F. Dahl in 1884. The natural moisture content of the paper is quite high and is much higher than permitted in transformer applications and so the insulation paper used in a transformer has to be dried which can take some days and during the process the DP of the cellulose is reduced. The pattern of cellulose deterioration is important for the prediction of insulation life and is generally monitored by the change of DP of the paper, which can be estimated from measurement of the viscosity of the paper when in solution [106].

Paper deteriorates inside the transformer and it degrades slowly as the polymer chains break down during service, releasing degradation products into the oil. The paper further degrades and loses all its mechanical strength and becomes brittle and susceptible to mechanical damage. The brittle paper may break away from the windings and cause overheating [83, 107].

Continuous on-line monitoring of the transformer oil temperature along with a thermal model of the transformer which can allow estimation of winding temperature can be used to estimate the loss of life of the transformer insulation due to overheating [74].

The temperature of the insulation directly influences the rate of ageing. Significant thermal cycling during the life of a transformer causes increased ageing of the cellulose material. During this process thermal expansion and contraction of windings and other solid parts and paper and oil cause an exchange of % moisture between the paper and oil. Since the oil can only hold a fraction of the water that paper can holds, the moisture content in the oil will be much smaller than in the paper. This will cause enhanced deterioration and ageing of the paper.

It appears that only a very small part of the water in the insulating paper can move into the oil. The process depends, once again, on the temperature. Warm oil can hold more moisture than the cold oil. Ageing adds moisture to the initial value and knowing its quantity allows a more exact interpretation of the ageing process. While the paper moisture content shows the state of ageing of the insulation, the moisture content in oil is more an indicator of the actual insulating strength of the system [39].

Ageing of cellulose material has an obvious effect on the thickness of material used for pressboard (chocks) under winding clamping pressure. The effect of ageing is more pronounced owing to the dual effect of temperature and pressure causing material decomposition due to degradation of the cellulose [36, 108].

3.2.7 Ageing Of Transformer Oil

Transformer oil is refined from crude oil and the choice of crude oil and refining technique forms the basis for final product. Normal transformer insulating oil can be classified as either paraffinic or naphthenic. Paraffinic oil has poor low temperature properties and low solvent power for oxidation products, leading to sludge. These properties of paraffinic oil can lead to precipitation of sludge on the winding paper and can cause blockages in the ducts.

On the other hand, oil oxidation products are soluble when they occur in naphthenic oil. The resistance of oil to oxidation is a crucial factor in its service life and it depends on the presence of antioxidants. Some oil will contain these naturally and the refining processes, typically hydrogenation, can enhance them. Oil that is deficient in natural antioxidants can be improved by the addition of oxidation inhibitor [33].

The main constituents of the crude oil contain carbon and hydrogen, small amount of compounds of sulphur, nitrogen, oxygen and water. Small traces of some metals and other elements can also be present in crude oil [33].

The refined transformer oil contains mainly saturated hydrocarbons, non-hydrocarbons and some aromatic oil content. The aromatic groups are organic compounds containing benzene type ring structures of carbon atoms, usually unsaturated, such as naphthalene, anthracene, acenaphthylene, etc. [33]. The ageing mechanism of oil is complicated as oxygen reacts with hydrocarbons and the acids are produced by oxidation. Oxidation in the presence of certain catalysts is responsible for oil ageing [109-110].

The role of insulating oil is not only to aid the heat dissipation but also to provide better electrical insulation by the displacement of air between the conductor windings and the metal housing. The ageing of transformer oil is detected due to presence of certain polar compounds. There are number of methods available to check the ageing of transformer oil in the laboratory. Some common ageing methods used to predict the service life of the transformer oils are discussed briefly below.

3.2.7.1 Oxygen Absorption Methods

There are many methods used to measure the rate of air or oxygen absorption during oil ageing. The basic technique used in outlined in reference [37] and involves filling the reaction vessel, containing a known amount of test oil, with dry air. The pressure drop in the reaction vessel as the oxidation of the oil takes place is measured by a mercury manometer. The parameter recorded usually is the time taken to deplete a fixed volume of oxygen as indicated by the pressure on the manometer. Catalysts such as solid copper wire or copper naphthenate solution may be added to the oil sample if required. When the samples of oils of similar weight are aged in a constant temperature bath, a comparative analysis of the time duration taken to consume a certain quantity of the gas will indicate the oxidation stability of the samples. The simplicity of this type of method is its advantage, but the accuracy of results with certain types of oils is a problem [33].

3.2.7.2 Double Sludge-Free Life Test And Power Factor Valued Oxidation Test

This is the method developed by the Doble Engineering Company to assess the quality of transformer oils. Very well known tests by Baker, Griffin and Oliver [109] are the

‘**Power factor value oxidation tests**’ and ‘**Sludge free tests**’ used by the power utilities for many years [109].

The apparatus used and described in [109] consists of a reaction cell, made from a glass tube, and constructed as a coaxial capacitor with the oil forming the dielectric medium. Dry air is bubbled into the cell which is held in a temperature controlled oil bath by means of a glass tube. A coil of copper wire is attached to the bottom of the cell as an oxidation catalyst. The power factor measurement tracks the changes in the power factor (dielectric dissipation factor or tanδ) of the oil during ageing. The sample of oil can be drawn into a small glass container using a pipette to be analysed chemically and mixed with n-pentene solvent. The mixture is kept in a cool and dark place for a day for monitoring sludge formation and determining the sludge free time, the time from the start to the time of collection of sludge. The satisfactory nature of the transformer oil is decided by plotting a graph of power factor versus time and comparing this with a standard limit curve [109].

3.2.7.3 International Standard Methods

The recognised international methods are described in Australian Standard AS-1767 (1975) for transformer oil ageing. This Standard covers the oxidation test, appearance, characteristics, methods of sampling, flash-point determination, viscosity determination, pour point, electric strength measurement and tests for initial acidity, corrosive sulphur, water contents, density, tanδ and resistivity of the oil sample.

The American Society of Testing and Materials (ASTM) have two standard methods for testing the oxidation stability of the oil. The sludge and acid levels test for uninhibited oil are laid down in ASTM D-2440 (1993) and in extremely accelerated ageing conditions the induction period of oxidation inhibitors such as ditertiary-butyl-para-cresol (DBPC) are laid down in ASTM D-2112. The test in ASTM D-2112 is carried out in severe environmental conditions to simulation of such operating conditions.

The International Electrotechnical Commission (IEC) Standards for evaluating the oxidation stability of transformer oils are detailed in IEC-1125 (1992). The Institute of petroleum (IP) offers 3 methods applicable for evaluating the oxidation stability of transformer oils they are found in IP-306 (1982), IP-307 (1980) and IP-335 (1980).

The International Organisation for Standardisation (ISO) has standard ISO-4263 for mineral oil used in low voltage power transformer. The other often used national standards include British Standards-BS EN 61125 [33].

3.3 Transformer Ageing by Temperature

The bounds of technical limitations for cellulosic materials have been extended by chemical and physical modifications during the manufacturing process. One of the principal limitations is the maximum temperature that the insulation system can tolerate while still providing an acceptable life. If it is necessary to operate above these temperatures for prolonged periods of time, the user must have a concern for the effect on the life of the insulation system. In term of ageing effects, mineral oil is more tolerant at elevated temperature than cellulose. Even if service conditions thermally degrade the oil, it can be removed and reconditioned [109]. Paper cannot be so reconditioned.

The thermal ageing of power transformer insulation is also accelerated by metal catalysts. During the ageing process the large molecule chain of the paper fibre is split and the DP is reduced, and accompanied by the decomposition of paper fibres, some harmful gasses are emitted into the oil. The impure oil impregnates the paper fibres which further aggravates the ageing. The sludge formed, which is a split product of fibre molecules particles of oil, can be deposited on the winding surface. The oil viscosity is increased, thus reducing the transfer of heat by the oil and resulting in increased temperature rise. This temperature rise can result in acceleration of the thermal ageing of the oil-impregnated paper insulation [110].

As noted previously, the moisture in the solid and liquid insulation of transformers in various forms deteriorates the electrical and mechanical strengths. The rule of thumb is that the mechanical life of the insulation is reduced by half for each doubling in water content and the rate of thermal deterioration of the paper is proportional to its water content [66]. Bubble formation, free water formation and static charge relaxation at the interface are associated detrimental effects due to moisture movement at high temperature [66].

Liquid filled transformer failures are frequently related to the thermal degradation of the solid insulation. The parts involved in these failures are generally, the paper insulating the conductors and the pressboard separating the layers of the coil. Paper close to the hottest-spot region has ageing accelerated beyond that which occurs at the average winding temperature [112].

Gas and water evolved by chemical action in oil, cellulose and at the conductor surface can be absorbed more readily in hot mineral oil until the point of saturation is reached. As a result, at high temperature the water absorbed in the oil may vaporise in the form of bubbles. The insulation may also be at risk as it cools after an overload since a heavy gas absorption in the oil will then be released in form of bubbles [113].

The electrical properties of an aged insulating paper are not changed significantly but mechanical properties are reduced tremendously during the ageing process [7]. Winding temperature may increase as a result during normal operation of transformers. This increase of temperature can cause cleavage of cellulose chains in the paper over a period of time. As a result, the mechanical strength of the paper is further reduced with time which can have an adverse effect on the performance of the insulation [114].

The state of insulating oil in a transformer can be directly evaluated because it is easily accessible for sampling. The same is not true for insulating paper for which the condition must be evaluated using an indirect method. This indirect method uses the furan levels produced by paper decomposition.

There are six furan derivatives that are dominantly present. They are: 2-furioc acid, 2-furfuryl alcohol, 5-hydroxymethyl-2furaldehyde, 2-furaldehyde, 2-acetyl furan and 5-methyl-2-furaldehyde [88]. Four amongst these six are useful for insulation monitoring.

These are 2-furioc acid, 2-furaldehyde, 2-acetyl furan and 5-methyl-2-furaldehyde [88]. These compounds are soluble in the insulating oil and can be measured [7].

The experience accumulated over years indicates that where transformer failure can be related to insulation faults, the primary cause of failure are due to paper ageing and consequently mechanical failure of the insulating paper, which in turn lead to electrical breakdown [115-121].

The evaluation of both oil and paper insulation strength are frequently used as diagnostic factors to determine end of life of transformer. Humidity in some cases has been recognised as a cause of variation in the properties of electrical insulation and cause of several types of insulation failure under electric stress. The absorption of moisture by solid insulation has a gradual effect of increasing dielectric loss, reducing insulation resistance and can contribute to a change in electric strength. Short time exposure to either very low or very high temperatures may be used as a diagnostic factor. In some cases it may be desirable to change the temperature rapidly so as to introduce a thermal shock, which is characteristic of service conditions [119].

An artificial version of paper insulation material, which is gaining attention, is "Nomex". Nomex is basically a particular commercial form synthetic paper made from polymide and has the advantage of a significantly higher temperature withstand than natural cellulose paper. Production of Nomex is complex and costly compared with cellulose insulation. However Nomex board possesses long term temperature stability, low dielectric constant in oil, no thermal degradation, is inherently non-flammable and exhibits excellent dielectric properties under oil [110]. Its primary disadvantage is its cost.

3.4 Bubble Formation and Transformer Ageing

For a bubble to form and grow within a liquid, the gas within the bubble must develop an internal pressure sufficient to overcome the external forces constraining it. The constraining forces are: (i) the interfacial tension force of the liquid, (ii) the gravitational force resulting from the column of liquid above the bubble and (iii) the force of atmospheric pressure acting on the surface of the liquid [122].

The formation of a bubble within the mineral oil involves gravitational and atmospheric forces and internal forces in the bubble. The source of gas pressure within the liquid, which tends to form a potential bubble, is the summation of partial pressures exerted by the various gases dissolved in the liquid. The principal gases found dissolved within the mineral oil of a transformer are nitrogen, oxygen, carbon dioxide and carbon monoxide. Some other hydrocarbon gases can also be present as a result of oil or cellulose decomposition due to partial discharges and sparking [122-125].

The insulation can also be at risk as the transformer cools after an overload since a heavy gas absorption in the oil will then be released as bubbles. The viscosity and density affect the rate of flow of the insulant through ducts and high voltage parts. The rate of flow of liquid affects electrical strength, assisting it through the breaking of fibre bridges and the dispersal of developing discharges but reducing it if streams of bubbles are carried into highly stressed regions as might happen at very high temperature breakdown can be facilitated [123].

In overload situations water vapour is more destructive because it can act as the root cause of failure if it produces bubbles. Water vapour is released from the surface of the cellulose insulation when it overheats under overload conditions. The released vapour adds to the internal pressure of the developing bubbles, thus increasing the bubbles' chances of growing and being released in a stream. Bubble evolution indicates that the relationship between moisture in the cellulose insulation and temperature are the predominant factors. Lower moisture content in paper lessens the chances of bubble formation [122].

The bubble evolution temperature is influenced by three variables: water content of the paper, gas content of the oil and total pressure. There are many cavities on the insulation paper filled with water vapour and dissolved gases. During overload the temperature of paper and of the cavity increases rapidly, and the cavity will expand at the same time getting more water from the paper driven out by the overload temperature. Finally the cavity would be large enough and the energy sufficient to release a free bubble [123].

Bubbles represent a potential dielectric problem in transformers in that, as a gas with unity relative permittivity, they will have a higher electric field stress in the bubble and, with a lower breakdown strength than the oil, partial discharge activity is promoted and the high temperature effects of PD activity can lead to increased rates of degradation of both the oil and the paper and thus reduce transformer life.

It is this aspect of transformer behaviour, bubble formation under such thermal shock conditions with moisture present, that the work described in this thesis is concentrated on.

3.5 Moisture in Transformer and Ageing

The migration of a small amount of moisture has also been associated with flow electrification at paper/oil interfaces. As water in transformer oil also brings risk of bubble formation, moisture presence in paper and oil systems has been a critical factor in transformer life and investigations into its effects began in the 1920s [125, 126].

Apart from being absorbed in the paper, water can exist in the transformer in three states. It is mostly found in the dissolved state in the oil. It can also exist as free water which is tightly bound to oil molecules when the dissolved moisture level in the oil exceeds the saturation level. Free water is also normally found at the bottom of the transformer tank. The capacity of moisture that the oil can hold is a function of the oil pressure and temperature [127-129].

It is difficult to ensure complete freedom of the transformer insulation from moisture under the various conditions of service. As moisture and oxygen are soluble in mineral oil it will absorb moisture and oxygen from the atmosphere at a rate dependent upon oil quality and temperature and can therefore become a medium for the transfer of moisture and oxygen from the atmosphere to the oil impregnated paper and pressboard materials.

Cellulose has great affinity for moisture, due to the presence of hydroxyl structure present in it. The moisture content is held in layers between the cellulose molecular chains [78].

Oil itself can also oxidise at elevated temperatures forming acids. Moisture and acid at high temperature levels cause scission of the glycosidic bonds in the cellulose chain. The scission of the glycosidic bonds reduces the degree of polymerisation and tensile strength of the cellulose. Most service-aged transformers fail in the lower part of the windings, which is the area where moisture concentration is highest. It is also an area of high electrical stress.

Drying of transformers can be an expensive process. However, it is much less expensive to perform a dryout than to allow transformer insulation to degrade faster than is normal as this substantially shortens transformer life. During heating and cooling in service, moisture will migrate back and forth between the cellulose and transformer oil. Due to the very low solubility of moisture in oil compared to paper, the oil will be supersaturated near the paper surface as the temperature increases, and this will result in water droplets and bubble formation and the attendant insulation damage that they will cause [78, 138].

3.6 Cavities in Transformer and Ageing

The process of oil-impregnation of the paper in transformers takes several days. The process of impregnation and the quality of the treatment during this time can have an impact on the electrical properties of the insulation under extreme conditions. An inadequate impregnation process may affect the insulation condition during operation.

As pressboard is formed from layers of paper, cavities may be formed during the production process, when the laminated material is moulded into its final shape. The application of such material as solid insulation for transformers may thus lead to extensive PD activity in the cavities if they are not completely filled with oil during the impregnation. A very rapid or insufficient impregnation will reduce the vacuum level, leading to residual gases which remain inside the cavities. These gases will, in most cases, not be dissolved in oil thus resulting in partial discharges and an accelerated deterioration of the solid insulation reducing lifetime of a transformer [39].

Overloading of transformers can raise the temperature of the paper and of the cavity rapidly. Such a sudden rise in temperature can expand the cavity, and simultaneously expel more water from the paper by the expansion due to the high temperature. Eventually, the cavity would become large enough and the thermal energy sufficient to release a free gas bubble. These phenomena can cause and accelerate transformer ageing and in the worst case lead to failure [123].

3.7 Apparatus for Measurement of Ageing

The test apparatus used in the laboratory work of this project to investigate electrical, and combined electrical and thermal ageing in transformer insulation has been previously described in detail in [39] which reported on results of investigations of transformer pressboard ageing. The test equipment consisted essentially of cylindrical vessels made of glass and nickel plated steel fittings. The operating temperature of the apparatus is designed to reach up to 135°C or higher. The vessels contains a heating plate at its base and hold 20 dm^3 of oil which is degassed at the beginning of the ageing procedure and the air in contact with the oil is almost free of moisture in the initial stage of investigations.

The solid pressboard samples have a volume of 0.1 dm^3 and are held between the flat plane electrode system which will provide effectively a uniform field of magnitude similar to that typically used in transformer applications. The measurement of dielectric loss factor and PD activity of the oil impregnated solid is able to be performed using leads incorporated in the chamber. Thus it can be done without opening the vessel or to remove the sample because of the test electrode in the shielding arrangement. The loss factor was measured at 1,000 volts, 50 hertz and at the relevant ageing temperature.

The test vessel used for the ageing measurements under combined electrical and thermal stress is shown in Figure 3-1.

The users of power transformers are interested in more detailed information about the insulation reliability and in particular about possible degradation of the electrical insulation of the equipment in service, as replacement or repair of power transformers can lead to enormous costs [63].

The research investigations described in this thesis used a generally similar insulation model chamber to investigate such ageing effects under conditions of high temperature and moisture. The experimental equipment used will be described in detail in a later chapter.

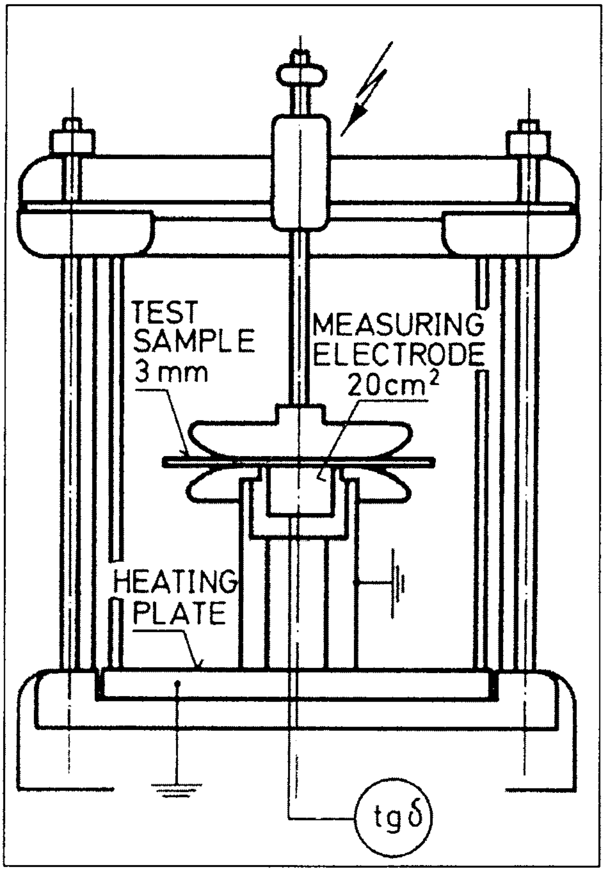

Figure 3-1. Test Vessel for Ageing Investigations under Combined Electrical and Thermal Stress [39]

3.8 Remnant Life of the Transformer

The life expectancy of a transformer is in part determined by the rate at which its electrical insulation is degraded under operating conditions. The external ambient and loading factors which influence the life of a transformer are the ambient temperature, humidity, magnitude of load, duration of loading, and the thermal conductivity of the transformer components [140].

Transformer loss of life refers to the reduction in life of a transformer due to a particular set of long term ambient temperature and load conditions. The loading of a transformer is governed by rules, relating to insulating temperature rise, which are derived by analysing the change with time of the chemical characteristics of insulating materials under the strong influence of heat and other degrading agents. These processes often interact with each other so that, for example, the products of decomposition of paper may then affect the deterioration of the oil.

Efforts to quantify the effect of temperature on insulation materials were based on a chemical reaction model using the Dakin approach (based on the Arrhenius reaction rate theory) which states that the chemical reaction rates, and hence deterioration rates, are exponentially dependent on temperature. By regarding ageing as a chemical process, a typical statement of the relationship between the useful lifetime of an insulation material and its long term operating temperature is represented as:

$$\text{Log (lifetime)} = A + (B / T)$$

Where A and B are empirical constants which are material dependent and T is operating temperature in absolute temperature units (Kelvins) [82].

A similar formula proposed previously by Montsinger is;

$$\text{Log (lifetime)} = C / \theta$$

Where C is an empirical constant of the material and θ is the operating temperature in degrees Celsius.

The values of the material constants A, B and C mentioned above are determined from test measurements on the relevant materials [82].

According to this formula the rate of ageing doubles for every 6 degree increase in the temperature of insulation. The Montsinger relationship forms the basis of many of the loading guides in general use. It is based on studies which equate life with the time taken for the tensile strength of paper to fall to half its initial value [82, 116].

In power transformers when moisture is present in uneven distribution it will tend to accumulate at the deepest point of the tank. The reason for the accumulation is that the specific density of the moisture is higher than that of the oil.

In the cold climate as the temperature reaches below the freezing point of water, the ice will float in the uppermost layers of the oil due to its lesser density. When the ice melts, the resulting water may invade regions of high field strength, causing a considerable reduction in dielectric field strength leading to the failure and breakdown of the dielectric strength of insulation [113].

Gases present in the oil may also reduce the dielectric strength of the oil. The dielectric strength of oil saturated with gas is not much lower than that of oil which is free of dissolved gas.

If the oil goes through a change of state, this can lead to some of the dissolved gas being released thus reducing the dielectric strength of the oil-gas combination because of the effect of the bubbles of gas and their PD activity. Gases present in the oil may also affect the life of oil. Air or oxygen present in the oil give rise to chemical changes which may bring about permanent deterioration of electrical properties of the oil and its ageing. In addition, these gases will promote the ageing of cellulose-based materials surrounded by the oil [33].

The properties of paper deteriorate under the effects of heat, water and oxygen. Ageing of paper causes a deterioration of mechanical properties through the reduction in degree of polymerisation value. As long as the paper retains its mechanical strength and does not carbonise and break up into pieces, it may remain electrically satisfactory. The ageing process is accelerated by both moisture and oxygen [83].

The dielectric strength of laminated paper such as pressboard impregnated with oil is considerably better than either of the individual component parts i.e. the paper or the oil. When combined together the role of the paper is to partition the oil into small gaps, and thus increase the dielectric strength of the composite material.

Both moisture content and ageing influence the properties of oil-paper insulation. If perfect degasification of paper is not achieved gas bubbles and voids will remain in the insulation. The gas bubbles will cause the dielectric strength of the paper to decrease, resulting in a higher electric stress in the voids. Gas bubbles are also developed under the effect of high field strength, from any moisture present in the paper [139-140].

The remnant life of the transformer is best explained by evaluating the condition of its components, especially those which have a role to play in the condition of insulation. The changes that occur from the working of transformers with the passage of time due to different stresses are described as ageing. Various insulation monitoring techniques applied to aged oil/paper composites are used to assess, in so far as it is possible, the remaining life of the transformer.

The life of a transformer can be extended by timely maintenance as a result of condition monitoring techniques. The well-known 'bath tub' curve shown below explains how effective condition monitoring based maintenance can prolong the life of transformers and increase the reliability of a population [63].

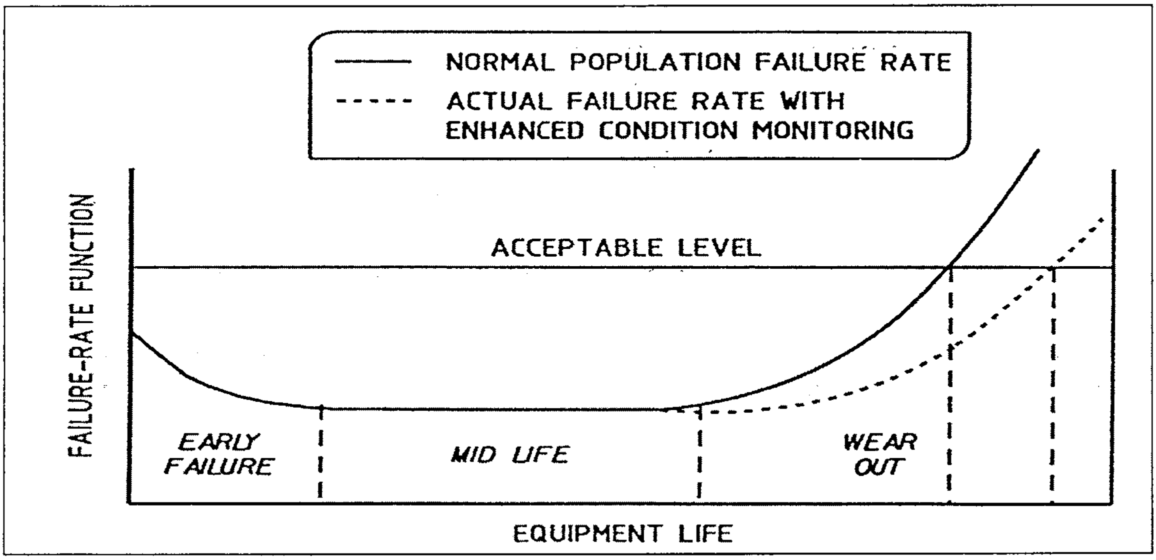

Figure 3-2: Bath Tub Failure Rate Curve [63]

The remnant life of transformers is calculated on the basis of a probabilistic approach after evaluation of the insulation condition. The presence of carbon monoxide and carbon dioxide, furans in the oil and PD activity in the paper provide data which makes it possible to obtain some rough estimate of the remaining life of a transformer. The following equations can help us to estimate remnant life of a transformer.

3.8.1 Montsinger Relationship

The relationship showing remnant life of the insulation at different temperatures can be given by following expression.

$$\text{Life} = a.e^{-b\theta}$$

Where θ denotes temperature in degree Celsius and "a", "b" are coefficients dependent on the material [82].

3.8.2 Arrhenius Law

The Arrhenius law is expressed as;

$$\text{Life} = e^{(A + B/T)}$$

Where A and B are positive coefficient and T is the temperature in degree Kelvin [82].

The results obtained by the Arrhenius law approach are more accurate as compared to the Montsinger relationship. The values obtained from the above two expressions give almost the same deterioration rate in a temperature range of 80 - 140°C.

3.8.3 Arrhennius-Dakin Formula

A classical method of calculating the remaining life of a transformer has been the Arrhenius Law;

$$\text{Remaining life} = Ae^{B/T}$$

Where A is the initial life, B is the constant depending on the properties of the material studied and T is the absolute temperature in degree Kelvin [74]

3.9 Failure and Reliability of the Transformer

The useful life period of a power transformer life cycle begins with its commission into service. Power transformers have one of the lowest breakdown rates of all electrical equipment but the effect of temperature during service is presently considered to be the key factor in the failures that do occur [141]. The overloading of transformers beyond nameplate rating can contribute to this increase in their failure rate. Therefore, as a result, temperature reduces transformer useful life and also affects its reliability.

Failure rate and reliability are related in the following way;

$$R = \exp(-\lambda t)$$

Where t is times in years, λ is the failure rate per transformer years in service, and R is the transformer reliability [141].

The ageing behaviour of oil-impregnated insulation is determined mainly by the thermal condition inside the transformer, especially the hot spot temperature. International standards state that the hot spot temperature can be estimated on the basis of the top oil temperature under consideration of the load and the winding temperature rise. However the closer the temperature measurement is carried out to the winding, the more accurate will be the approximation of the measured temperature to the actual hot spot temperature [119-121].

Recently, fibre optic sensor monitoring systems for point measurements and for distributed measurements along the winding conductor length have been tested for application inside large power transformers. The accuracy available is sufficient for online monitoring [142].

End of life of a transformer may be dictated by any one factor or by a combination of factors. Much attention has been given to paper ageing, as it is undoubtedly a factor in reducing life leading to failure of insulation. Determining the probable life of operating transformers that have reached the end stage of their service life is complex and there is no single scientific method available to determine the condition or end-of-life of an operating transformer. Experienced engineers, chemists and technicians are required to conduct analysis, tests, visual inspections and review of historical data to help form the decision about the probable condition of transformer [34]. In order to delay ageing of insulation material used in oil-impregnated power transformer, all insulating material should possess outstanding electrical, thermal, environmental and mechanical characteristics, to withstand high electrical stress and thermal loading even after years of service [37, 143].

3.10 Partial Discharges and Transformer Ageing

Partial discharges damage the insulation by heating the surface of insulation. The gas discharge and its high temperature cause significant ionisation level in the voids. The high temperature and the ions in the discharge will interact with the walls of the voids and will cause carbonisation and similar damage to the solid insulation material. The heating and interaction of ions with insulation can cause chemical change and ageing and make the insulation erode away as well as degrading to conducting carbon. This can also cause stress cracking and tiny crazes may appear at the surface of the material. Ultra-violet light transmitted by discharges can also cause damage to the dielectric and further promote the stress-cracking [37].

The deterioration caused by partial discharges in cavities (formed mostly due to improper impregnation) follows several stages. In the first stage, the dielectric surface is attacked; in the second stage, preferential areas are formed where the deterioration is far more severe than at other places. And in the last stage, one of these preferential areas develops into a deep pit. The discharges are then concentrated at the pit, making it further erode, and the dielectric material degrades so much by molecular scissions that the breakdown strength falls below the applied field strength and electrical treeing is then initiated.

This treeing then causes carbonised tracking paths on the dielectric surface and can ultimately result in full and complete breakdown. The initial phase during which the dielectric surface is attacked can take several years at operating stresses. The final stage, which includes treeing and breakdown can be very short and can take minutes to some hours [143].

Deterioration by surface discharges follows the same lines as in cavities but, because of the larger surface available, the effect tends to be less severe and larger discharge magnitude is allowable without the same degradation [37]. Internal and surface discharges are known to cause deterioration to the dielectrics by several means. Firstly, by heating the dielectric boundary: secondly, by causing charges to be trapped on the surface: thirdly, by ultraviolet radiation from the discharge and, finally, by formation of chemicals such as nitric acid and ozone by the discharge activity. These discharges can also cause de-polymerisation, stress cracking and gassing leading to erosion of the dielectric surface [143].

In oil-impregnated insulation discharges in voids adjacent to the conductor attack the insulation and, after some time penetrate the first paper layer. Surface discharges can then occur along the layers after penetrating the first paper layer and so electrical trees or carbonised tracks are formed longitudinally between paper layers. These tracks follow the weakest points in the insulation, which is along the tangential path along the paper layers. At the foot of the electrical tree local overheating takes place, which results ultimately in thermal breakdown of the insulation. If breakdown has taken a long time, such as with the development to breakdown at operating voltage, these trees and carbonised track can quite long lengths [37].

Deterioration by surface discharges follows a similar pattern as for internal discharges between layers. As surface discharges are easier to study than internal ones, they are often used to compare the discharge resistance of different materials. Usually the time to break down is taken as a measure. Deterioration by corona discharges (PDs in air only) usually occur around bare conductors, they cannot attack insulation in the same way as internal and surface partial discharges. Only indirect action by ozone formed by the corona discharge may deteriorate neighbouring dielectric surfaces [143].

Harmful discharges can be distinguished with the help of the partial discharge patterns. Internal discharges and their presence or absence is a crucial consideration for the life of the insulation. The discharges in oil-impregnated transformer can occur due to, insufficient drying of the insulation, imperfect impregnation of the oil-impregnated insulation, presence of dirt or other foreign particles and ageing of insulation during operation [143-145]. By using the characteristics of the PD patterns it is possible to determine the effect of the PD activity (magnitude and number) in terms of the insulation condition at the time of PD monitoring.

Chapter 4

Partial Discharge Measurements and Analysis

4.1 Partial Discharge Basics

The study of partial discharge (PD) measurement and location in oil-impregnated power transformer can be tracked back to the early 1940's, when this test was known as the hissing test [146]. PDs are defined as localised electrical discharges that only partially bridge the insulation between conductors and which may or may not occur adjacent to a conductor [147]. The discharge may result from gas ionisation (a process that produces positive or negative ions and electrons from neutral atoms or molecules) causing an electron avalanche (cumulative ionisation in gases, liquid or voids in solid insulation caused by collision between field-accelerated electrons and neutral atoms or molecules). The movement of electrical charges through an insulating medium initiated by electron avalanches can be maintained by various secondary processes that generate further avalanches causing an electrical discharge [148].

The discharge may result from ionisation in gases, in cavities in solid insulation, in gas bubbles, in insulating liquids, or along dielectric interface surfaces. Between the partial discharge and one or both of the electrodes some sound dielectric is still present in the shape of a solid, liquid, or gaseous insulator barrier to full breakdown: hence the breakdown is only partial. The current magnitude of such discharges is very small; but they can cause progressive deterioration and ultimate failure [143].

Because of their ionisation processes in their interaction with solids, PDs have a significant effect on the life of insulation in high voltage (HV) equipment. Every discharge event may deteriorate the insulation material by the energy impact of high energy electrons or accelerated ions causing many types of chemical transformations. The primary cause of the chemical change is the scission of the chemical bonds of the insulation material by the high energy electrons and ions of the discharge. A major result of this interaction is the formation of free carbon. An eventual breakdown of insulation of HV equipment while in service may result, causing considerable damage to the equipment and to the system to which it is connected. The technique of measuring and analysing PDs occurring in insulation structures or assemblies can thus be used to detect weaknesses before they lead to catastrophic failure [149].

The detection of PDs is based on direct or indirect monitoring of the energy exchange processes which takes place during the interaction of the discharge with the (usually) solid material. The exchanges are manifested as any of the following:

- electrical impulse currents or electromagnetic radiation (VHF, UHF and light),
- pressure pulses (ultrasonic waves),
- chemical reaction
- gas generation from oil.

Discharge detection and measurement techniques may be based on the observation of any of the above phenomena. As to locating PDs in high voltage equipment, the techniques fall mainly into two areas: electrical and acoustic. Despite the fact that the acoustic location method is important in some transformer and cable applications, the more frequently used, and in most cases, the most successful detection methods for transformer applications are electrical PD monitors [143].

4.2 Partial Discharges in the Transformer

Partial Discharges in a transformer may be a result of improper construction or they can appear during service as a result of ageing processes or contamination in the oil-impregnated transformer insulation. The PDs in a transformer are mainly generated due to sources such as voids or cavities in the solid insulation, surface tracking, gas bubbles in oil and floating metallic particles in the oil. Internal discharges occur in cavities in a dielectric, surface discharge along an insulator, and corona discharges along a sharp edge. In transformers, an obvious source of these cavities arising is poor vacuum filling with oil of the cellulose, which results in air being trapped in the major insulation between the windings.

Discharges in a transformer can arise at the voids in the insulation, at the boundary layer between the oil and paper, in contaminated insulating material, in over-stressed joints in the insulation subjected to excessive electrical fields and in parts not under high voltage but capacitively coupled and poorly earthed. PD activity normally originates either in gas-filled voids within the dielectric or at interfaces between different materials where the electrical stress can have tangential or surface components which are potentially the most difficult to sustain by insulation or at contaminated sites that do not have good adhesion with the base insulation. PDs also occur inside electrical trees that are initiated at electrical stress enhancements caused by interfacial protrusions or contamination within the dielectric [143, 150-151].

PD detection is thus an important means of testing the reliability of HV apparatus because PD measurement provides information on the quality of insulation systems. The wide acceptance of using non-destructive PD testing to assess the condition of insulation system has instigated the development of advanced PD analyser systems. The accompanying developments in fast data acquisition systems and advances in computer based measuring techniques has made it possible to store a large amount of PD Data with very high sampling rates to measure very high frequency PD signals [26, 152].

The PD is not a complete insulation failure but is indicative of local insulation damage present with high electric stress and a certain amount of ionisation or charge transport underway somewhere in the insulation. An increased magnitude and rate of the PD activity can result in the dielectric breakdown of the electrical insulation and the ultimate failure of the power equipment. Detecting PDs in the power equipment in the early stages and early rectification of the faulty insulation can help to prevent major loss and severe damage to the equipment. PD activity has the advantage over other diagnostics and that is an instantaneous monitor of the insulation condition at the time that the measurement is made. Most other techniques such as DDF and DGA provide only results that indicate cumulative effects of insulation damage. For example the detection of hydrogen and acetylene in transformer oil by dissolved gas analysis is a clear indication of arcing problems but it does not provide any information about where the fault is located and what the instantaneous fault severity is. [153-154].

Total insulation failure in equipment is generally preceded by intense PD activity. PDs at their inception are generally small magnitude and are apparently relatively insignificant. However they cause progressive degradation and eventually a total insulation failure. Detecting PDs would not only help to establish a quality control but also can help detect a change in the general quality of insulation, occurring due to overloading etc. Different forms of devices are used to detect the discharges for assessing strength of insulation. The sensitivity of the detection system must be high enough to satisfy the basic purpose of the test, which may be conducted in the presence of unavoidable electrical noise. Similarly the issue of calibration is of critical importance in PD measurements. Calibration is necessary to provide standard methods of interpretation of PD results and their intensity, both for future comparison on the same equipment and for comparison with other types of equipment. The discharge magnitude for PDs is given in units of pico-coulombs (pC) [155-157]. However there are cases such as in EM radiation coupling methods for PD sensors where calibration in pC terms is difficult. However some form of calibration or sensitivity check is necessary for PD monitoring so that trend analysis can be performed. Trend of PD activity over time is a primary means of identifying problems with insulation.

In PD measurement we are dealing with a small quantity of energy, as we measure the voltage amplitude of a discharge pulse or the amount of charge it dissipates. Alternatively the relationship can be expressed mathematically as $q = CV$, q being of the order of pico- coulombs and the capacitance (C) of the order of pico-farads or even less. This means that V can be of the order of few milli-volts before it is amplified. Consequently a PD is a typically a very limited energy phenomenon and a high sensitivity is required for the PDs detecting equipment because of the very low voltage level. The low voltage level also means that electrical interference is a major problem and can be a limiting factor in on-site tests.

It is desired that substantial importance should be given to the nature of the application, which may include PD tests on transformers for example, and the calibration required for measurement correction. While conducting PD measurements the background level of noise must be as low as possible because of the very low signal levels. However in the case of on-site application this is not always possible given the fact that corona discharges occur over a very wide range of the frequency spectrum. In order to suppress the electromagnetic noise and to get more information from the PD signal, The Rogowski coil with its non-magnetic core (and thus very high frequency response) is quite suitable for on-line PD monitoring in a transformer. The Rogowski coil is an air core coil with the coil cross-section arranged perpendicular to the magnetic flux lines of a current carrying conductor. It is very similar to a current transformer (CT) but without the magnetic core and the limitations that are imposed by that material [35, 158-161]. The problem is that the lack of the magnetic core reduces sensitivity of response.

As noted above there is always some electrical interference to be contended with during PD testing. The interference that is encountered while conducting on-line tests may be different to that which is encountered while conducting tests in the laboratory and thus must be addressed in a different way. The interference in the laboratory can include surges of various forms, electrical disturbances generated due to other electrical equipment operating at the same time in laboratory and the disturbances due to incandescent lights or fluorescent lights etc. Disturbances can also be caused due to switching operation in other circuits, commutating machines, high voltage testing in the vicinity, radio transmission and inherent noise of the measuring instrument itself.

The major source of interference in PD measurements performed in on-site applications is predominantly corona discharge [143], AM radio broadcasts, television, mobile radios, car ignition systems etc.

4.3 Types of Discharges

There are three types of partial discharges according to the usual classification method: these are (i) internal discharges, (ii) surface discharges and (iii) corona discharges. The first two of these in particular can damage and thus cause deterioration to the insulation where they occur and will eventually escalate with the result being a breakdown to the HV apparatus. The corona discharge occurs primarily in a gas and is usually not likely to cause damage to the insulation unless it is in a gas in a confined volume such as a GIS chamber where the chemical changes due to corona will accumulate. Each of the three types of discharge is briefly explained and discussed below.

4.3.1 Internal Discharges

The cavities and small cracks in otherwise homogeneous solid insulation cause internal discharges because of the stress enhancement that occurs in the gas inclusion in the void or crack. Often the voids are the result of the poor design or a defect in manufacturing process, such as inadequate curing of an epoxy casting. PDs also occur in local regions of high concentration of non-uniform electric field, particularly in gaseous and liquid dielectrics parts of the overall insulation. Within the areas of such local field stress weakness exists and PDs may commence at voltage levels (the PD inception voltage level-PDIV) below the normal operating voltage of the equipment insulation. The effect of these discharges is to deteriorate the insulation, imposing higher stresses upon it with a corresponding decrease in the insulation overall life expectancy.

The rate of decay of the insulation is a complex function of many variables including:

- the level of electric stress acting upon the insulation,
- the type of breakdown mechanism, i.e. thermal, chemical, electrical etc,
- the internal and external environment,
- the repetition rate of the discharges,
- the location of the PDs and the inception voltage.

Internal discharges in high voltage insulation arise in cavities where the field gradient of the gas in the cavity causes electric breakdown. These types of discharges are generally permanently injurious to insulation [26]. Figure 4-1 shows the typical internal discharge mechanism.

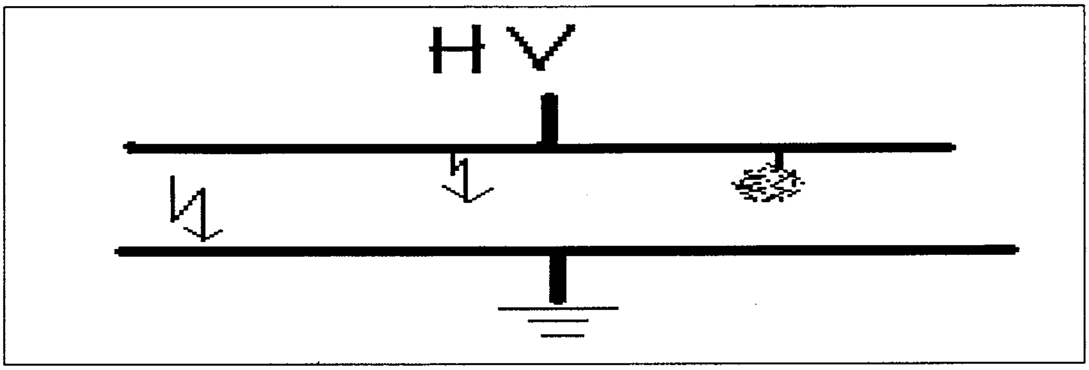

Figure 4-1: Internal Partial Discharges

Internal discharges normally occur on both parts of the voltage waveform (positive and negative half cycles). The study of the typical elliptical waveform display shows the amplitude and the number of discharges being substantially symmetrical on both sides of the waveform. However a variation of 3:1 in the magnitude is possible in such situations [37]. Normally a certain degree of random variation in amplitude or location is observed as well. PDs initiate at a particular voltage level and do not exist below a certain voltage level.

4.3.1.1 Partial Discharge Inception Voltage

The lowest voltage at which PDs above some stated magnitude occur as the applied voltage gradually increases from a value where no such discharges are observed is the PD inception voltage. Different test and sample parameters can affect PD inception voltage value and in some cases duplication may be difficult to achieve [143, 147].

4.3.1.2 Partial Discharge Extinction Voltage

The highest voltage at which PDs above some stated magnitude no longer occur as the applied voltage is gradually decreased from above the inception voltage is the PD extinction voltage level - PDEV. The test and sample parameters can affect this value and in some cases duplication of PDEV may be difficult to achieve. In the case of internal discharge there is little or no variation in magnitude of discharges as the voltage is increased. The discharge extinction voltage is generally lower than the discharge inception voltage, but may in some cases be about the same level [143, 147].

4.3.1.3 Discharges Occurring Below The Inception Voltage

Following the initiation of a discharge the discharge activity can persist for some time, even to the extent that a voltage lower than the inception voltage can sustain the discharge once initiated. The applied voltage over the cavity is then smaller than the inception voltage. This voltage and the residual charge in the cavity co-operate and the discharge can sometime persist at approximately half the inception voltage [37]. The extinction voltage is very often found in practice to be lower than inception voltage although not normally as low as half. This is the reason for samples being pre-stressed in many test procedures at 1.5 to 2 times the nominal voltage before being turned down to a test voltage [37, 147] to perform measurements.

4.3.2 Surface Discharges

Surface Discharge usually occur at the interface between two different dielectric materials. These may include solid-gas, solid-solid, solid liquid and liquid gas interfaces. This interface can cause a high discharge electric stress along the interface and initiate discharges. This will be particularly the case if the relative permittivities of the two materials are dissimilar. The discharge will then spread along the surface, perhaps following the shape of the ground plane very closely, until it reaches the ground electrode. Figure 4-2 shows the surface discharge mechanism.

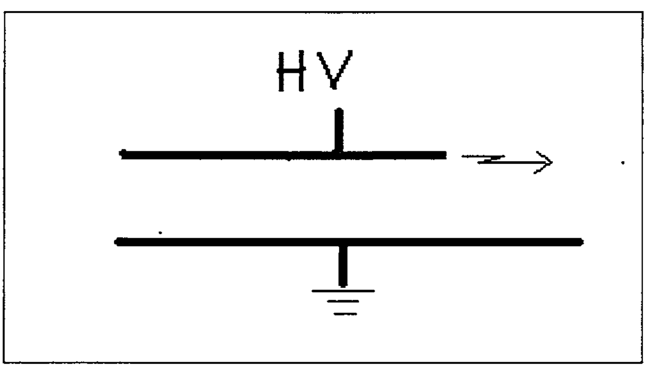

Figure 4-2: Surface Discharge

Surface discharges will occur if there is an electric stress component parallel to the dielectric surface. This applies to bushings, terminations of cables, the end sections of generator windings, and over a solid air surface with contamination on it. In the latter case it will be surface tracking. The discharges will damage the surface and affect the electric field, so that in general the discharges extend beyond the region where the original surface component of the electric field is high enough to cause discharges. Surface discharges occur along dielectric interfaces where substantial tangential field strength is present. The interface is either gas or liquid bounded. The discharges or an external dielectric surface which occur at areas of high tangential stress can be found to occur in a badly designed bushing which may result in an overstressed foil. A careful study of the external field and the configuration and the size of insulator will avoid flashover from the outer insulation. The whole point is to avoid the concentration of the electrical field at a particular site [35, 161].

4.3.3 Corona Discharges

Corona discharge occurs in a gas at the surface of a metal electrode at some high electric stress level. The result is ionization of the gas around the sharp edges of the HV electrodes. In general there is no permanent damage to the insulation if it is air, but if it is a contained gas such as SF6, some damage to the gas may accumulate. It is also possible for corona discharge to occur at floating metal items which are subject to the influence of an electric field from a high voltage conductor. The floating metal object may attain some high voltage due to capacitive coupling.

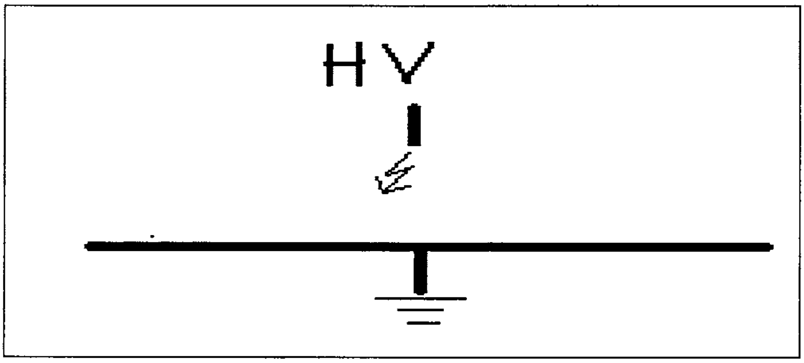

Figure 4-3: Corona Discharge

Figure 4-3 shows the corona discharge mechanism. Corona discharge appears with ac voltage generally during the negative half cycle of the voltage waveform only. They are usually found at the high voltage electrode, however they can sometimes occur at low voltage (even earthed) electrodes if the electric field at the surface is very non-uniform and is thus high enough to cause inception. Corona discharge from sharp edges such as isolator switch contacts in substations is a major source of electrical interference while conducting PD tests, so the test area should be as free of sharp pointed edges as possible [162-164].

4.3.3.1 Negative PD's

As a positive ion comes close to a point electrode it moves towards the electrode following the attraction of the electric field. The ion releases one or more electrons from collision with the electrode and as the process repeats a cloud of positive ions come near the point and the negative electrons travel away from the point. The electrons slow down at a greater distance from the point and attach themselves to the ionised molecules in air. These result in two regions of space charge, a positive space charge forms in the nearest vicinity of the point electrode by slow positive ions and at greater distance negative ions, which are formed by adhesion of the electrons to the oxygen (for example) and end up as a negative space charge. The entire process takes place at a distance of only about 0.1mm from the point and in a time of about two microseconds extinguishes [143, 163] for each individual discharge.

4.3.3.2 Positive Corona

The electron avalanche causes a distribution of space charge. As the electron disappears at a greater speed the slower positive ions end up shielding the point electrode from the electric field. The corona discharge stops as the positive ions have drifted away. Following this a new discharge starts. This process repeats itself quite regularly [143, 163].

4.3.3.3 Recurrence of Corona at ac Voltages

As the ac voltage slowly increases, the corona discharges occur at or near the negative peak of the voltage only, after the inception voltage level is exceeded. Oscilloscope displays are helpful for this case. At first only one discharge peak per cycle may be seen. A rapid increase in number of discharges results if the voltage increases even fractionally. They are generally equal in magnitude and their number increases linearly with the applied voltage. At higher voltages, impulses also appear on the positive half cycle. These are usually more irregular and are of larger size. When observed on an oscilloscope display, corona discharges can be easily distinguished from other discharges [37]. Typical traces of corona discharge due to a sharp point at the negative half cycle and internal discharge in a cavity at both positive and negative half cycle is shown in Figure 4-4 [26].

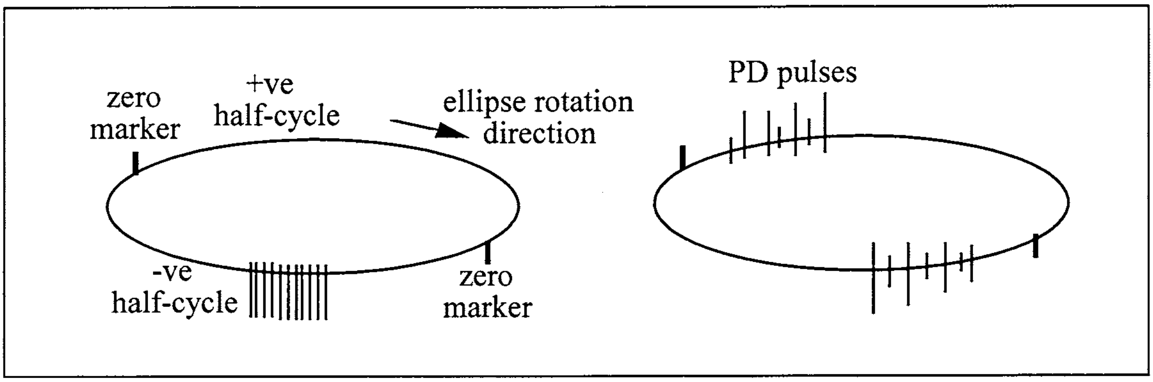

Figure 4-4: Corona Discharge and Internal Discharge in Air

Left pattern is Corona Discharge due to Sharp Point

Right pattern is Internal PDs in a Cavity

4.4 Partial Discharge Measurement

Partial discharge magnitude measured by the discharge detector in pico-coulombs is not equal to the actual charge transfer that occurs in a case of surface, internal or corona discharge. However it is a good representation of the intensity of the discharge as it is directly related to the energy (charge) dissipated in the volume of a discharge [37].

The basic circuit for discharge measurement includes a high voltage source, preferably free of discharges, a coupling capacitor (providing a closed circuit for the discharge displacement), an amplifier, a discharge detector and a discharge analyser. The sensitivity of a detection circuit is defined as the smallest discharge pulse that can just be distinguished from the background noise.

Before testing, the measurement system is calibrated using an external calibration source by injecting known quantities of a fast pulse discharge of charge. Calibration test source must be removed before high voltage can be applied and no calibration can be made during tests [147]. The basic PD measurement circuits specified in the IEC-60270 Standard and the basic PD measurement circuit used in the experiments using the CDA3 detector that was used in the experiments described here are shown in Figures 4-5 and 4-6 respectively [26].

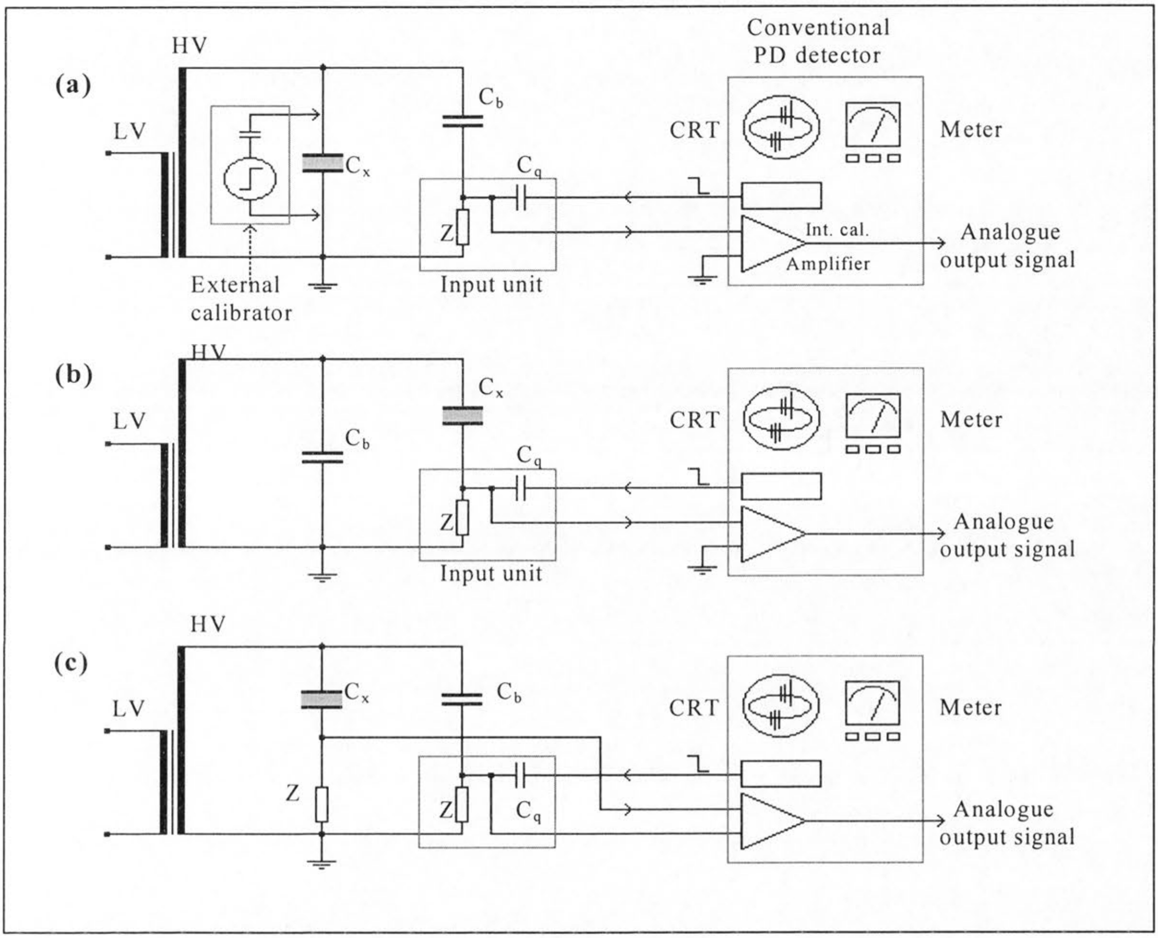

Figure 4-5: Basic Partial Discharge Measurement Circuits
As specified in IEC-60270 Standard

In Figure 4-6, Cs denotes the capacitance of the test sample. The capacitance C_b represents a HV discharge-free coupling (and blocking) capacitor. The analogue output signal of the conventional PD detector is connected to the input of the CDA3 circuit board, which then processes the PD signals digitally. The basic PD measurement circuit is explained in detail later in section 5.6.

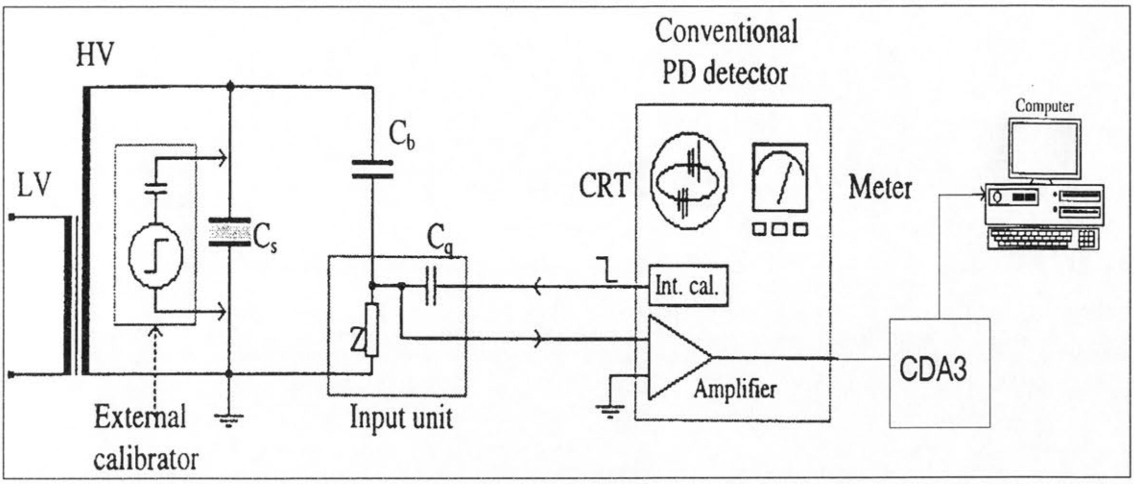

Figure 4-6. Basic Partial Discharge Measurement Circuit Using CDA3

Much progress has been made by developing and applying statistical techniques for the analysis of partial discharge patterns. These statistics are based on the basic magnitude vs. phase and Count vs. phase plots. The shape of these distributions is displayed on positive and negative half of the voltage cycle. The statistical analysis method assumes that these variations are Gaussian in shape: this is a substantial approximation, but one which yields very useful results in terms of correlation of PD characteristic patterns with insulation damage.

It has been found that these shapes are characteristic for the type of defect from which they originate. Each distribution is analysed by means of a number of statistical operators. Each defect for a dielectric model shows a typical combination of operators as a fingerprint. The observation of discharges with a statistical analyser is thus an effective means of distinguishing the discharge source type. The shape of the discharge pattern gives supplementary information for the distinction between internal, surface and corona discharges. In addition thickness and width of a detected cavity can be estimated using neural networks and can be made to determine extent of deterioration [26, 152].

4.5 Partial Discharge Location Tests

Basic indication of PD activity and also the location of the PD can be determined by acoustic methods using piezoelectric sensors. PDs generate pressure waves and sensors operating at acoustic frequencies of 100 to 300 kHz throughout the transformer tank can pick up the acoustic signals. The location of the PDs can be detected through the process of triangulation if sensors are located at a number of points around the tank and if the acoustic velocity and the internal structure of the transformer are known [5, 16]. In recent time PD acoustic testing has greatly improved by housing the transducers inside the transformer tank [165-166] to remove complications caused by the interaction with the tank wall.

The main component of the acoustic detection system is the transducer design which has to provide adequate sensitivity as well as reliability and ease of operation. Logically, to achieve maximum sensitivity, transducers should be placed inside the tank as close as possible to the source. Since the position of the source is unknown and the hardwired transducer cannot be installed safely and easily anywhere inside the electric field region in the tank, so external transducers are generally used. The pressure wave is transmitted to the transducer through the transformer tank wall. The wave thus reaches the sensing element on the wall (piezoelectric ceramic element). The piezoelectric ceramic element converts the pressure wave into an electrical signal which is displayed on an oscilloscope. The display shows the signal from the pressure wave emitted by the discharge after its travel through the transformer insulation (oil). This signal requires processing to provide information for enabling the location of the discharge [143, 167].

As the energy associated with PDs is very low, the resulting signal can be quite close to the background level and thus difficult to exploit. The signal ratio is increased by using an averaging device. The time interval between occurrence of the discharge indicated by the electrical signal at the terminal of the measuring impedance and the time of arrival of the pressure wave after travel through the ambient environment at velocity v, the distance is then calculated by formula: $d = vt$.

The instrument commonly used for measuring this transit time is the basic digital oscilloscope, which is normally triggered by signals from electrical PD detectors monitoring the discharges. The transit time of the acoustic pulses is able to be read directly from the screen as the difference between arrival times of the electrical and acoustic signals.

An iterative process is required to locate the source if a response can be detected on one transducer. A locating operation is generally performed in steps. The first step is to determine the section of the transformer where the source is located. The second step is to place the maximum number of transducers on the transformer wall near the predicted location and to record the responses and co-ordinates of the transducers in relation to the reference point. The operator then identifies on the recordings the time that appears to correspond to the direct path through the transformer oil. A computer provides considerable help since it is not easy to determine the intersection of three spheres from 3 sensors [143, 167].

Ultrasonic locating methods have been in use for many years. The accuracy depends on the position of the fault in relation to the location where the transducer can be mounted. Electrical locating is part of the required measurement technique and ultrasonic locating technique has made it possible to pinpoint location of the PDs. Electrical locating and ultrasonic locating methods are fully operational and have been used to enhance significantly the state of art in PD measurement and locating of the PD source with good accuracy within the short time for effective decision making [166-167].

Ultrasonic detectors can detect external discharges such as corona and surface discharge. Internal discharges can sometime be detected with the aid of piezoelectric sensors placed at the metal surface of the transformer [37, 147], but the shielding of some of the internal components of the transformer windings and core make detection difficult.

While useful, acoustic monitoring has considerable limitations for PD activity monitoring. It cannot give information on the magnitude of the PDs and their phase relationship with voltage and thus it cannot be used to identify PD types and to provide trend analysis of insulation condition based on the PD properties. Only electrical methods of monitoring allow such flexibility of analysis to determine condition trends.

4.6 Partial Discharge Detection in Transformer

While PDs are normally detected by electrical rather than non-electrical methods, one of the simplest detection methods for transformers consists of the monitoring of gases generated by PD activity in the oil. This also applies to transformer oil-impregnated paper insulation. If a discharge occurs in the insulation, gas is produced by breakdown of oil which can be detected by the Buchholtz relay. The method is simple but on the other hand rather insensitive. A more definitive and sensitive means is achieved by dissolved gas analysis [205].

Reference [156] describes a highly innovative method of on-line monitoring for the power transformer which combines a number of techniques. The American Electrical Power Services Corporation (AEP) is one of several companies to produce a transformer monitoring system. The system is called the Transformer Performance Analysis System (TPAS). It is actually designed for use in very expensive extra high voltage power transmission transformers. TPAS is basically a form of expert system that employs model-based condition monitoring. The system is provided with sensors that gather operating data of transformer and compares it with standard normal predicted readings. On that basis TPAS can predict future performance of the unit. The system can also chart trends and detect when there are any deviations from the predicted performance. TPAS actually continuously monitors several key parameters, which give vital clues regarding the performance of the transformer; these are PDs, water content of oil and gases in oil. Further data is collected on load current, operating voltage, solar magnetic disturbances, and oil temperature status of pumps and fans. Sensors inside the transformer transmit their information with the predicted readings, store data and transfer data to a master computer station when needed [156].

The application of the modern personal computer and digital equipment for both recording of large data quantities and for analysis has allowed better interpretation of the complicated PD distributions and have opened up a new era of research into PD activity and its interpretation and has also increased the reliability of modern insulation systems by providing a more quantitative means of analysing PDs data and allowing storage of the data for future comparison.

PD measurements have gained a position of utmost importance, and extensive research has been carried out for more accurate and reliable detection and location techniques for PD applications, especially for on-line condition monitoring of PD activity in transformers [26, 152].

4.7 Partial Discharge In Transformer Oil

PDs can often lead to ageing of insulating fluids and therefore influence their electric and dielectric behaviour in a negative way. They also decompose the fluid by producing different gaseous or composite products. Even though PDs are very important, their formation and the parameters that are important in determining the PD behaviour, such as moisture, temperature and pressure and how they influence the PD behaviour of mineral-based oil are not yet fully understood [143, 150]. There is much more information required in this regard. This thesis work has been aimed at partly addressing this area.

Transformer oil normally has to withstand varying temperatures, which influence the electrical behaviour of the insulating fluid. The electrical strength of insulating oil strongly depends upon the dissolved and undissolved gas component inside the fluid. [41]. Transformer oil has to withstand such contaminants which can accelerate the ageing processes.

To determine the influence of the age of the oil on the relevant PD parameters, several researchers have explained the initiation of PDs in insulating liquids by assuming the breakdown of gas-filled voids in the liquid and others explain the initiation in a more general way by postulating that impurities such as particles provide PD initiation sites. The influence of the water content on the electrical and especially on the PD behaviour of mineral based transformer oil has been investigated in detail by a number of workers. Mostly it is assumed that water molecules migrate due to their higher permittivity compared with insulating oil in the direction of the electrode. They can the initiate PD activity by distorting the electric field and by acting as impurities sites for initiation of PDs [143, 150].

4.8 Partial Discharge Causes in Oil-Impregnated Insulation

Transformer oil-impregnated insulation contains mainly oil and cellulose based paper and pressboard. Transformer oil and cellulose both are organic based materials, which are vulnerable to thermal and moisture-based degradation. Degradation can affect their function seriously. The Thermal ageing of the cellulose insulation system will also produce water, in addition to any that may enter from the atmosphere.

The moisture is soluble in oil; it can absorb the moisture produced from the cellulose degradation and from the atmosphere. The atmospheric moisture in the oil can eventually transfer to the cellulose insulation due to its very hydroscopic nature. High moisture content in oil and cellulose will decrease the dielectric strength of both materials. As the temperature of a transformer is increased during overloading the moisture is then forced from the cellulose into the oil. So, the moisture does not remain at the same concentration but rather, it is continuously changing between the solid and liquid insulation of a transformer [See Figure 2.7]. High moisture contents in cellulose may produce bubbles at sudden high temperature shock and PD activity can be initiated, leading to a potentially dangerous condition of the transformer [207]. Paradoxically, the very high temperatures and bubble formation may, by virtue of the expulsion of moisture, have some impact in reducing ageing of the paper. This is one issue which is being addressed in the work of this thesis.

When the insulation of a transformer is stressed by alternating voltage, either induced or applied from a separate high voltage source, PDs may occur in different parts of the windings, connecting leads, or other components and may involve different configurations of conductors and/or dielectric materials. They may occur, for example, within cavities in the solid insulation of the windings or bushings, in cavities or gas bubbles between conductors and solid insulation, or in free oil spaces adjacent to either insulation or conductors at earth potential or at high voltage [37, 175].

Because of their almost constant presence in high voltage equipment, PDs are regarded as the most hazardous of the insulation degradation processes with respect to the service life of the transformer insulation. Therefore it is of fundamental importance to be able to identify the hazardous PDs during testing. The magnitude of the individual discharge and the number can be of great help in identifying hazardous discharges. Overall PD activity must be carefully monitored by continuous maintenance testing procedures to establish the trends in the insulation degradation [36, 39].

4.9 Breakdown Theory in the Transformer

An increase in the operating temperature will change the properties of the insulation very significantly. This lack of thermal stability at elevated temperatures limits the use of cellulose for continuous operation at high temperatures. Thus the characterisation of PD phenomena and their impact on the cellulose paper insulation under various conditions becomes a necessity. Often the overloading occurs when the plant or the utility slowly increases the load in small increments over time. The capacity of the transformer may eventually be exceeded resulting in excessive temperatures that prematurely age the insulation. Pressboard and paper are hydrophilic materials capable of absorbing the surrounding water molecules and the dielectric strength of transformer oil decreases rapidly with the absorption of moisture: this can lead to breakdown or failure of the insulation [8]. A related area where there is still much lack of detailed knowledge is in the impact of sudden thermal shocks, due to short circuit effects for example. These thermal shocks can cause gas and bubble formation and these can cause a significant change in the PD behaviour and its impact on the insulation degradation, particularly that of the paper.

The source of possible gas bubble formation caused by thermal shock is not very clear but this is obviously of importance in oil/solid systems as PD activity in the bubbles might occur near to an insulation surface and cause failure of the solid dielectric, before flashover of the oil itself. High voltage power transformers are not totally discharge free, even in a new condition: a certain level of partial discharge activity is allowed and the interpretation of the measurement results and their potential impact and change of insulation properties depends on the knowledge of the test engineer. In most cases these changes can be seen as a degradation of the insulation properties [8, 175].

PD test data and analysis characteristics can be used to analyse the nature of different PD sources. The most frequently used PD quantity is the phase resolved PD pattern [26]. The quantities observed over the whole cycle provide statistical distributions of the discharge magnitude, distribution of the number of discharges and combination of PD magnitude and its intensity. Each distribution is characterised by its specific shape and these shapes can be explained in terms of PD inception conditions. With regards to the PD pulse spectrum, discharge magnitude and discharge phase position as well as the repetition rate can be used in the analysis of insulation defects [26].

The use of the computer-aided PD analysis system offers an opportunity to store sequences of the discharge pulses and to perform post-processing of these results in the course of time. In this way a complete data recording is made for further evaluation and diagnosis of the insulating system. It is known that the behaviour of discharges may be very complex due to their dependency to a wide range of conditions like the discharge site and the voltage stress. Moreover, depending on ageing effects at the discharge site different types of behaviour can be observed in the course of time. The observation of these PD intensity spectra can give interesting and useful information about discharge sources like transformers by showing internal defects and differences in the PD patterns [26]. The use of digital diagnosis support provides additional information about the PD process, particularly indicating if the PD is a regular one (no deviation from the normal situation) or that the process is irregular which means that discharging defects are present. The digital PD diagnosis can also be used to investigate and evaluate different defects in service aged of the transformer by linking together all information gathered from periodic or continuos monitoring [26, 176].

4.10 Computerised Discharge Analyser (CDA 3)

The PD monitoring system used in the experiments was a Computerised Discharge Analyser (CDA3). This is a computer-based PD measurement and analysis system developed at The University of New South Wales. The system is used regularly both in the laboratory and on-site. The hardware consists of a single printed circuit board, which enables direct interfacing between conventional PD detector and a standard PC.

The board can be plugged directly into a standard PC with a free full size 16-bit ISA slot without any modification to either the discharge detector or the PC [26].

The board receives two analogue input signals from a conventional commercial PD detector. One is of the 50Hz voltage supply signal, trapped from the HV output of the supply through a resistive divider or equivalent device. The other input signal to the CDA3 is the amplified PD pulse from the output of the conventional discharge detector. The PD pulse contains basic discharge information, which is stored in memory under direct memory access (DMA). The PD pattern and the complete history of the discharge activity can be easily recalled for future investigation and comparison. A menu-driven program controls the CDA3 operation. Results are displayed in tabular or graphical formats on a monitor. The CDA3 software can discriminate an internal calibrator in the presence of live PDs. This discrimination technique can also be used to eliminate the effect of certain types of external interference.

The CDA3 system provides the peak discharge magnitude (PD max), the average discharge magnitude (PD avg.), discharge current (I), discharge power (P), quadratic rate (Q) and repetition rate (R) for characterising discharge activities. If the positive and negative half-cycles are analysed separately, the result is a set of 12 integrated quantities. This may be used to form a simple database instead of raw discharge data [26].

The programme software calculates for each phase window (ϕI) and over the integration period, the total number of PD pulses detected (nI), the peak (mI), average (aI) discharge magnitude and the average discharge current (cI). To characterise these four distributions, statistical analysis can be applied to calculate their moments. For example, with the current distribution, the mean is denoted as c1, standard deviation as c2, skewness as c3 and kurtosis as c4. As the two half-cycles are analysed separately, there are two sets of moments for each distribution and overall there are 32 statistical moments for the four distributions. The various PD signatures can be stored in a database and recalled later for comparative analysis. The software design of the CDA3 as developed previously at UNSW is detailed in [26] and Appendix B.

The CDA3 system is extremely valuable in assessing the different PD characteristics for various potentially dangerous PD conditions which may arise in power system equipment; in particular oil-impregnated power transformers. This system provides a more quantitative means of acquiring and analysing PD data, which allows storage of data for future comparison, an essential requirement for maintenance and for any life assessment and life extension programs [26, 152].

Chapter 5

Effects of High Temperature and Moisture on Partial Discharges in Oil-Impregnated Insulation: An Experimental Investigation

5.1 Introduction

As most transformer failures occur in the insulation, monitoring of transformer insulation is required to provide an early indication of any degradation that may be caused by abnormal electrical, thermal, environmental and mechanical stresses which may occur during operation [178-179].

Temperature is the major cause of degradation of the cellulose insulation that is the predominant dielectric material used in oil-impregnated transformer insulation. Increased temperature accelerates chemical change in the insulation thus reducing its lifetime. Paper insulation in particular may deteriorate rapidly if the operating temperature in the oil-impregnated insulation is too high. The operating life of cellulose based insulation thus depends heavily on temperature rise above ambient. In addition to normal temperature variations during operation, transformers are sometimes subject to sudden thermal overload and the effect of such thermal shocks on transformer insulation has not yet been fully investigated. Dynamics of water migration between paper and oil insulation is not researched. The intermittent status of released water particles and its role in triggering major failure like fire explosion are to be understood. With that point of view, systematic experimental study and data analysis using PD's, RVM and PDC are made. The novel findings of this investigation are presented in the subsequent three chapters.

The ingress of moisture, coupled with high operating temperature in the insulation reduces the dielectric strength of the cellulose paper, the pressboard and the transformer oil. The deterioration of the oil-impregnated insulation is due to the operating temperature and voltage, excessive oxygen in the oil and moisture in the insulation. Excessive moisture in the insulation causes PDs within the moisture soaked cellulose paper reducing its ability to withstand high electric field stresses. The combination of very high temperatures with the presence of moisture in both oil and paper is an area which has not received a great deal of attention thus far, but is nevertheless an important component of the operational degradation process. Thermal shocks can generate gas bubbles and they have significant impact on PD levels in the insulation system. Thus this area of thermal shock in conjunction with elevated moisture levels is an important area of study and work and results of this chapter were designed to provide some better knowledge of this aspect.

As most transformer failures occur in the insulation, condition monitoring (preferably continuous and on-line) of transformer insulation is required to provide an early indication of any degradation that may be caused by abnormal electrical and thermal stresses which may occur during operation. In order to recognise deterioration from PD patterns, it is necessary to catalogue and to understand the correlation of the PD patterns to the insulation condition [5, 180]. This requires investigation of the physical processes that take place and to identify them from the PD patterns. This also needs to be done to cover all operational aspects of the transformer and this is the reason for the work described here.

This chapter reports results of a laboratory experimental investigation aimed at a detailed investigation of the PD characteristics and patterns in a test model of transformer-type oil-impregnated insulation. The tests were performed over a range of parameters, including abnormally high temperature levels with different levels of moisture contamination of both oil and paper. The frequency variation was from 50 Hz to 200 Hz. The experiments were performed and investigated in the laboratory with an environment and configuration similar to practical operating conditions in a transformer under load. The PD patterns were recorded and analysed during increasing and decreasing of the temperature. The PD patterns together with inception and extinction data were recorded and correlated with moisture and temperature effects.

The work investigated the thermal dependence of PD activity in new and aged paper insulation, using temperatures up to 140-145 ^{o}C. The temperature levels used were much higher than normal operation to simulate the transient over-temperature conditions that may occur during a heavy overload of a transformer. At these temperatures there is substantial gas bubble formation and these bubbles have a significant impact on the PD activity. One particular condition of temperature that is known to present problems is the thermal impact due to sudden changes in the load. Such thermal shock can generate such gas bubbles, involving moisture, which will have substantial impact on PD activity [124]. Thus the effect of high temperature on PD activity is of importance in insulation monitoring. The thermal generation of gas bubbles and associated temperature levels, moisture levels and PD pattern characteristics were also recorded and analyzed. The effect of aged and new transformer oil on PD pattern is recorded in this chapter.

Typical configurations of paper insulated copper windings and pressboard spacers were subjected to long-term tests in a heated oil test cell. The level of PD activity and the effects on PD pattern due to temperature, moisture and ageing in oil-impregnated insulation is considered here. PD activity over a range of temperatures with and without bubble formation is also studied. The effects of prolonged operation at high temperatures on moisture levels and changed PD behaviour due to moisture in paper are also covered in this chapter.

There are a number of methods available which can provide reliable information of ageing processes of oil and paper. Degree of polymerisation (DP) tests and dissolved gas analysis (DGA), including furan analysis, and dielectric dissipation factor (DDF) tests are some of the more common and often used monitoring tests. However they give an integrated or global assessment of the insulation condition rather than an instantaneous and localised evaluation. In contrast, PD measurement of insulation gives an instantaneous and time-resolved assessment of condition and they can in some circumstances be used to locate the fault site.

PD monitoring is thus one of the more important tools available to assess the condition of oil–impregnated insulation. PDs are also a major cause of insulation damage and degradation and thus their monitoring is a very useful diagnostic tool of the insulation degradation in large power transformers. PD monitoring is not an infallible monitor, but nevertheless it is a very sensitive indicator of insulation condition. PD monitoring is thus one of the more important tools available for the maintenance engineer to assess the condition of transformer insulation [26, 152].

5.2 Transformer Insulation Model

All transformer parts which operate at different potential require some form of insulation between them, whether it is a liquid, or a solid. The operating lifetime of any transformer is effectively determined by the life of this insulation. Insulation lifetime, apart from some very abnormal damage, is dependent primarily on the temperature at which the insulation operates. Transformer insulation has the two major components of mineral oil and paper-based materials. The major constituent of paper (and pressboard) is cellulose, which is a natural long chain polymer of glucose molecules joined together by the glycosidic bond. The paper derives its tensile strength from its fibrous nature, which arise from intramolecular and intermolecular hydrogen bonding. The rate of loss of this mechanical tensile strength is temperature dependent because of the chemical scission of the bonds, which hold the molecular chains together. The chemical reactions, which cause this scission, are also temperature dependent. Cellulose material degrades, especially at high temperatures and in the presence of oxygen. The degradation products include water, furan products, glucose molecules, solids and carbon oxides. The degradation from the thermal stress affects the electrical, chemical and mechanical properties of the paper. Indeed, the degradation of the tensile strength of the paper is a useful determinant of the paper insulation lifetime.

The natural level of moisture in paper under atmospheric conditions is about 5% by weight. When used as transformer winding insulation, the paper must be dried after construction to a moisture level of less than 0.5% in new transformers. The natural degradation of the paper during operation will then produce moisture, which will then be maintained in the paper and may also enter the oil.

During a sudden overload condition which causes thermal shock the water vapour in the cellulose insulation expands, thus causing bubble formation, and in this process moisture from the paper transfers into the oil and because moisture migrates very slowly into paper it can lead to the presence of free water in the oil. Free water droplets in the oil, when their molecules are subjected to the ac electric field inside a transformer, become polarised and electric dipoles of water move around inside the bubble, trying to align with the applied field. The result is elongation of the bubble along the electric field lines. Eventually, the molecules break through the interfacial tension and small water spheres escape and move in opposite directions, forming a moisture bridge that can cause PD activity or even transformer failure in the long term. Such PDs, at their inception are generally of small magnitude but they can still cause progressive degradation of material and eventually total insulation failure. Detecting these PDs and their characteristics can help to detect small changes in the general quality of insulation, such as those occurring due to the thermal effects of overloading [181-184].

5.3 Degradation of Insulation Material

Overloading of the insulation in a high voltage power transformer causes a high thermal stress that will accelerate degradation of the insulation. All insulation subject to any sustained temperature rise above ambient will degrade insulation in accordance with the Ahrrenius model of chemical reaction rate increase with temperature [82]. Also, sudden or sustained thermal overload in the transformer will increase the reaction rate and thus further decrease lifetime. In addition to this purely thermal degradation, PDs will occur as insulation degrades (or they may arise from other causes) and these will further increase the degradation rate. The exact relationship of the PD activity level to such high over-temperature conditions has not been widely investigated. The aims of the investigations reported here were to investigate this relationship with temperature and to determine degradation modes of the insulation due to high temperatures coupled with PD activity. To achieve this investigation, typical model configurations of paper-insulated copper windings and pressboard spacers were used in an oil test cell, able to be heated, with attendant continuous PD monitoring.

5.4 Insulation Condition Monitoring

Overloading of a transformer is a major cause of the thermal stress that may degrade the insulation. Detecting PD activity during overloading establishes not only quality control but also can help in detecting a change in the insulation quality. PD activity is not a complete failure of the insulation, but is indicative of local high fields and a certain amount of ionisation or charge transport underway somewhere in the insulation. The increased level/rate of PDs can result in dielectric breakdown of the electrical insulation and the failure of the power equipment. If we can understand and correlate the PD properties with insulation condition and potential faults, it should be possible to prevent catastrophic failure.

The experiments reported here were aimed at a detailed investigation of the PD patterns in oil-impregnated insulation at different temperature, moisture, applied voltage and frequency and their effect in accelerating ageing [80, 83, 105]. The PD activity related to the deterioration of this particular insulation system was recorded and analysed. The experimental model was designed to give electrical stresses typical of working transformers and also to allow application of high thermal and environmental stresses.

5.5 Experimental Procedure

The winding insulation test objects are mounted in a small steel tank, which is 280mm wide, 330mm long and 210mm high, with high voltage bushings and windows for observation of bubble formation and movement. Heater pads under the base heat the tank and its contents to the desired temperature and the paper insulation on the windings can also be heated by ohmic heating of the conductor system, using an external low voltage, high current supply. The total oil capacity of the tank is 12 litres. Normal transformer insulating oil was used. Figure 5.1 shows the test chamber used.

The test electrode configuration consisted of a high voltage (HV) copper electrode attached to the HV supply for applying electrical stress and a low voltage (LV) copper electrode, through which heating current could be circulated to raise the temperature of conductor and the insulation. A duct space between the electrodes, which is the location of the test insulation, contained mineral oil, paper layers and pressboard spacers as shown in Figure 5-2. This structure and the electric fields applied by the external supply were designed to simulate oil-filled interturn spacings and conditions in transformers. The temperature of the conductor was monitored by a fibre optic temperature sensor.

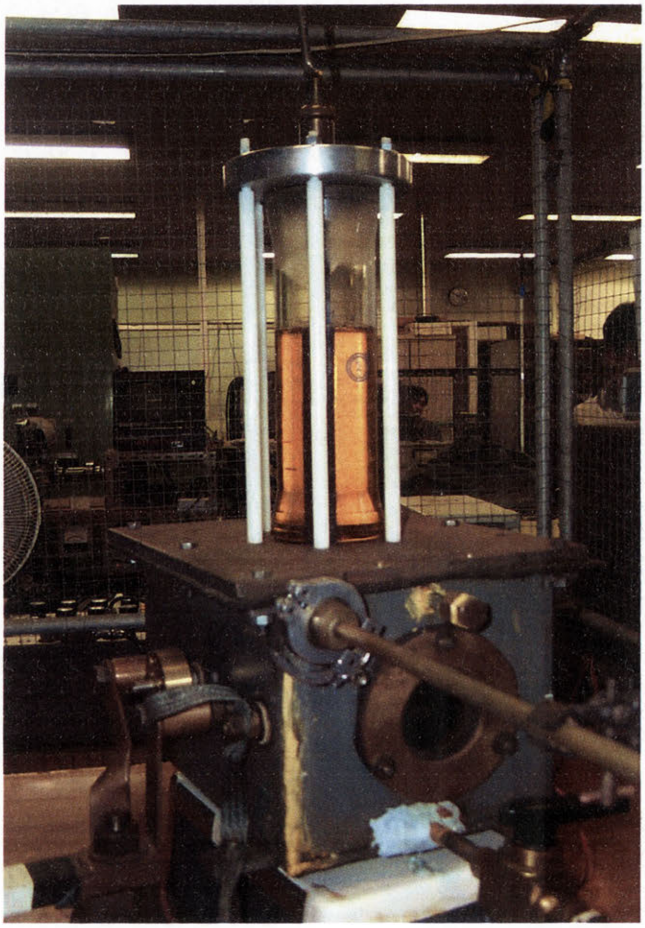

Figure 5-1. Steel tank used for tests

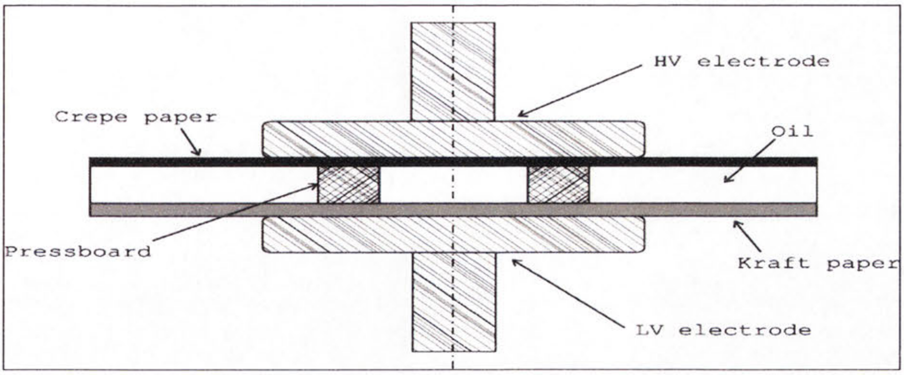

Figure 5-2. Arrangement of Test Sample

Copper HV Electrode, Two Layers of Crepe Paper, Pressboard spacers, Mineral Oil filling, 10 Layers of Kraft Paper and LV Copper Electrode

The HV electrode is 96mm x 58mm, had radius edges of 6.35mm and was covered by two layers of 0.25mm crepe paper to give a total thickness of 0.5mm insulation on the HV electrode. Figure 5-3 illustrates the HV electrode insulation configuration.

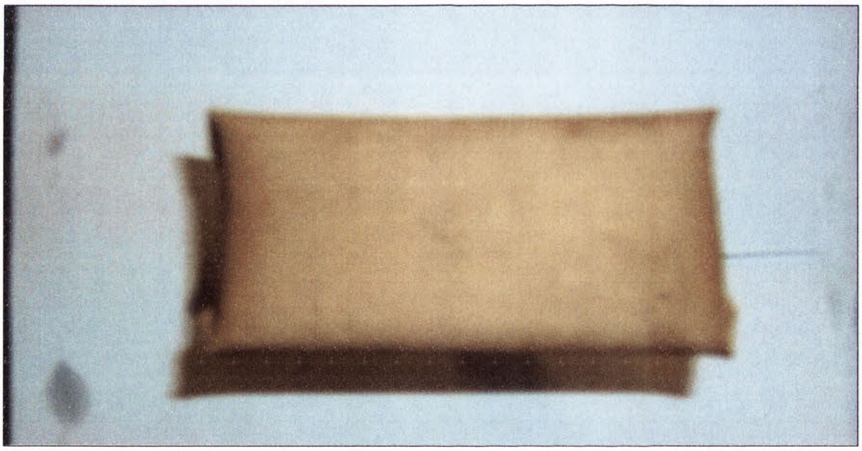

Figure 5-3. Insulated High Voltage Electrode

Insulation covering is two layers of 0.25mm thick crepe paper

The LV electrode consisted of six segments, each of effective length of 100mm in series and arranged side-by-side in a rectangular configuration giving an overall area of 60mm x 100mm (See the detail in Fig 5-7). The individual insulated conductor section (10mm wide and 3mm thick) had a covering of three layers of 0.06mm thick Kraft paper and the six segments were covered as a whole by seven sheets of the same paper. This made the total thickness of Kraft paper insulation 0.6mm.

Figure 5-4 illustrates the LV electrode configuration. Two 3mm-thick pressboard spacers (shown in detail in Figure 5-8) were used as spacers between the HV and the LV electrodes.

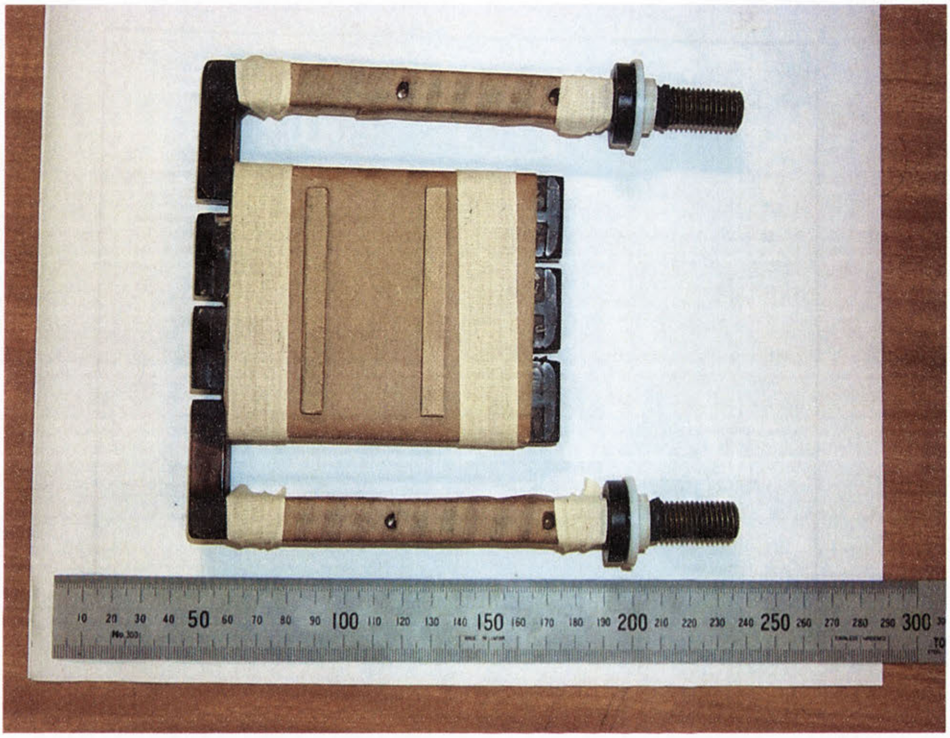

Figure 5-4. Insulated Low Voltage Electrode

Three wraps of 0.06mm Kraft Paper and then seven sheets of similar paper.

Two 3mm thick pressboard spacers are shown on the LV Electrode

The model winding test configuration used is typical of that used in oil-impregnated power transformers. It consists of a paper insulated copper strip configuration and is designed for application of an electric stress (1.83 kV/mm minimum occurring across the paper, with dielectric constant $\varepsilon_{oil} = 2.2$, $\varepsilon_{paper} = 3.2$ and $\varepsilon_{pressboard} = 4.2$) which is equivalent to that used in transformer windings when the windings are located between a parallel electrode structure.

In the model, the required electric stress is obtained with application of voltages up to 10 kV between the electrodes. The winding can be heated independently of the oil heating by current circulated in the winding by a high capacity LV transformer. This can raise the temperature of the copper conductor to 145°C quickly when required. A fibre optic temperature sensor (Figure 5-5) monitors the temperature of the conductor.

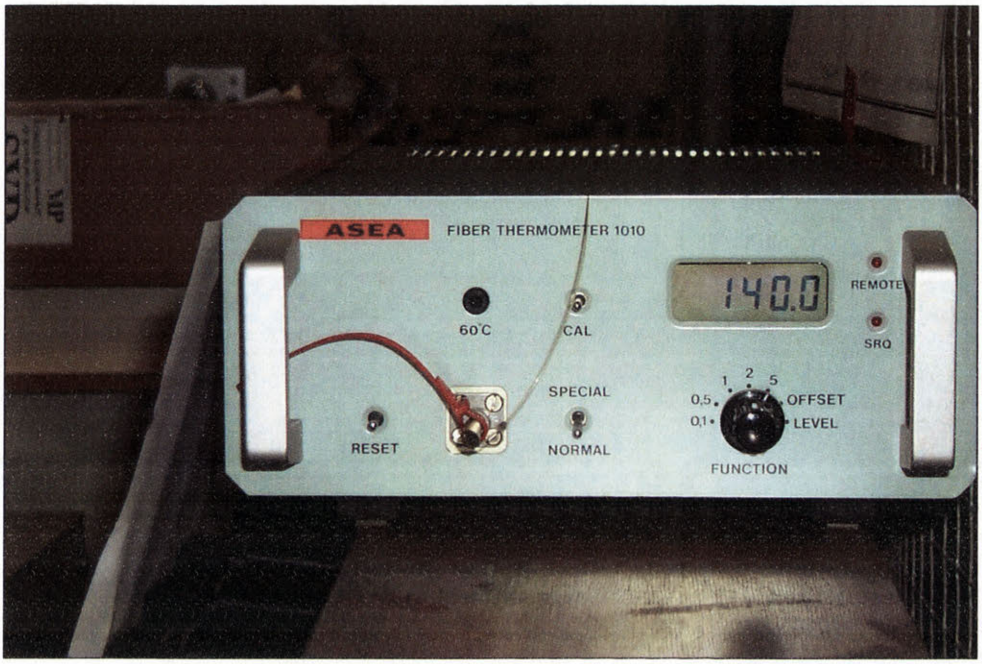

Figure 5-5. Fibre Thermometer ASEA Model 1010
Showing a typical overload temperature of 140 C

The uncovered HV and LV electrode are shown in Figures 5-6 and 5-7 respectively.

Figure 5-6. Uncovered High Voltage Electrode
(96mm length x 58mm wide)

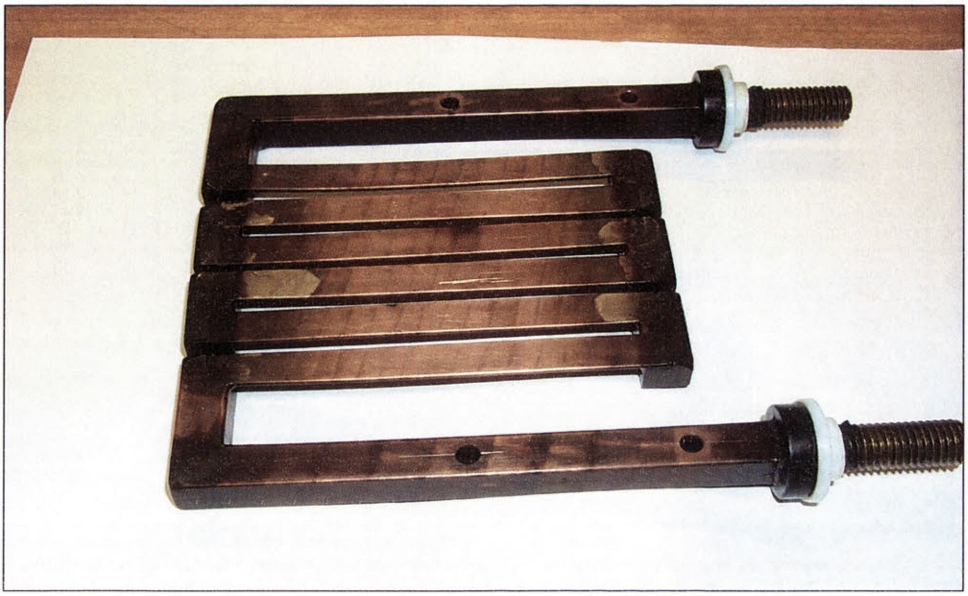

Figure 5-7. Uncovered Low Voltage Electrode

Six Conductors (100mm x10mm x 3mm) with overall area of 60 x100mm.

The duct between HV and LV electrodes contains both the oil and pressboard spacers as well as the paper insulation. The pressboard spacer length and width are 65mm and 6 mm respectively (Figure 5-8). Total thickness of the insulation between the HV and LV electrodes is ~ 4.1mm.

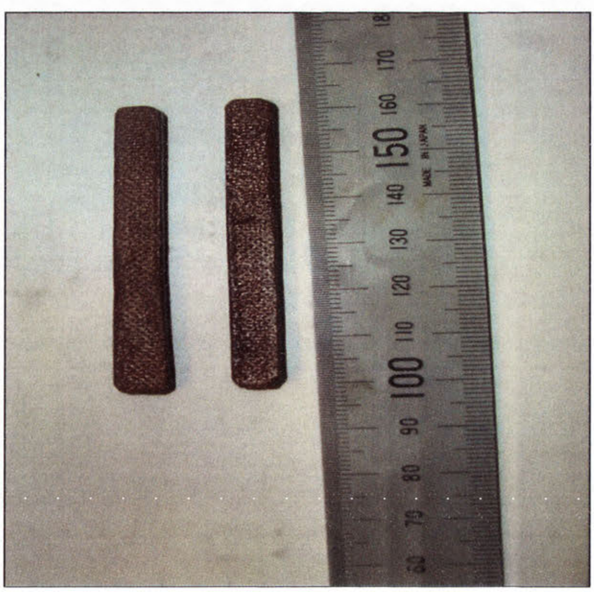

Figure 5-8. Pressboard Spacers; Length and Width are 65mm and 6 mm

5.6 Measuring Equipment

The PD pulses generated in the test insulation were recorded using a computerised discharge analyser (CDA3) system. This system provides phase resolved PD patterns of magnitude and number and their various statistical distributions for each half cycle of voltage. It also displays the IEC60270 integrated discharge quantities of discharge current, quadratic rate, discharge power and repetition rate of the PD pulses. Statistical moments for pattern characterisation are also calculated and displayed. These are the mean, the standard deviation, the skewness and the kurtosis of the (assumed Gaussian) PD patterns, are displayed on a PC [26] and are updated every few seconds, with the data being continuously recorded by the PC. The system has the capacity to record every PD event that occurs.

The circuit for PD measurement and calibration procedure follows IEC-Standard 60270 on PD measurement. Figure 4-6 (Chapter 4) shows the detail of the PD measurement circuit used. The CDA3 is contained on a circuit board inserted within an IBM-PC. It interfaces the analogue output of a conventional discharge detector (Robinson Model 5) and the computer recording system [26, 147]. In Figure 4-6 the Cs denotes the capacitance of the test object. The C_b is a HV discharge-free coupling capacitor providing appropriate isolation. Z is an appropriate input unit, chosen depending on the test object. The analogue output signal of the conventional PD detector (Robinson) is connected to the input of the CDA3 circuit board, which then processes the PD signals digitally. A voltage reference is also given to the PC to provide the phase resolution of the PD patterns. Figure 5-9 is a photograph of the recording system.

Before testing, the measurement system is calibrated using an external calibration source. The parameter set up of the CDA3 system is also calibrated. This latter includes calibration of integration time, detector calibration, analyser calibration and the lower signal threshold. To prevent electrical interference in the measurements, the signal threshold of the CDA3 was set to 30 pC. Thus, any signal with PD magnitude lower than 30 pC was rejected. This level was chosen after consideration of typical test levels obtained and the typical interference level in the test area.

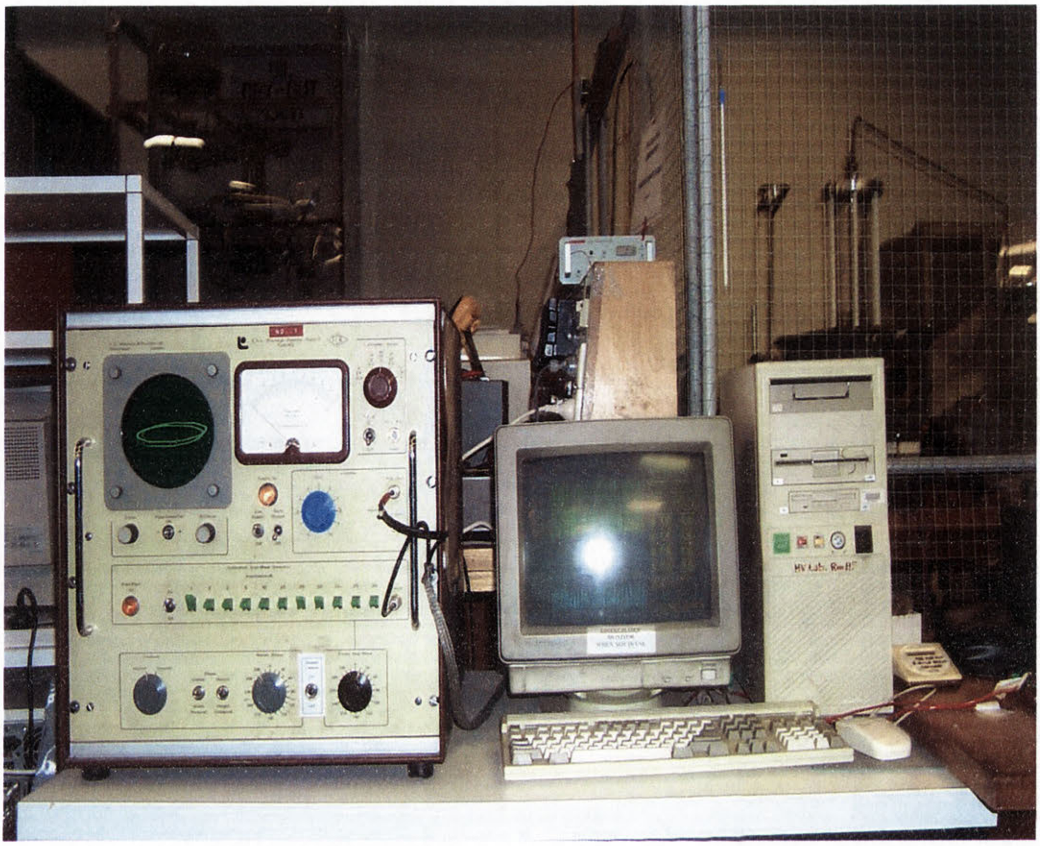

Figure 5-9. Partial Discharge Measurement Apparatus
A typical output pattern is displayed on the monitor unit

5.7 Discharge Quantities

The analysis of the experimental results reported here is focused on the peak and average discharge magnitude and the PD repetition rate. The peak discharge magnitude (q_m) is defined as the magnitude of the largest apparent charge recorded in a selected time interval. The peak discharge magnitude is expressed in Coulombs as;

$$q_m = \max[q_1, q_2, q_3, \cdots, q_n],$$

Where $q_1, q_2, q_3, \ldots\ldots, q_n$ are the magnitudes of the apparent PD charges measured.

The average discharge magnitude (q_a) is defined as the ratio between the sum of the measured discharge magnitude and the total number of PD pulses recorded in a selected time interval. The average discharge magnitude is also expressed in Coulombs as below;

$$q_a = \frac{1}{n}\sum_{i=1}^{n} q_i$$

Where n is the total number of discharges within the measurement time interval T and the q_i are the apparent charges of individual PD events.

According to IEC 60270 [132], the repetition rate (r) is defined as the ratio between the total number of PD pulses recorded in a selected time interval and the duration of this time interval and can be expressed mathematically as;

$$r = \frac{n}{T}$$

Where n is the total number of discharges within a selected time interval T.

5.8 Test Results And Discussion

The dominant ageing or degrading factors used in the experimental tests were a combination of thermal and electrical stress. Facilities were also available to accelerate ageing by operating the system at higher frequency. The operating frequency used was 50 and 200 Hz in the tests reported here, with the higher frequency used to accelerate ageing.

The voltage applied to the model (10 kV) was designed to give operation at electrical stresses typical of those occurring in working transformers. After setting up the test equipment, the constant 10 kV test voltage was applied to a well-aged sample which had already been aged for almost three years (at about normal room temperature) in previous tests and experiments. Although the aims of previous experiments performed were quite different from that detailed here, a study of previous records found some data to be very useful in correlating different PD patterns especially with the moisture in the paper.

5.8.1 Effect of Temperature and Frequency

The temperature of the oil in the steel tank was maintained constant at 80°C by the heater control system. At 80°C the insulation system PD level was checked prior to initiating the high temperature tests and was found to be discharge-free. The temperature of the copper winding and the paper was then increased rapidly by injecting high current to the windings via the LV electrode.

The PD inception temperature in the sample at 10 kV was found to be 110°C. Figure 5-10, shows the PD pattern measured at this inception level. As can be seen the PDs at inception were few in number and quite consistent in magnitude with a peak value of about 142 pC and an average value of 110 pC. They also appeared at the peaks of voltage, indicating possibly a void type source, although the PD number is so small that such conclusions are not conclusive.

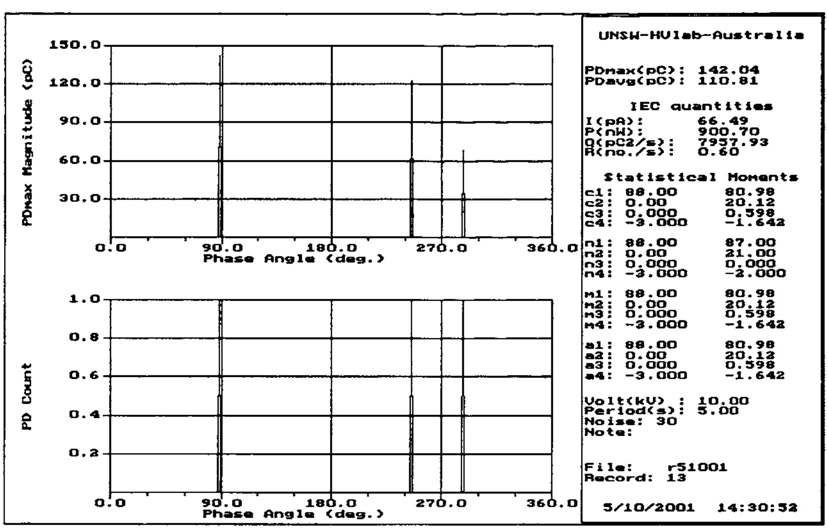

Figure 5-10. PD Phase resolved Patterns and statistical data at inception at 10kV, 50 Hz and 110°C

1. Left Top is PD maximum, 2. Left Bottom is PD Count,

3. Top right are IEC parameters [PD max, PD ave, Discharge Current (I), Power (P), Quadratic Rate (Q) and Repetition rate (R)]

The temperature was then raised uniformly by increasing current until the conductor temperature reached 145°C. During the temperature rise the PD levels and patterns were recorded after each 10°C rise after inception. The conductor (and thus insulation) temperature was then maintained at 145°C for 30 minutes and the PD levels were recorded at five minute intervals.

Many gas bubbles were observed to be discharged / released at a temperature of 140-145°C with some small and some large bubbles generated (Figure 5-11). The phenomenon of bubble formation can be explained by development from high electric stress in voids in the insulation or, more likely, by production due to high moisture content in the paper vaporising ie. since it is above boiling point of water as the temperature is raised very quickly with an almost adiabatic process during which the moisture acquires heat energy and, when the vapour pressure is greater than the external pressure, a gas bubble escapes.

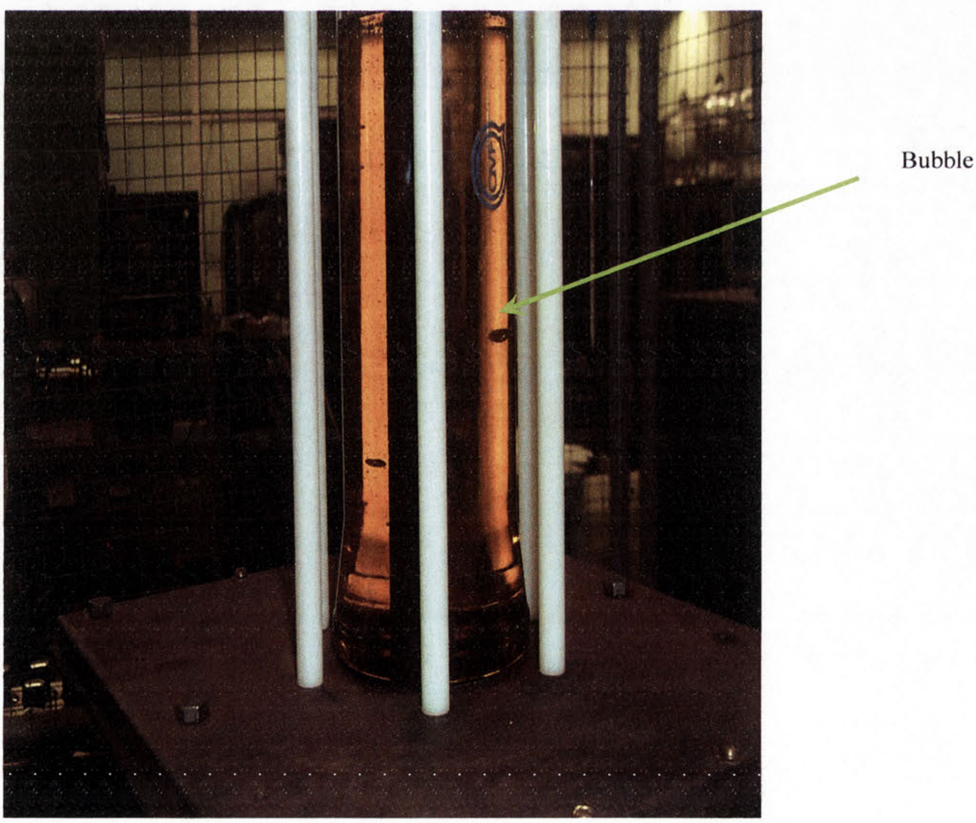

Figure 5-11. Gas Bubbles Released in the top glass bushing of the cell
[10kV, 50 Hz and a temperature of 140-145°C.]

It was also observed that the discharge/release of large bubbles was accompanied by a dramatic decrease in the **maximum** PD magnitude. However although the maximum level decreased substantially, the average PD magnitude and repetition rate however did not change much as a result of the bubbles, as can be seen by comparing Figure 5-12 (before the bubble release) and Figure 5-13 (after the bubble release). The maximum PD level after the release of bubble decreased from 1.37 nC before bubbles to 336 pC after. However the average magnitude decreased only marginally from 100 to 95 pC. The PD rate changed from about 1016 to 960.

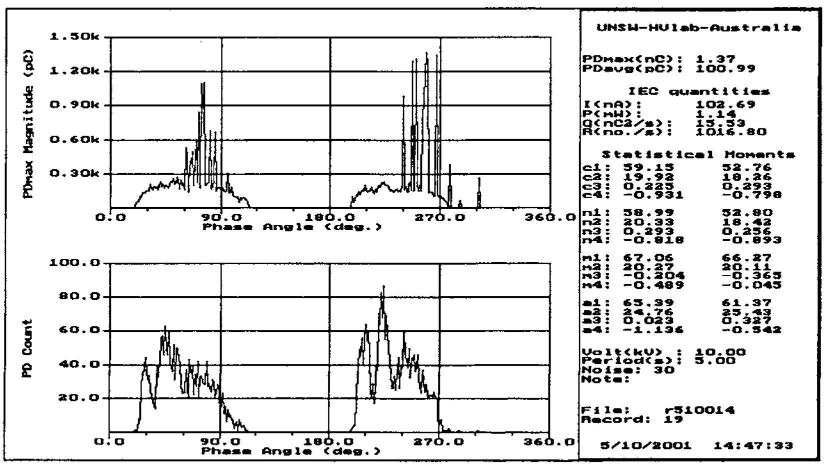

Figure 5-12. PD Pattern Before Release of Bubble at 10kV, 50 Hz and 145°C

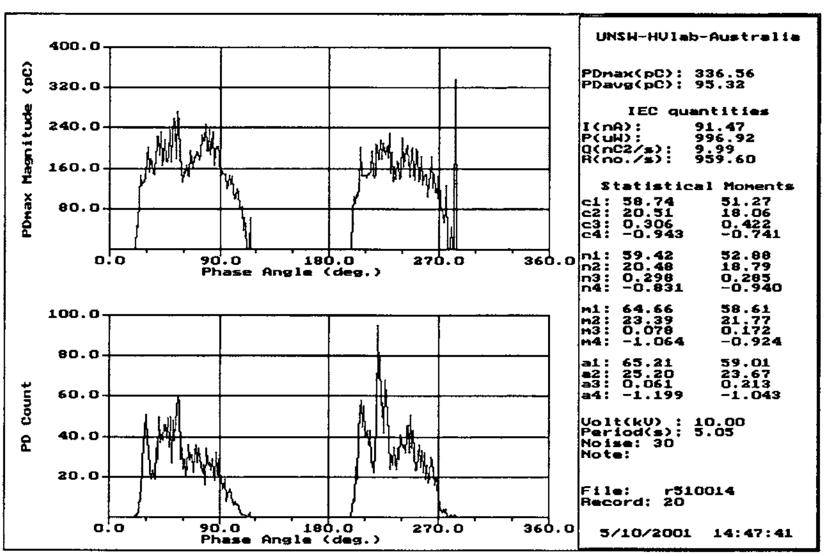

Figure 5-13. PD Pattern After Release of Bubbles at 10kV, 50 Hz and 145°C

(recorded only 8 seconds later than the record shown in Fig. 5-12)

Note also that the PD inception and extinction phase angles do not vary much between the two sets of pattern shown in Figures 5-12 and 5-13. Also, the patterns of the discharge numbers are very similar in each case, indicating that there is little difference in the base PD behaviour except for the relatively few discharges of high magnitude that occur just before the bubbles are released. Thus it is likely that the "before" example of Figure 5-12, shows PDs in bubbles which are held, or generated, within the solid insulation and that the large discharges are due to the influence of the solid insulation material interacting with the bubble. The "after" pattern thus shows the PDs activity within the isolated bubbles when only surrounded by the liquid.

The temperature was then reduced in stages and the PD levels were recorded after each decrease of 10°C in temperature. The PD extinction temperature was found to occur at 100°C ie. boiling point of water. The oil temperature was then maintained at 80°C for fourteen days and the insulation system was overloaded daily for 30 minute periods to temperatures of 140-145°C in order to determine the effects of short duration period of increased temperature on the oil-impregnated insulation.

It was found that maximum PD levels in this situation had increased from 3.24 nC (see Figure 5-14) to 3.46 nC (Figure 5-15) over a period of eleven days. The average PD magnitude as well as the PD number also increased significantly, from 219 pC to 477 pC and the PD repetition rate number increased from 39 to 109 (no./s). These can then be taken as an indication of some substantial degradation of the insulation material over the eleven day period.

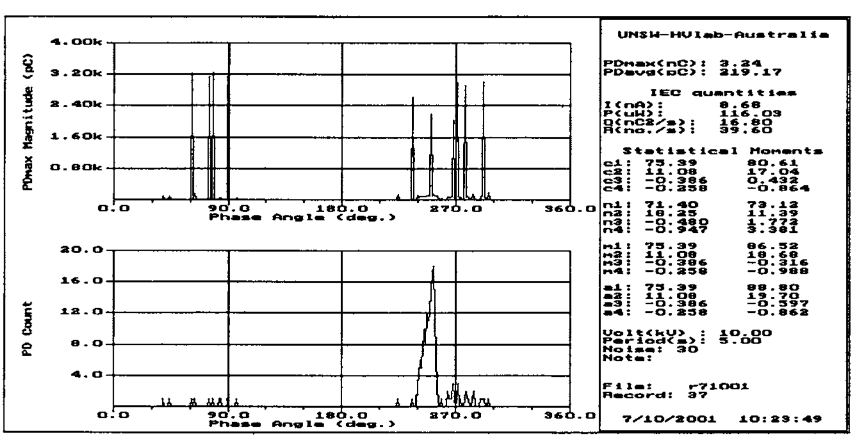

Figure 5-14. Maximum PD 3.24 nC at 10kV, 50 Hz and 145°C

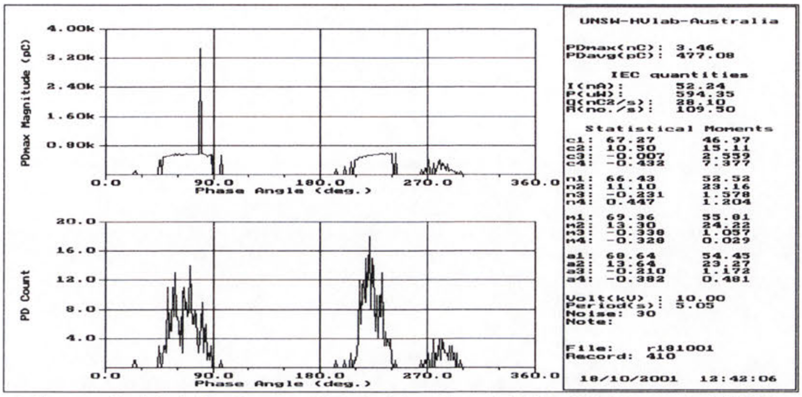

Figure 5-15. Maximum PD 3.46 nC at 10kV, 50 Hz and 145°C

(taken 11 days after 5-14)

It was also observed that during the heating phase water droplets accumulated on the bushing glass (Figure 5-16). The accumulation of water droplets at the glass bushing can be explained by the fact that at high temperature water is driven from the paper into the oil and then from the oil to the air above the oil in the form of bubbles/vapours and, after condensation, accumulates on the inner face of the glass bushing.

Figure 5-16. Water Accumulated on the Glass Bushing

Some of these condensed moisture drops eventually dropped back into the oil. When this happened the effect was the production of very different PD patterns lasting for less than five seconds (the sampling period for the PD patterns). These changing patterns and their sequential behaviour are shown in Figures 5-17, 5-18 and 5-19.

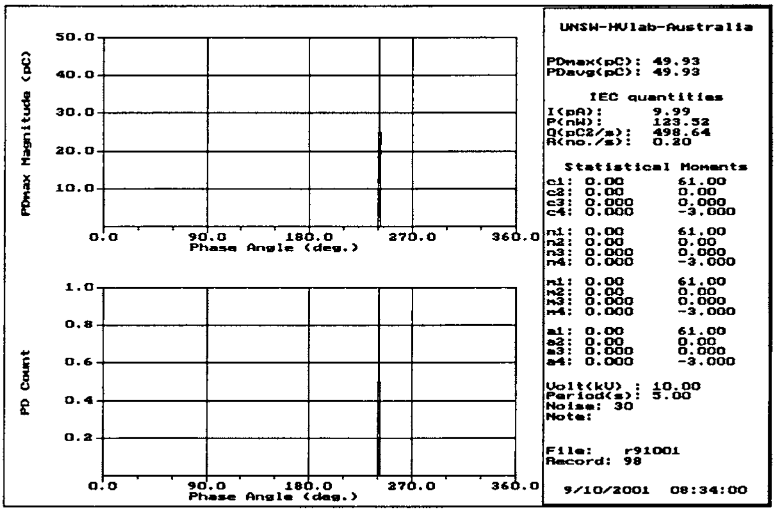

Figure 5-17. PD Pattern Before the fall of Water Droplets into the Oil

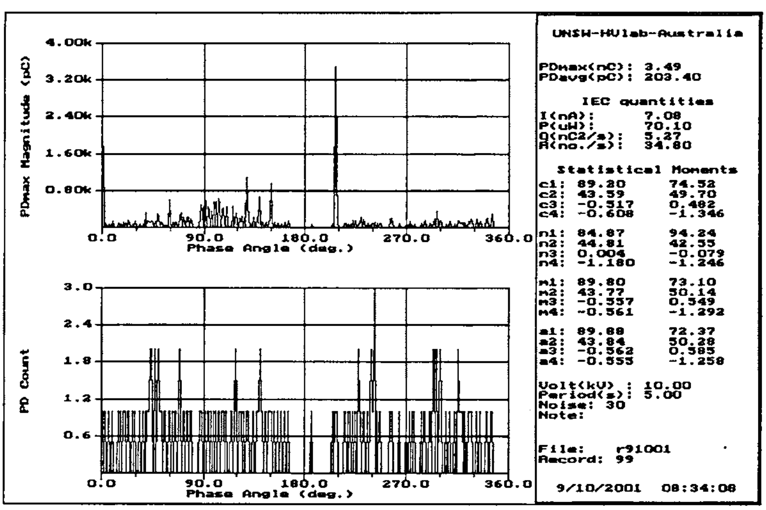

Figure 5-18. PD Pattern After a Water Droplet Enters the Main Oil Volume

Prior to the water droplet entering the oil and after its dispersion, the PD activity was at very low level and with very small magnitude and limited to the region at negative peak voltage (Figure 5-17). However immediately after the droplet enters the oil the PD activity then becomes very high and the phase distribution is distributed almost uniformly over the whole voltage cycle (Figure 5-18). The peak PD magnitude, average

PD magnitude as well as the PD number all increased with the water droplet entering the oil. The peak PD magnitude increased from 49 pC to 3.49 nC, the average PD magnitude increased from 49 pC to 203 pC and the PD repetition rate number increased from 0.20 to 34 (no./s). The time between the measurements of Fig 5-17 and Fig 5-18 is only nine seconds.

The change in PD activity can be explained by the fact that, because the density of oil is less than that of water, as the water droplet falls in the oil from the glass bushing it tends to go to the bottom of the steel tank and during that process the water droplet can disperse and enter regions of high electric field strength causing a considerable reduction in the local dielectric strength leading to high levels of PDs and leading to damage and dielectric breakdown of the insulation. This can also be explained by the fact that electrical discharges can occur in a high voltage region due to disturbance by the change in moisture equilibrium causing PDs of higher intensity.

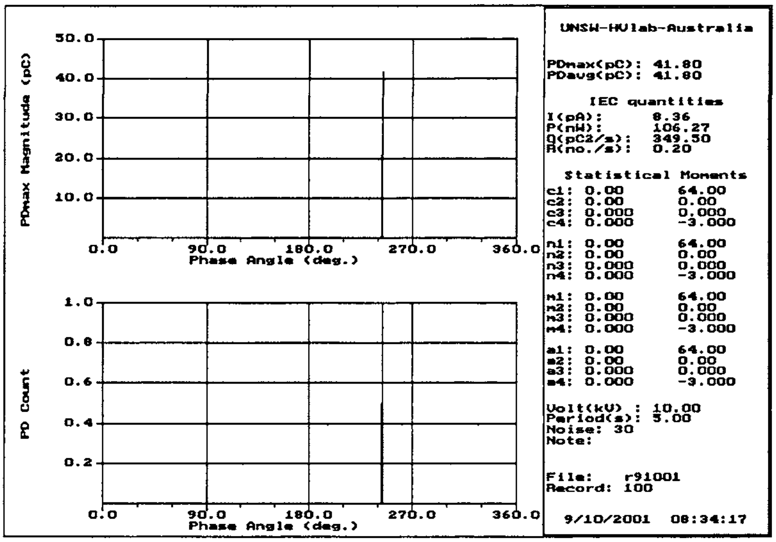

Figure 5-19. PD Pattern after water droplet has dispersed in the oil volume

Figure 5-19 shows the PD activity shortly after the droplet has dispersed. In Figure 5-19 the PD activity is shown 17 seconds after the droplet entered the oil. It can be seen that the PD activity has been restored to its pre-moisture level. The magnitude is now 41 pC and the repetition rate is 0.20 (cf 49 pC and 0.20 prior to the droplet insertion).

However, although the duration of the high PD levels due to moisture was short, the potential for some permanent damage with peak PD levels of about 3 nC and repetition rates of 34 is significant.

The experiment was then repeated with an acceleration of the insulation ageing rate. The ageing was accelerated by increasing the excitation voltage frequency from 50 Hz to 200 Hz by using an AC power supply/frequency converter (Figure 5-20) [5, 26].

Figure 5-20. AC Power Supply/Frequency Converter Kikusui Model PCR-1000

The insulation system was then thermally loaded as previously at 50 Hz for fourteen full days and it was found on the sixth day that, instead of little PD activity as was the case at 50 Hz, the system was then starting to generate discharges at 80°C with the PD activity levels and distribution as shown in Figure 5-21, where the pattern is almost symmetrical over the two voltage half cycles. The average PD level is 142 pC and the repetition rate is 216 per sec.

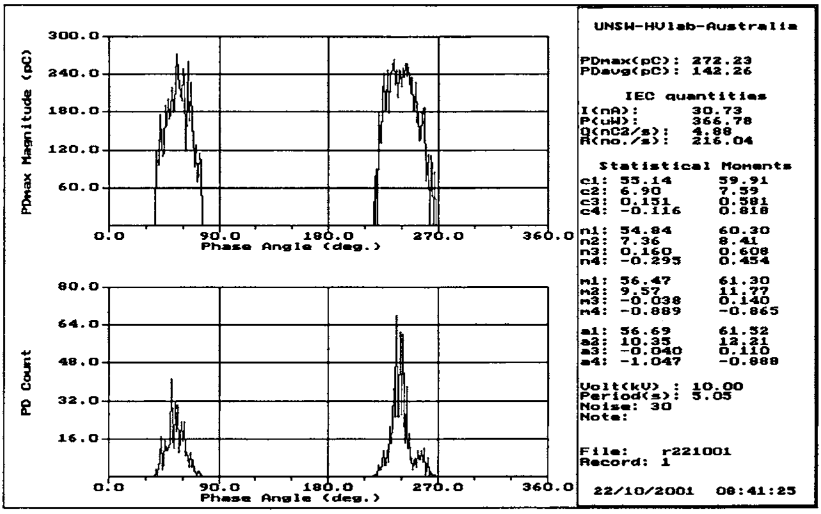

Figure 5-21. PD Pattern at 10kV, 200 Hz and 80°C

During this experiment gas bubbles were again produced. In the test model structure used it is likely that bubbles are generated and then trapped between the layers of paper or between the paper and pressboard, thus initiating the PDs at 80° C.

A very similar almost symmetrical PD pattern on the same insulation system had been observed in previous tests on the same model. These were performed in October 1996 during experiments after the system was loaded for three weeks at 140°C and 50 Hz and the next day the insulation system was found to be discharging at 80°C (see Figure 5-22).

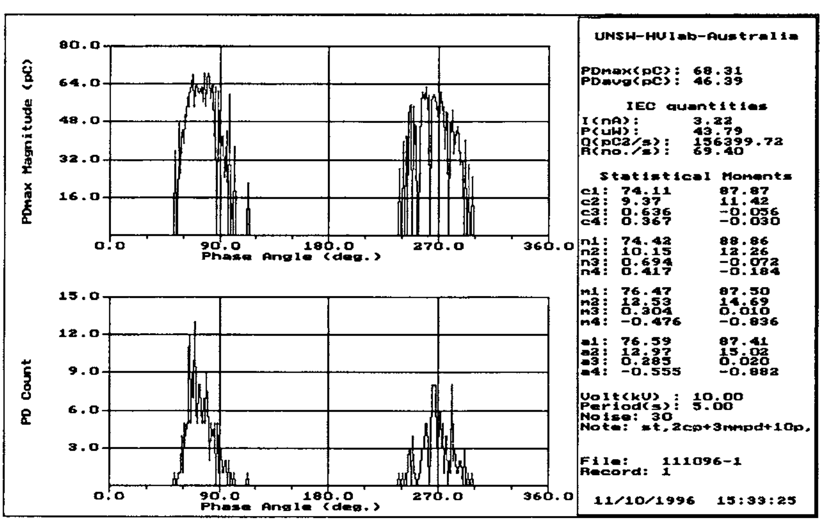

Figure 5-22. PD Pattern at 10kV, 50 Hz and 80°C in October 1996

At the overload temperature of 145 C and with accelerated ageing in the investigations reported here the maximum PD magnitude rose from an initial level of 3.24 nC (see Figure 5-14) to 3.88 nC (see Figure 5-23 below). The average PD magnitude increased from 219 pC to 1.42 nC and the PD repetition rate number increased from 39 to 216 (no./s).

On the fourteenth day it was observed that the maximum PD level had decreased to 1.52 nC (Figure 5-24) from the peak of 3.88 nC (Figure 5-23) and that the number of bubbles that were discharged/released was very few compared to the number previously found. The average PD magnitude decreased from 1.42 nC to 97 pC and the PD repetition rate number decreased from 216 to 70 (no./s).

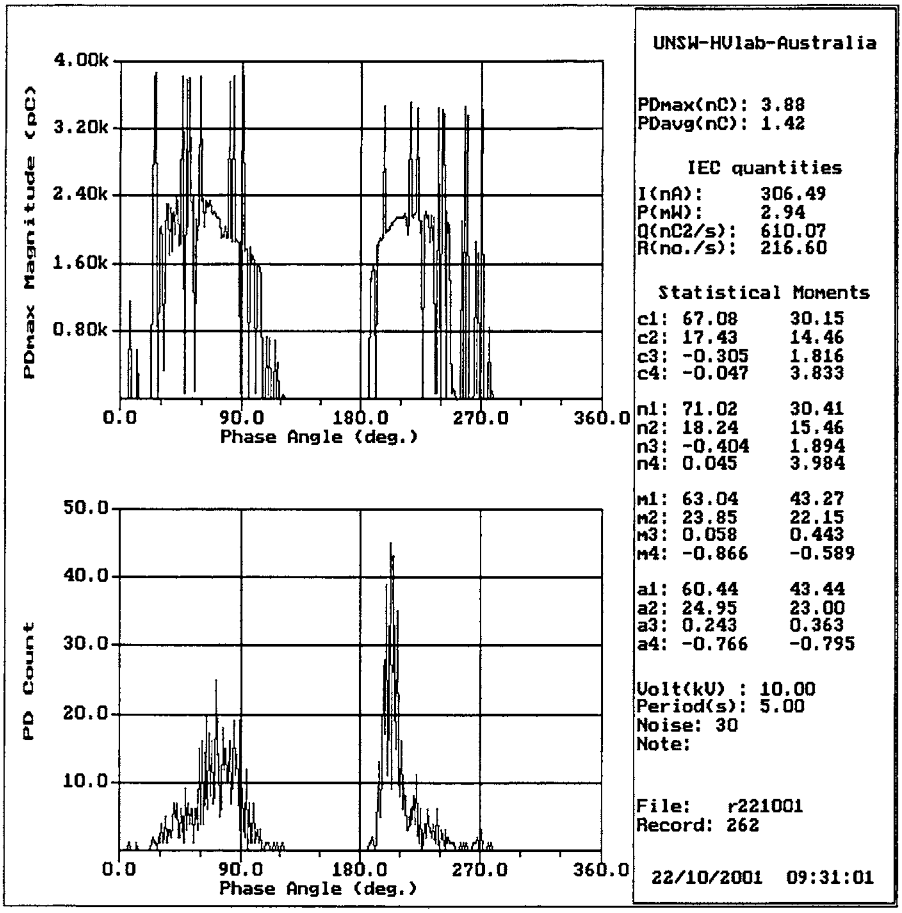

Figure 5-23. Maximum PD 3.88 nC at 10kV, 200 Hz and 145°C

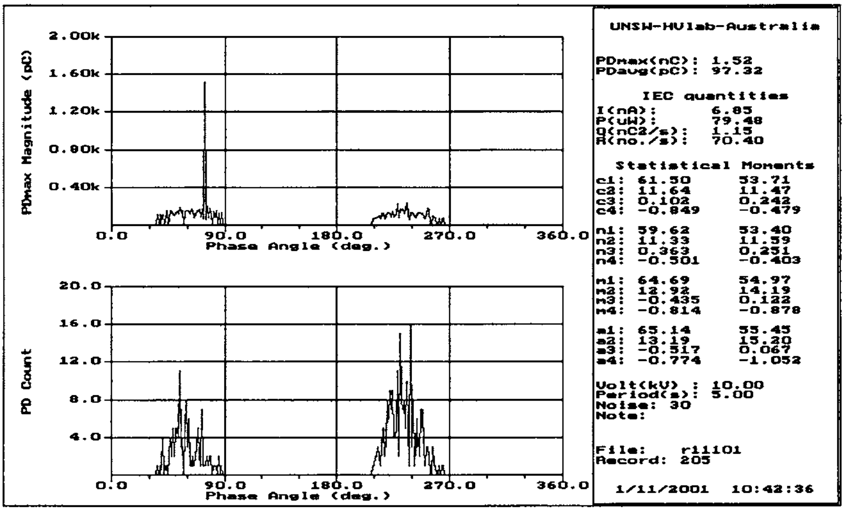

Figure 5-24. Maximum PD 1.52 nC at 10kV, 200 Hz and 145°C

(on fourteenth day)

5.8.2 Effect of Moisture

The frequency was then changed back to 50Hz, and the system was thermally overloaded daily once again for 30 minutes. After a few days it was observed that the maximum PD level had reduced substantially, from 1.52nC to 131 pC (Figure 5-25), and that the PD inception/extinction temperature had increased.

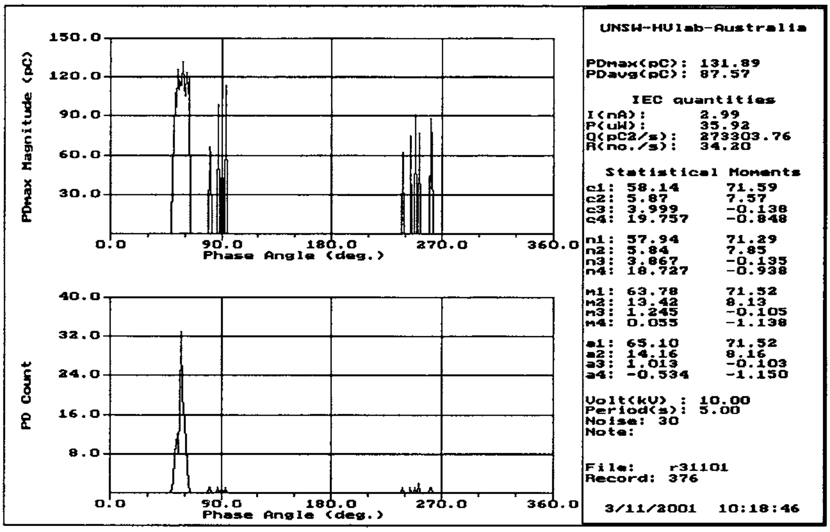

Figure 5-25. Maximum PD 131 pC at 10kV, 50 Hz and 145°C

Thus this indicated some recovery of the insulation properties of the model. The next day the insulation system was found to be discharge-free at the overload temperature. A sample of oil was taken and the moisture content in the oil was found to be 100 ppm less than that measured at the start of experiment.

The system was not then overloaded again on the basis that the prior overloading had somehow dried out the moisture in the oil-paper system. The system temperature was kept at 80°C and then, when overloaded again after two months, no partial discharges were found and the temperature was then decreased from 80°C to room temperature keeping in mind that the paper might re-absorb moisture at the lower temperature levels. The system was then overloaded after three weeks and was found to be still discharge-free. Thus it can be concluded that some drying had indeed occurred.

The system was then shut down and water drops were added directly to the oil. When tested again three weeks later at overload temperature the system was still found to be discharge-free. The system was again shut down and further water drops added directly to the paper this time. The temperature was then again raised to 80°C and when the voltage was applied after a few days it was found that the system was again discharging but now at only 8kV of applied 50 Hz voltage. The PD pattern at this level is shown in Figure 5-26.

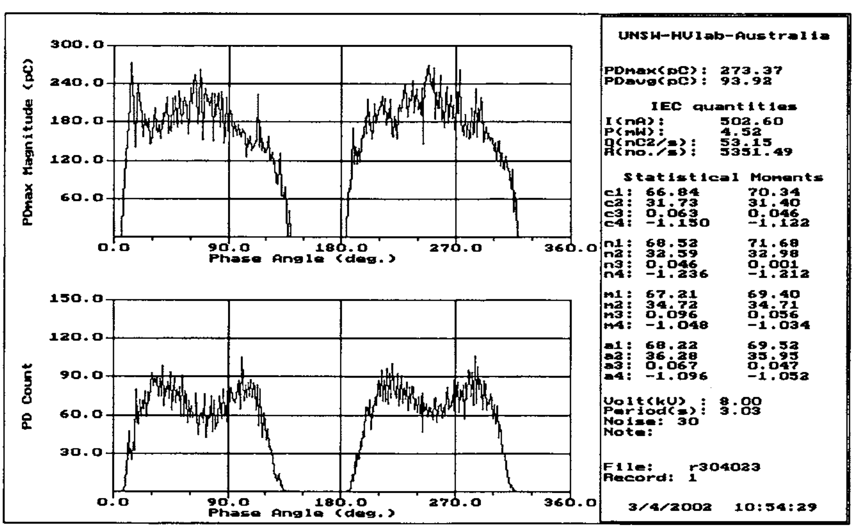

Figure 5-26. PD Pattern After Moisture was Added at 8kV, 50 Hz and 80°C in April 2002

This decrease of the inception level was thus caused by the moisture added to the paper and by the resulting thermal damage caused by the overloading. The PD pattern shown in Figure 5-27 was observed during experiments in December 1997, at the time when water was added directly to the paper of an insulation system that was new and was initially discharge-free after overloading.

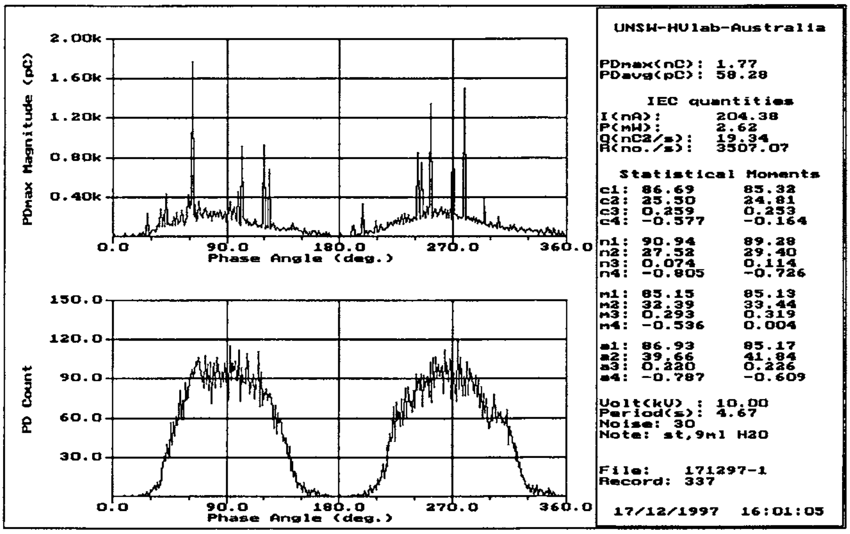

Figure 5-27. PD Pattern After Moisture was Added at 10kV, 50 Hz and 80°C in December 1997 (9 years later)

5.8.3 <u>Effect of Ageing</u>

The PD patterns in the similar investigations reported here (Figure 5-26) have changed as a result of this damage and the overloading. Note that the repetition number pattern in Fig 5-26 has a dip at about the peak voltages and that the PD activity now starts at a much lower phase angle than was previously the case, indicating some permanent damage. The dip in the repetition number pattern at about peak voltage can be explained as due to the high repetition rate. This change in the PD pattern behaviour can thus be associated with ageing of the cellulose material due to moisture and thermal effects.

It was also observed that the colour of the oil had changed during the tests (see Figure 5-28) from clear to light brown due to thermal ageing of the cellulose materials and to oxidation of the oil. The change of colour of the oil is quite typical and can be explained by the fact that at high temperature oil absorb more moisture, gases and contaminants. The gas consists mainly of oxygen, which acts as an oxidant to the oil and in the presence of high temperature and contaminants causes oxidation of oil those results in darkening of the oil.

Figure 5-28. Change in Oil Colour; Left is Aged Oil and Right is New Oil

The signs of ageing damage and deterioration were also observed on the high voltage electrode crepe paper insulation covering (Figure 5-29) and the low voltage electrode kraft paper and pressboard (Figure 5-30). The colour of the paper and pressboard were also changed to a dark colour from the original light colour. The signs of black carbonised marks caused by the PD activity are also very prominent on the aged crepe paper, kraft paper and pressboard. Figures 5-3 and 5-4 show the new condition of the insulation for comparison.

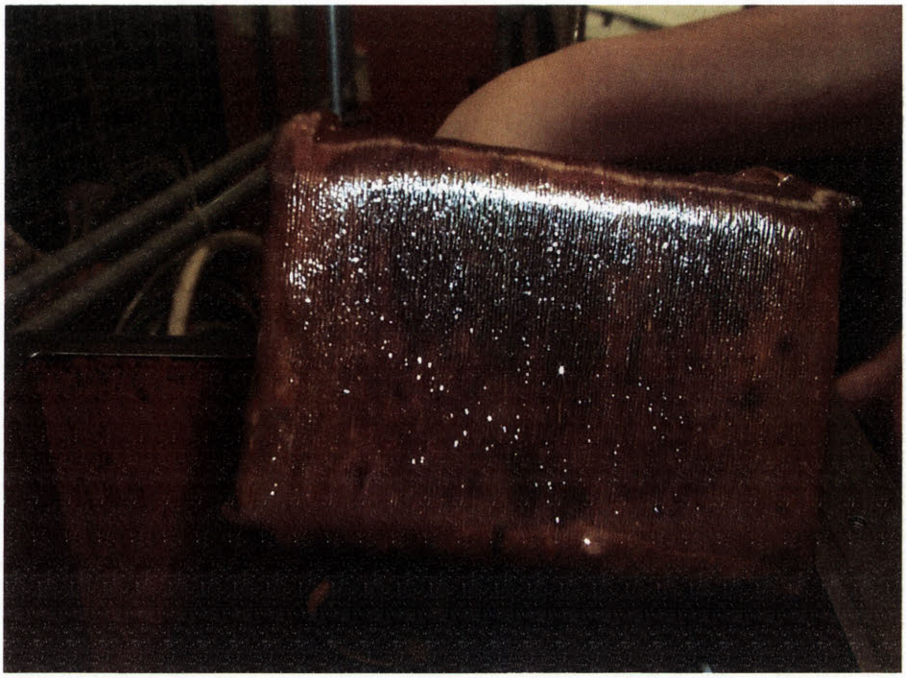

Figure 5-29. Damaged Caused to Crepe Paper at High Voltage Electrode

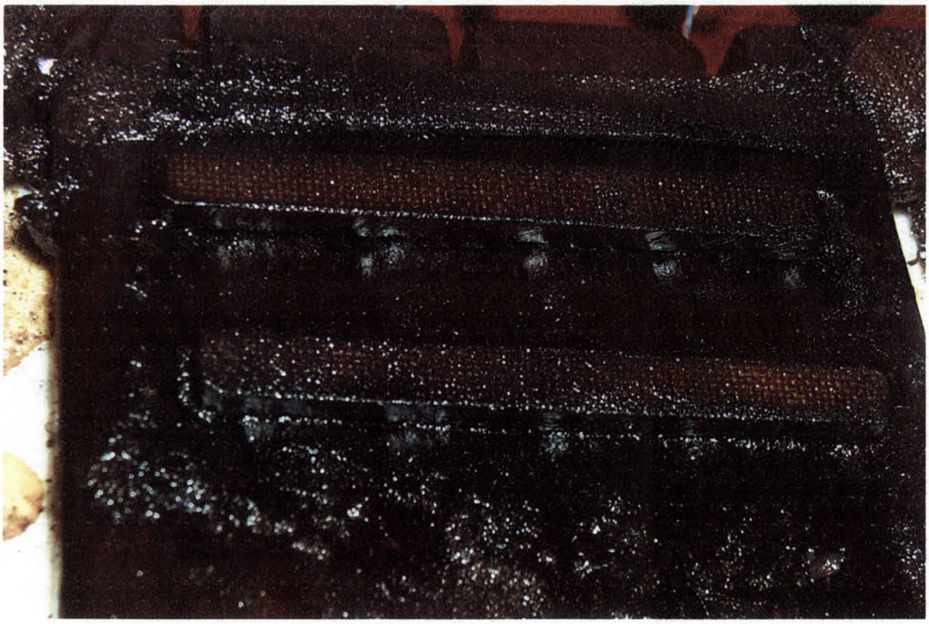

Figure 5-30. Damaged Caused to Kraft Paper and Pressboard at the Low Voltage Electrode

This can be explained because paper and pressboard materials contain 90% cellulose which is a natural polymer of glucose. At high temperatures the polymer chains break and form water especially in the presence of oxygen. The moisture generated, the oxygen and high temperature then cause oxidation that results in the change of colour of the cellulose material. High moisture content in cellulose-based materials also reduces the dielectric strength and cause PD activity to occur. The PD activity is low level in the start but this grows with ageing and forms then forms black carbonised conducting paths along the surface of the cellulose based materials. In this escalation process the PD activity can ultimately lead to total failure of the insulation.

5.8.4 New Transformer Oil with Aged Paper and Pressboard

The system was then overloaded at a temperature of 140-145°C for five weeks for 30 minutes daily in order to dry the paper insulation out by expelling the internally generated moisture. The PD pattern then recorded at the overload temperature is shown at Figure 5-31 below.

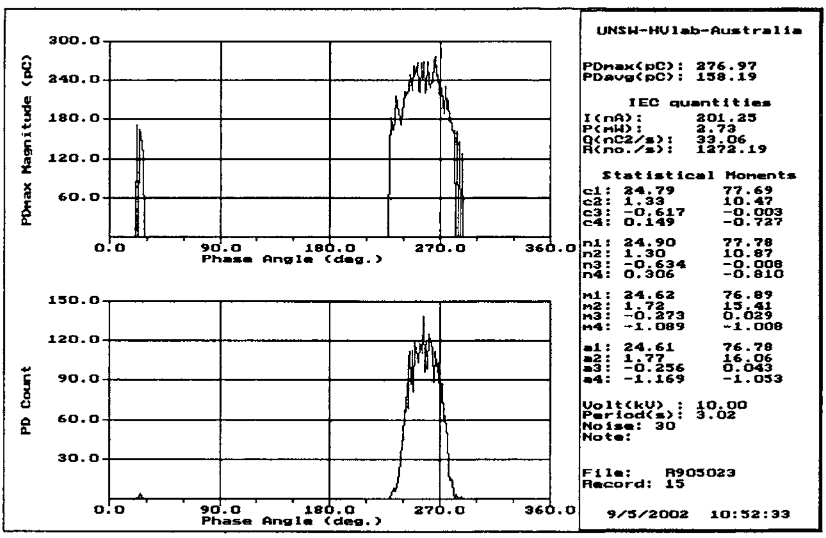

Figure 5-31. PD Pattern Before Oil Change at 10kV, 50 Hz and 140-145°C

To study the effects of new transformer oil in conjunction with an aged sample, the aged transformer oil used for the tests in Figure 5-31 was replaced by new transformer oil. When the system was again overloaded then it was found to be not discharging while raising the temperature from 80 to 145°C. However, after overloading for 20 minutes at a temperature of 140-145°C (Figure 5-32) it then started discharging.

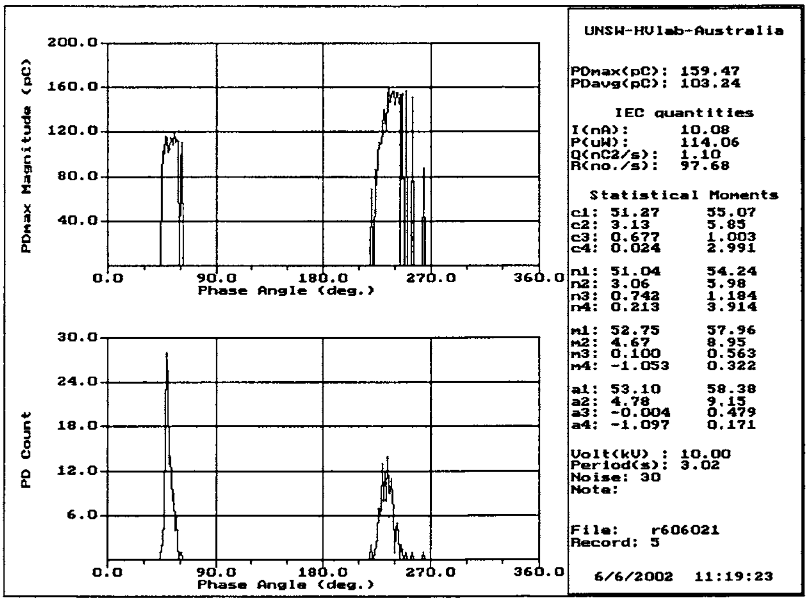

Figure 5-32. PD Pattern After Oil Change at 10kV, 50 Hz and after 20 minutes Overloading at 140-145°C

The discharge level was quite low at about 103 pC average and the repetition rate was about 100 per sec. The low discharge level showed the improvement in the insulating properties due to the increased dielectric strength of the new transformer oil. The PD pattern of the activity was very similar to that obtained previously but due to the new insulating oil the PD values reduced. The PD maximum reduced from 276 pC to 159 pC and PD average from 158 pC to 103 pC. There was a great change in the values of repetition rate. It decreased from 1272 (no./s) to 97 (no./s).

After overloading for a further two weeks on a daily basis, it was observed that the system was not discharging at the 140°C overload temperature. It was also observed of the insulating paper of the high voltage and low voltage electrodes that very thin fibres of paper were produced due to long term exposure of the insulation paper to high temperature and moisture levels. This phenomenon can be explained by loss in mechanical strength of the paper due to heavy loading resulting in a low DP value and as long as the paper does not break into pieces it remains electrically satisfactory, even though some fibres are generated due to loss of tensile strength due to low DP.

5.8.5 New Transformer Oil with New Paper and Pressboard

The system was then shut down and all of the insulating material used, including the degraded paper on the LV and HV electrodes, the degraded pressboard and insulating oil was fully replaced by new paper insulating material to study the comparative effects of aged and new insulating material in terms of partial discharge activity. The temperature of the oil in the tank was initially maintained constant at 80°C. The temperature was then raised uniformly by increasing current until the conductor temperature reached 145°C.

The temperature was then maintained at 145°C for 30 minutes. After thermal overloading for 30 minutes it was observed that the maximum level PD attained was 561pc, and the phase pattern was as shown in Figure 5-33. These are very different to the PD patterns of the aged materials and thus comparison and analysis of the patterns for the two may allow some means of identifying aged material. Comparing Figure 5-32 with Figure 5-33 we can see that the PD count and magnitudes and distributions in Figure 5-33 are similar in both half cycles, whereas in Figure 5-32 the PD count and magnitude are quite dissimilar in the two half cycles. The PD count rate is very small in the new material, as would be expected. The magnitude of the PD has increased with the new insulation but with the much lower count the IEC integrated current is much lower (4 nA after compared to 10 nA before).

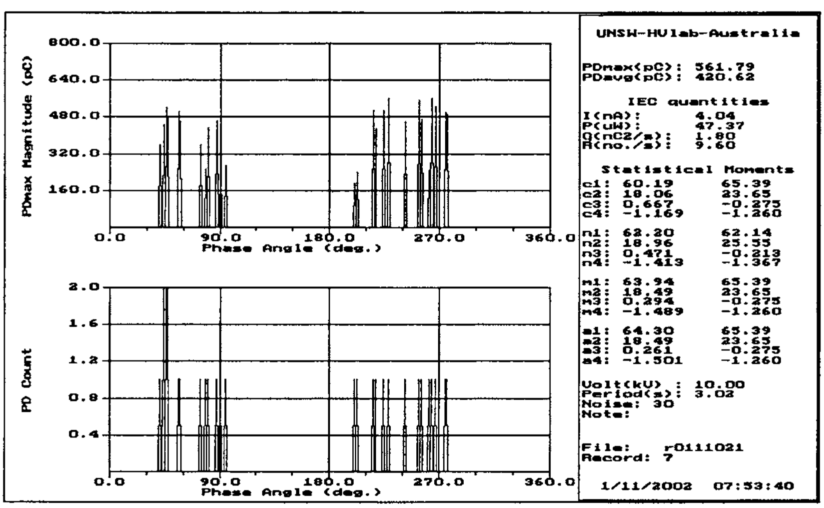

Figure 5-33. PD Pattern for New Insulating Material

[at10kV, 50 Hz and 140-145°C]

The increase in maximum PD level with new insulation is likely to be the result of some intrinsic moisture content initially in the paper that was not removed by the initial conditioning process. After overloading for a few days it was observed that the oil-impregnated system was then not discharging even at the overload temperatures. Thus it was likely that the prior overloading had dried substantially the initial moisture out of the paper in the oil-paper system. The system was then shut down and left at ambient temperature for almost eight months to see the long term ageing effects and to allow the moisture that was dried from the paper insulation to be gradually re-absorbed by the paper again.

The system was then again overloaded after the eight month period and it was found that at an overload temperature of 140-145°C the system was then discharging again and showing signs of ageing of the paper. The PD maximum magnitude increased to 946pC from the 561 pC prior to the layoff period, and the PD average increased to 527pC from 420pC and the repetition rate increased to 166 (no./s) from 9 (no./s), all as shown in Figure 5-34 below.

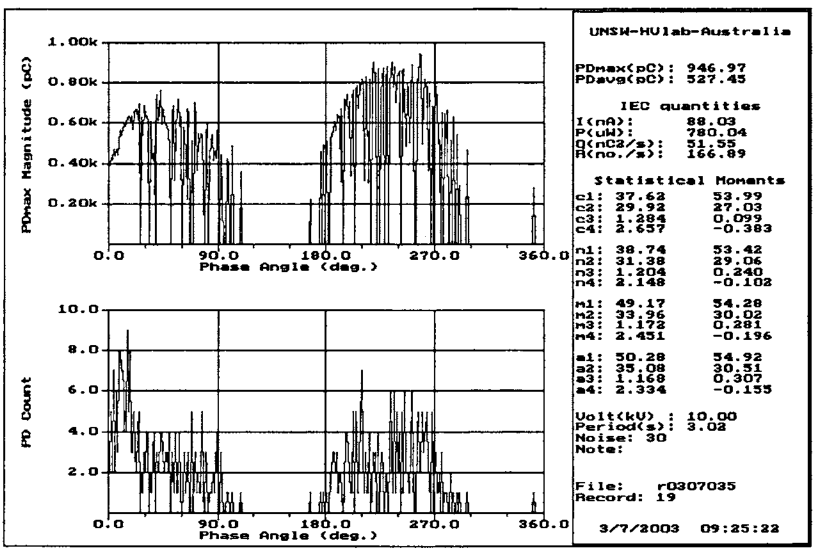

Figure 5-34. PD Pattern for New Insulating Material after 8 Months layoff [tests done at 10kV, 50 Hz and 140-145°C]

It is of some importance also to note that the phase dependence of the PD activity has also changed substantially over the period. The PD activity after the rest period starts at an inception angle lower than zero degrees, as compared to before when it started at an angle of more than 30 degees (see Figure 5-33). This is most likely due to ingress of moisture into the paper insulation at room temperature and ageing of the the sample over the almost eight month lay off period so the system can degrade even it is not energized. A Polarisation/Depolarisation Current test (PDC) was also carried out by KEA Consultants on the test cell before the CDA3 tests were performed and these results also indicated significant ageing of insulation. The results are shown in Annexure "C".

5.8.6 Effect of temperature, voltage and frequency on PD activity

The experimental tests reported here were combinations of high thermal and electrical stresses applied to the new oil-impregnated insulation. The aim of the experiment was to see the effect of overload temperatures reached during sudden high level overloading of transformers and also to determine the effects of overvoltages (and undervoltages) imposed on the insulation system.

In addition to these effects, tests were also performed to study the effects of ageing caused by change of frequency. Increased frequency excitation is frequently used to accelerate PD ageing of insulation on the basis that an increased number of voltage cycles will increase the number of PDs linearly with frequency. There are some indications that this linear increase is not fully applicable in all test configuration conditions [206] and the tests reported here were performed to determine whether such a linear ageing rate is applicable in this case and to determine whether such an accelerated ageing technique is valid, in terms of the quantification multipliers (linear) normally used.

After setting up the test equipment, different sets of experiments were conducted using different voltages, frequencies and temperatures. The applied voltages used were 10, 13 and 16 kVrms and the corresponding electric stress imposed across the paper insulation was 1.8, 2.4 and 2.9 kV/mm respectively. The test voltage frequencies used were 50 Hz and 200Hz and the test temperature levels were 80, 100, 120 and 140°C. The temperature of the oil was maintained at 80°C.

The temperature of the low voltage winding was raised by use of the current transformer and was monitored by the fibre optic sensor. The test voltage magnitude and frequency were varied by utilising a variable voltage and variable frequency converter. In total, forty two experiments were performed with different conditions and parameters. These were divided into three groups or Test Cases.

In Test Case-1, the test voltage magnitude was fixed at 10kV, while the test voltage frequency and the test temperature of the conductor winding were varied. The test parameters (temperature, applied voltage and frequency) of the sequence of the 14 experiments performed in Case-1 are shown in Table 5-1.

Test 1	80°C/10kV/50Hz	Test 2	80°C/10kV/200Hz
3	100°C/10kV/50Hz	4	100°C/10kV/200Hz
5	120°C/10kV/50Hz	6	120°C/10kV/200Hz
7	140°C/10kV/50Hz	8	140°C/10kV/200Hz
9	120°C/10kV/50Hz	10	120°C/10kV/200Hz
11	100°C/10kV/50Hz	12	100°C/10kV/200Hz
13	80°C/10kV/50Hz	14	80°C/10kV/200Hz

Table 5-1. Frequency and Temperature Levels for a Test Voltage of 10kV

In Test Case-2 and Test Case-3, the experiments were repeated with test voltage levels of 13 and 16kV as shown in the sequences in Tables 5-2 and 5-3 respectively. In each case, there were fourteen sets of readings. Thus, altogether forty-two sets of results were obtained. The experiments were also repeated to reduce any inconsistencies.

Test 1	80°C/13kV/50Hz	Test 2	80°C/13kV/200Hz
3	100°C/13kV/50Hz	4	100°C/13kV/200Hz
5	120°C/13kV/50Hz	6	120°C/13kV/200Hz
7	140°C/13kV/50Hz	8	140°C/13kV/200Hz
9	120°C/13kV/50Hz	10	120°C/13kV/200Hz
11	100°C/13kV/50Hz	12	100°C/13kV/200Hz
13	80°C/13kV/50Hz	14	80°C/13kV/200Hz

Table 5-2. Frequency and Temperature Levels for a Test Voltage of 13kV

Test 1	80°C/16kV/50Hz	Test 2	80°C/16kV/200Hz
3	100°C/16kV/50Hz	4	100°C/16kV/200Hz
5	120°C/16kV/50Hz	6	120°C/16kV/200Hz
7	140°C/16kV/50Hz	8	140°C/16kV/200Hz
9	120°C/16kV/50Hz	10	120°C/16kV/200Hz
11	100°C/16kV/50Hz	12	100°C/16kV/200Hz
13	80°C/16kV/50Hz	14	80°C/16kV/200Hz

Table 5-3. Frequency and Temperature Levels for a Test Voltage of 16kV

During the experiments, it was observed that with an increase in applied voltage from 10 to 16kV, while keeping other parameters constant, the peak and the average PD magnitude as well as the PD number, all increased with the increase of applied voltage. The peak PD magnitude increased from 85 pC (Figure 5-35) to 1.31 nC (Figure 5-37) and the average PD magnitude increased from 35 pC to 115 pC. Similarly, the PD repetition rate number increased from 3 to 1483 (no./s).

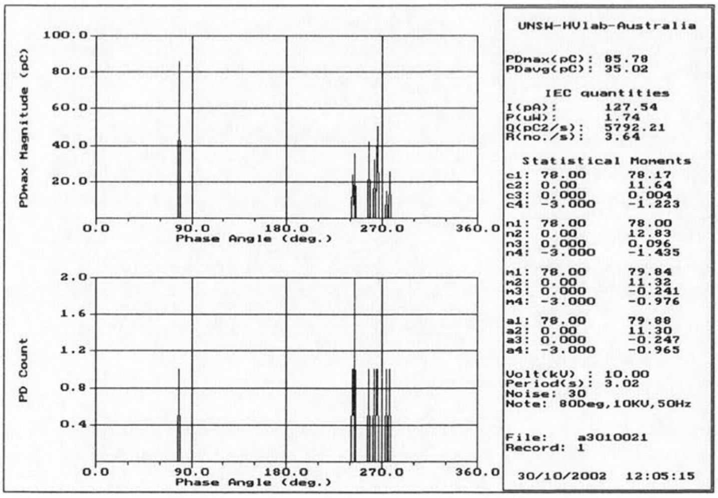

Figure 5-35. PD Pattern at 80°C, 10kV and 50Hz

The inception phase angles decreased with increase of voltage from 10 kV to 16 kV. The inception angle decreased from around 75 degrees at 10 kV to 30 degrees at 13 kV. Also it further deceased at 16 kV to less than zero degrees. The overall total shift of inception angle from 10 kV to 16 kV was around 105 degrees. Figures 5-35 to 5-37 show the shift of PD inception angle from 10kV to 16 kV.

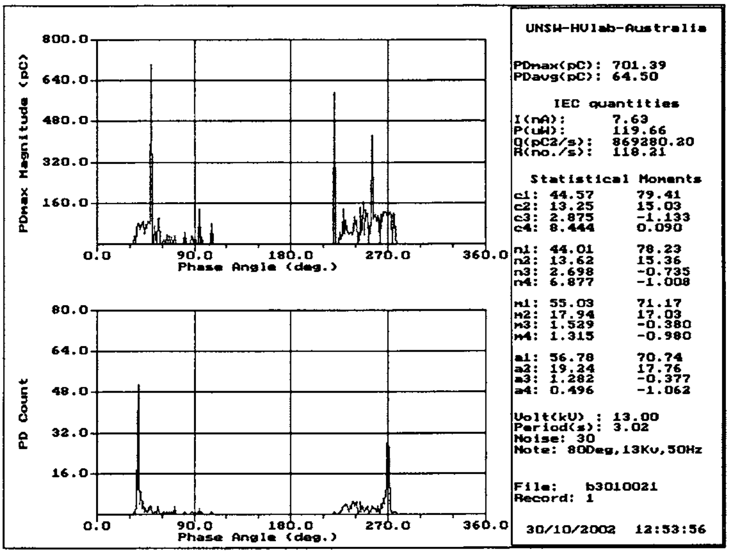

Figure 5-36. PD Pattern at 80°C, 13kVand 50Hz

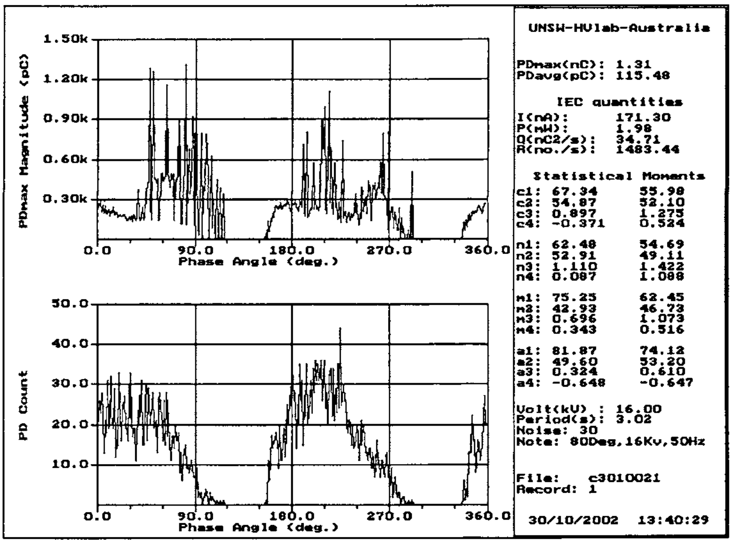

Figure 5-37. PD Pattern at 80°C, 16kV and 50Hz

It was also noted that with a change of frequency from 50 to 200Hz, the peak and the average PD magnitude decreased (the peak from 1310 to 447 pC and the average from 115 to 80 pC), however the PD repetition rate increased from 1483 to 3637 no. per sec. The inception angle did not change with the change of frequency (Compare Figures 5-37 and 5-38).

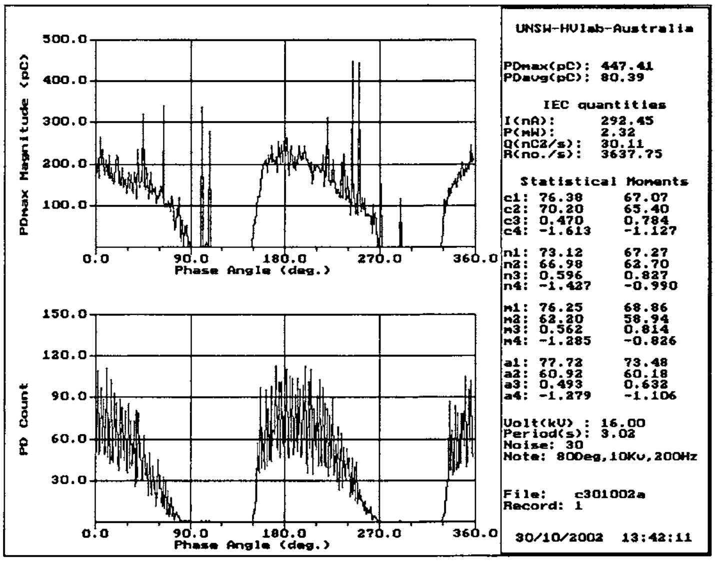

Figure 5-38. PD Pattern at 80°C, 16kV and 200Hz

Similar observations were noticed while observing previous PD data recorded in November 1996 (See Figure 5-39 for 50 Hz and 5-40 for 200Hz).

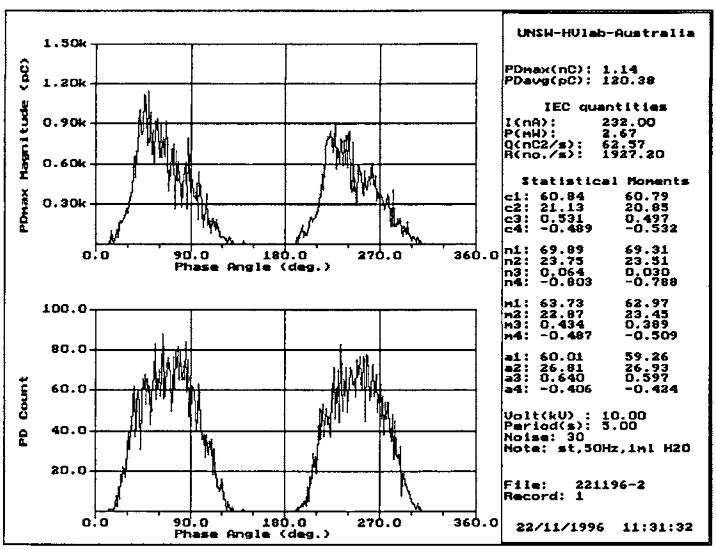

Figure 5-39. PD Pattern at 80°C, 10kV and 50Hz in November 1996

Although the inception levels were quite different in 1996, the relative magnitudes were quite similar between the two frequency conditions. It is noted that in 1996 the PD number ratio of 200 Hz activity to 50 Hz, a frequency ratio of 4, was 2.66, while in the current tests reported here it was 2.45. The ration of the IEC power was 2.45 and of the quadratic rate was 2.11.

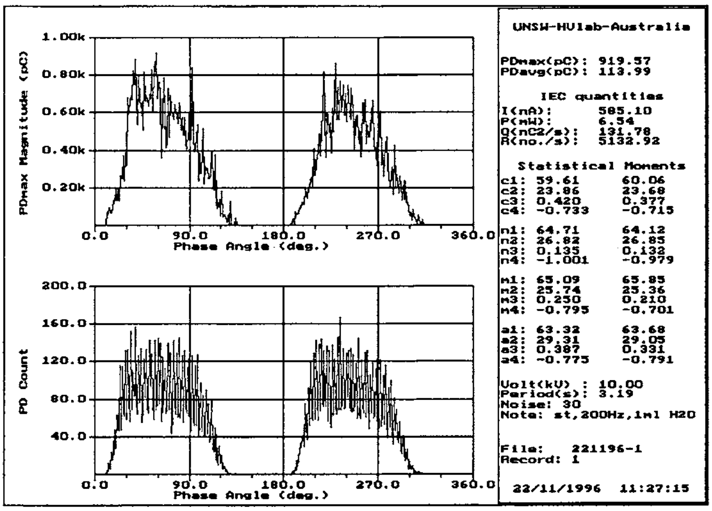

Figure 5-40. PD Pattern at 80°C, 10kV and 200Hz in November 1996

The test results also indicated that the peak PD magnitude, the average PD magnitude and the PD number increased with an increase in the test temperature (see Figures 5-37 and 5-41 for comparison). All of these values decreased with the decrease in temperature. However, the inception angle did not change with the change of frequency. In this instance, the peak PD magnitude had increased from 1.31nC (Figure 5-37) at 80°C to 3.59nC (Figure 5-41) at 140°C. For a similar range of temperature, the average PD magnitude had increased from 115 to 235pC and the PD repetition rate number had increased from 1483 to 2993 (no. /s).

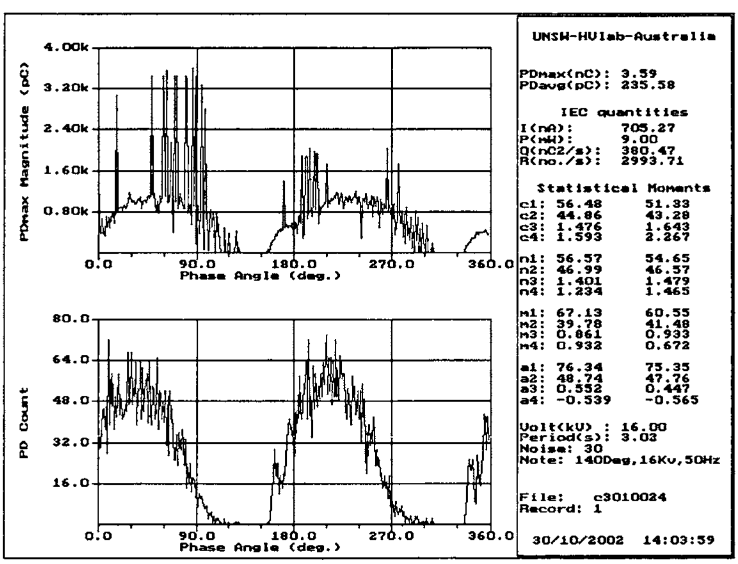

Figure 5-41. PD Pattern at 140°C, 16kV and 50Hz

5.8.7 Effect of Temperature, Voltage and Frequency on PD current waveform

The above results were supported by monitoring of the PDs using a high frequency current transformer (Figure 5-42) on the earth connection to pick up the true PD current waveform signals. The discharges picked up by high frequency current transformer were displayed on a digital storage oscilloscope model Lecroy 9362C (Figure 5-43). The frequency range of the HFCT was 10 kHz to 250 MHz. The advantage of using the HFCT was its simplicity and high sensitivity. The voltage and frequency were again changed using AC power supply/frequency converter model PCR-1000 (Figure 5-20).

Figure 5-42. Clip–On High Frequency Current Transformer

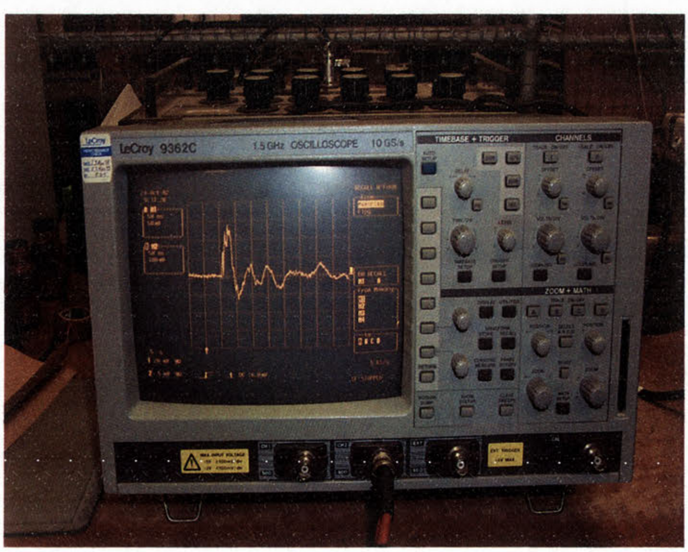

Figure 5-43. Oscilloscope Model Lecroy 9362C

First tests were performed with the HFCT and the oscilloscope on the insulation model using an applied voltage varying from 10 kV to 16kV and by keeping other parameters (temperature and frequency) constant. Then, the frequency was changed from 50 to 200Hz for the voltage range with other parameters constant and also temperature was increased from 80°C to 140°C, keeping other parameters constant.

The peak PD voltage magnitudes were recorded. Figures 5-44 to 5-48 show the true PD current waveforms obtained with the HFCT.

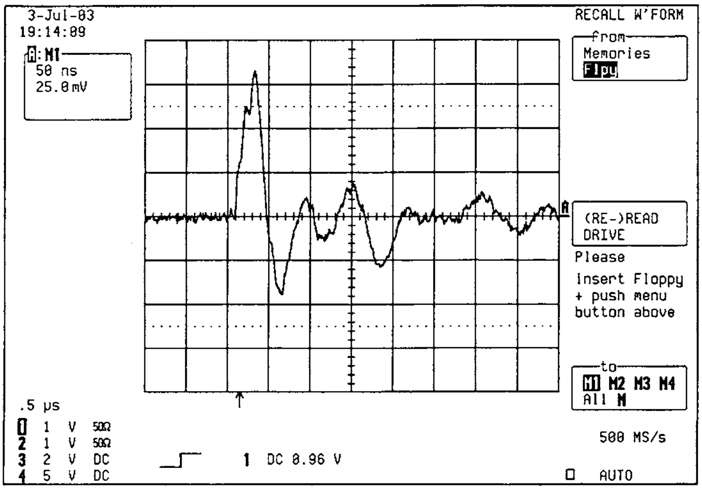

Figure 5-44. True PD Pattern at 80°C, 10kV and 50Hz:

25 mV per division: 50 nsec per division:

PD Voltage Peak Magnitude ~ 85 mV

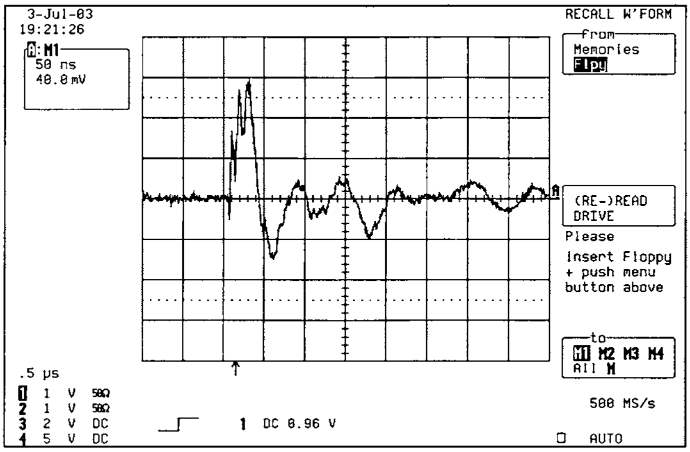

Figure 5-45. True PD Pattern at 80°C, 13kV and 50Hz:

40 mV per division: 50 nsec per division:

PD Voltage Peak Magnitude ~ 120 mV

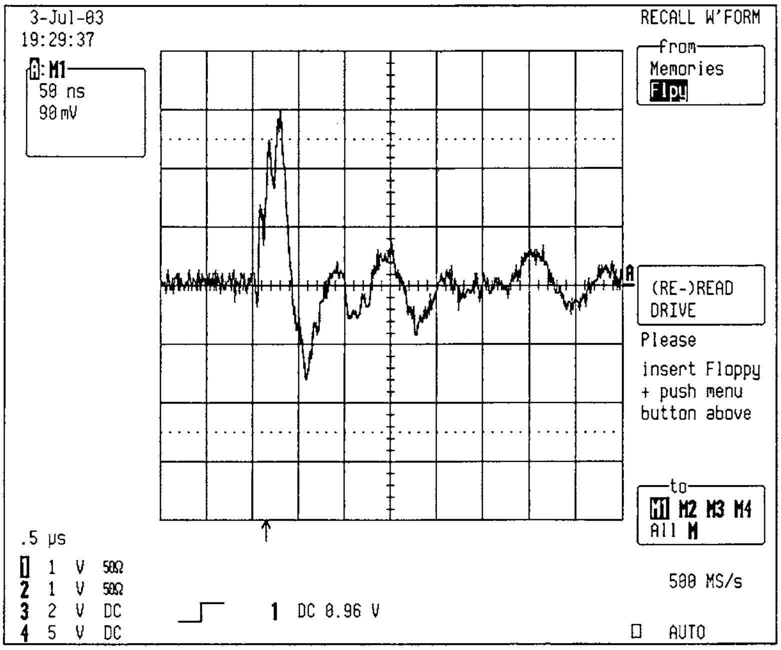

Figure 5-46. True PD Pattern at 80°C, 16kV and 50Hz:

90 mV per division: 50 nsec per division:

PD Voltage Peak Magnitude ~ 270 mV

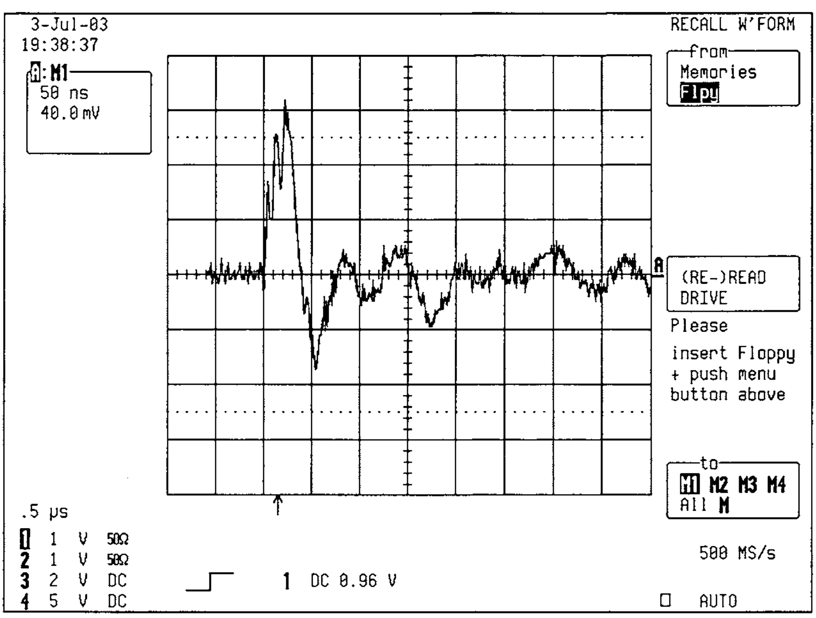

Figure 5-47. True PD Pattern at 80°C, 16kV and 200Hz:

40 mV/div: 50 nsec/div:

PD Voltage Peak Magnitude ~ 128 mV

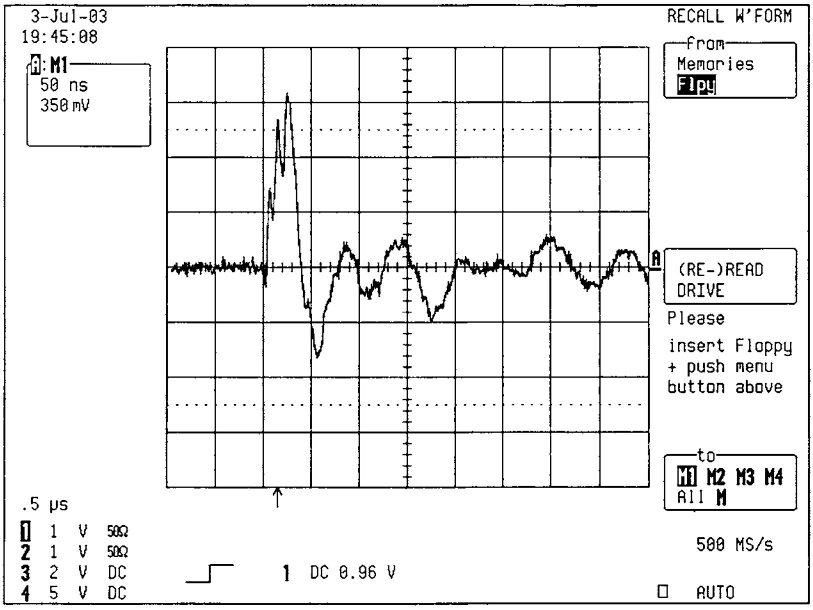

Figure 5-48. True PD Pattern at 140°C, 16kV and 50Hz:

350 mV/div: 50 nsec/div:

PD Voltage Peak Magnitude ~ 1120 mV

During the experiments, it was observed from the reading on the oscilloscope that with an increase in applied voltage from 10 to 16kV, keeping other parameters constant, the peak PD voltage magnitude increased with the increase of applied voltage. The peak PD voltage magnitude increased from 85 mV (Figure 5-44) to 270 mV (Figure 5-46) between 10 and 16 kV. It was also noted that with a change of frequency from 50 to 200Hz, the PD voltage magnitude decreased. The PD voltage magnitude decreased from 270 mV (Figure 5-46) to 128 mV (Figure 5-47). Further it was noted that an increase in temperature from 80 °C to 140°C and by keeping other parameters constant the peak PD voltage magnitude increased with the increase of temperature. The peak PD voltage magnitude increased from 85 mV (Figure 5-44) to 1120 mV (Figure 5-48).

5.8.8 <u>Effect of Moisture, Temperature and Ageing</u>

The temperature of the system was then lowered from 80°C to room temperature by switching off the heaters at the base of the steel tank. The aim was to allow more moisture to be absorbed by the paper at room temperature. Prior to lowering of the temperature the system was found to be not discharging at even an overload temperature of 140-145°C.

The aim of this particular experiment was to see the combined effects of moisture, temperature and ageing on the oil-impregnated insulation. The temperature of the tank was then once again raised from the room temperature level after absorption of moisture to 80°C after ageing for almost three years to see the extended long-term effects of ageing in the oil-impregnated insulation.

The voltage was raised to 10kV and it was found that the system was discharging at 80°C. Figure 5-49 shows the PD pattern obtained and it indicates degradation of the insulation due to the effect of moisture absorbed in the oil impregnated insulation model and also due to prior overloading. The results obtained for the ageing of oil-impregnated insulation support the assertion that the transformer in service can absorb less moisture as compared to a transformer in storage. The paper insulation in the transformer can absorb more moisture at ambient temperature compared to a transformer in service at higher temperatures.

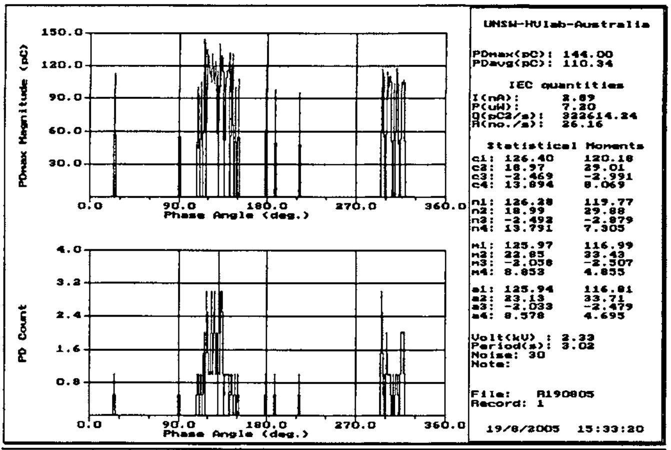

Figure 5-49. PD Pattern at 10kV, 50Hz and 80°C; (After Ageing for Three Years)

The temperature of the copper winding and paper was then increased until the conductor temperature reached 145°C. This was done in order to dry out the paper insulation. The temperature was then maintained at 145°C for 30 minutes and then reduced to 80°C. Many bubbles were observed to be released with some large and some small at temperatures of 140-145°C and it was also observed that water droplets accumulated on the glass bushing. The cycle of increasing temperature from 80°C to 145°C and then reducing back to 80 C after 30 minutes was repeated four times daily to remove moisture present in the paper quickly. After one week of such overloading cycles the insulation system was found to be discharge-free even at the overload temperature, indicating that the moisture had been removed from the paper.

The system voltage was then shut down and system temperature allowed to drop to ambient and water drops were added directly to the paper. The temperature was then again raised to 80°C and when the voltage was applied after a few days it was found that the system was again discharging, now at only 8kV applied voltage. The PD pattern recorded is shown in Figure 5-50. The water added directly to the paper and the resulting thermal damage caused by the overloading thus caused this decrease in the PD inception level.

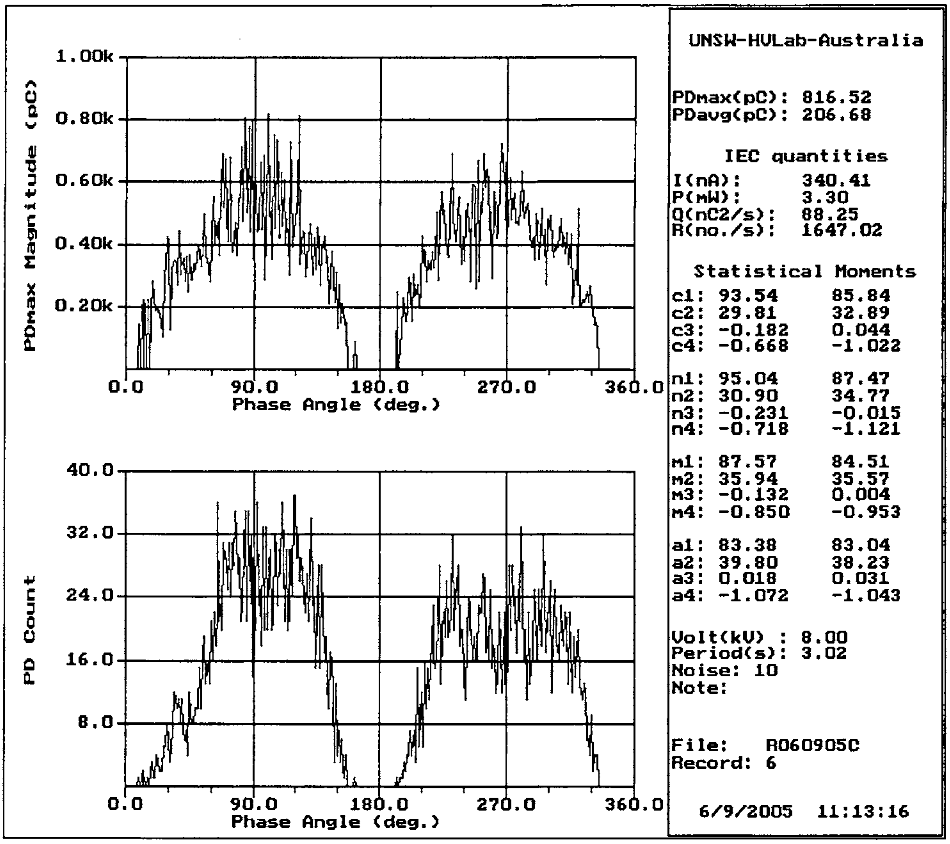

Figure 5-50. PD Pattern at 8kV, 50Hz and 80°C in September 2005; Moisture Added to Paper Insulation

The PD pattern and results obtained now show close similarity with the results of experiments performed earlier in April, 2002 (Figure 5-26) and in December 1997 (Figure 5-27). This similarity is especially the case in comparison with Figure 5-26.

The decrease of the inception level voltage to 8 kV and the low inception phase angle of less than 10 degrees as seen in Figure 5-50 and Figure 5-26 was thus caused directly by the water added to the paper and by the resulting thermal damage caused by the overloading.

The most common feature of all in the above three Figures is the low inception angle and the high repetition rate (no./s). Therefore, it can be taken that the change of PD pattern with moisture in the paper and ageing in a phase resolved plot to a low PD inception angle and high PD repetition rate can be used as a very useful diagnostic tool in identifying moisture and ageing affects in oil-impregnated cellulose-based transformer insulation.

5.9 Discussion and Conclusions

The following observations and discussion are based on over five years of extensive research investigations of the oil impregnated paper insulation model, and over four years of my own experimental work and detailed scrutiny of previous experimental work carried out on the same sample as used and reported on here since 1996 on new and aged oil-impregnated insulation.

- Gas bubble formation occurred at temperatures of the oil-paper insulated conductor at 140-145°C. Such temperatures may be reached in transformers during transient overload conditions that may occur during a heavy overload of a transformer and thus the results of the investigations reported, which were also performed at typical electrical stresses, are relevant to practical transformer configurations.

- The release of large gas bubbles caused a significant decrease in the maximum PD level, due to the change of the involvement of the cellulose material in the PD activity. That is, the bubbles in free oil rather than in the cellulose limited the PD level generated.

- The formation of gas bubbles at high temperature can cause ageing of the paper insulation and this can cause the discharge inception to occur at lower paper temperatures.

- During thermal overloading in the oil-impregnated paper insulation, moisture from the paper will move freely into the oil and to the air space above the oil but the reverse process, moisture transfer from oil to paper, is much slower.

- Incursion of moisture into high electric field strength regions can cause PDs of high intensity due to a reduction in breakdown field strength or some disturbance in the moisture equilibrium.

- The reduction in the bubble generation frequency at high temperatures can eventually result in lower moisture content in the paper.

- During thermal overloading from 80°C to 145°C, the peak PD magnitude, the average PD magnitude and the PD number increases with increase of temperature and when temperature decreases, PD number decreases also.

- When the applied voltage changed from 10 to 16kV, the peak PD magnitude, the average PD magnitude and the PD number increased with the increase of the test voltage and vice-versa.

- When the test voltage frequency changed from 50 to 200 Hz, the peak and the average PD magnitude decreased, whereas the PD number increased with the increase of frequency. A reverse trend occurred when the test voltage frequency was reduced. The increase in PD number and in the other related IEC integrated parameters of power and quadratic rate did not indicate an increase consistent with the increase in frequency: i.e. the change was not linear with frequency.

- Paper is the primary source for the moisture content of the oil during overloading and moisture in the insulating paper is more dangerous in term of PD activity as compared to moisture in the insulating oil.

- The colour of oil changes from clear to light brown and for paper/pressboard change similarly with ageing due to thermal, environmental and electrical stress.

- Cellulose paper loses its mechanical strength with ageing. It was observed during visual inspection during replacing aged insulating oil with new oil that thermal overloading caused the fibre of the crepe paper to separate slightly. As the paper did not break up into pieces, however, it remained electrically satisfactory.

- The change of the PD phase pattern to a low PD inception angle and high PD repetition rate when the insulation ages can be used as a very useful diagnostic tool in identifying moisture and ageing affects in oil-impregnated cellulose based transformer insulation.

The results of this investigation have shown the complexity involved in correlation of the effects of moisture with temperature on PD activity in transformer type insulation. The level of PD activity is affected directly by the temperature itself. Results indicated that the PD activity varies considerably under simultaneous voltage and thermal stresses. It was also found that prolonged operation at high temperatures reduced moisture levels and changed PD behaviour, and moisture in insulating paper is more dangerous in term of PD activity as compared to moisture in insulating oil.

This complexity may lead to some potential problems in interpretation of the results of PD measurements performed on transformers. Much further work is needed to elucidate the impact of the various parameters on PD activity before any definitive indicators of ageing quantification can be derived. Despite shortcomings, the above research nevertheless can be extremely useful in analysing PD data and monitoring of high voltage transformers. However further detailed and long-term investigations are needed to better quantify the results.

Chapter 6

The Effect of Elevated Temperature in Oil-Impregnated Insulation: Statistical Analysis of PD Activity

6.1 Introduction

As with all organic insulation the ageing of oil-impregnated transformer insulation is very dependent on operating temperature rise above ambient. PD measurements of such insulation gives an instantaneous and time-resolved assessment of condition so it is one of the more important tools available for monitoring the transformer insulation [4-6]. However, although technology enables the application of such a diagnostic technique, the interpretation and correlation of the PD characteristics obtained with the ageing of the insulation is an area that still requires some considerable investigation. There is also still a problem with electromagnetic interference on-site that can limit the sensitivity of the PD tests. Although the sensitivity of the PD detection system has been substantially improved since it was first established, there is a possibility that major faults within electrical equipment, especially oil-insulated transformers, may remain undetected [170]. This reality thus requires further investigation in increasing measurement sensitivity within obviously reasonable cost and in improving interpretation of the results of tests. Developments in these areas must be accompanied by fundamental investigations of the PD behaviour under varying conditions; e.g. the temperature and moisture effects in aged insulation. Such investigations will provide better means of interpretation of the test results in terms of insulation condition [171].

This chapter presents the results of a detailed laboratory experimental investigation of PD activity at high temperature in oil-impregnated paper and pressboard material similar to practical transformers. The experiments were aimed to investigate the effects of high temperature similar to that experienced by transformers during very high loads or during through-faults and also to determine the affects of ageing on new mineral oil, on crepe paper, on kraft paper and pressboard materials. The results of the tests will provide useful information on the relationship between PD patterns and activity and ageing of the insulation.

The glass cell model was used in this series of tests and was operated at elevated oil temperatures (80-85°C) from ambient to simulate high temperature conditions such as may occur during abnormal (overload) operation of a transformer. The temperature was then reduced to ambient to study the variation of the phase resolved PD patterns during increase and decrease of the temperature. In the previous chapter the tests reported were obtained from experiments performed on the insulation model in a steel tank and the system temperature was maintained continuously at 80°C with bursts of overload temperature up to the range 140-145°C.

Condition monitoring, especially continuous and on-line, of transformer insulation can provide an early indication of any degradation that may be caused by abnormal electrical, thermal, environmental and mechanical stresses, which may occur during operation. In order to recognise such deterioration from PD patterns and their characteristics, it is necessary to catalogue and understand the correlation of the PD patterns with the insulation condition [47, 77,171].

Thus, in order to obtain better interpretation of the PD patterns so that subtle differences could be determined, the PD patterns were recorded and their derived representative statistical parameters were determined and analyzed for the test conditions when the temperature was increasing and decreasing. The experiments were repeated to eliminate any inconsistency in the test results.

The effects on PD patterns and their characteristics due to aging in the oil-impregnated insulation are also considered in this chapter. The analysis was focused on the statistical discharge quantities that include peak and average PD magnitudes and the IEC integrated parameters of average PD current and PD repetition rate. In addition, observations of the discharge phase distributions were performed using different statistical moments were also conducted. The statistical parameters used were the mean value, the standard deviation, the skewness and the kurtosis of the phase-resolved patterns. These were calculated taking the PD distributions to be Gaussian in distribution. This is not always the case as will have been seen from the previous patterns shown in chapter 5, however the above statistical parameters do provide useful information that can characterise, in a sensitive way, change in PD characteristics.

The results of these tests indicate that the PD activity is greatly affected by the temperature change and ageing and that the statistical parameters do provide a useful indicator of ageing. Thus the use of PD patterns analysis can be a useful ageing condition monitor.

6.2 Experimental Details

6.2.1 <u>Test Configurations</u>

The insulation system that was used in the work described here is designed to simulate the configurations and stress levels at 10kVrms that occur in typical transformer insulation. The electric field stress level used was 2.25kV/mm minimum occurring across the pressboard. The relative dielectric constants of the materials used were: ε_{oil} = 2.2, ε_{paper} = 3.2 and $\varepsilon_{pressboard}$ = 4.2. The test cell is of glass, containing oil impregnated paper insulation and pressboard insulation. The glass cell has a crossed cylindrical shape (vertical and horizontal arms) with an inner diameter of 8 cm. The height of the vertical cylinder and the horizontal cylinder are both 40cm. The structure of the glass cell has a total volume of approximately 3.6 litres. Viewing windows are available at both ends of the horizontal cylinder.

The High Voltage (HV) electrode is attached to the HV connector on the top of the cell. The metal covering is secured by PVC screws and bolts. Next to the HV connector is the breathing hole, which provides access for vacuum impregnation with oil. The low voltage (LV) electrode is attached to the base of the glass cell. Also attached to the base is an inlet/outlet valve, through which the oil is either injected or drained from the glass cell. The cell is designed to withstand continuous high temperature operation and is heated by heating tape wrapped around the lower part of the glass cell. Figure 6-1 shows the test cell used in the experimental investigation and Figure 6-2 shows a schematic of the cell.

Natural heat convection in the hot oil forces the oil to circulate and to transfer heat throughout the test sample. The maximum test temperature reached during the experiments was in the range 80-85°C. After reaching the maximum, the heating source was disconnected and the temperature was then allowed to reduce to ambient by natural thermal dissipation. The ambient temperature during the experiments was in the range 23.5 - 25.5°C. A fibre optic temperature sensor was used to monitor sample and oil temperature. The fibre sensor head was placed on the top surface of the paper/pressboard sample through a breathing hole on the top of the glass cell.

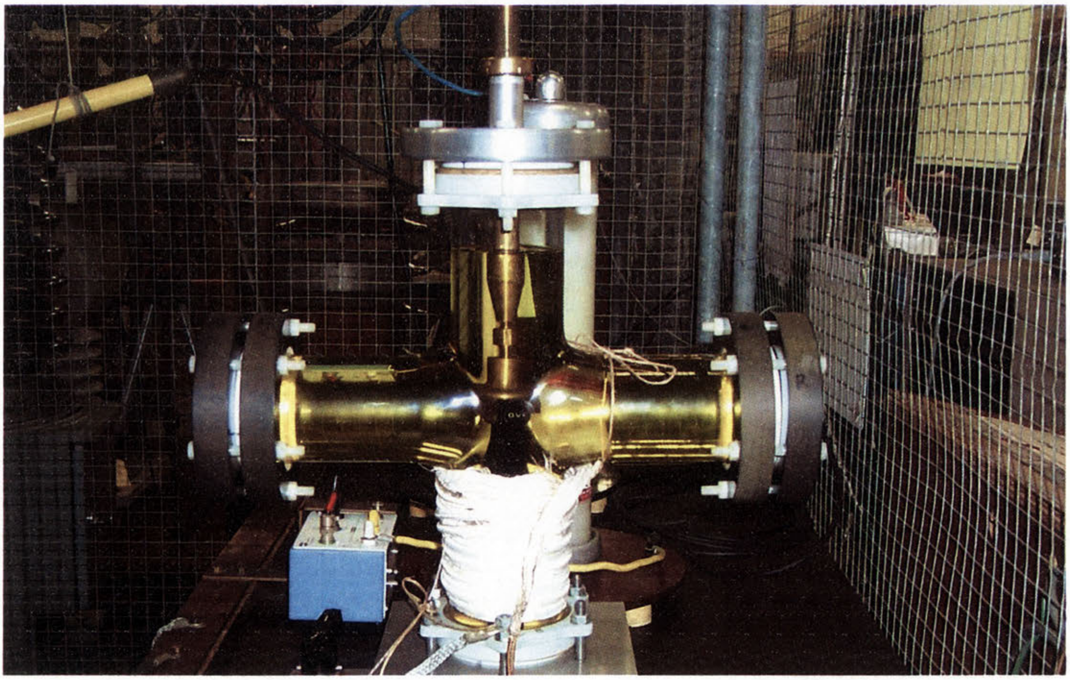

Figure 6-1. The Glass Test Cell

Heights of the vertical and horizontal sections are both 40cm

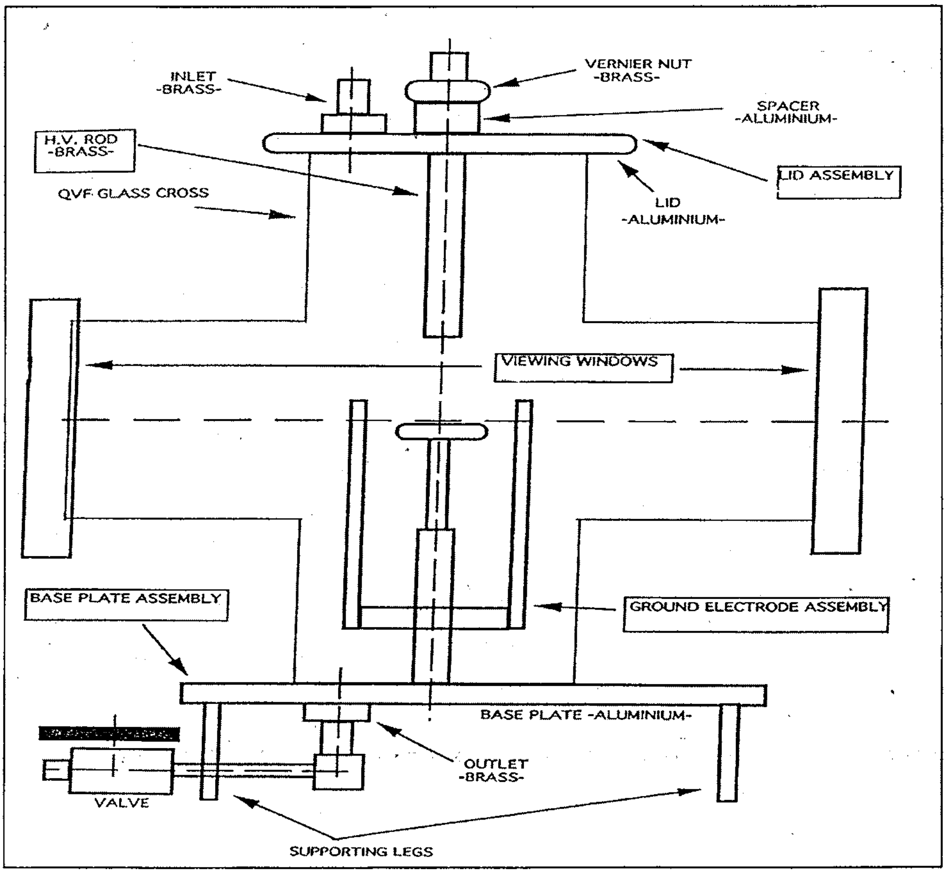

Figure 6-2. The Glass Test Cell Drawing

Heights of the vertical and horizontal sections are both 40cm

Oil-impregnated paper and pressboard material insulate the circular cross-section high voltage (HV) and low voltage (LV) electrodes. The HV and LV electrodes are both of brass, of plane face, and have diameter of 40mm. Figure 6-3 shows the HV and LV electrodes.

The insulation between the high voltage and low voltage electrodes has three compartments. Immediately adjacent to the low voltage electrode are ten layers of kraft paper each of thickness 0.06mm, making a total thickness of paper equal to 0.6mm. Immediately adjacent to the high voltage electrode are two layers of 0.25mm thick crepe paper making a total thickness 0.5mm. The insulation component is a pressboard layer 3mm thick sandwiched between the two paper layers. Overall, the kraft paper, crepe paper and pressboard combination make up a 25 sq.cm area bounded by the electrodes. Figure 6-4 shows the crepe paper, pressboard and kraft paper materials used.

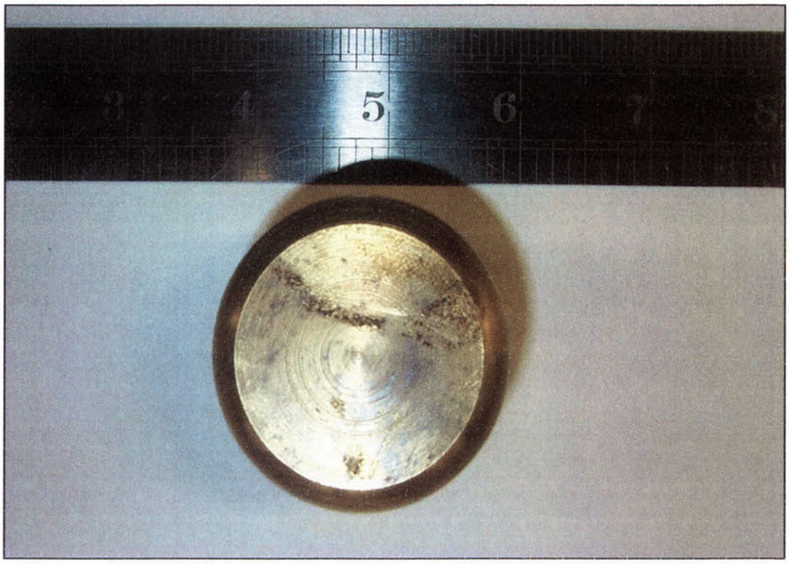

Figure 6-3. The High Voltage and Low Voltage Electrode configuration

(Diameter = 40mm)

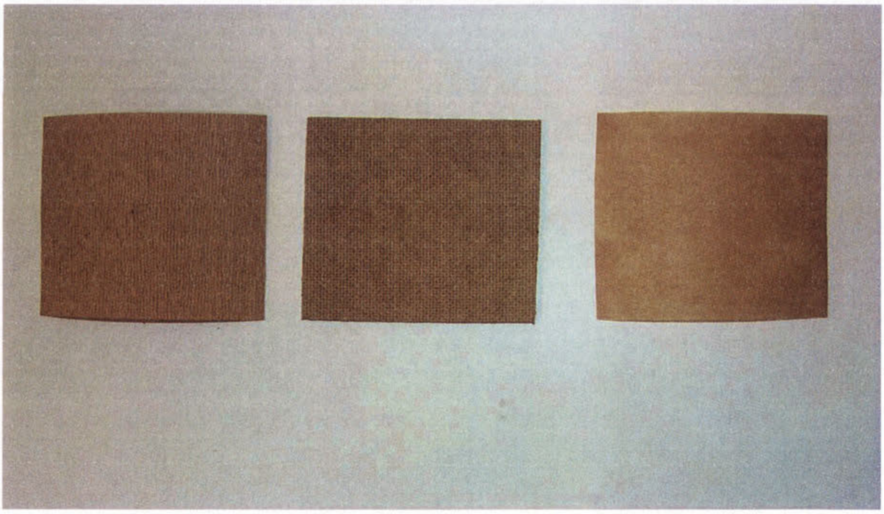

Figure 6-4. Crepe Paper, Pressboard and Kraft Paper

Left is crepe paper, Middle is pressboard and Right is Kraft paper

[Each is of area 25 sq.cm.]

The total separation thickness between the high voltage electrode and low voltage electrode is ~ 4.1mm. Figure 6-5 shows the arrangement of the electrodes and the insulation test sample.

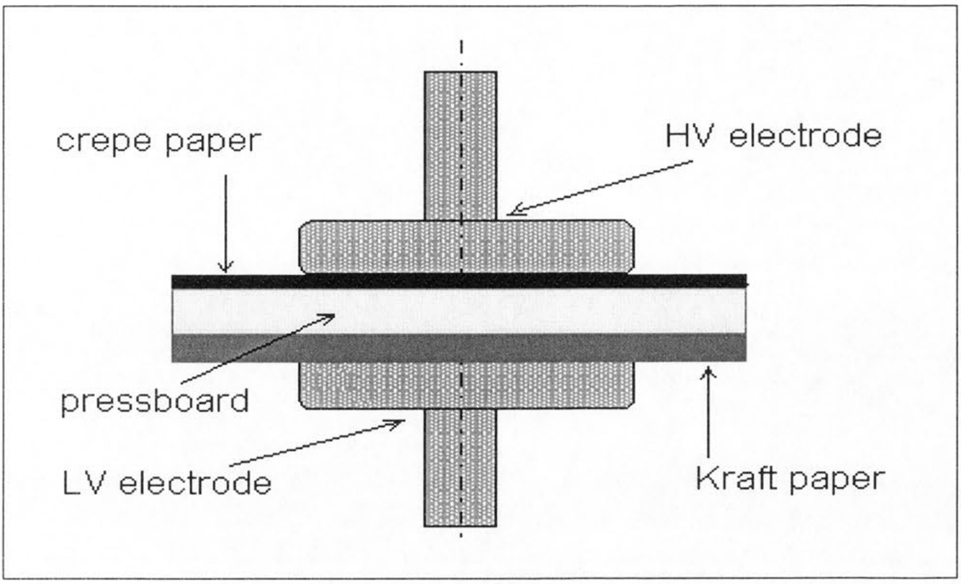

Figure 6-5. Arrangement of the Test Sample

2 Layers of Crepe Paper, Pressboard, 10 Layers of Kraft Paper

6.2.2 <u>Measuring Equipment</u>

PD activity in the insulation during the experiments was recorded using the CDA3 computer-based analyser. This system and the PD measurement circuit used have been described earlier. The circuit for PD measurement and calibration procedure follows the IEC-60270 Standard for PD measurement [26, 147]. To prevent electrical interference in the measurements, the signal threshold of the CDA3 was set to reject background noise. In practice, the lower limit of PD detection was about 30pC.

The analysis of the experimental results reported here is mainly focused in the examination of the statistical parameters of the PD characteristics, including the mean, the standard deviation, the skewness, the kurtosis of the phase resolved patterns and the peak and average discharge magnitudes as well as the PD repetition rate.

6.2.2.1 <u>PD Integrated Quantities</u>

The PD integrated quantities used are derived from the basic individual PD quantities by the CDA3 system. They are the IEC integrated PD parameters. These PD integrated quantities are normally calculated from PD pulses recorded over some defined time period. In this chapter, the PD pulse recording time used was three seconds. A brief description of these integrated quantities is given below [26, 147].

6.2.2.1.1 PD Peak Discharge Magnitude (q_m)

The PD peak discharge magnitude (q_m) is defined as the magnitude of the largest apparent charge of PD recorded in a selected time interval [26]. The PD peak discharge magnitude is expressed in Coulombs and is written as;

$$q_m = \max[q_1, q_2, q_3, \cdots, q_n]$$

Where $q_1, q_2, q_3, \ldots\ldots, q_n$ are the magnitude of the apparent charge.

6.2.2.1.2 PD Average Discharge Magnitude (q_a)

The PD average discharge magnitude (q_a) is defined as the average of the total PD charges recorded in a selected time interval [26]. The PD peak discharge magnitude is expressed in Coulombs and is written as;

$$q_a = \frac{1}{n}\sum_{i=1}^{n} q_i$$

Where n is the total number of the discharges within time interval T and $q_{i's}$ are the apparent charges.

6.2.2.1.3 PD Average Discharge Current (I)

PD average discharge current (I) is defined as the sum of the absolute values of individual apparent charge magnitudes q_i during a chosen time interval T, divided by this time interval [147]. The PD average discharge current is expressed in amperes and is written as;

$$I = \frac{1}{T}\sum_{i=1}^{n} |q_i|$$

Where n is the total number of the discharges within the time interval T.

6.2.2.1.4 PD Quadratic Rate (*D*)

The PD quadratic rate (*D*) is defined as the sum of the squares of the individual apparent charge magnitudes q_i during a chosen reference time interval T, divided by this time interval [26]. The PD quadratic rate is expressed in Coulombs^2/s and is written as;

$$D = \frac{1}{T}\sum_{i=1}^{n} q_i^{\ 2}$$

6.2.2.1.5 PD Discharge power (*P*)

PD discharge power (*P*) is defined as the average pulse power fed into the terminals of the test object due to apparent charge magnitudes q_i during a chosen time interval T. The PD discharge power is expressed in watts and is written as;

$$P = \frac{1}{T}\sum_{i=1}^{n} q_i v_i$$

The v_i's are the instantaneous values of the test voltage at the instant of the discharge occurrence [147].

6.2.2.1.6 PD Repetition Rate (*r*)

PD repetition rate (*r*) is defined as the ratio between the total numbers of PD pulses (n) recorded in a selected time interval (T) and the duration of this time interval [147-148]. The PD repetition rate is expressed in pulse per second (pps or no./s) and is written as;

$$r = \frac{n}{T}$$

6.2.2.2 Partial Discharge Statistical Distributions Analysis

The PD's phase distribution patterns provide the basis for performing some statistical analysis on the magnitude-phase (q-φ) patterns. On the basis of PD statistical distributions, various digital statistical analysis techniques have been developed. The analysis techniques are briefly discussed.

Phase-resolved analysis provides information of the statistical distribution of discharges in relation to the ac voltage cycles. The voltage time base is divided into a number of small equal windows, representing the position of discharges. Various discharge parameters are calculated based on the discharge phase position (φ) over a specified integration period that covers a number of ac voltage cycles. The variation of the parameters can be represented in different distributions.

An assumed univariate phase-resolved PD distribution is used in this work for statistical analysis of the characteristics of the discharges. The application of univariate phase-resolved distribution to the digital PD analysis was first introduced by T Tanaka of CRIEPI in Japan and by later contributions from others [26, 187-190]. The univariate phase-resolved analysis covers the following four different distributions [12].

6.2.2.2.1 Discharge Number (n-φ) Distribution

The discharge number (n-φ) distribution is the total number of PD pulses, counted in each phase window of the voltage waveform, by the PD detector system, and plotted as a function of phase angle of the supply voltage waveform.

6.2.2.2.2 Average Discharge (q_a-φ) Distribution

Average discharge (q_a-φ) distribution is the average magnitude of PD pulses detected in each phase window plotted as a function of phase angle.

6.2.2.2.3 Maximum Discharge (q_m-φ) Distribution

Maximum discharge (q_m-φ) distribution is the peak magnitude of PD pulses detected in each phase window as a function of phase angle.

6.2.2.2.4 Discharge Current (i-φ) Distribution

Discharge current (i-φ) distribution is the average current of PD pulses detected in each phase window as a function of phase angle.

Separate analysis for both the positive and negative half-cycles is based on the fact that the discharges on the positive half-cycle may have different characteristics from those on the negative half-cycle. This further division creates eight different statistical distributions; each set of the four above parameters for the positive half-cycle and another set for the negative half-cycle. The properties of the distributions are characteristic for particular defects and hence many more PD defects can be characterised using this statistical analysis technique. This possibility leads to the development of the large size PD "fingerprint" catalogue associated with the numerous different defects that can occur in insulation. This statistical analysis is used here in analysing the PD data obtained in the experiments described.

The variation of the parameters can also be characterised using a bivariate distribution with both PD number and magnitude (n-q-φ). A two-dimensional array (q-φ) that consists of a finitely divided pulse magnitude (q) and the phase position (φ) are included in this distribution form. The number of PDs occurring for a particular magnitude and at an associated phase angle is entered as a value of each array (n). The PD characteristics can be displayed in a three- dimensional graphic (n-q-φ) using the bivariate distribution. The PD count is displayed as function of the q-φ plane. A three-dimensional perspective thus given provides a more comprehensive display. The viewing angle can be adjusted hence providing the user with a more flexible observation and the analysis results can also be viewed in a two-dimensional graphic. Instead of the height, the pulse counts are represented in different colour scales.

Other displays that can be created using bivariate distribution are the (q-φ) scatter plot and the (q-φ) polar plot. The scatter plot uses every single PD event and is a useful record for pattern analysis [26]. As the bivariate distribution analysis requires a large size of computer memory and a lot of computing time, development in the computer technology recently provides a better possibility in applying bivariate distribution analysis for real-time applications.

Another method used is pulse-height analysis. In this method the pulse magnitude is divided into equally small windows. Two types of univariate distributions that apply to the pulse-height analysis are discharge number distribution as a function of discharge magnitude (n-q) and discharge energy (n-w) [26].

The characteristics of PD distributions can also be determined using a similar approach to the one in phase-resolved analysis by calculating the statistical operators, such as mean, standard deviation, skewness and kurtosis. It should be noted that there is no variable related to the phase angle, which has been proved to be sensitive for particular defect types. Consequently, this analysis is not now used.

Voltage-difference analysis (VDA) [Pulse sequence analysis] and Voltage-resolved-PD-pattern (VRPD) analysis techniques have been introduced recently as further statistical tools for PD pattern characterisation and classification [189]. As compared to the phase-resolved and pulse-height analysis techniques, the simplicity of the both VDA and VRPD is an advantage.

In VDA the voltage difference between consecutive partial discharges is treated as a parameter for the statistical analysis. VDA analysis is presented in a two-dimensional scatter plot of discharge sequence [10]. As this method could be used for simple PD classifications, it is not extensively used, whereas VPRD analysis provides the identification of PD distributions related to the normalised ac voltage value and is presented in two-dimensional graphic. In VPRD analysis the integrated parameters (e.g. peak magnitude, average magnitude and the number) of discharges are plotted against the normalised voltage value [26]. This technique enables us to observe directly the stress between the PD activity and the applied voltage. The physical process of discharges, such as space charge phenomena in corona can also be interpreted by using VRPD approach. Moreover, the utilisation of the statistical parameters for pattern characterisation is possible using this technique. Furthermore the application of mean, standard deviation and average discharge range parameters has successfully shown the change of PD activity as the applied stress changes by the use of this technique. As the voltage phase angle is not available in this analysis, it is difficult to determine the exact time when the discharge starts to occur and extinguish [26].

6.2.2.3 PD Characterisation

For PD characterisation, four different statistical parameters for PD distributions are used. They are the mean, the standard deviation, the skewness and the kurtosis [26]. The analysis of measured PD data in this chapter is primarily performed by using these statistical parameters. [26, 147]. They are defined below.

6.2.2.3.1 Mean (μ)

The mean (μ) represents a central value of a PD distribution and is calculated for each half-cycle of voltage. It is determined from the equation:

$$\mu = \frac{\sum_{i=1}^{n} x_i \cdot f(x_i)}{\sum_{i=1}^{n} f(x_i)}$$

Where f is the general (PD) function of variable x_i and i = 1, 2, ….n for each discharge. The mean has the same unit as x_i. In phase-resolved PD analysis, the mean is in degrees.

6.2.2.3.2 Standard Deviation (σ)

The standard deviation (σ) gives a measure of the variability of the PD distribution around its mean value. The standard deviation is also calculated for each half-cycle by using the following equation.

$$\sigma^2 = \frac{\sum_{i=1}^{n} (x_i - \mu)^2 \cdot f(x_i)}{\sum_{i=1}^{n} f(x_i)}$$

Where f is the general function of the variable x_i , μ is the mean and i = 1, 2, ….n. In phase-resolved PD analysis, the standard deviation is also in degrees.

6.2.2.3.3 Skewness (S_k)

The skewness (S_k) indicates the degree of symmetry or asymmetry of a half cycle of the PD distribution about its mean. It is calculated using the following equation:

$$S_k = \frac{\sum_{i=1}^{n} (x_i - \mu)^3 \cdot f(x_i)}{\sigma^3 \cdot \sum_{i=1}^{n} f(x_i)}$$

Here, μ and σ are the mean and the standard deviation of the PD distribution respectively, f is the general function of variable x_i and i = 1, 2, ….n. A skewness $S_k = 0$ indicates a symmetrical distribution. An extended tail of distribution on the left ($\varphi < \varphi_\mu$) gives a negative S_k, while extension on the right ($\varphi > \varphi_\mu$) gives positive S_k. φ is the phase position and φ_μ is the mean phase position.

6.2.2.3.4 Kurtosis (Ku)

Kurtosis (Ku) indicates the flatness or peakedness of a half cycle distribution of PD pattern relative to a normal distribution and is calculated using the following equation:

$$Ku = \frac{\sum_{i=1}^{n} (x_i - \mu)^4 \cdot f(x_i)}{\sigma^4 \cdot \sum_{i=1}^{n} f(x_i)} - 3.0$$

Where, μ and σ are the mean and the standard deviation of the PD distribution respectively, f is the general function of variable x_i and i = 1, 2, ….n. A zero value of Ku corresponds to the normal (Gaussian) distribution. A positive value of Ku indicates a sharper distribution, while a negative value Ku means a flatter distribution. Both skewness and the kurtosis are non-dimensional quantities.

6.2.2.4 Partial Discharge Pattern Fingerprints

The PD statistical moments make it possible to develop PD pattern "fingerprints" from various measured PD patterns. There are 32 different operators that can be used for such characterisation purposes. The PD statistical moments are shown in Table 6.1. The more simplified notations of the PD statistical moment are shown in Table 6.2.

	Positive half-cycle				Negative half-cycle			
	Mean	Std	Skewness	Kurtosis	Mean	Std	Skewness	Kurtosis
(q_m-φ)	$\mu^+(q_m\text{-}\varphi)$	$\sigma^+(q_m\text{-}\varphi)$	$Sk^+(q_m\text{-}\varphi)$	$Ku^+(q_m\text{-}\varphi)$	$\mu^-(q_m\text{-}\varphi)$	$\sigma^-(q_m\text{-}\varphi)$	$Sk^-(q_m\text{-}\varphi)$	$Ku^-(q_m\text{-}\varphi)$
(q_a-φ)	$\mu^+(q_m\text{-}\varphi)$	$\sigma^+(q_m\text{-}\varphi)$	$Sk^+(q_m\text{-}\varphi)$	$Ku^+(q_m\text{-}\varphi)$	$\mu^-(q_m\text{-}\varphi)$	$\sigma^-(q_m\text{-}\varphi)$	$Sk^-(q_m\text{-}\varphi)$	$Ku^-(q_m\text{-}\varphi)$
(n-φ)	$\mu^+(q_m\text{-}\varphi)$	$\sigma^+(q_m\text{-}\varphi)$	$Sk^+(q_m\text{-}\varphi)$	$Ku^+(q_m\text{-}\varphi)$	$\mu^-(q_m\text{-}\varphi)$	$\sigma^-(q_m\text{-}\varphi)$	$Sk^-(q_m\text{-}\varphi)$	$Ku^-(q_m\text{-}\varphi)$
(i-φ)	$\mu^+(q_m\text{-}\varphi)$	$\sigma^+(q_m\text{-}\varphi)$	$Sk^+(q_m\text{-}\varphi)$	$Ku^+(q_m\text{-}\varphi)$	$\mu^-(q_m\text{-}\varphi)$	$\sigma^-(q_m\text{-}\varphi)$	$Sk^-(q_m\text{-}\varphi)$	$Ku^-(q_m\text{-}\varphi)$

Table 6.1: PD Statistical Moments for Pattern Characterisation [26]

	Positive half-cycle				Negative half-cycle			
	Mean	Std	Skewness	Kurtosis	Mean	Std	Skewness	Kurtosis
(q_m-φ)	$m_1^{(+)}$	$m_2^{(+)}$	$m_3^{(+)}$	$M_4^{(+)}$	$m_1^{(-)}$	$m_2^{(-)}$	$m_3^{(-)}$	$m_4^{(-)}$
(q_a-φ)	$a_1^{(+)}$	$a_2^{(+)}$	$a_3^{(+)}$	$a_4^{(+)}$	$a_1^{(-)}$	$a_2^{(-)}$	$a_3^{(-)}$	$a_4^{(-)}$
(n-φ)	$n_1^{(+)}$	$n_2^{(+)}$	$n_3^{(+)}$	$n_4^{(+)}$	$n_1^{(-)}$	$n_2^{(-)}$	$n_3^{(-)}$	$n_4^{(-)}$
(i-φ)	$c_1^{(+)}$	$c_2^{(+)}$	$c_3^{(+)}$	$c_4^{(+)}$	$c_1^{(-)}$	$c_2^{(-)}$	$c_3^{(-)}$	$c_4^{(-)}$

Table 6.2: Simplified PD Statistical Moments for Pattern Characterisation [26]

Where the notation m, a, n and c are used to denote the peak discharge, average discharge, discharge number and the average discharge current distributions respectively. The subscripts 1, 2, 3 and 4 represent the mean, standard deviation, skewness and kurtosis. And the superscripts positive and negative indicate the corresponding value for each half cycle. The simplified notations m, a, n and c are used for the description of the measured PD properties in the experiments.

Application of expert systems, for example neural network and fuzzy logic, for automated PD recognition has provided the partial discharge technique as a powerful tool for insulation condition monitoring [26].

The other PD statistical operators that can be used for pattern characterisation are the cross-correlation coefficient and the number of peaks [26, 38]. The cross-correlation coefficient (cc) is used to measure the degree of difference in terms of shape between distribution at the positive and at the negative half-cycles. A value of 1 (complete positive correlation) indicates both distributions are similar in shape, while a value of zero (un-correlated) means they are completely different. The cross-correlation coefficient is also a non-dimensional quantity. The cross-correlation coefficient is determined using the following formula:

$$cc = \frac{\sum_{i=1}^{n} x_i y_i - \sum_{i=1}^{n} x_i \sum_{i=1}^{n} y_i \Big/ n}{\sqrt{\left[\sum_{i=1}^{n} x_i^2 - \left(\sum_{i=1}^{n} x_i\right)^2 \Big/ n\right] \cdot \left[\sum_{i=1}^{n} y_i^2 - \left(\sum_{i=1}^{n} y_i\right)^2 \Big/ n\right]}}$$

Where x_i, y_i are variables and $i = 1, 2, \ldots.n$.

The number of peaks (Pe) is used to distinguish different distributions by counting the number of local peaks (tops) of the distribution. This distribution operator can distinguish up to eight different peaks for each analysed distribution. However, it is difficult to observe the exact number of peaks because the PD distributions usually have non-distinguishable small peaks. This can result in an inaccurate value, so this operator is not often used for pattern recognition. It is subjected to the following criterion [38]:

$$\frac{dyi-1}{dxi-1} > 1 \quad \text{and} \quad \frac{dyi+1}{dxi+1} > 1$$

Where x_i and y_i are variables.

6.3 Results and Discussion

The experimental tests were performed with a combination of thermal and electrical stress. The voltage applied to the model (10kV) was designed to give operation at electrical stresses typical of working transformers (2.25kV/mm minimum occurring across pressboard as mentioned earlier). The temperature of the sample containing oil, crepe paper, pressboard and kraft paper in the glass cell was raised from ambient temperature in the range of 23.5-25.5°C to 80-85°C by heating tape wrapped around the lower part of the glass cell. The temperature of the sample was then reduced to ambient by switching off the heating and allowing natural cooling. The process of increasing and decreasing of the temperature during the cycle took almost three hours to complete. The experiments were repeated to ensure consistency in the results. The temperature of the system was monitored by fibre optic sensor. The fibre optic sensor head was placed very close to the crepe paper, pressboard and kraft paper to ensure accurate measurement of their temperature.

The aim of the experiment was to simulate high temperature insulation conditions (80-85°C) such as that may occur during abnormal (overload) operation of a transformer. The purpose of reducing the temperature back to ambient was to study the resulting PD patterns during increasing and decreasing temperature phases in the oil-impregnated transformer type insulation. Such information is needed to determine whether any change in temperature may mask the PD characteristics representative of condition at the higher temperature phase.

The temperature high of 85°C of the paper was chosen to simulate the maximum permissible operating temperature which is taken to be a hot spot temperature of 97°C.

At a surface temperature of 85°C, the internal temperature of the paper (the hot spot) should be about the limit of 97°C.

6.3.1 Increasing Temperature

It was observed that during increase of temperature from ambient to 60°C the peak discharge magnitude on the positive half-cycle was higher than the level on the negative half-cycle, as shown in the phase-resolved plot of Figure 6-6 below. In the temperature range from 60 to 70 C (Figure 6-7 shows the PD activity at 70°C), the PD repetition rate increased dramatically from 863 (no./s) (Figure 6-6) to 4800 (no./s) (Figure 6-7).

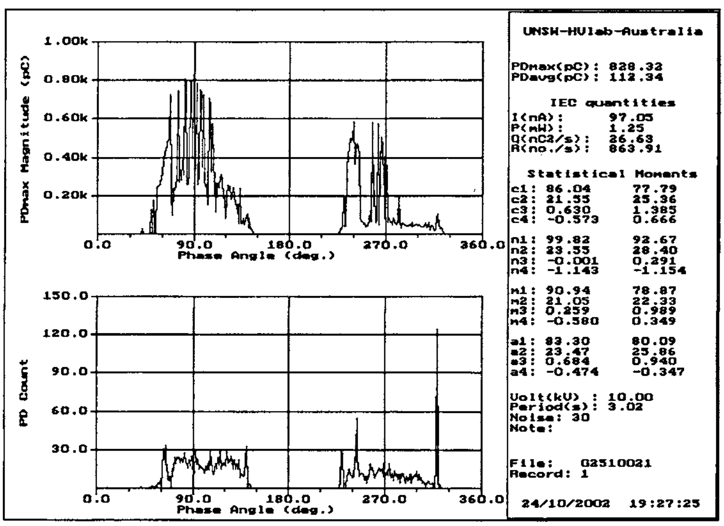

Figure 6-6. PD Pattern at 10kV, 60°C and 50Hz: Temperature Increasing;

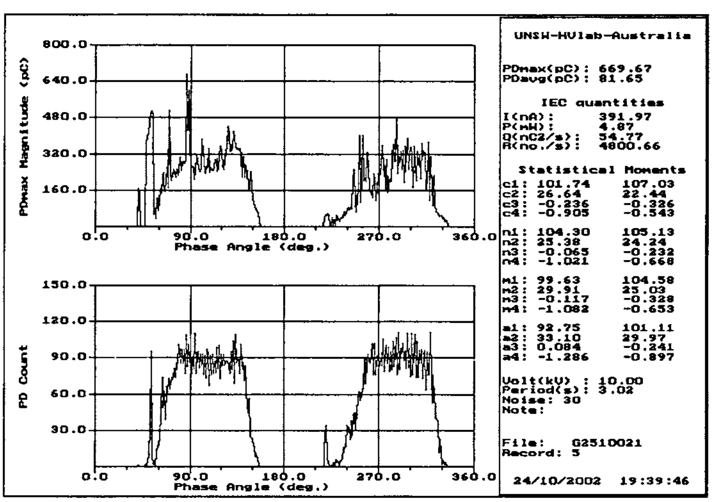

Figure 6-7. PD Pattern at 10kV, 70°C and 50Hz: Temperature Increasing;

As the surface temperature reached the upper limit range of 81 to 85°C from 70°C (Figure 6-8 shows results at 81-85°C) the maximum PD level changed its behaviour and the peak PD pattern magnitude on the negative half-cycle became larger than on the positive half cycle.

At the same time, the maximum and average discharge magnitudes increased significantly. A significant increase in the repetition rate was also observed. The maximum PD increased from 669pC (Figure 6-7) to 1.45nC (Figure 6-8), average PD increased from 81pC to 325pC and the repetition rate increased from 4800 (no./s) to 5533 (no./s).

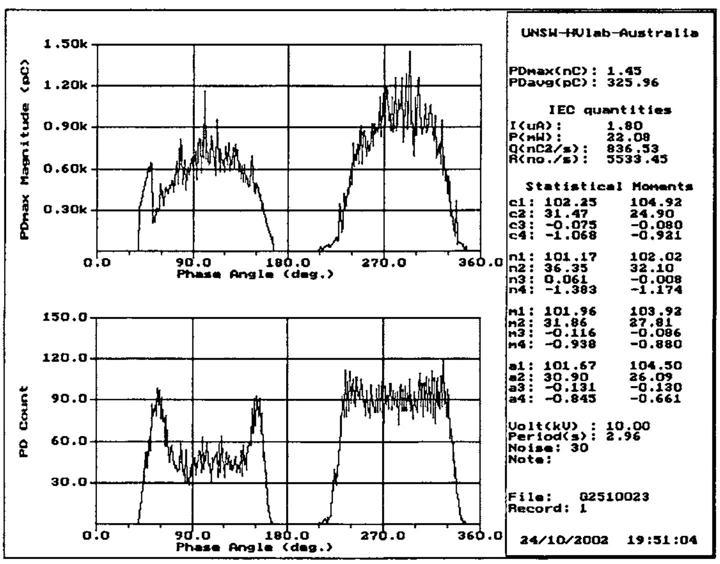

Figure 6-8. PD Pattern at 10kV, 81-85°C and 50Hz: Temperature Increasing; Peak of the PD Pattern has shifted to the negative half cycle.

It can also be seen that there is a steady trend, with increasing temperature, to earlier PD inception on both the PD and repetition rate plots versus phase angle of the voltage waveform.

Following the simulated sudden increase in loading, the PD behaviour was then investigated during the cooling part of the thermal cycle, with the heater turned off and the chamber and contents allowed to cool naturally to ambient.

6.3.2 Decreasing Temperature

When the temperature was decreased from the peak level of 85°C back to 80°C, the largest peak PD magnitudes on both the positive and the negative half-cycles become almost equal (see Figure 6-9).

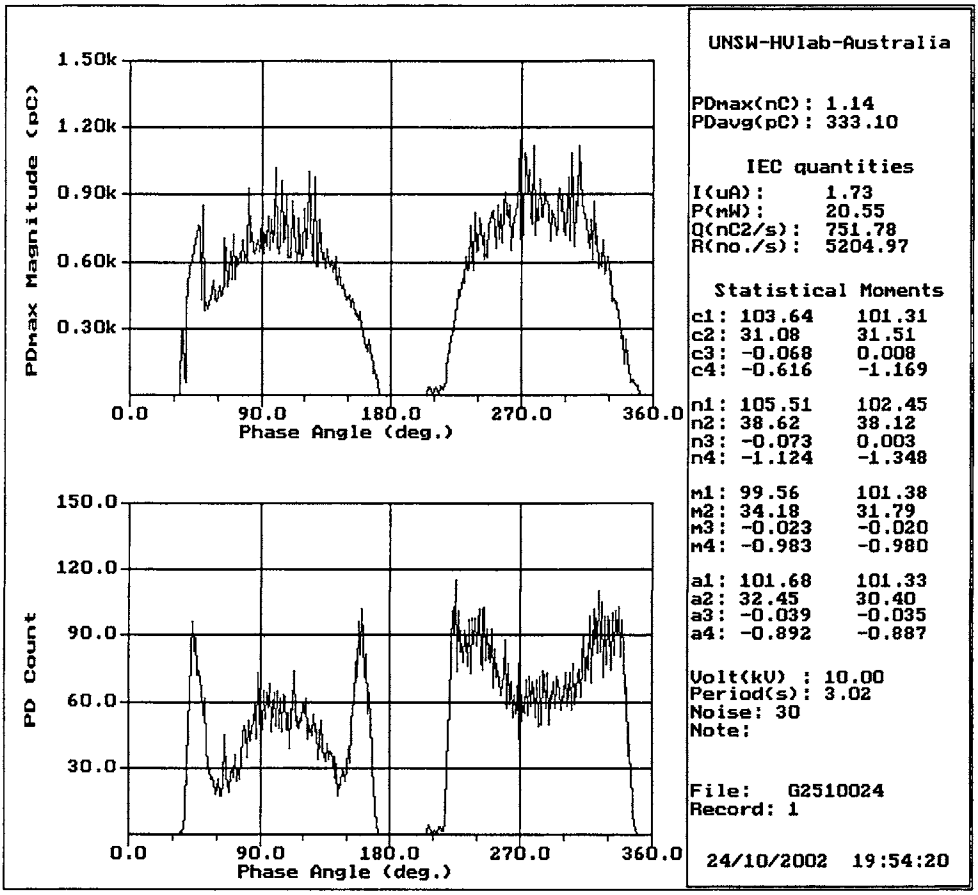

Figure 6-9. PD pattern at 10kV, 80°C and 50Hz: Temperature Decreasing; New sample in Glass Cell without Moisture
Peak PD Pattern at Positive Half Cycle and Negative Half Cycle Almost Same.

As the temperature was further decreased to 60°C, the largest peak PD magnitude has again shifted to be again in the positive half-cycle. Figures 6-10 and 6-11 depict the phase-resolved pattern of PDs at temperature 70°C and 60°C.

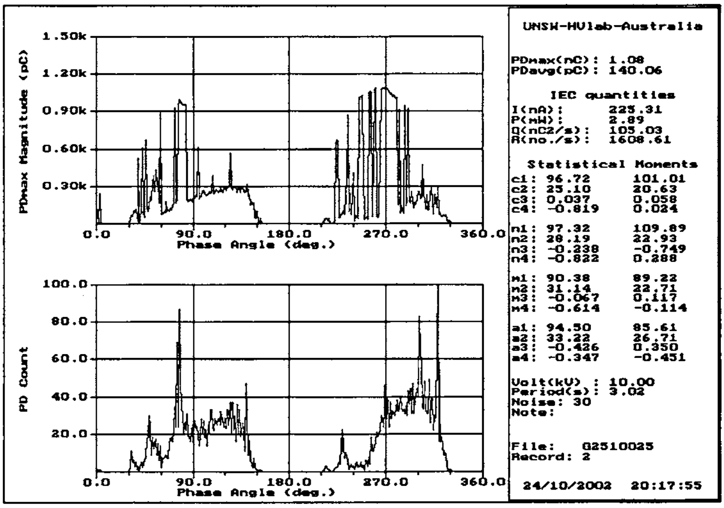

Figure 6-10. PD Pattern at 10kV, 70°C and 50Hz: Temperature Decreasing; Peak PD Pattern at Positive Half Cycle.

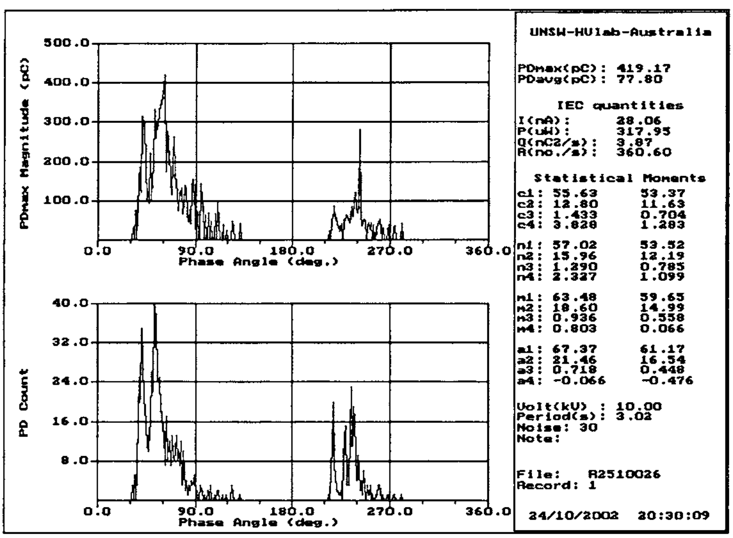

Figure 6-11. PD Pattern at 10kV, 60°C and 50Hz: Temperature Decreasing; Peak PD Pattern at Positive Half Cycle.

It was observed during the experiment that the PD magnitude and the PD repetition rate increased with increase of temperature between 60 to 85°C and when temperature decreased the repetition rate also decreased. It was also observed that 80°C was the temperature where the peak PD magnitudes for both positive and negative half-cycles were almost the same.

The temperature above 80°C is most likely the temperature at which the cellulose materials in the oil-impregnated insulation starts to feel the effect of temperature increase and this causes the change in pattern from the positive half cycle to the negative half cycle with the cellulose material and moisture effects become more involved. If this is indeed the case, then drying of transformer oil below 80 degrees can be considered safe for drying of transformers without affecting its insulation.

Further it was observed that in the phase resolved plots at temperatures 60°C (Figure 6-6; temperature increasing) and at 81-85°C (Figure 6-8; temperature increasing), the maximum PD, average PD and PD repetition rate all increased. The maximum PD increased from 828pC to 1.45nC, average PD increased from 112pC to 325pC and the PD repetition rate increased from 863 (no./s) to 5533 (no./s).

Furthermore it was also observed that at temperatures 81-85°C (Figure 6-8) and 60°C (Figure 6-11; temperature decreasing), the maximum PD, average PD and PD repetition rate all decreased. The maximum PD decreased from 1.45nC to 419pC, average PD decreased from 325pC to 77pC and the PD repetition rate decreased from 5533 (no./s) to 360 (no./s).

The inception angles in all the experiments during increase and decrease of temperature did not change significantly. This is an important indication that there was no significant change in the overall insulation condition over the period of these tests, despite the PD magnitudes and numbers changing substantially in that time. It is an indication that the inception angle is an important parameter in condition assessment of the insulation.

6.3.3 Comparison with Previous Tests in Steel Tank

It was observed during the experiment that the PD pattern at 10kV, 80°C and 50Hz in the glass cell are similar to those monitored during previous test configuration enclosed in a steel tank. In Figure 6-12 the test conditions used were 8kV, 80°C and 50Hz mentioned in the previous chapter. The pattern in Figures 6-9 (in glass cell) and Figure 6-12 (in steel tank) can be compared.

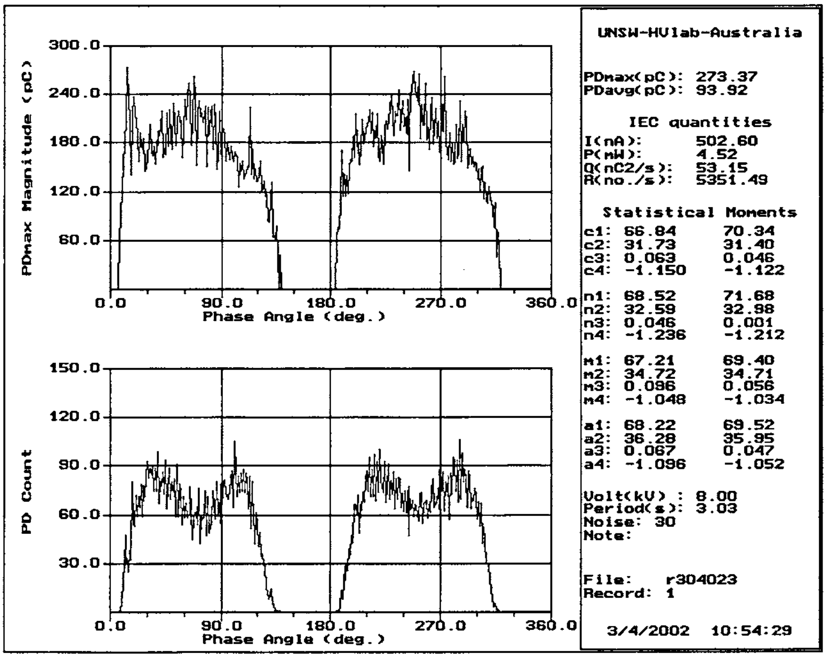

Figure 6-12. PDs at 8kV, 50Hz, 80°C : Aged Sample with Moisture in steel tank); Peak PD Patterns at Positive Half Cycle and Negative Half Cycle Almost Same [6].

The general shapes of the patterns and the PD repetition rates are almost similar. The similarity in shape is due to similarity in the insulation configuration between the high voltage and low voltage electrodes in a steel tank which also contained kraft paper, crepe paper and pressboard and the total separation thickness between high voltage electrode and low voltage electrode was also 4.1mm, as in the glass cell. Thus the electric field would be the same for the same voltage in the two cases. The temperature of 80°C can also be one of the reasons for similarity in PD shape pattern as discussed earlier.

The voltage used in the above comparison was different in the steel tank and glass cell: the stress levels are 2.25 kV/mm in the glass cell and 1.46 kV/mm in the steel tank. Therefore, there is some difference in the inception angles and the PD magnitudes are different, consistent with the different stress levels. It was noted that the PD patterns in Figure 6-12 (Aged sample in steel tank with moisture) had changed, with discharges on the positive half-cycle starting at about 5 degrees of voltage phase as compared to Figure 6-9 (New sample in glass tank without moisture) where the discharges were very consistent in starting at about 30 degrees. Similarly, discharges on the negative half-cycle started at around 185 degrees (Figure 6-12) compared with at 210 degrees (Figure

6-9). The decrease in the inception angle in aged sample in steel tank is probably due to more moisture in the sample and ageing.

6.3.4 Test Using Aged Insulation

The new insulation structure used in the previous tests in the glass test cell was then subjected to voltage excitation for a total period of five months to investigate the effects of longer term ageing on the oil-impregnated sample in this chamber. It was found that the maximum PD magnitude and the average PD magnitude increased in the aged sample at 80°C.

Figure 6-13 shows the phase-resolved pattern of peak PD magnitude and PD number distribution measured during the test using the well-aged insulation. The peak PD magnitude had increased from 1.14nC previously (see Figure 6-9) to 2.46nC after ageing (see Figure 6-13) and the PD average magnitude had also increased from 333 pC previously to 571 pC after the ageing.

It was also noted that the PD pattern phase distribution in the aged sample had changed, with discharges on the positive half-cycle starting at about 5 degrees (Figure 6-13) of the voltage waveform as compared to previous results where the discharges were very consistent in starting at about 30 degrees (see Figures 6-6 to 6-11). Similarly, for the test using an aged sample, the discharges on the negative half-cycle started at around 185 degrees compared with 210 degrees in the previous tests. The decrease in PD inception angle on both positive and negative half cycles is thus due to the ageing of the oil-impregnated glass cell insulation. A PDC (Polarisation - depolarisation test) was also carried out by KEA consultants on the test cell after the CDA3 tests and the results also indicated ageing of the insulation. The PDC results are included at Annexure "D".

These results again emphasize the importance of the PD inception angle on ageing condition of the transformer insulation.

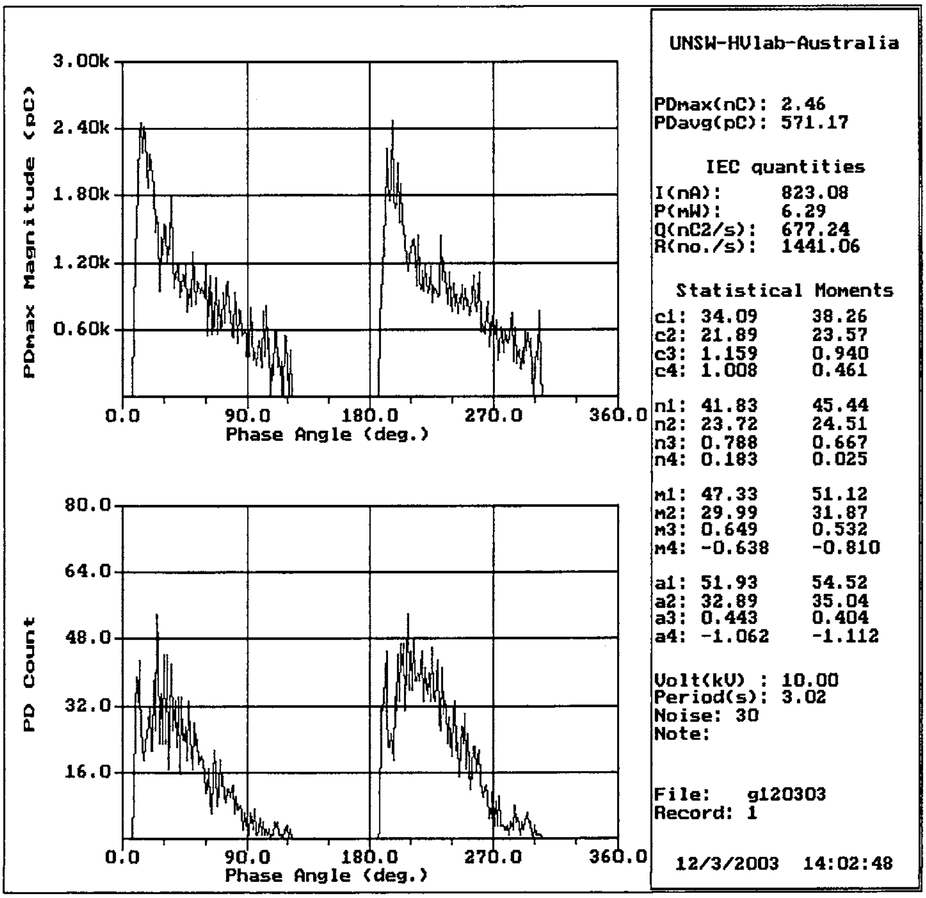

Figure 6-13. PD Pattern at 10kV, 80°C and 50Hz,:

Aged sample after ageing for five months in glass cell;

Peak PD pattern on positive half cycle and negative half cycle are almost the same.

A similar change of colour of the oil from clear to light brown was also observed again due to thermal damage to cellulose materials and oxidation of oil. Figures 6-14 and 6-15 show the colour change of the oil.

The change of colour of the kraft paper, crepe paper and pressboard from light brown shade to dark brown was also observed during the ageing process. At high temperatures the cellulose polymer chains break up reduce in length and, as part of the degradation, form water especially in the presence of oxygen. The excessive moisture, oxygen and temperature caused the oxidation that results in the change of colour of the cellulose material.

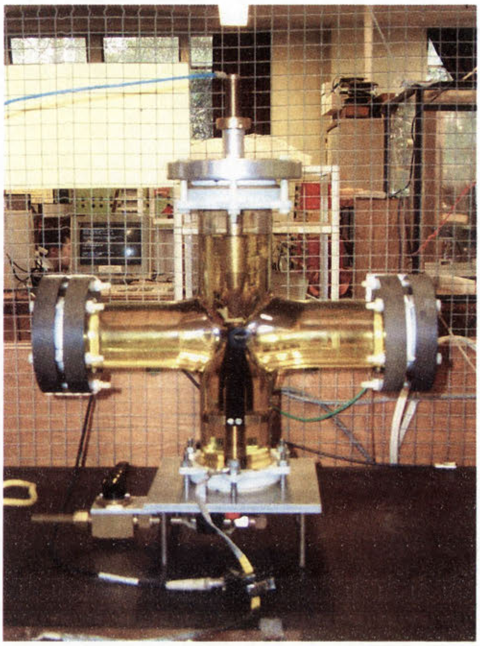

Figure 6-14. Colour of Oil in Glass Cell Before the Ageing Process

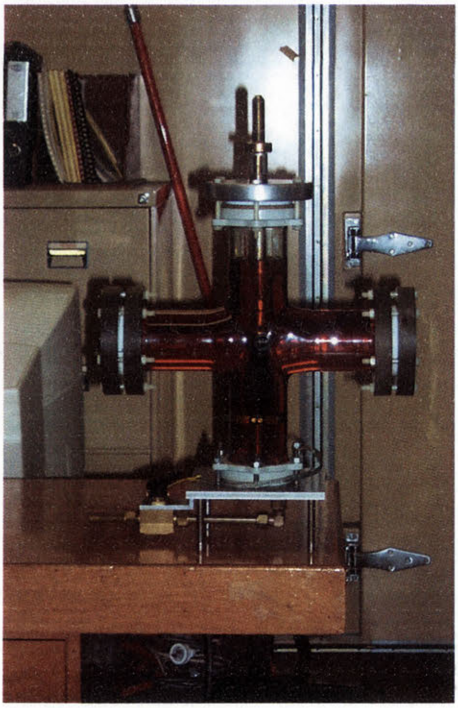

Figure 6-15. Colour of Oil in Glass Cell After the Ageing Process Caused Oxidation of Oil that Results in Darkening of Oil Colour

The effects of ageing are also very obvious from the damage caused to the crepe paper, pressboard and kraft paper. Signs of water treeing can be seen on the crepe paper and significantly so on the pressboard. Electrical treeing can be seen on the kraft paper showing clear signs of black carbonised conducting paths causing burning and brittleness of the paper.

The water treeing is caused when water migrates to high stress areas and reduces the dielectric strength of the material and water treeing also produces third harmonics. No PD activity is present when the water trees are present. The water treeing is then followed by electrical treeing. In the electrical treeing mode the PD activity starts and causes black carbonised conducting paths ultimately leading to the failure of the insulation. Figures 6-4 and 6-16 show the quality of cellulose material before and after the Ageing Process.

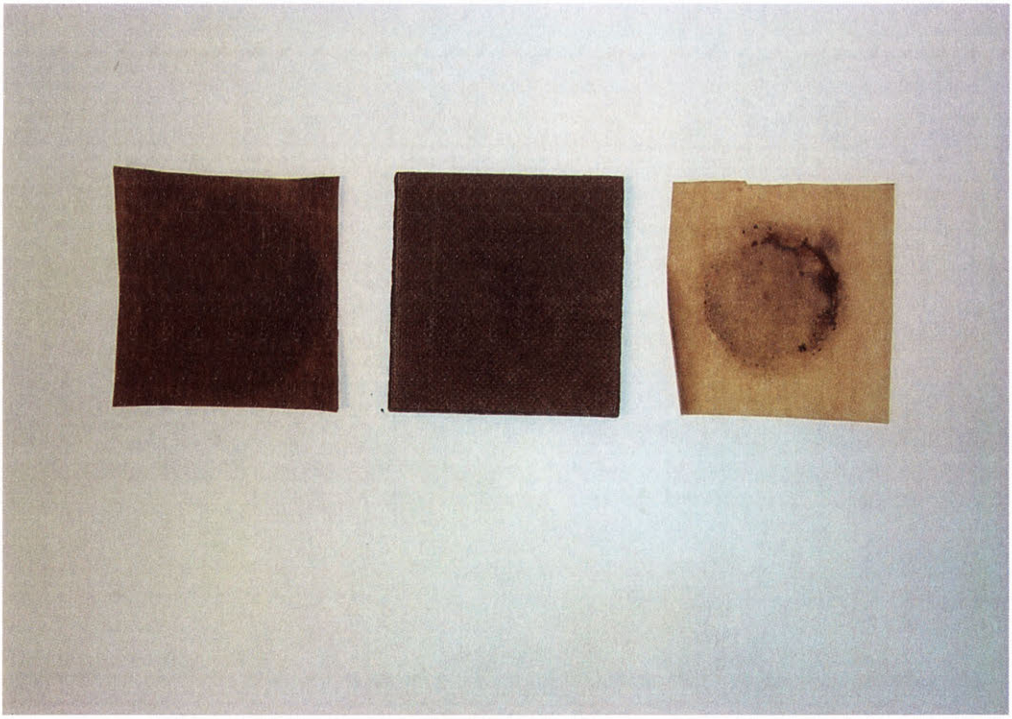

Figure 6-16. Quality of Crepe Paper, Pressboard and Paper After Ageing;
Left is Crepe Paper, Middle is Pressboard and Right is Kraft Paper with Black Marks Showing Clear Signs of Carbonised Conducting Paths Causing Burning and Brittleness

6.3.5 Investigation of Temperature Effects on PDs: Use of Integrated Parameter Distributions in Oil-Impregnated Insulation

6.3.5.1 The IEC Quantities

The test results indicated that the peak and the average PD magnitudes were slightly decreased when the test temperature increased from ambient to about 70°C. The peak and average discharge magnitude increased significantly when the test temperature was further increased. Figure 6-17 shows the trend of peak and the average PD magnitude as the temperature is increased. The actual PD values are shown as individual points: the curves drawn are curves of best fit (obtained using a second order polynomial approximation) of the actual discrete values of the peak and the average PD magnitudes. Note that there is a minimum reached during the temperature variation, followed by a rapid rise of magnitudes at higher temperature.

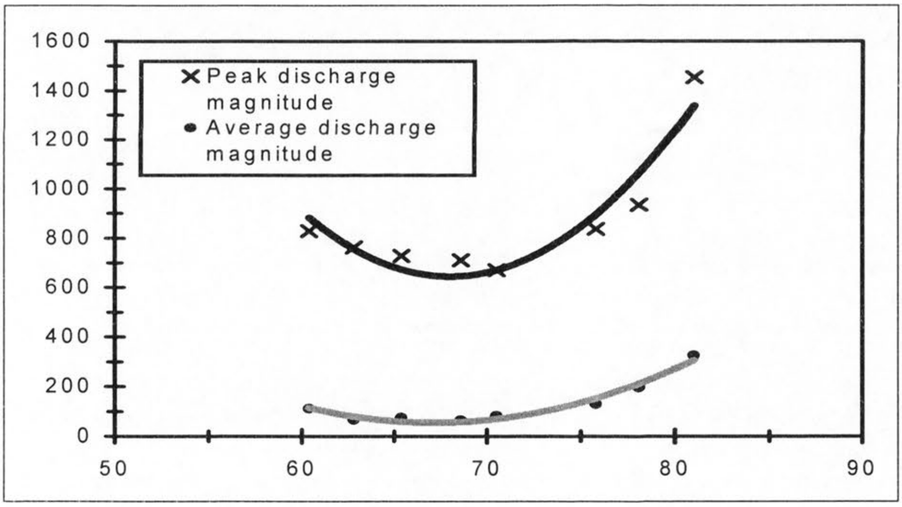

Figure 6-17. Peak and Average PD Magnitude (pC) vs. temperature (°C)
Temperature increasing at 10kV

Figure 6-18 illustrates the temperature dependence of the IEC discharge current and the PD repetition rate at a test voltage level of 10kV. It is clear from the results that there was a significant increase in the PD repetition rate as the test temperature increased. A substantial increase in discharge current, although not as substantial as the repetition rate increase, was also observed when the test temperature was increased.

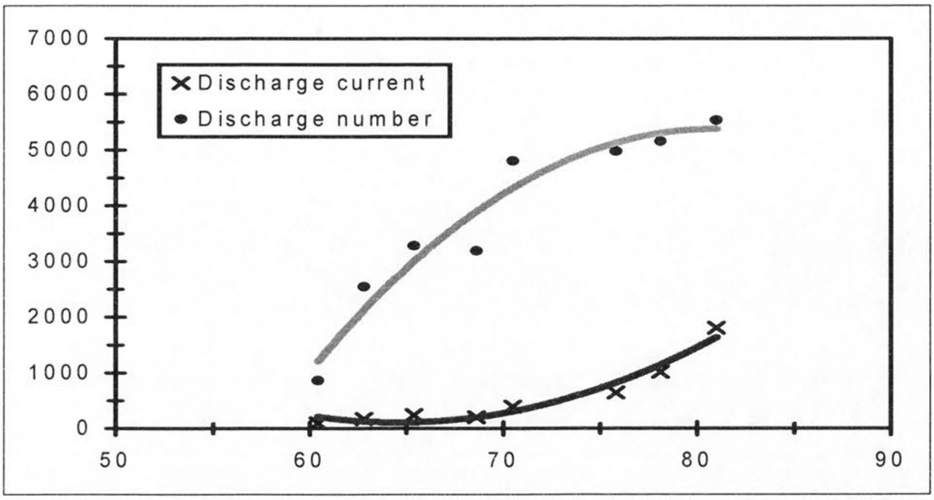

Figure 6-18. PD Current (nA) and PD Number (pps) vs. temperature (°C)

Temperature increasing at 10kV.

Contradictory trends were found when the test temperature was reduced back down to the ambient. The peak PD magnitude was slightly increased when the test temperature decreased to about 74°C and the sharply decreased when the test temperature further reduced. The average PD magnitude, the PD current and the PD repetition rate all decreased monotonically as the temperature reduced. Figure 6-19 depicts the trend of the peak and the average PD magnitude as the temperature decreased. The behaviour of discharge current and PD repetition rate are shown in Figure 6-20.

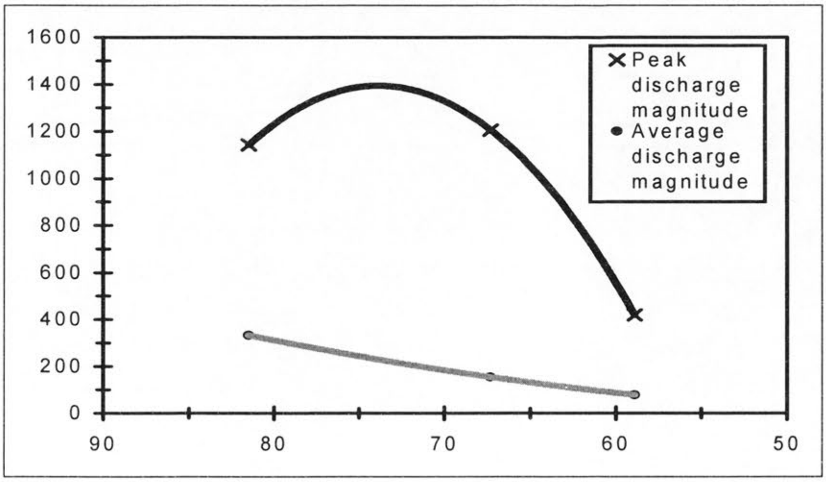

Figure 6-19. Peak and Average PD Magnitude (pC) vs. temperature (°C)

Temperature decreasing at 10kV.

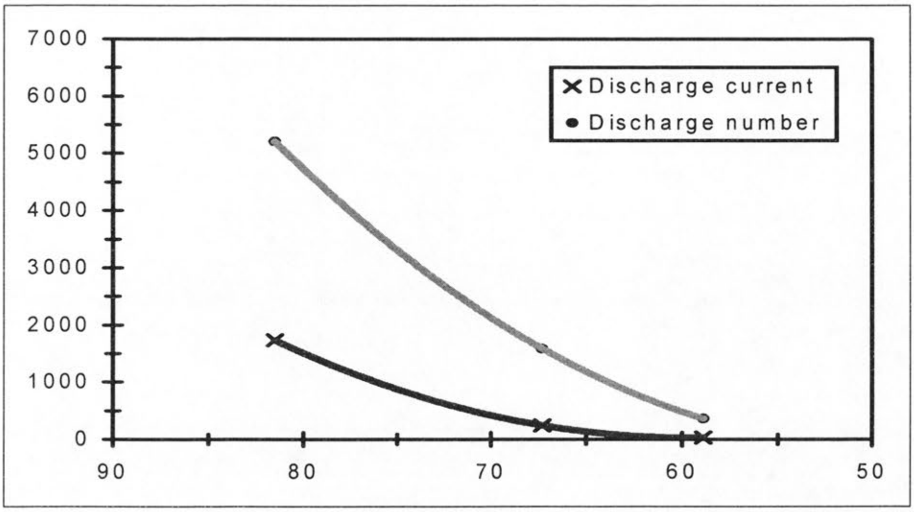

Figure 6-20. PD Current (nA) and PD Number (pps) vs. temperature (°C)

Temperature decreasing at 10kV.

The PD behaviour reported here has a slightly different characteristic to that reported previously. Results show that during increase of temperature from 60 to 85 C (see Figures 6-17 and 6-18) the peak PD magnitude, the average PD magnitude, the PD current and the PD number increased at 85°C as compared to PDs with temperature at 60°C and all those values decreased with decrease of temperature from 85 to 60°C (see Figures 6-19 and 6-20).

A slightly different intermediate trend (which was not linear) was observed as the temperature increased and then decreased between 60 and 85°C. It was also observed that the PD peak magnitude, average magnitude, average current and repetition rate are greatly affected by the temperature change. The variation of PD characteristics with temperature can be used as a diagnostic tool to assess condition of the oil-impregnated insulation.

6.3.5.2 The Statistical Moments

The previous investigations on this test configuration by other authors showed that the statistical parameters, such as the mean, the standard deviation, the skewness and the kurtosis of the phase resolved partial discharge patterns are all meaningful and are unique for particular insulation defects [26, 187-190]. Thus statistical analysis was conducted on the results of this investigation to examine whether there were any distinctive properties that could be used as indicators for the assessment of condition of oil-impregnated insulation.

6.3.5.2.1 The Mean and the Standard Deviation

The mean of the PD maximum distribution shifted to a larger phase angle as the test temperature increased for both the positive and negative half-cycles. The mean of the distribution then tended to shift back to a lower phase angle when the test temperature was decreased. Figures 6-21 and 6-22 exhibit the correlation between the mean value of the maximum PD distribution and the test temperature at a test voltage level of 10kV for both positive and negative half-cycles.

The average PD distribution had similar trends to that of the mean values. The mean of the PD number distribution and the PD current distribution, however, are relatively steady at about 105° when the test temperature was increased. The mean shifted to a lower phase angle as the test temperature reduced.

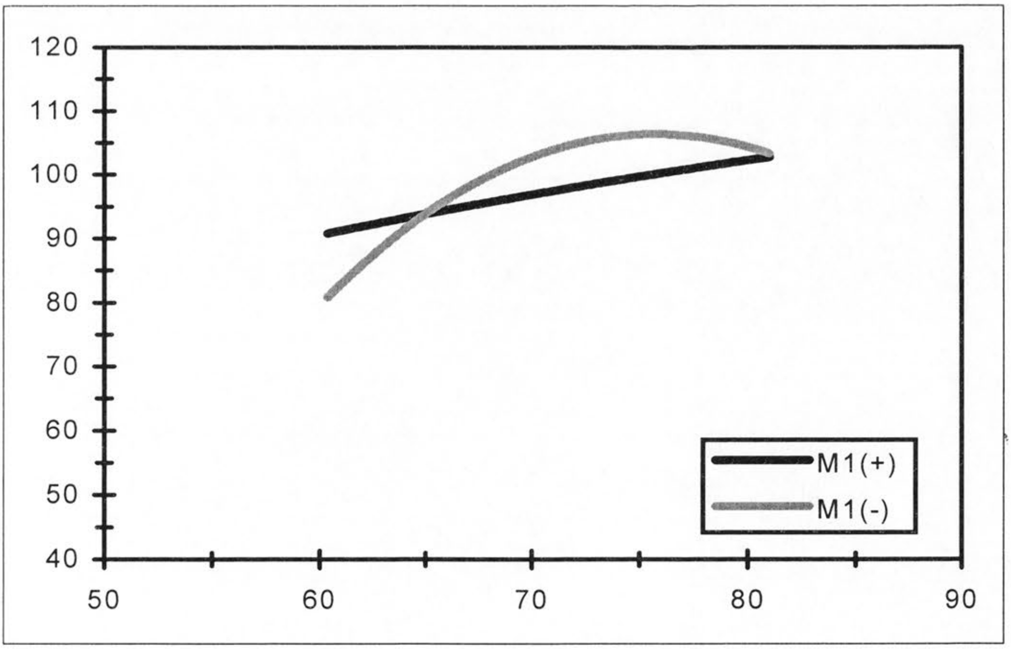

Fig. 6-21. Mean of Maximum PD Distribution (Phase Angle) vs. temperature (°C) Temperature Increasing at 10kV; Positive (M1+) and Negative (M1-) Half Cycles

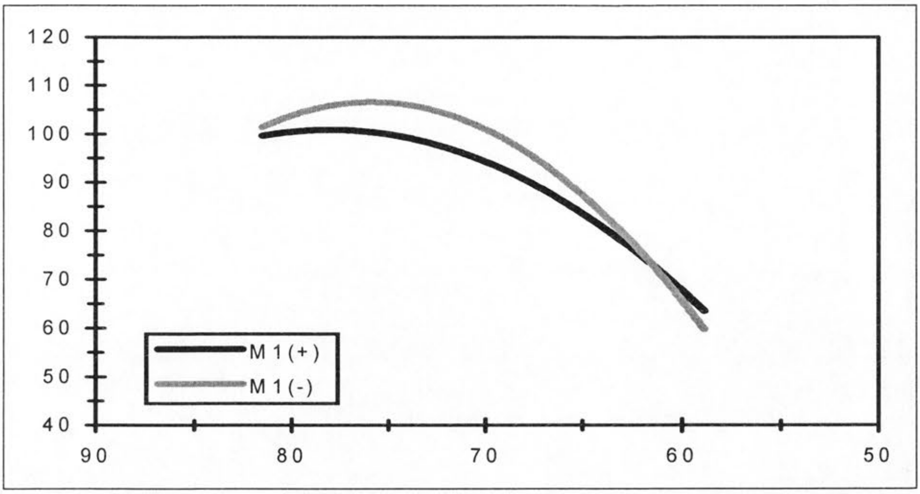

Fig. 6-22. Mean of Maximum PD Distribution (Phase Angle)Vs Temperature (°C)
Temperature Decreasing at 10kV; Positive (M1+) and Negative (M1-) Half Cycles

A slight increase in the standard deviation of the PD number distribution was seen as the temperature increased. A reverse trend occurred as the test temperature reduced. This indicated that the distribution extended when temperature increased and reduced when the temperature reduced. The correlation between the standard deviation of the PD number distribution and the test temperature at 10kV is illustrated in Figures 6-23 and 6-24. In general, the standard deviation of all other distributions (maximum PD, average PD and PD current) behaved similarly to those for the PD number distribution.

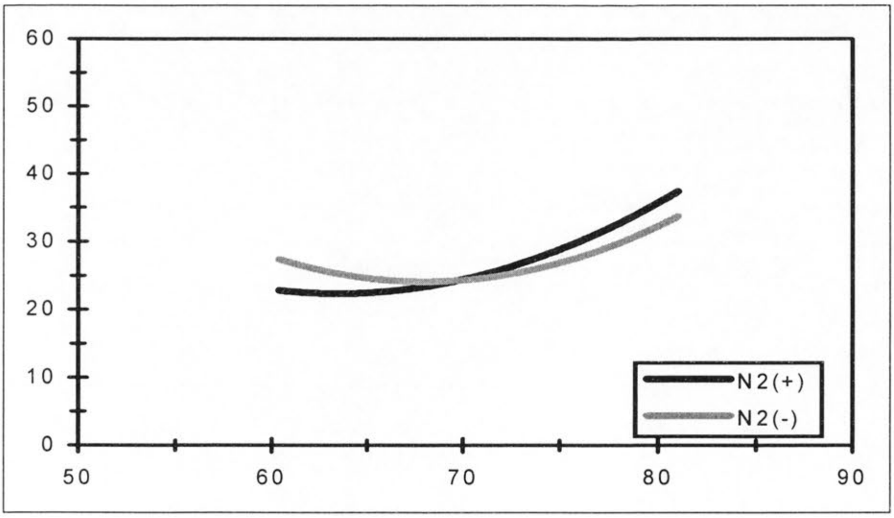

Figure 6-23. Deviation of PD Number Distribution Vs Temperature (°C)
Temperature Increasing at 10kV; Positive (N2+) and Negative (N2-) Half Cycles

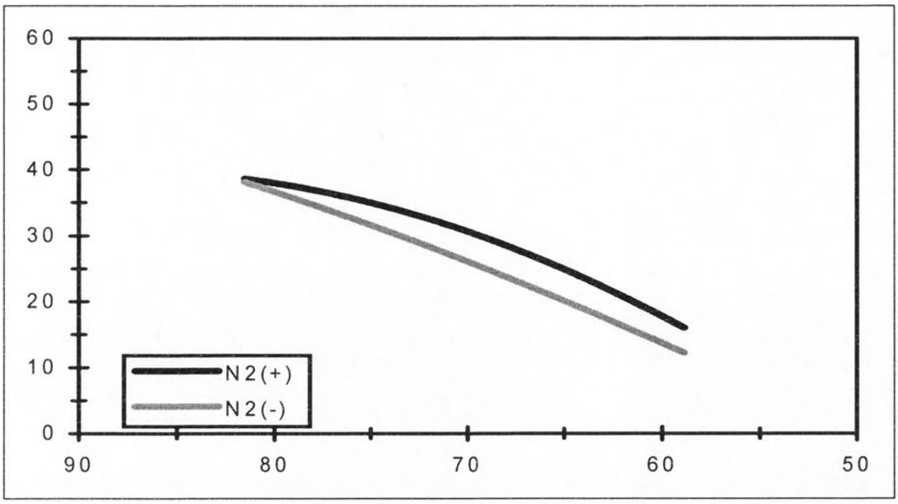

Figure 6-24. Deviation of PD Number Distribution Vs Temperature (°C)
Temperature Decreasing at 10kV; Positive (N2+) and Negative (N2-) Half Cycle

6.3.5.2.2 The Skewness and the Kurtosis

In general, the skewness value of the PD distributions decreased when the test temperature increased, although passing through a shallow minimum (Figure 6-25). It decreased generally when temperature then decreased, but again passed through a very shallow minimum (Figure 6-26). A trend towards a larger negative value of skewness indicates that there is an extension on the tail of the distribution to a lower phase angle, as noted previously on the phase-resolved plots. Thus as the temperature increased, a higher number of discharges appeared at the lower phase angles of the mean.

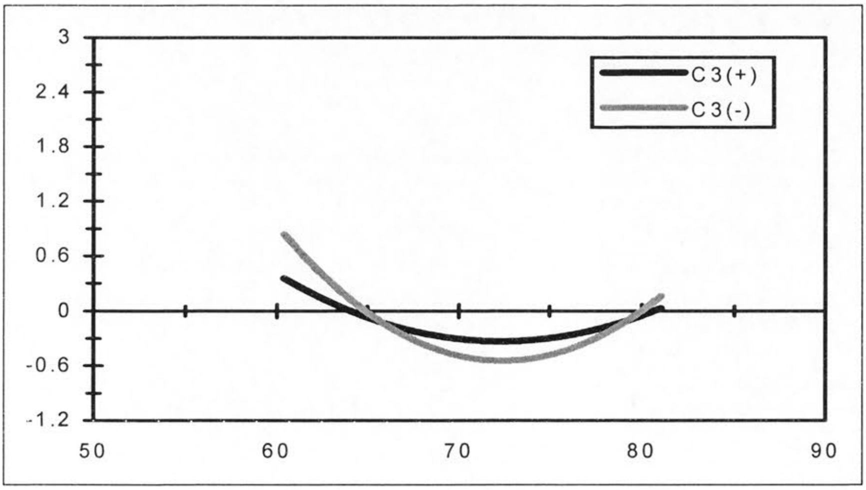

Figure 6-25. Skewness of PD Current Distribution Vs Temperature (°C)
Temperature Increasing at 10kV; Positive (C3+) and Negative (C3-) Half Cycle

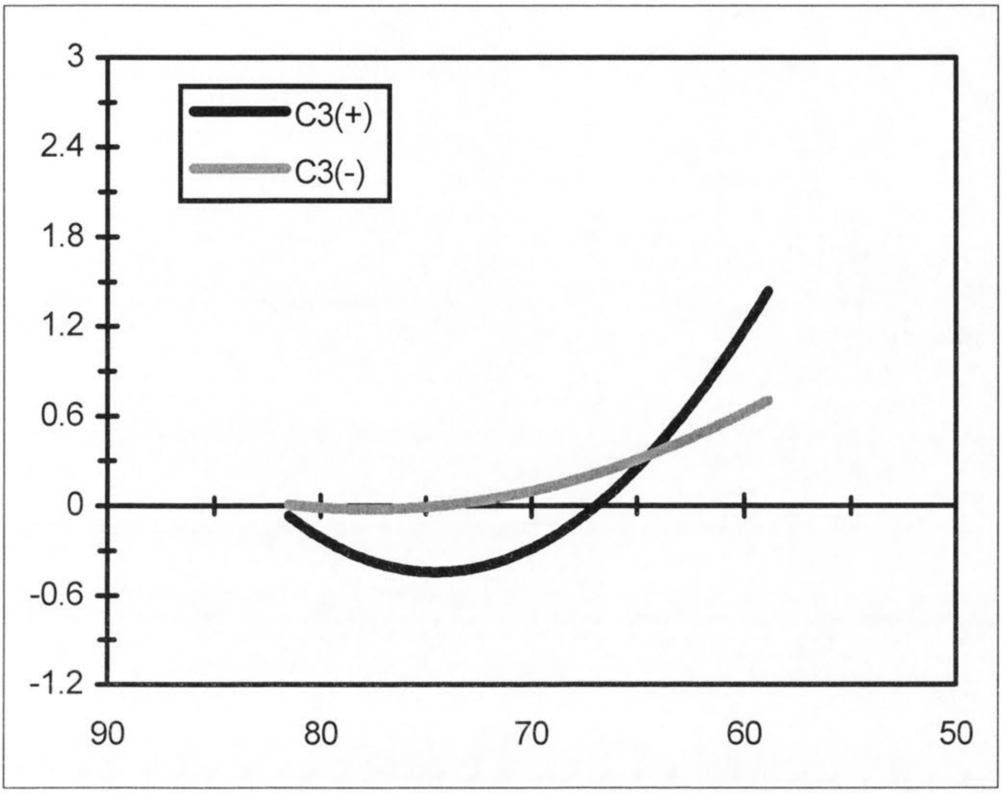

Figure 6-26. Skewness of PD Current Distribution Vs Temperature (°C)
Temperature Decreasing at 10kV; Positive (C3+) and Negative (C3-) Half Cycle

The kurtosis value that measures the sharpness of a PD distribution relative to a normal (Gaussian) distribution behaved differently for each PD distribution considered. Figures 6-27 and 6-28 show the trend of the kurtosis values of the average discharge magnitude distribution as the test temperature changed (increasing in 6-27 and decreasing in 6-28). The kurtosis value at the positive half-cycle tended to decrease to a minimum peak and then increase as the temperature further increased. A reverse trend was observed when the temperature reduced back to ambient.

The discharge current and discharge number distributions had a relatively constant value of the kurtosis as the test temperature increased above 60°C. However, when the temperature reduced back below 70°C, a sharp increase in the kurtosis value was observed. Meanwhile, the kurtosis of PD maximum amplitude distribution changed with the temperature. The value tended to increase as the temperature increased and decrease as temperature decreased.

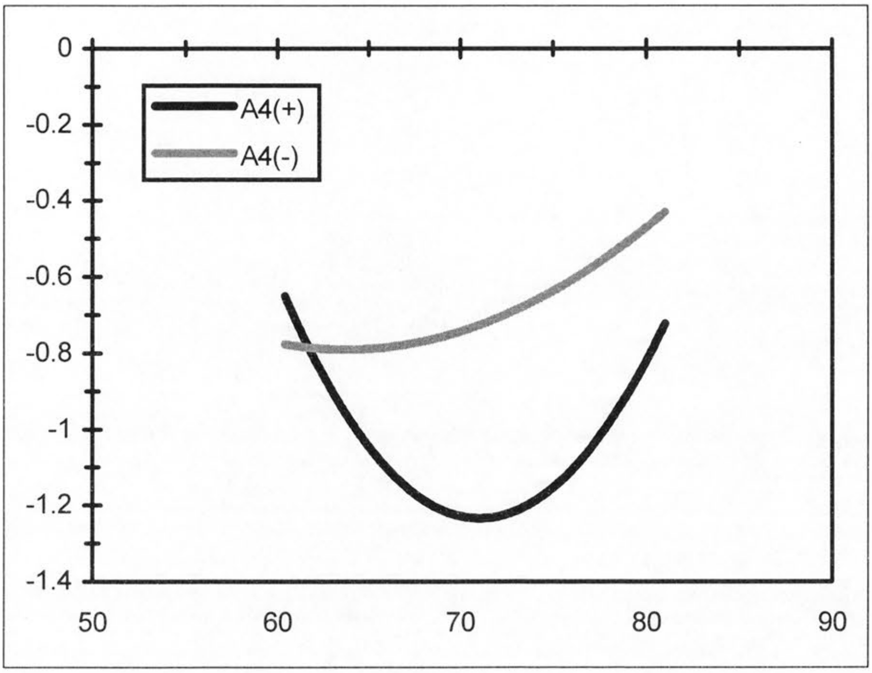

Figure 6-27. Kurtosis of Average PD Distribution Vs Temperature (°C)
Temperature Increasing at 10kV; Positive (A4+) and Negative (A4-) Half Cycles

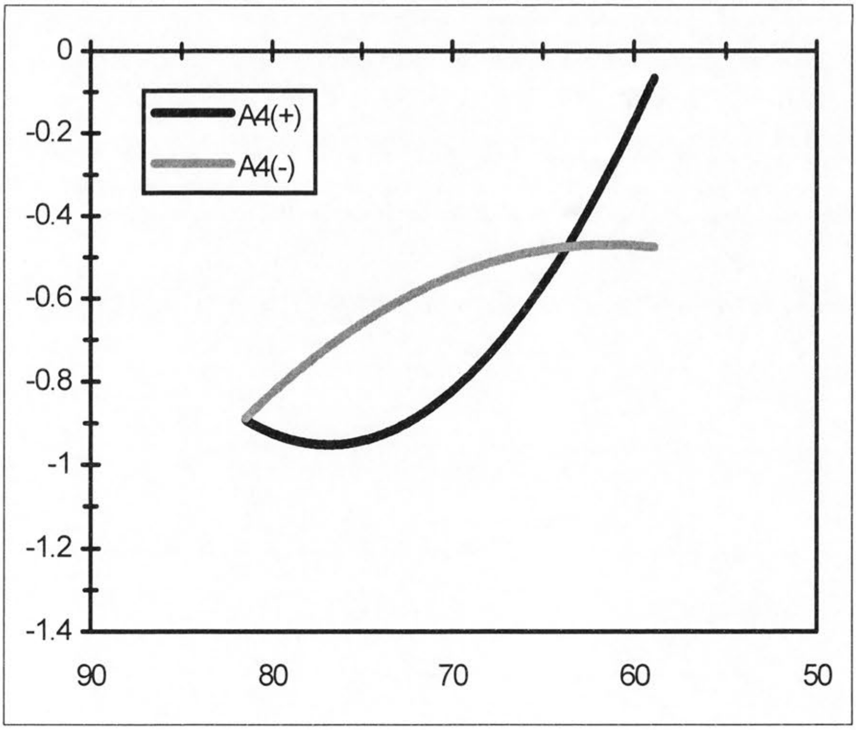

Figure 6-28. Kurtosis of Average PD Distribution Vs Temperature (°C)
Temperature Decreasing at 10kV; Positive (A4+) and Negative (A4-) Half Cycles

6.3.6 Summary of the Statistical Analysis of Results

The statistical analysis results of the tests conducted showed that the mean of the maximum PD distribution shifted to a larger phase angle as the test temperature increased for both positive and negative half-cycles and the PD mean distribution tended to shift back to a lower phase angle when the test temperature decreased. The PD average distribution had similar trends of the mean values. The mean of the PD number distribution and the PD current distributions, however, are relatively steady at about 105° when the test temperature was increased. The mean shifted to a lower phase angle as the test temperature reduced. A slight increase in the standard deviation of the PD number distribution was seen as the temperature increased. A reverse trend occurred as the test temperature reduced. This indicated that the distribution extended when temperature increased and reduced when the temperature reduced.

Generally, the standard deviation of all other distributions (maximum PD, average PD and PD current) behaved similarly to that for PD number and the skewness value of the PD distributions decreased when the test temperature increased and increased when temperature decreased. A trend towards a larger negative value of skewness indicates that there is an extension on the tail of the distribution to a lower phase angle. Thus as the temperature increased, a higher number of discharges appeared on the lower phase angle of the mean. The kurtosis value that measures the sharpness of a distribution relative to a normal distribution behaved differently for each PD distributions considered. The kurtosis value on the positive half-cycle tended to decrease to a minimum peak and then increase as the temperature further increased. A reverse trend was observed when the temperature reduced back to ambient.

The statistical parameters, such as the mean, the standard deviation, the skewness and the kurtosis of the phase resolved partial discharge patterns are meaningful and are considered unique for particular insulation defect conditions. The statistical analysis was conducted to examine whether there was some distinctive properties that could be used as indicators for the assessment of oil-impregnated insulation during the change of temperature. Results showed that the PD distribution might change significantly when the temperature is changed. The careful study of the statistical operators for PD classification in condition monitoring can be used as indicators for the better assessment and understanding of oil-impregnated insulation.

6.4 Conclusions

A number of significant observations of the tests using the glass cell were noted during the increasing and decreasing temperature phases in the experiment. The following PD pattern analyses were observed during the variation of temperature and ageing of the oil-impregnated transformer insulation.

- During simulated thermal overloading when temperature increased from ambient to 80-85°C the largest peak PD magnitude measured was initially on the positive half cycle, but the peak then shifted from the positive to the negative half-cycle.

- During the cooling phase from 80-85°C to the ambient temperature the PDs with largest peak magnitude shifted back again from the negative half cycle to the positive half-cycle.

- At 80°C the PDs with largest peak magnitude were found to be similar on both the positive and negative half-cycles.

- The colour of the oil changed from clear to light brown after the ageing due to thermal stress causing oxidation.

- The colour of the kraft paper, the crepe paper and the pressboard changed from the original light brown shade to dark brown with ageing. The ageing due to PD activity can cause a burning or carbonisation effect on both pressboard and paper and also caused the paper to become brittle through de-polymerisation.

- The peak magnitude of the discharges and the PD repetition rate increased with the increase of temperature and decreases with decrease of temperature.

- Similar test configurations result in similar partial discharge patterns at a same temperature stress level.

From the experimental results, it can be concluded that the peak and the average PD magnitude are greatly affected by the temperature change. The discharge number and the discharge current varied significantly with the test temperature. The variation of PD levels with temperature is an important factor in using PD diagnostics to assess insulation condition in transformers.

Observation of the statistical moments of PD distributions of the phase resolved partial discharge patterns are meaningful and showed that the distributions change significantly when the temperature is changed. This indicates that the use of statistical operators for automated PD classifications in insulation condition monitoring has to be conducted carefully. The use of separate PD signatures for different test temperatures and insulation condition would be appropriate indicators for the better assessment and understanding of oil-impregnated insulation.

Chapter 7

Effect of High Temperature and Moisture on Recovery Voltage Measurement Results: An Experimental Investigation

7.1 Introduction

The reliability of the power transformer largely depends upon the condition of the oil-paper insulation. Extending transformer life beyond its design life is not only economically valuable, but also prevents loss of revenue caused when power failure occurs. Insulation condition monitoring is therefore becoming increasingly important, as this tool can be used to determine the integrity of the insulation [74, 191]. Thus the development of all potential diagnostic techniques is an important consideration.

The dielectric system of a typical oil-impregnated power transformer is used to provide insulation for the high voltage windings and connections while the oil performs a dual function as an insulant and as a cooling medium. The presence of moisture in the oil/paper insulation plays a critical role in determining the life span of a transformer. Moisture in the transformer reduces the insulation strength by decreasing the electric strength of the transformer's insulation system. As we have seen, when the transformer warms up during operation and particular when it supplies excess load, at the high temperatures attained moisture migrates from the solid insulation into the oil and the gas space above the oil. Transformer oil has a low affinity for water but even low levels of dissolved moisture can cause problems. The solubility of moisture in oil increases noticeably as the temperature increases.

On the other hand paper can absorb very significant amounts of moisture and is thus there is likely to be much more moisture in the paper than in the oil. The moisture in paper will also reduce significantly the dielectric strength of the paper insulation. The rate of migration of moisture to the paper in a transformer is dependent on the conductor temperature and the rate of change of the conductor temperature. As the transformer conductors (and the paper) heats the moisture is expelled from the paper into the oil as we have seen and can form bubbles. Then, as the transformer cools, the moisture returns to the solid paper and the pressboard insulation but at a somewhat slower rate. Both the paper and pressboard in a transformer can absorb more moisture at ambient, whereas the oil can absorb more moisture at overload temperature. Moisture in paper is usually measured in percentage, while in oil it is usually given as parts per million of the oil mass [192-193].

The magnitude of the load and the climate and the resulting temperature are the major influences in determining the ageing of the insulation and thus the remnant life of an aged transformer. The ageing and life expectancy of the insulation, in turn, are greatly dependent on environmental conditions, which involve hydrolytic, oxidative and thermal degradation. The moisture in a transformer is absorbed from the atmosphere and is also produced by the ageing of the cellulose based paper and pressboard insulation. At high temperatures the hydrocarbon chains in the cellulose break down into smaller chains and this breaking process involves the release of hydrogen and oxygen atoms. The released gases then combine to form water. Excessive amounts of moisture in the transformer can then accelerate the ageing process of the cellulose and prematurely age the transformer's insulation system.

Moisture in the paper and oil also brings the risk of bubble formation as documented in the previous experimental results; it is a significant risk in paper insulation especially at overload temperatures. High moisture content in the oil/paper due to ageing can cause failure of the transformer [28, 194-196]. Therefore, the level of moisture content in the oil/paper is one of the decisive factors used in determining the total breakdown strength of an insulation system. To assess the extent of degradation of an insulation system, it is therefore necessary to know the moisture content of oil/paper. Insulation diagnostic techniques have therefore become increasingly important as they can be used to determine the integrity of the insulation and also allow us to estimate the remaining life of the insulation.

A number of insulation diagnostic techniques are available and can be categorised into electrical, mechanical and chemical methods. One of the electrical insulation diagnostic techniques introduced in the mid 70s is the Recovery Voltage Measurement (RVM). RVM is a technique for determining the level of moisture content and hence, potentially, the degradation of oil/paper insulation [192-195]. Although it is not possible to use RVM to obtain quantitative estimates of moisture in the insulation, it is nevertheless a very useful technique.

Recovery Voltage Measurement experiments were conducted on the insulation models used in this thesis, using a LabVIEW (Laboratory Virtual Instrument Engineering Workbench) based software [28, 197]. Comparison of the change in relaxation phenomena in each test object under particular condition with DC RVM measurement in relation to partial discharge measurement is made and the obtained new results are reported in this chapter.

7.2 Recovery Voltage Measurement

The RVM technique used to assess the state of oil-paper insulation has been undergoing research and development over the world for almost thirty years. The main aim is to develop new insulation diagnostic methods for assessing large transformers in service [194]. RVM is a non-intrusive and non-destructive test that can be performed on-site and also in the laboratory. The data acquisition is not very sensitive to external disturbances, but temperature and humidity may influence the results of the measurements. It relies on the dielectric properties of oil/paper insulation and gives a general indication of moisture content in insulation system [195-196].

RVM is based on use of the dielectric response of insulating materials to the application of electric fields and is thus part of the general area of dielectric spectroscopy. In order to understand the method in detail we need to discuss briefly the dielectric response of polar insulating materials to a step change of a DC voltage applied to the dielectric material by means of some form of metal electrode configuration.

Solid and liquid dielectric insulation materials have a dielectric response to an applied DC electric field that is determined by the intrinsic structure and composition of the material, including in particular their polarization properties which may feature any of the following aspects:

- molecular dipole structure,
- electronic polarisation,
- ionic polarisation,
- interfacial polarization

Many other facets, including in particular the chemical composition, may also affect the dielectric response [200].

The actual dielectric response of the dielectric material is thus a sensitive indicator of the material insulation state and hence of its dielectric condition. Any impurities such as moisture or change in the material structure and chemistry, caused for example by thermal ageing, should theoretically be able to be characterised by a determination of the dielectric response of the material to an applied DC voltage.

Moisture in this case is both an impurity and a by-product of ageing of insulation. It is arguably the most common cause of problems with service-aged insulation. Because of its high molecular dipole moment and its consequent high relative permittivity and loss factor, moisture as a foreign material can have a quite disproportionate effect compared to its quantity in the dielectric. Fortunately, its effect on the dielectric properties of insulation also makes its presence relatively easy to detect.

7.2.1 Recovery voltage measurement for transformers

In developing the techniques to use for moisture detection, one of the characteristics of moisture that can be utilised is its high dielectric dissipation factor (DDF) and high relative permittivity which render its contribution to the polarization response very substantial when DC voltage steps are applied. The moisture will increase DDF and also the capacitance. However the use of standard DDF techniques is not sufficiently sensitive and accurate enough to quantify moisture. But the effect of the moisture on the polarization properties of the insulation can be monitored and thus can be used to give some indication of moisture levels.

The DDF of insulation results from the overall polarization effect of the applied electric field on the dielectric material. The overall polarization of an insulator dielectric is thus the integrated result of the individual polarization components listed above, including atomic, electronic, ionic, thermal and interfacial polarization.

In the case of moisture in the dielectric, it is the interfacial polarization that gives the most important contribution. This can result from moisture effects on the interface between the paper and the impregnating oil, for example. Interfacial polarisation occurs whenever there is an accumulation of charge at the interface between two materials, e.g. in the interfacing of paper and oil in the power transformers. More moisture content results in more conduction and lower resistance, which leads to a lower time constant in the response [28].

Moisture presence will affect the overall polarization properties very significantly and this is the basis of the technique of the recovery voltage measurement (RVM) for moisture assessment. The recovery voltage method for transformers is similar to the more general polarization-depolarization current (PDC) method except that recovery voltages across the insulation are measured during the final open circuit phase. The current response is not used in this method. The shape and magnitude of the recovery voltage in terms of its peak value and its initial rate of rise are the important quantitative considerations as will be seen later.

The time constant of the interfacial polarization response, which is so highly influenced by the moisture content of the oil/paper insulation and the absorption of by-products of aging, falls in the range of 10ms to 1000s of the time domain response.

7.2.1.1 General polarization response

In insulation containing components of different permittivity and conductance, the ions can accumulate on the surface of various insulating materials and thus form dipoles. More moisture in the insulation results in more free charge on the interface and the polarization field will thus increase. The polarization process can only exist in the presence of an external electric field. However, when that field is removed, the dipoles will return to their original state as they relax and the charge is dissipated. In the case of moist oil-paper insulation, there is a significant polarization effect due to the water molecules contained in the insulation. By applying a DC electric field, these molecules (which were electrically neutral) acquire a polarization and try to drift or move or just orient in the direction of the electric field. Measurement of the current in the time domain during the polarization phase will thus give a response dependent on the moisture level. Similarly, when the field is removed and the insulation sample short-circuited, the depolarization current in the time domain will give a response determined by the moisture level. This is the pure PDC technique. The RVM method is slightly different in that it measures a recovery voltage rather than a depolarization current.

In the RVM method, the sample is first short circuited but is then open circuited to monitor the recovery voltage of the open-circuit. The equivalent circuit of the RVM charging phase in a homogeneous insulation is shown in Figure 7-1. The voltage applied is denoted by Vc, Cg is the geometric capacitance, Rg is the geometric resistance, Cp is the polarization capacitance and Rp is the polarization resistance.

Each RVM test cycle consists of 4 phases: (1) charging, (2) discharging, (3) measurement and (4) relaxation. The sample is to be charged with a DC voltage for a charging time t_c, during which molecules are polarised and align in the direction of the DC electric field. The sample is then short-circuited for a pre-determined period of time t_d (usually half of the charging time), causing the molecules to be partially depolarised and relaxed. The test sample is then open-circuited and the voltage monitored in the time domain.

Upon opening the short circuit, a voltage due to the remaining charge will build up between the terminals of the insulation sample. This residual polarisation results in a voltage known as the recovery voltage. Two measurements are taken in each test cycle and they are the maximum recovery voltage (V_{max}) and central time constant (time to peak; t_{peak}). The four phases of RVM are shown in Figure 7-2. The ratio dV/dt in Figure 7-2 is the initial slope of the recovery voltage.

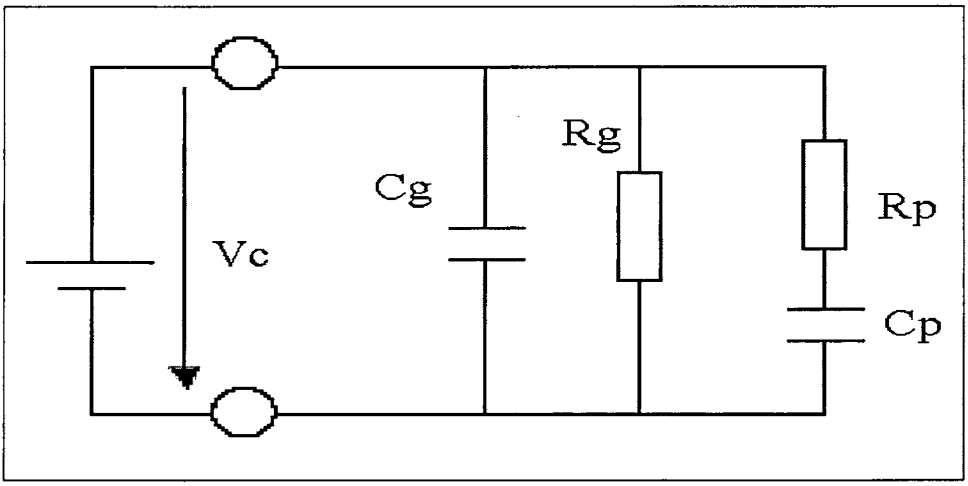

Figure 7-1. Equivalent Circuit of RVM in Homogeneous Insulation [28].

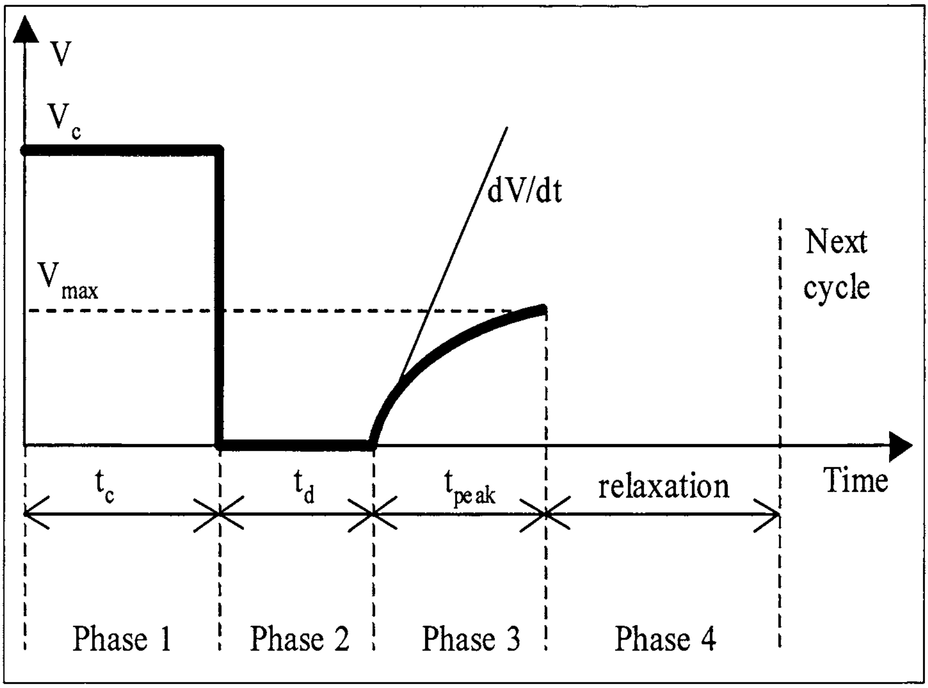

Figure 7-2. Test Phases in One RVM Measurement Cycle [28].

The charging/discharging procedure is repeated using a sequence of increasing charging times range from fractions of a second to thousands of seconds. A curve of maximum recovery voltage (V_{max}) against charging time (t_c) is then plotted. This curve is known as the polarisation spectrum, as shown in Figure 7-3.

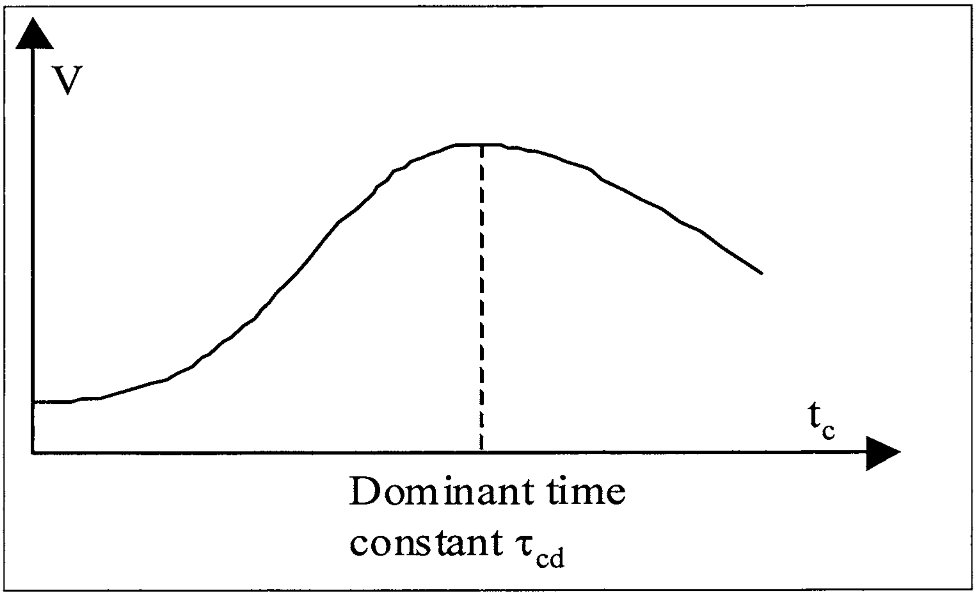

Figure 7-3. Recovery Voltage Measurement Polarisation Spectrum: Maximum Recovery Voltage (V_{max}) along Y- Axis Vs Charging Time (t_c) along X-Axis; Dominant Time Constant (τ_{cd}) [28]

A significant characteristic of the polarisation spectrum is the time at which the peak occurs: this is known as the dominant time constant (τ_{cd}). This value is dependent on the properties of the insulating material. More precisely, this value directly reflects the moisture content of the oil/paper insulation system. The displacement of the peak of the curve towards a smaller time constant indicates a higher moisture level and thus some degradation of the insulation system.

The insulation system with higher moisture content has a relatively fast polarisation response in which the polarisation capacitance charges and discharges faster, resulting in the maximum recovery voltage being attained at shorter charging time. On the other hand, an insulation system with lower moisture content has a relatively slow polarisation response in which the polarisation capacitance charges and discharges slowly. Hence, the value of maximum recovery voltage can only appear at longer charging time. The polarization spectrum is also affected by temperature. At higher temperatures the peak of the curve shifts towards smaller time constant indicating insulation degradation.

The polarisation spectra obtained can be divided into two basic groups: standard and non-standard spectra.

The standard group of polarisation spectra have only one maximum peak in the curve, which reasonably provides an estimate of the moisture content in the oil/paper insulation.

Curves with multiple peaks, flat curves and curves with discontinuities are considered as the non-standard spectrum group. More information on the test object and experience are required to interpret this kind of graph.

7.3 Measurement System

Figures 7-4 and 7-5 below show the configuration and measurement system layout diagram of the RVM system developed and used in the High Voltage Laboratory for these tests. The computer is used as a controller to automate the measurement process. Interfacing is through a National Instruments data acquisition card (DAC→PCI-6025E). Three digital output channels are used for controlling the relays in the switching unit. One analog input channel (Analogue to Digital Converter; ADA) is used for recording the recovered voltage signal from a Keithley electrometer. The peak recovery voltage for each RVM test cycle is recorded from the output of the electrometer.

The relays in the switching box are controlled by the computer to switch the system on and off at predetermined charging, discharging and measurement times. The user can programme the time interval values in. At the end of each RVM cycle, the test object will be discharged for a certain period of time to remove the residual charge. The charging voltage is provided by a variable high-voltage DC supply, which can be set in the range 0-3000V.

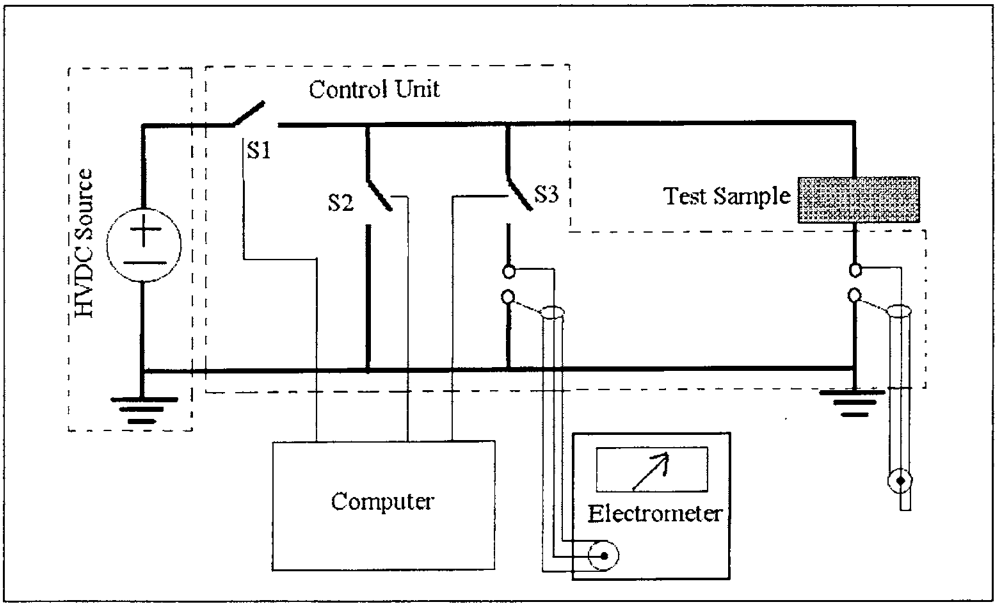

Figure 7-4. Configuration of Recovery Voltage Measurement System [28]

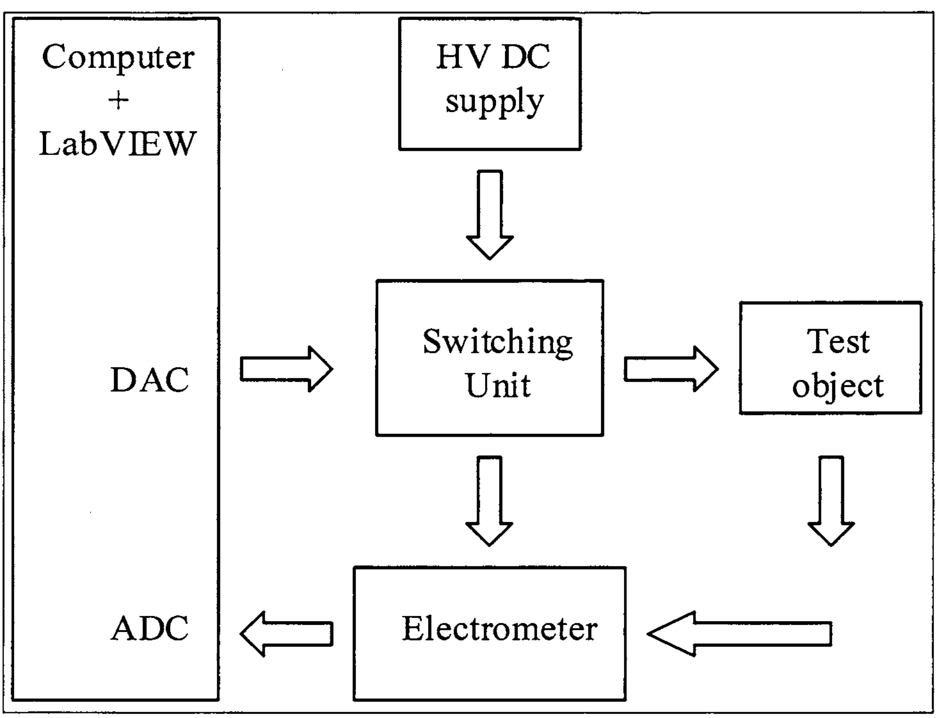

Figure 7-5. Recovery Voltage Measurement System Layout Diagram [28]

LabVIEW acts as the "brain" of the system, and controls the relays, captures the signal and calculates the required parameters. The front Panel of the RVM system used in these experiments is shown in Figure 7-6.

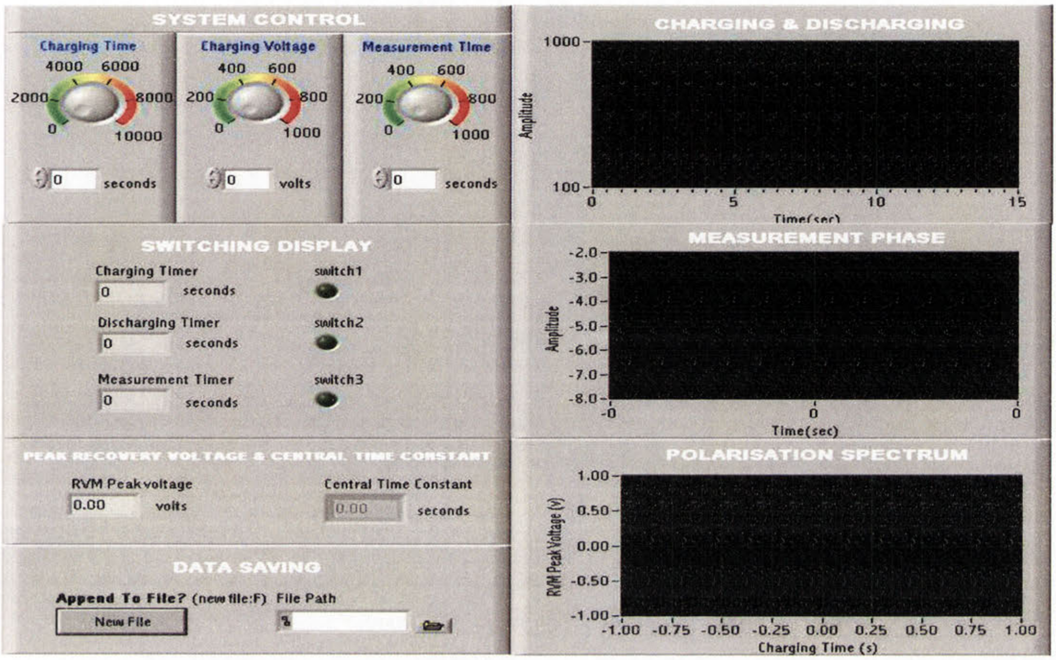

Figure 7-6. Front Panel Of The RVM System [28].

The recovery voltage obtained from the electrometer can be somewhat noisy and a filtering circuit is used to clean up the signal [28]. Features such as data storage, plotting of the recovery voltage of individual measurement, plotting of the polarisation spectrum and concurrent temperature sensing are added features of the system. The detailed RVM operational manual for the system is included in Annexure "E" [28, 197].

7.4 Experimental Results and Discussions

The experiments were carried out in the laboratory on the previously described laboratory models of transformer oil-impregnated insulation at different temperatures and with different moisture contamination levels. An oil sample extracted from the tank was sent to an industrial laboratory for measuring its moisture content. The configuration of steel tank and oil-impregnated paper/pressboard insulation has already been explained in chapter 5 (section 5.5). Figure 7-7 shows the recovery voltage measurement experimental set up.

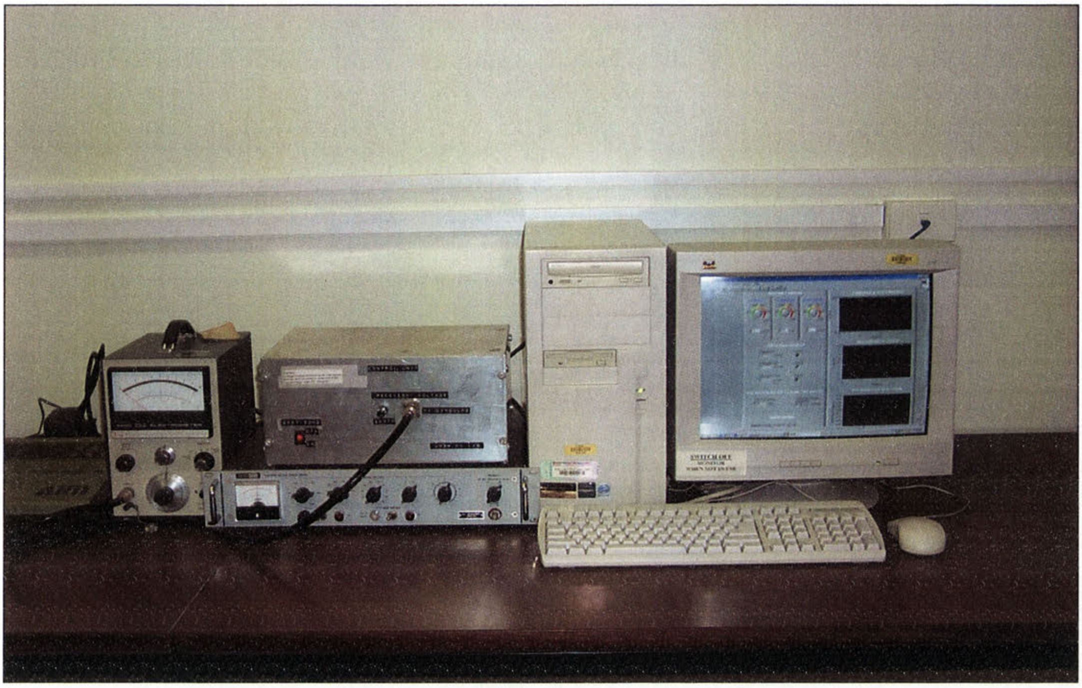

Figure 7-7. Recovery Voltage Measurement Experiment Set-Up.

The experiments were performed at three different temperatures: 20°C (room temperature), 80°C (normal operating temperature) and 140-145°C (overloading condition). The temperature was monitored using the fibre optic thermometer. The charging voltage was set to 500V and 1000V. A relaxation time of 10 minutes was applied in all the tests. A complete set of reading for each set of voltage and temperature took approximately 2.5 hours. Normally six complete sets of readings (500V- room temperature, 80°C, 140-145°C and 1000V- room temperature, 80°C, 140-145°C) were required for comparison purposes. To raise or lower the temperature of the test conductor and insulation from 140-145°C to ambient took around 4-5 hours.

In addition to recovery voltage measurement, partial discharge measurements tests (135 and 255ppm moisture content in oil at 80°C) were carried out using the CDA3 PD system to assess the insulation of the oil-impregnated aged insulation from the PD aspect.

Many tests were carried out under different conditions of moisture content, temperature and charging voltage. Figure 7-8 shows the polarisation spectrum for the tests conducted at temperature of 80°C with moisture content of 135ppm. It can be seen that an increase in the charging voltage results in an increase in the recovery voltage and that the scaling effect of the charging voltage on the polarisation spectrum is reasonably constant. The dominant time constant is ~10 seconds. Figure 7-9 shows the corresponding PD pattern at moisture content in the oil of 135 ppm.

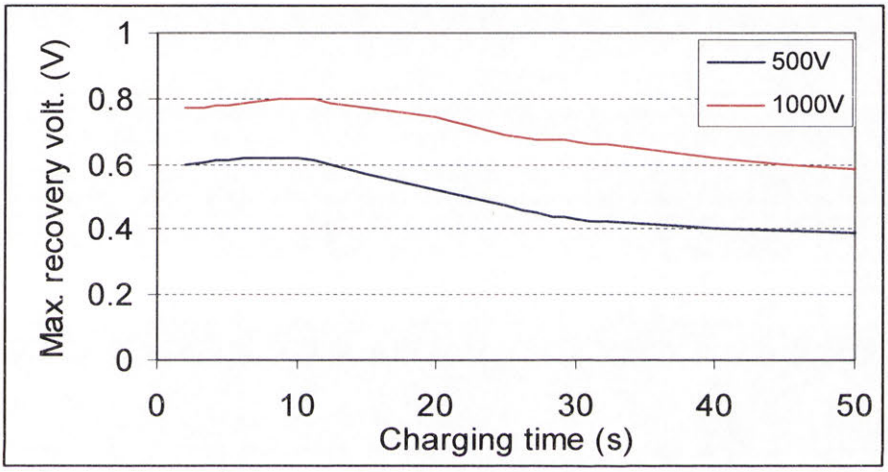

Figure 7-8. Polarisation Spectrum (80°C, 135ppm at 500V and 1000V):

Maximum Recovery Voltage (volts) Along Y-Axis Vs
Charging Time (seconds) Along X-Axis

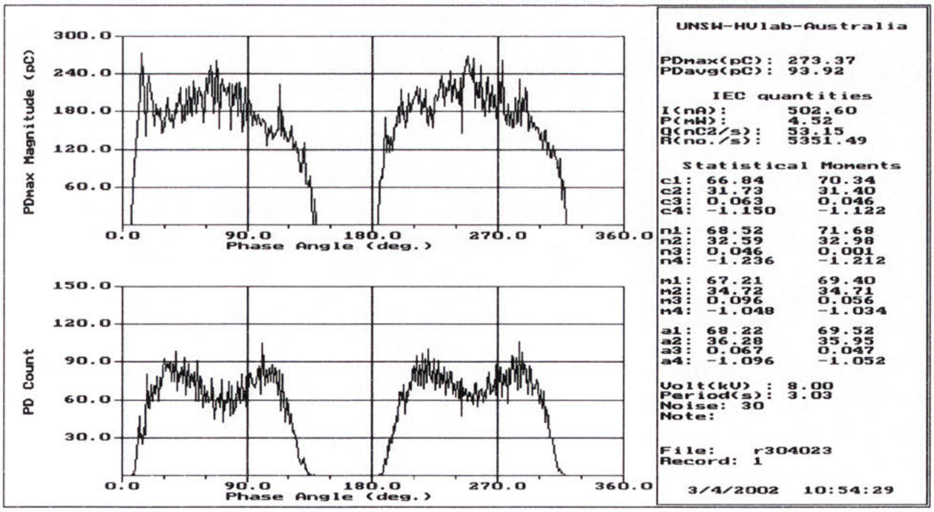

Figure 7-9. PD Pattern at 8KV (80°C, 135ppm).

Figure 7-10 shows the polarisation spectrum for the tests conducted at the same temperature of 80^0C but with higher moisture content of 255ppm. The dominant time constant is ~5 seconds.

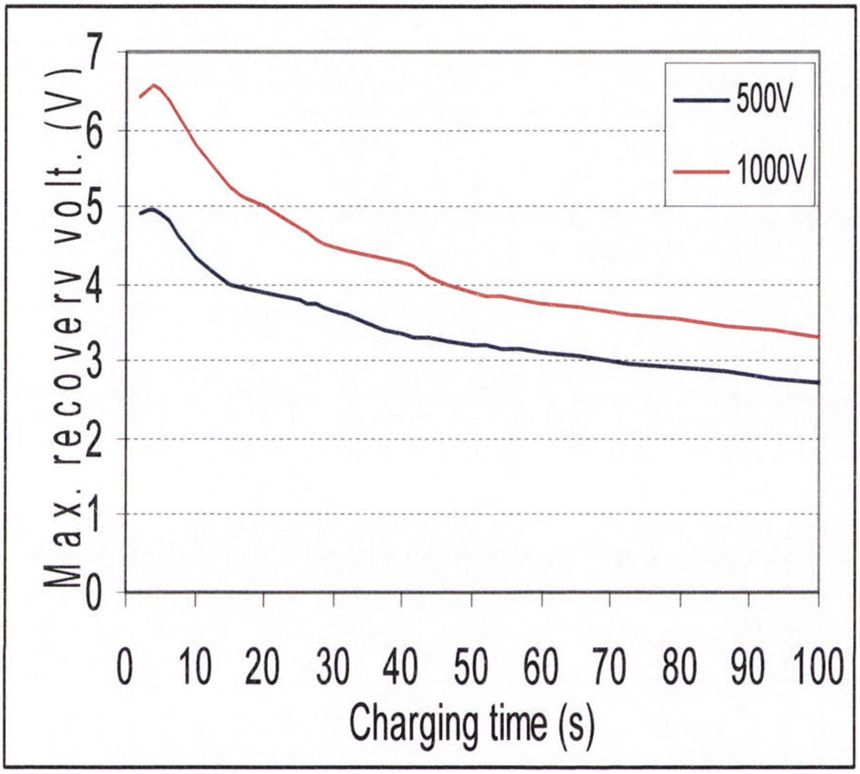

Figure 7-10. Polarisation Spectrum (80°C, 255ppm at 500V and 1000V):

Maximum Recovery Voltage (volts) Along Y-Axis Vs
Charging Time (seconds) Along X-Axis

Comparison of Figures 7-8 and 7-10 shows the respective polarisation spectra for the tests conducted at temperature of 80^0C with moisture content of 135ppm (Figure 7-8) and for moisture levels of 255 ppm (Fig 7-10). In figure 7-8, it is seen that increasing the charging voltage results in an increase in the recovery voltage and that the scaling effect of the charging voltage on the polarisation spectrum is reasonably constant and the dominant time constant is ~10 seconds. The polarisation spectrum for the tests conducted at the same temperature of 80^0C but with higher moisture content of 255ppm (Figure 7-10) show that the smaller dominant time constant is now about 5 seconds.

Thus, the insulation system with higher moisture content has a relatively faster polarisation response, and therefore the value of the maximum recovery voltage is attained at a shorter charging time. The shorter charging time is due to the higher moisture content in the oil causing the faster polarisation response, which means the polarisation capacitance charges and discharges faster, which then caused the maximum recovery voltage (V_{max}) to appear at the shorter starting time and so the dominant time constant is ~5 seconds. Figure 7-11 shows the PD pattern for the system at moisture content in oil at 255 ppm. Note that there is some difference in the PD patterns.

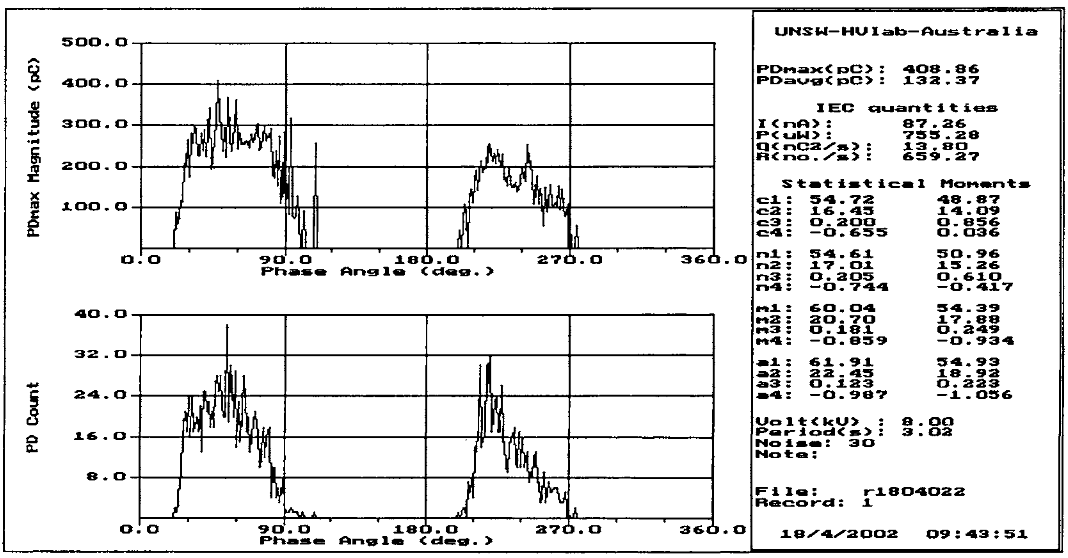

Figure 7-11. PD Pattern at 8KV (80°C, 255ppm).

Figure 7-9 shows higher PD, current, power, quadratic rate and repetition rate at the temperature of 80^0C and moisture content of 255ppm in oil. And Figure 7-11 shows lower PD, current, power, quadratic rate and repetition rate at the temperature of 80^0C and moisture content of 255ppm in oil. The higher PD current (502nA), power (4.52mW), quadratic (53 nC^2 /s) , repetition rate (5351 no./s) and low inception angle less than 10 degrees in a phase resolved plot (Figure 7-9) is possibly due to higher moisture content in paper. The lower PD current (408 nA), power (755uW), quadratic (13 nC^2 /s) , repetition rate (659 no./s) and higher inception angle more than 20 degrees in a phase resolved plot (Figure 7-11) is possibly due to less moisture content in the paper. The water added directly to paper in the steel tank migrated from paper to oil during overloading raising moisture content in oil from 135 to 255ppm. With increase in water content from 135 to 255ppm at a temperature, peak voltage increased due to increase in polar water content. With increase in temperature more water may be dissolved in oil but the peak is found to decrease due to increased mobility of active ions in relation to polarised water molecules. Increased max. PD peaks with increase in moisture content were observed. Apart from that I and R reduced by increasing moisture content.

When comparing the results obtained from both the recovery voltage measurement and partial discharge measurements tests to assess the insulation of the oil-impregnated aged insulation it was observed that RVM tests conducted at the same temperature of 80^0C but with higher moisture content of 255ppm in oil has a smaller dominant time constant of 5 seconds in the polarisation spectrum showing there is moisture in the oil/paper insulation and degradation. Contrary to this, in the PD test results the higher PD current (502nA), power (4.52mW), quadratic (53 nC^2 /s), repetition rate (5351 no. /s) and low inception angle less than 10 degrees in a PD's phase resolved at same temperature of 80^0C but with lower moisture content of 135 ppm in oil show there is moisture in the oil/paper insulation and degradation.

The results obtained from the PD tests seem more promising and logical to the author as they are in line with the results obtained in the previous chapter, namely that moisture in paper (which can cause PDs) is more dangerous as compared with moisture in the oil. Further, the PD results show low PD inception angle and high PD repetition rate can be used as a very useful diagnostic tool in identifying moisture and ageing affects in oil-impregnated cellulose based transformer insulation.

The RVM results for the case of 500V in Figures 7-8 and 7-10 are combined for comparison and shown in Figure 7-12.

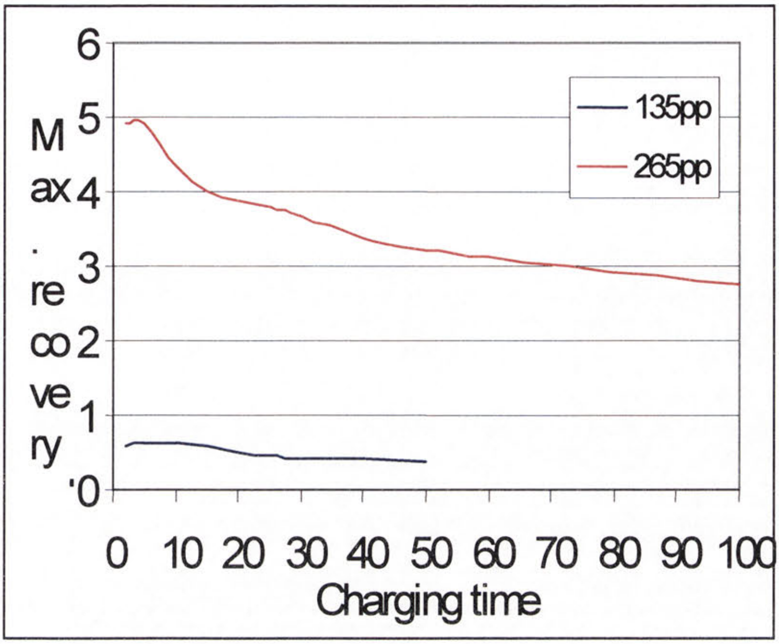

Figure 7-12. Polarisation Spectrum (80^0C,135 and 255ppm at 500V):

Maximum Recovery Voltage (volts) Along Y-Axis Vs
Charging Time (seconds) Along X-Axis

Figures 7-10, 7-13 and 7-14 show the effect of temperature on the polarisation spectrum. The actual temperatures recorded on the conductor, paper and oil for the three different temperature conditions are shown in the Table 7-1 below.

Condition	**Conductor Temperature**	**Paper Temperature**	**Oil Temperature**
Ambient	24^0C	24^0C	24^0C
Normal Operating Temperature	80^0C	80^0C	80^0C
Overloading Conditions	140-145^0C	115-120^0C	80-85^0C

Table 7-1. Measured Temperatures of Test Conditions.

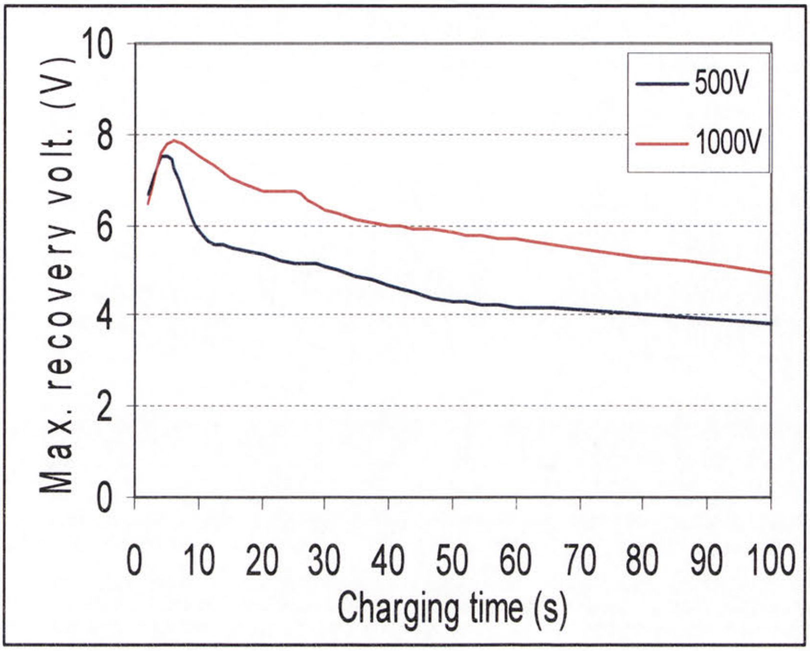

Figure 7-13. Polarisation Spectrum (20°C, 255ppm at 500V and 1000V):

Maximum Recovery Voltage (volts) Along Y-Axis Vs
Charging Time (seconds) Along X-Axis

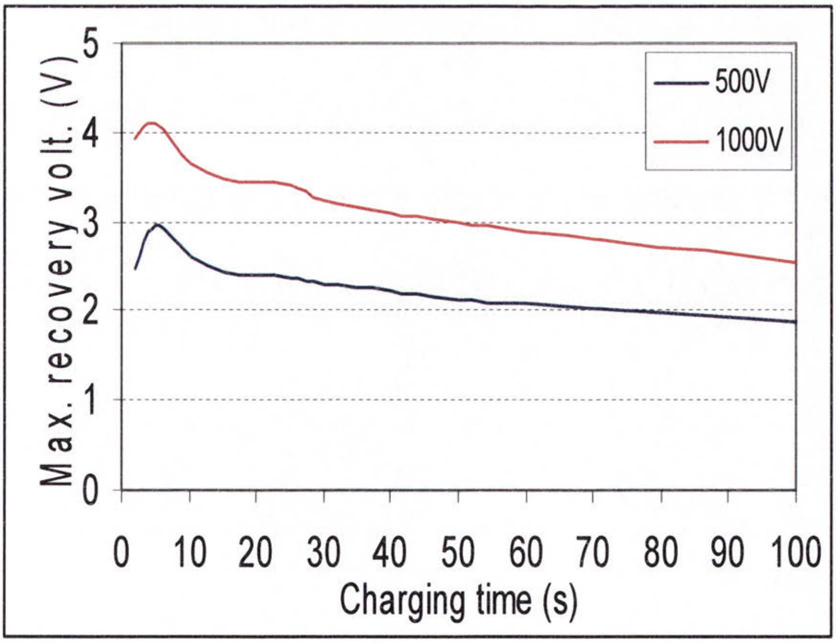

Figure 7-14. Polarisation Spectrum (140-145°C, 255ppm at 500V and 1000V):

Maximum Recovery Voltage (volts) Along Y-Axis Vs
Charging Time (seconds) Along X-Axis

The results are combined and shown in Figure 7-15 for the case of a 500V charging voltage. It can be seen that the recovery voltage decreases with increasing temperature. However, there are no significant changes in the dominant time constant, which is an unexpected result. The possible reason for this is that the moisture exchange between paper and oil and the polarisation process tends to be more active at higher temperature [91], thus resulting in more free charges in the interface. Consequently, the electrical conductivity is higher and the resistance is lower, leading to the maximum recovery voltage being attained in a shorter period, as the time constant is directly proportional to the electrical resistance.

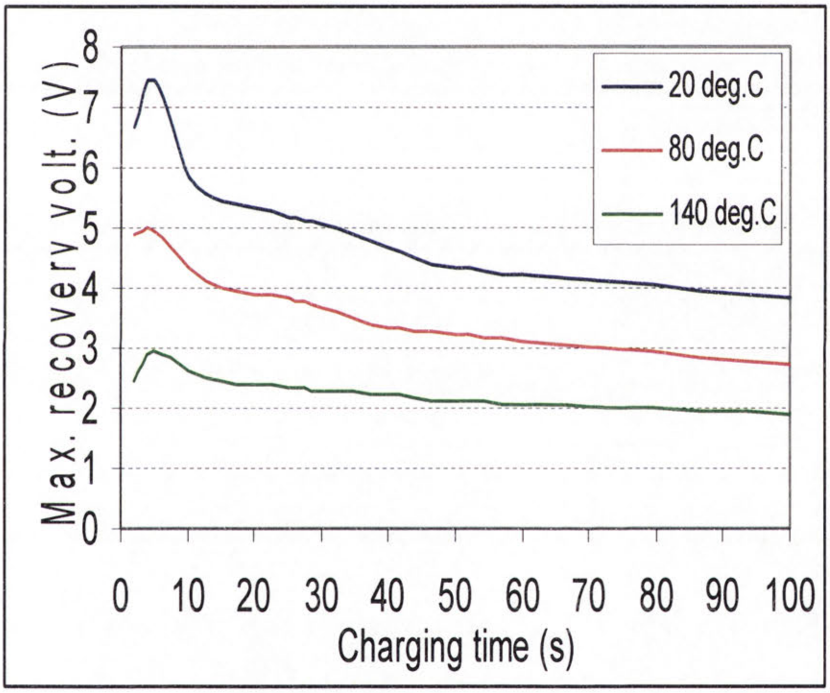

Figure 7-15. Polarisation Spectrum (20°C, 80°C and 140°C, 255ppm at 500V):

Maximum Recovery Voltage (volts) Along Y-Axis Vs
Charging Time (seconds) Along X-Axis

One possible explanation for the failure to obtain a reduction in the time constant with increasing temperature is that, following the injection of water into the oil, the test cell was not allowed to stand for long enough so that the paper could absorb the moisture totally within its whole structure.

7.5 Conclusions

The following discussion and observations are based on the results obtained from the experiments conducted on the oil-impregnated paper insulation laboratory models.

- The peak of the polarisation spectrum shifted to a smaller time constant with increase of moisture content in the oil. The study also indicated a good degree of linearity in response to variation of charging voltage.

- Uneven distribution of moisture or other ageing products may complicate the evaluation of the measurement of recovery voltage. Therefore, moisture equilibrium of the test object plays an important role in determining the conditions of the insulation system and in analysing the results of global monitoring systems such as polarization spectroscopy and its derivative methods.

- Overall, recovery voltage measurement is an insulation diagnostic technique which is capable of assessing the conditions of the aged transformer from moisture in oil/paper insulation, although it is not able to give quantitative indications of moisture content. Additionally, the results of analysis of moisture in oil/paper insulation can also be used as a tool for the planning of maintenance.

- Monitoring transformer insulation using PD diagnostic methods along with another diagnostic method allows better understanding of the insulation condition and of the reliability in the interpretation of the results.

With the introduction of the LabVIEW program in the recovery voltage measurement system, the whole measurement process becomes easier and straightforward. It provides data storage capability and allows development of a data bank, which can be used for future reference and research. As LabVIEW offers online monitoring over the Internet using Transmission Control Protocol (TCP)/Internet Protocol (IP), future implementation of this feature can improve the development of a computer based data logger for RVM.

Despite the advantages of the RVM measurement technique, it is not as useful as PD measurement in enabling sensitive interpretation of the health of oil-impregnated transformer insulation. PD measurement is more sensitive indicator, whereas RVM is very much a general tool that cannot give moisture information if you are looking at moisture over a long period of time. Also on-line PD measurement is easier to do. Monitoring the oil/paper insulation using polarisation and depolarisation current (PDC) and dielectric spectroscopy is perhaps a bit more flexible than RVM but still not as sensitive/useful as monitoring insulation condition by PD measurement.

Chapter 8

Conclusions and Recommendations for Further Work

8.1 Conclusions

8.1.1 Diagnostics and assessment

Power transformers are the most expensive and indispensable components of an electrical transmission system. Many power transformers in operation in power systems today have passed their nominal design life under different electrical, thermal, mechanical and environmental stresses. Their sudden insulation failure can cause long-term interruption, costly repairs and loss of revenue. It is the insulation system of the transformer that will eventually determine the condition of the transformer and when it either reaches the end of its life or when its condition requires major remedial action or repairs. There is thus a need to develop and improve both monitoring diagnostics and interpretation techniques when assessing the insulation condition of such transformers.

There have been new (or in some cases, improved versions of older methods) diagnostics developed in recent years for transformers. These include Recovery Voltage (RV) techniques, Polarization-Depolarization Current (PDC) methods and dielectric spectroscopy in general, Frequency Response Analysis (FRA), a variety of methods of PD monitoring, including UHF methods and methods of analysis such as Pulse Sequence Analysis (PSA) and PD frequency domain analysis. The application of these techniques is aimed at providing better methods of condition assessment of the transformer insulation under normal operating conditions. However one area of the operation of transformers that has not been investigated in as much detail as it should be is the impact of sudden and then prolonged high thermal stress on the transformer insulation, particularly when there is moisture present in the oil and paper materials.

The combination of such thermal stress and moisture can have severe impact on the insulation, including accelerated deterioration, bubble formation in the oil and between paper layers, partial discharge activity and the increased transfer of moisture between the oil and the paper insulation as the thermal shock heats the paper insulation very quickly. The generation of bubbles in the oil and paper layers increases partial discharge activity with the accompanying increase in degradation that such activity can cause.

This thesis work has attempted to investigate such effects on transformer insulation using test models of typical transformer-type insulation in the laboratory. The insulation condition has been monitored using phase resolved partial discharge analysis with the aim being to determine the rate of deterioration due to such effects and to try to identify from the PD analysis the best methods of analysis and interpretation that can be used to identify the condition of the insulation.

There are many non-PD methods additional to those listed above which are available to provide some information on the ageing processes thus providing means of assessment of the insulation condition. These include dielectric dissipation factor (DDF), dissolved gas analysis (DGA), furan compound analysis, degree of polymerisation (DP) and interfacial tension test methods. The problem with most methods is that they are:

(i) not able to be applied on-line
(ii) not able to provide continuous monitoring
(iii) difficult to interpret in terms of the correlation of the results with the insulation condition.

For example DDF, DGA and furan methods are not able to give information on the instantaneous and local insulation condition. Instead they are only able to provide a measurement which is the accumulation of deterioration over a period of time. They are global methods in that their results are averaged over the whole insulation rather than able to be localised in the insulation.

Unless they are performed frequently enough to give detailed trend analysis they are of limited use in providing assessment of instantaneous condition of insulation, unless the data provided are indicative of imminent failure.

DP measurements are able to give better indication of the paper insulation condition in transformers, but they have the problem that the samples of paper that are obtainable for test from a transformer are not available from the internal hot spot area of the windings which is where the main deterioration of the paper will occur. Thus the DP measurements are not able to give an unequivocal assessment of the age of the most degraded paper present in the windings. While there has been much progress in relating furan levels to DP measurements of the paper the results are still empirical and do not provide absolute assessment of condition. Also in any case they do not cover the oil condition, only that of the paper.

In contrast, PD measurements give an instantaneous and time-resolved assessment of the insulation condition especially in complex oil-impregnated insulation such as the transformer. The assessment by PDs will include all insulation, including the paper and the oil in particular. Phase resolved partial discharge measurements enable the condition to be assessed and the patterns obtained can be correlated with fault type and, to a degree, to localisation. Further it has been shown by many workers over the years that statistical analysis of these phase resolved patterns will provide very sensitive indication of condition and fault type and deterioration.

To this end the investigations preformed have used phase resolved PD analysis to analyse the insulation condition when subject to high electrical and thermal stress, as such PD methods are seen as the most useful means of monitoring being able to be used in the field. Other PD methods such as frequency domain analysis and UHF methods are still in the early stages of development and while they will certainly eventually provide sensitive means of assessment they still require some further development. For the current purposes where the types of measurements used can be performed and recorded on-site using commercial PD equipment, phase resolved analysis and the statistical analysis of the PD patterns are seen as the most useful methods for the investigations reported here.

The use of the CDA3 Phase resolved PD monitoring system with a standard commercial PD detector thus provides a better quantitative means of analysing PD data especially on line. In addition, the results reported here can thus be used for comparison with measurements obtained on real insulation. In this way the results will enable some possible application to ageing and deterioration and the effects of moisture in real transformers.

8.1.2 Outcomes of the investigations

The following observations and conclusions are based on results obtained from over five years of extensive research on the laboratory models described, over four years of my own experimental work and on detailed scrutiny of previous experimental work carried out on the same sample reported here since 1996 on new and aged oil-impregnated insulation in the steel tank vessel. In addition my extended experimental work included the study of new and aged oil-impregnated insulation in a glass test cell, with particular emphasis on the effects of thermal shock. The investigations were carried out on models with an environment, insulation configuration and stresses similar to those which exist for the insulation under practical operating conditions in transformers under normal load and under abnormally high loads.

During thermal overloading of the oil-impregnated transformer insulation temperatures of between 80 -145°C were imposed by the test conditions. During the tests significant small gas bubble formation was seen to occur in the oil at temperatures of 140-145°C and then the release of larger bubbles (originating from within the paper insulation) caused a very significant decrease in the maximum PD level. The decrease resulted from the release of bubbles from the paper layers where, when kept within the paper layers they provided the typical void which generates PD activity. Once released from the paper they no longer gave a source of PD activity. In addition, the peak PD magnitude, the average PD magnitude and the PD number all increased with increase in temperature and then decreased as temperature was reduced.

Moreover, during this high temperature overloading phase, moisture from the paper was forcibly transferred by thermal action to the oil and eventually to the air above the oil as a result of the gas bubble moisture transfer. However the reverse process of moisture transfer from oil to paper was much slower and the incursion of moisture into the high electric field strength region of the paper caused PDs of high intensity due to the effect of the increase in moisture content.

The formation of the gas bubbles at high temperature and the high temperature operation was found to cause subsequent reduction of partial discharge inception level at lower temperature level (typical of normal transformer operation under load) indicating significant ageing of the insulation. In addition it was found that a reduction in bubble generation frequency at the high temperatures could eventually result in lower moisture content in the paper. Higher moisture content in insulating paper (around the winding conductor) is more dangerous in terms of PD activity compared to moisture presence in the insulating oil.

The colour of the paper, the pressboard and the oil changed very markedly during the tests from the light shade of normal un-aged materials to a very dark shade indicative of ageing due to the combined thermal, environmental and electrical stresses. The PD activity was seen to have caused a significant carbonisation of both the paper and pressboard and also caused the paper to become brittle, with obvious decrease of DP number.

The change of the PD pattern to a lower PD inception angle and higher PD repetition rate after the high temperature phase can thus be used as a very useful diagnostic tool in identifying moisture and ageing affects of the paper.

The change of electric stress by an increase of 60% (by applied voltage increase from 10 to 16kV in the test sample) caused the peak PD magnitude, the average PD magnitude, and the PD number to increase with the increase of the test voltage and then to decrease with stress reduction, although with decrease in inception level.

Additionally, when the test voltage frequency was increased from 50 to 200 Hz, the peak and the average PD magnitude all decreased, whereas the PD number increased with the increase of frequency. A reverse trend occurred when the test voltage frequency was reduced. However the increase in number of PDs was not linear with frequency increase. The increase was only about 2.6 times for an increase of frequency of 4 times. This is consistent with a PD activity which is not totally dielectric based, but indicates that some surface discharges were present.

During the overloading of the oil-impregnated transformer insulation from ambient temperature to 85°C, the highest peak PD magnitude measured was initially located on the positive half cycle but then shifted after a time from the positive to the negative half-cycle. During the cooling phase from 85°C back to the ambient temperature, the PDs with highest peak magnitude then shifted back from the negative half cycle to the positive half-cycle again. The peak discharge magnitude and the PD repetition rate increased with the increase of temperature and then decreased as temperature decreased to ambient. The experimental results showed that the peak and the average PD magnitudes are greatly affected by the temperature change. The discharge number and the discharge current also varied significantly with the test temperature.

This variation of PD level with temperature is an important factor in using PD diagnostics to assess insulation condition in transformers. The observation of the statistical moments of the PD pattern distributions showed that the statistical distributions changed significantly when the temperature changed. This indicates that the use of statistical moments for automated PD classifications in condition monitoring has to be conducted carefully and the use of separate PD signatures for different test temperature and insulation condition would be appropriate and would provide potentially useful condition indicators.

It also indicates that, given the variation of PD magnitude and number activity with temperature, it is perhaps the statistical parameters such as the skewness and particularly the kurtosis rather than the simple magnitude and number that may be best for use in determining insulation condition. This result illustrating the need to take temperature into account is a parallel of the case of DDF measurements such as used in the Doble method where the DDF is measured at one voltage only and must be carefully normalised in its temperature to achieve useful results that can be used for comparison with the usual guidelines and criteria.

The results obtained from the experiments conducted on the oil-impregnated transformer insulation using the Recovery Voltage Measurement (RVM) technique showed that the peak of the polarisation spectrum shifted to a smaller time constant with the increase of moisture content, and a good linearity of response in variation of charging voltage was found. The moisture equilibrium of the test object plays an important role in determining the conditions of the insulation system as uneven distribution of moisture or other ageing products may complicate the evaluation of the measurements of recovery voltage. The recovery voltage measurement using LabView program is an insulation diagnostic technique, capable of assessing the conditions of the aged transformer from moisture in oil/paper insulation and can also be used as a tool for the planning of maintenance but Polarisation and Depolarisation Current (PDC) and dielectric spectroscopy is perhaps a bit more flexible but still not as sensitive or useful as monitoring by PD measurement.

Despite the potential advantages of some other measurement techniques, such as DP number and furan level testing, the PD measurement diagnostic has been demonstrated to be a more sensitive condition indicator as it provides an instantaneous and time resolved assessment, whereas the other methods provide only an integrated and global assessment of the accumulated deterioration or, as in the case of the DP measurement are difficult to apply to appropriate samples of the service aged insulation. It has been observed that monitoring of PD activity can provide an extremely useful and consistent monitor in terms of the individual results and in particular in its use as a trend analyser. Such trend analysis can provide better understanding of the oil-impregnated insulation degradation processes. PD diagnostics are particularly beneficial when using trend analysis but due to the unpredictable nature of PDs and the complicated nature of oil-impregnated insulation, time-to-failure prediction using PD analysis alone is not possible.

The PD diagnostic method, combined with another diagnostic tool, preferably Dissolved Gas Analysis (DGA) of the oil, can be a more useful means to understanding the transformer's insulation condition and can improve the reliability in the interpretation of the results and provide better understanding of oil-impregnated transformer insulation deterioration. Transformer condition monitoring can not only provide an early indication of any degradation caused by abnormal electrical, thermal, mechanical and environmental stress, but also can save cost, improve reliability of supply, provide better safety of personnel and prevent potential environmental damage.

Voltage (electric stress), frequency, oxygen content, moisture level and temperature all affect the PD behaviour. In particular PD behaviour is substantially affected by the test temperature and the moisture level. The variation of PD level with temperature and moisture (especially in paper) is an important factor in using PD diagnostics to assess insulation condition in a transformer.

The results of all of the above investigations have shown the complexity involved in correlation of the effects of moisture with temperature on PD activity in transformer type insulation. This complexity may lead to some potential problems in interpretation of the results of PD measurements performed on transformers. Much further work is needed to elucidate the impact of the various parameters on PD activity before any definitive indicators of ageing quantification can be derived. The result of these experimental works and conclusions can be used in analysing PD data obtained using both off-line and, preferably, on-line measurements, particularly in oil-impregnated power transformers.

However, further long-term investigations are needed to better quantify the results and the following section provides some detail as to the areas of investigation that would be useful to follow.

8.2 Recommendations for further work

The power transformer insulation is mainly comprised of mineral oil and cellulose based products. The insulation thus contains both solid and liquid insulation. There are many factors which effect the properties of these materials under electrical, thermal, mechanical and environmental stress both individually and in combination. The chemistry of materials and knowledge of individual involvements and chemical changes that the insulating materials experience under single and multistresses is so complex that currently there is no definite single electrical, chemical or theoretical explanation which gives a certain answer regarding the current health and time of failure of the oil-impregnated insulation.

Recommendations arising from the work described here are that for such a complex type insulation the properties, behaviour and effects of insulating materials (mineral oil, paper and pressboard) should be studied individually and also in combination and further more detailed experiments should be conducted to see the effects of voltage, frequency, temperature, moisture and gases (oxygen in particular) using single stress and multistress models to find out the way these factors play a role under normal and abnormal (thermal and moisture affected) conditions of an operating power transformer. A team containing at least one chemical engineer as well as electrical engineers is highly recommended for a better understanding of the electrical and chemical phenomena involved.

There are many methods available to monitor the insulation but PD monitoring provides better diagnostics and quality control tools. The difficulty in obtaining definitive answers due to variability of PD phenomena when using both CDA3 measurement (using blocking capacitor and input unit) and oscilloscope measurement of PD waveforms (using high frequency current transformer and Lecroy) should be used to cross-check the CDA3 PD data with true PD data. Apart from PD measurements, oil tests should not only include moisture content but DGA including furan analysis. The DP value of cellulose based products should also be monitored regularly. These measures will guide step by step to understand better the health of oil-impregnated insulation. Despite the numerous advantages of CDA3, its compatibility with Pentium four will definitely improve data storage and data sharing.

The implementation of the above mentioned recommendations is time consuming and costly. However the combined electrical and chemical engineering department involvement in this research to share their respective expertise, and financial support from electrical utilities and oil and paper companies can definitely help to monitor the most expensive equipment of power transmission system, so avoiding unexpected failure causing catastrophic results.

References

[1] B. H. WARD, "A Survey of New Techniques in Insulation Monitoring of Power Transformer", IEEE Electrical Insulation Magazine, Volume: 17, Issue: 3, pp. 16-23, May/June 2001.

[2] B. SHI and L. YANG, "An Investigation on the Influencing Factors on On-Line Insulation Monitoring of HV Apparatus", IEEE International Symposium on Electrical Insulation, CA USA, pp. 81-84, 2-5 April 2000.

[3] J. P. V. BOLHUIS, E. GULSKI and J. J. SMIT, "Monitoring and Diagnostic of Transformer Solid Insulation", IEEE Transactions on Power Delivery, Volume: 17, Issue: 2, pp. 528-536, April 2002.

[4] F. H. KREUGER, E. GULSKI and A. KRIVDA, "Classification of Partial Discharges", IEEE Transaction on Electrical Insulation, Volume: 28, Issue: 6, pp.917-931, December1993.

[5] R. E. JAMES et al., "Effect of Moisture and Temperature of PD Behaviour of an Oil-Impregnated Insulation System", Proceedings 1997 Australasian Universities Power Engineering Conference (AUPEC 1997), Sydney, Australia. Conference proceedings Volume: 3, pp. 607-614, 29th September–1st October 1997.

[6] R. H. KHAWAJA, W. G. ARIASTINA and T. R. BLACKBURN, "Partial Discharge Behaviour in Oil-Impregnated insulation", Proceeding of 7th International Conference on Properties & Applications of Dielectric Material (ICPADM 2003), Nagoya, Japan, Volume: 3, pp.1166-1169, 1-5 June 2003.

[7] T. K. SAHA et al., "Investigating the Effects of Oxidation and Thermal Degradation on Electrical and Chemical Properties of Power Transformers Insulation", IEEE Transaction on Power Delivery, Volume: 14 Issue: 4, pp. 1359-1367, October 1999.

[8] W. H. BARTLEY, "The Locomotive Executive Story Summary: An Analysis of Transformer Failures, Part 1- 1988 through 1997", Hartford Steam Boiler Inspection and Insurance Company, USA.

[9] D. CHU and A. LUX, "On-Line Monitoring of Power Transformers and Components: A Review of Key Parameters", Electrical Insulation Conference and Electrical Manufacturing & Coil Winding Conf. 1999 Proc, pp.669-675, 1999.

[10] T. R. BLACKBURN et al., "Investigation of Partial Discharge Mechanisms in a Void under AC Electric Stress", 1999 11th High Voltage Engineering Symposium, IEE Conference Publ. No: 467, Volume: 4, pp. 364-368, 22-27 August 1999.

[11] B. GARCIA et al., “A Moisture Model for Power Transformer Monitoring-Part 1: Theoretical Foundation”, IEEE Transactions on Power Delivery, Vol. 20, No. 2, pp. 1417-1422, April 2005.

[12] B. GARCIA et al., “A Moisture Model for Power Transformer Monitoring-Part II: Theoretical Foundation”, IEEE Transactions on Power Delivery, Vol. 20, No. 2, pp. 1423-1429, April 2005.

[13] T. WEEKES T. MOLINSKI and X. LI, “Risk Assessment Using Transformer Loss of Life Data”, IEEE Electrical Insulation Magazine, Vol. 20, No. 2, pp. 27-31, March/April 2004.

[14] L. E. LUNDGAARD et al., “Ageing of Oil-Impregnated Paper in Power Transformer, IEEE Transactions on Power Delivery, Vol. 19, No. 1, pp. 230-239, January 2004.

[15] M. A. ELBORKI et al., “Detection and Characterisation of Partial Discharges in Transformer Defect Models”, IEEE Power Engineering Society Summer Meeting 2002: Volume 1, pp. 405-410, 2002.

[16] A. CAVALLINI and G. C. MONTANARI, “A New Methodology for the Identification of PD in Electrical Apparatus: Properties and Applications”, IEEE Trans. on Dielectrics and Electrical Insulation, Vol. 12, No. 2, pp. 203-215, 2005.

[17] D. ASCHENBRENNER et al., “On Line PD Measurements and Diagnosis on Power Transformers”, IEEE Transactions on Dielectrics and Electrical Insulation, Vol. 12, No. 2, pp. 216-222, April 2005.

[18] A. J. KACHLER and I. HOHLEIN, “Ageing of cellulose at Transformer Service Temperatures. Part 1: Influence of Type of Oil and Air on the Degree of Polymerization of Pressboard, Dissolved Gases, and Furanic Compounds in Oil”, IEEE Electrical Insulation magazine, Vol. 21, No. 2, pp. 15-21, 2005.

[19] M. K. PRADHAN and T. S. RAMU, “On the Estimation of Elapsed Life of Oil-Immersed Power transformers”, IEEE Transactions on Power Delivery, Vol. 20, No. 3, pp. 1962-1969, July 2005.

[20] T. K. SAHA P. PURKAIT and D F. MULLER, “Deriving an Equivalent Circuit of Transformers Insulation for Understanding the dielectric Response Measurement”, IEEE Transactions on Power Delivery, Vol. 20, No. 1, pp. 149-157, January 2005.

[21] M. H. LI et al., “Return Voltage Measurements of Oil Impregnated Paper Insulated Transformers”, Proceedings of the 2005 International Symposium on Electrical Insulating Materials, Kitakyushu, Japan, pp. 273-276, 5-9 June 2005.

[22] M. DONG et al., “Synthetic Furfural Analysis for Paper Insulation Ageing Diagnosis of Transformers”, Proceedings of the 2005 International Symposium on Electrical Insulating Materials, Kitakyushu, Japan, pp. 439-442, 5-9 June 2005.

[23] C. T. DERVOS C. D. PARASKEVAS and P. SKAFIDAS, "Dielectric Characterization of Power Transformer Oils as a Diagnostic Life Prediction Method, "IEEE Electrical Insulation Magazine, Vol. 21, No. 1, pp. 11-19, 2005.

[24] M. DUVAL and J. DUKARM, "Improving the Reliability of Transformer Gas-in Oil Diagnosis, "IEEE Electrical Insulation Magazine, Vol. 21, No. 4, pp. 21-27, 2005.

[25] V. G. ARAKELIAN, "The Long Way to the Automatic Chromatographic Analysis of Gases Dissolved in Insulating Oil, "IEEE Electrical Insulation Magazine, Vol. 20, No. 6, pp. 8-25, November/December 2004.

[26] B. T. PHUNG, "Computer-based Partial Discharge Detection and Characterisation", PhD Thesis, School of Electrical Engineering, The University Of New South Wales, Sydney, Australia, 1997.

[27] D. J. WOODCOOK, "Condition Appraisal of Power Transformers", Weidmann ACTI Portal, Technical Library", Weidmann Systems International Inc., Weidmann.

[28] Y. H. LU, C. K. TAN, B.T. PHUNG, R. H. KHAWAJA and T. R. BLACKBURN, "Development of a Computer-Based Data Logger for Recovery Voltage Measurements", Proc of 2002 Australasian Universities Power Engineering Conference (AUPEC 2002), Melbourne, Australia, October 2002.

[29] M. J. HEATHCOTE and D. P. FRANKLIN, "The J & P Transformer Handbook: A Practical Technology of the Power Transformer", 12th Edition, Butterworth-Heinemann, 2000.

[30] J. J. KELLY, S. D. MYERS and R. H. PARRISH, "Transformer Maintenance Guide", Transformer Maintenance Institute, 1981.

[31] A. E. FITZGERALD, C. KINGSLEY and S. D. UMANS, "Electrical Machinery", Sixth Edition, McGraw-Hill International Book Company, New York, 2002.

[32] K. KARSAI et al., "Large Power Transformers", Elsevier Science Publishing Company Inc., Budapest, Hungary, 1987.

[33] H. LEE and J. RUNGIS, "Laboratory ageing of Transformer oils", CSIRO Division of Applied Physics, Australia, 1996.

[34] WEIDMANN ELECTRICAL, "Condition Appraisal of Power Transformers/Solution for Transformer Asset Managers", Weidmann-ACTI Asset Management Portal, Engineering Services, Weidmann.

[35] F. H. KREUGER, "Industrial High Voltage", Volume 1, Delft University Press, Netherlands, 1991.

[36] H. P. MOSER et al., "Transformerboard", Translated by W. Heidemann, EHV-Weidmann Limited, St. Johnsbury, Vermont, USA, 1979.

[37] F. H. KREUGER, "Industrial High Voltage Volume 2", Delft University Press, Netherlands, 1992.

[38] J. D. GLOVER and M. S. SARMA, "Power System Analysis and Design with Personal Computer Applications, 3rd Ed., Brooks Electrical Engineering Services, 2001.

[39] H. P. MOSER et al., "Transformerboard II Properties and Application of Transformerboard of Different Fibres", H. Weidmann AG, CH-8640 Rapperswil, Switzerland, 1987.

[40] B. D. SPARLING, "Transformer Monitoring from Monitoring to Diagnostics", Proc. IEEE/PES Transmission and Distribution Conference, 2002, Asia Pacific, Volume: 2, pp. 1506-1509, 6-10 October 2002.

[41] R. E. JAMES, "Fundamental of PD Testing/Review of Equipment Standards and PD Calibration Methods", Electricity Supply Association of Australia (ESAA) Short Course on Insulation Condition Monitoring and Partial Discharge Techniques, Sydney, 18-20 June 2003.

[42] F. JACOB, "Oil: The Four Rs Retain, Recondition, Reclaim, Replace", Weidmann ACTI Portal-Condition Appraisal of Power Transformers, Technical Library, Weidmann.

[43] I. FOFANA et al., "Challenge of Mixed insulating Liquids for use in High-Voltage Transformers II: Investigation of Mixed Liquids", IEEE Electrical Insulation Magazine, Volume: 18 Issue: 4, pp. 5-16, July/August 2002.

[44] J. HEIGHES, "High Voltage Transformer Insulation and its Processing", AEI Engineering, AEI Transformer Division, pp. 84-87, March/April 1966.

[45] S. ITAHASHI et al., "Analysis of Water in Oil Impregnated Kraft Paper and its Effect on Conductivity", IEEE Transactions on Dielectrics and Electrical Insulation, Volume: 2 Issue: 6, pp.1111–1116, December 1995.

[46] V. WASSERBERG, H. BORSI and E. GOCKENBACH, "A New Method for Drying the paper Insulation of Power transformer During Service", Conf. Record: 2000 IEEE International Symposium on Electrical Insulation, pp. 251-254, 2000.

[47] A. SIEROTA and J. RUNGIS, "Electrical Insulating Oils Part 1: Characterisation and Pre-treatment of New Transformer oils", IEEE Electrical Insulation Magazine, Vol. 11, Part 1, pp. 8-20, January/February 1995.

[48] IEC 422:1989/ AS 1883-1992, "Supervision and Maintenance Guide for Mineral Insulating Oils in Electrical Equipment/Guide to Maintenance and Supervision of Insulating Oil in Service, 1989/1992.

[49] B. PAHLAVANPOUR, M. A. MARTINS and A. D. PABLO, "Experiment Investigation in to the Thermal Ageing of Kraft Paper and Mineral Insulating Oil", Conference Record: 2002 IEEE International Symposium on Electrical Insulation, Boston, MA USA, pp. 341-345, 7-10 April 2002.

[50] M. G. DANIKAS, “Breakdown of Transformer Oil”, IEEE Electrical Insulation Magazine, Volume: 6 Issue 5, pp. 27-34, September/October 1990.

[51] M. POMPILLI, C. MAZETTI and R. BARTNIKAS, “Effect of Reduced Viscosity on the Electrical Characteristics of Transformer and Switchgear Oils”, Conference Record of the 2002 IEEE International Symposium on Electrical Insulation, Boston, MA USA, pp. 363-366, 7-10 April 2002.

[52] WESTINGHOUSE ELECTRIC AND MANUFACTURING COMPANY. “Insulating Oil for Electrical Apparatus”, Westinghouse No: IB-5336-D, London.

[53] POWER GRID COMPANY OF INDIA LIMITED, “Oil Tests Information”, New Delhi, India.

[54] B. PAHLAVANPOUR, G. WILSON and R. HEYWOOD, “Insulating Oil in Service: Is Fit for Purpose?”, Insulating Liquids Conference (No. 1999/119), IEE, London, pp. 3/1-3/4, 1999.

[55] D. WOODCOCK, “How Contamination Causes Transformer Failure”, Electrical World, Volume: 210, Issue: 2, pp. 27-29, February 1996.

[56] A. SIEROTA, “Loss Angle Measurement on Insulating Materials and their Relevance to Condition Monitoring”, Lecture presented at the ESAA/UNSW Workshop on Partial discharge measurement and insulation condition monitoring, Australia, 24-26 May 1993.

[57] C. S. HUH, J. I. JEONG and H. W. CHO, “Study on the Breakdown Characteristics of Flowing Insulating Oil”, Proceedings of 13th International Conference on Dielectric Liquids (ICDL 99), Nara, Japan, pp. 160-162, 20-25 July 1999.

[58] E. T. NORRIS, “IEE High Voltage Power Transformer Insulation”, Proceedings IEE, Volume: 110 Issue: 2, pp. 428-439, February 1963.

[59] K. SIODLA, W. ZIOMEK and E. KUFFEL, “The Volume and Area Effect in Transformer Oil”, Conference Record of the 2002 IEEE International Symposium on Electrical Insulation, Boston MA USA, pp. 359-362, 7-10 April 2002.

[60] L. D. TOIT, “On-Site Regeneration of Transformer Oil, An Essential Element of Preventive Transformer Maintenance”, Karabo Transformer Oil, pp. 1-15, Fichardt Park, South Africa.

[61] C. R. ROEHRIG, “Reclaiming Transformer Oil”, Plant Engineering, Westinghouse Electric Co., San Francisco, CA, pp. 163-166, 15 September 1977.

[62] D. ALLAN et al., “New Insulation Diagnostic and Monitoring Techniques for In-service HV Apparatus”, Proceedings of the 3rd International Conference on Properties and Applications of Dielectric Materials (ICPADM 1991), Tokyo, Japan, Volume: 1, pp. 448-451, 8-12 July 1991.

[63] D. ALLAN, "Service Ageing and Assessment", Electricity Supply Association of Australia Short Course on Insulation Condition Monitoring and Partial Discharge Techniques, Sydney, 18-20 June 2003.

[64] A. M. EMSLEY and G. C. STEVENS, "Review of Chemical Indicators of Degradation of Cellulosic Electrical Paper insulation in Oil-filled transformers", IEE Proceedings of Science, Measurement and Technology, Volume: 141, Part 5, pp. 324-334, September 1994.

[65] A. M. EMSLEY and G. C. STEVENS, "A Reassessment of the Low Temperature Thermal Degradation of Cellulose", Sixth IEE International Conference on Dielectric Materials, Measurements and Applications, pp. 229-232, 7-10 September 1992.

[66] C. HONGYAN and S. BIRLASEKARAN, "Temperature Dependant Relaxation Studies on Oil–filled Transformer", Conference Record: 2002 IEEE International Symposium on Electrical Insulation, Boston, pp. 174-178, 7-10 April 2002.

[67] T. K. SAHA and Z. T. YAO, "Experience with Return Voltage Measurements for Assessing Insulation Conditions in Service-Aged Transformers, IEEE Transactions on Power Delivery, Volume: 18, Issue: 1, pp. 128-135, 2003.

[68] D. M. HEPBURN, A. J. SHEILDS and I. J. Kemp, "High Voltage Plant Monitoring Through Oil/Paper Analysis", Dielectric Material, Measurement and Applications, IEE Conf. Publication No. 473, pp.218-223, 17-21 September 2000.

[69] Y. DU et al., "A Review of Moisture Equilibrium in the Paper-Oil Systems", Department of Electrical Engineering and Computer Science, MIT, Cambridge MA, and Electric Power Research Institute Palo Alto CA USA.

[70] D. COUDERC, P BOURASSA and J. M. MUIRAS, "Gas-in-Oil Criteria for the Monitoring of Self-Contained Oil-Filled Power Cables", IEEE Annual Report: Conference on Electrical Insulation and Dielectric Phenomena, San Francisco, Volume: 1, pp. 283-286, 20-23 October 1996.

[71] Y. SHEIRETOV and M. ZAHN, "A Study of the Temperature and Moisture Dependant Dielectric Properties of Oil–Impregnated pressboard", Conference on Electrical Insulation and Dielectric Phenomena, Pocona Manor PA, pp. 487-492, 17-20 October 1993.

[72] Y. P. NERKAR, R. N. NARAYANACHAR and R. S. NEMA, "Characterisation of Partial Discharges in Oil–Impregnated Pressboard Insulation System", Eleventh International High Voltage Engineering Symposium, Conference Publication No. 467, Volume: 5, pp.208-211, 22-27 August 1999.

[73] W. G. ARIASTINA and T. R. BLACKBURN, "Characteristics of Partial Discharge in Oil Impregnated Insulation Using Different Test Voltage Frequencies", Proceedings of the 6th International Conference on Properties and Applications of Dielectric Materials (ICPADM 2000), Xi'an, Vol. 1, pp. 487-492, 21-26 June 2000.

[74] M. WANG, A. J. VADERMAAR and K. D. SRIVASTAVA, "Review of Condition Assessment of Power Transformer in Service", IEEE Electrical Insulation Magazine, Volume: 18 Issue: 6, pp. 12-25, November/December 2002.

[75] L. M. NIKOLOSKI and D. D. HRISTOVSKI, "Drying of Already Impregnated Oil-Paper Insulation", IEEE Annual Report: Conf. on Electrical Insulation and Dielectric Phenomena, Vol, 1, pp. 178-181, San Francisco, 20-23 October 1996.

[76] M. HASSIG et al., "On-Site Applications of Advanced Diagnosis Methods for Quality Assessment of Insulation of Power Transformers", IEEE Annual Report Conference on Electrical Insulation and Dielectric Phenomena, pp. 441-447, 2001.

[77] THE ELECTRICITY COMMISSION OF NSW, "Electrical Testing Training Manual", Transmission Division Supply Group, Staff Training Homebush, Sydney, Australia, 1984.

[78] FACILITIES INSTRUCTIONS, STANDARDS AND TECHNIQUES (FIST), "Transformer Maintenance", Volume 3-30, United States Department of Interior: Bureau of Reclamation, December 1991.

[79] M. DARVENIZA et al., "Investigations into Effective Methods for Assessing the Condition of Insulation in Aged Power Transformers, IEEE Transactions on Power Delivery, Volume: 13 Issue: 4, pp. 1214-1223, October 1988.

[80] R. ADAMS, "Condition Monitoring of Ageing Power Equipment: Part 1 Electrical Plant, Electricity Trust of South Australia.

[81] S. D. LIZUNOV, "Condition of Transformer Insulation in Service: Method of Assessment and Required Criteria for Satisfactory Operation, CIGRE Report 12-03, Paris 1976.

[82] R. E. JAMES and T. R. BLACKBURN, "Lecture Notes: School of Electrical Engineering & Telecommunications", University of New South Wales, Sydney, Australia, 1996.

[83] B. PAHLAVANPOUR, R. HEYWOOD and G. WILSON, "Power Transformer Insulation Ageing", CIGRE Study Committee 15 Symposium "Service Ageing of Materials in HV Equipment", Sydney, Australia, pp. 11/1- 11/7, 4 October 1999.

[84] M. DUVAL, "A Review of Faults Detectable by Gas-in Oil Analysis in Transformer", IEEE Electrical Insulation Magazine, Volume: 18 Issue: 3, pp. 8-17, May/June 2002.

[85] J. H. PROVANZANA et al., "Transformer Condition Monitoring - Realising an Integrated Adaptive Analysis System", CIGRE paper 12-105, Paris 1992.

[86] T. LEIBFRIED and A. J. KACHLER, "Insulation Diagnostics on Power Transformers Using the Polarisation and Depolarisation Current (PDC) Analysis", Conference Record of the IEEE International Symposium on Electrical Insulation, Boston, MA USA, pp. 170-173, 7-10 April 2002.

[87] A. BOSSI et al., "Criteria for Checking Insulation Condition of Power Transformers in Enel`s 420kV and 245kV Systems", CIGRE Paper 12-09, Paris 1976.

[88] J. UNSWORTH and F. MICHELL, "Degradation of Electrical Insulating Paper Monitored with High Performance Liquid Chromatography", IEEE Transactions on Electrical Insulation, Volume: 25 Issue: 4, pp. 737-746, August 1990.

[89] R. BOZZO et al., "Design of Experiments (DOE) Procedures for the Optimisation of a Digital Partial Discharge Measurement System", 1996 IEEE Annual Report-Conference on Electrical Insulation and Dielectric Phenomena, San Francisco, Volume: 1, pp. 64-68, 20-23 October 1996.

[90] T. SCHOLEY AND D. GORGIUS, "Ultrasonic Detection of Discharges in Power Transformers", Ninth International Symposium on High Voltage Engineering, Graz Convention Centre, Austria, 5604-1, 28 August-1September 1995.

[91] V. ASCHENBRENNER and T. UEIK, "Using Parameters of RVM Measurement for Qualitative Appreciation of Power Transformers Insulation State", IEEE/PES Asia Pacific Transmission and Distribution Conference and Exhibition 2002, Volume: 3, pp. 1829-1833, 6-10 October 2002.

[92] J. REASON, "On- Line Transformer Monitoring", Electrical World, Volume: 10, pp. 19-26, October 1995.

[93] P. GUUINIC and J. AUBIN, "CIGRE's Work on Power Transformers", EPRI "Substation Equipment Diagnostics Conference IX", New Orleans, Louisiana, USA, pp. 1-15, 18-21 February 2001.

[94] C. BENGTSSON, "Status and Trends in Transformer Monitoring", IEEE Transaction on Power Delivery, Volume: 11 Issue: 3, pp. 1379-1384, July 1996.

[95] J. BINGGELI et al., "The Treatment of Transformers", CIGRE Session, Paper No. 10, 1966.

[96] F. M. CLARK, "Water Solution in High Voltage Dielectric Liquids", General Electric Company, London, U.K., 1940.

[97] D. W. AUCKLAND et al., "Degradation of Oil-Paper Systems due to the Electrical Field Enhanced Absorption of Water", 7th International Conference on Dielectric Materials Measurements and Applications, Conference Publication No. 430, IEE 1996, pp. 197-200, 23-26 September 1996.

[98] R. FERGUSON, A. LOBEIRAS and J. SABAU, "Suspended Particles in the Liquid Insulation of Ageing Power Transformer", DEIS Feature Article: IEEE Electrical Insulation Magazine, Volume 18, Part 4, pp. 17-23, July/August 2002.

[99] L. D. TOIT, "The Life of a Transformer; Controllable or Uncontrollable", Karabo Transformer Oil, Fichardt Park, South Africa.

[100] V. ASCHENBRENNER and T. UEIK, "The Possibilities and Limits of Estimation of Ageing Degree of Paper-Oil Insulation in Power Transformer by Recovery Voltage Method", IEE Conf, Dielectric Materials Measurements and Applications: IEE Publication No. 473, pp. 335-340, 17-21 September 2000.

[101] R. BALANATHAN, "Summary Report: Transformers for Power Systems", EA Technology, Chester, England, 4-5 October 2000.

[102] H. OKUBO et al., "Electrical Insulation Diagnostic Method and Maintenance Criteria for Oil-Immersed Power Transformers", Proceedings 13th International Conf. on Dielectric Liquids (ICDL 99), Nara, Japan, pp.372-377, July 1999.

[103] J. K. WOODCOOK and J. C. WRIGHT, "Power Transformer Design Enhancements Made to Increase Operational Life", Weidmann ACTI Portal, Technical Library, Weidmann Technical Services Inc. Weidmann.

[104] IEEE STANDARD 259-1994, "IEEE Standard Test Procedure for the Evaluation of Systems of Insulation for Speciality Transformers", 1 December 1994.

[105] P. CYGAN and J. R. LAGHARI, "Models for Insulating Ageing under Electrical and Thermal Multistress, IEEE Transactions on Electrical Insulation, Volume 25, Part 5, pp. 923-934, October 1990.

[106] A. M. EMSLEY et al., "Degradation of Cellulosic Insulation in Power Transformers. Part 2: Formation of Furan Products in Insulating Oil, IEE Proceedings Science Measurement and Technology, Volume147, No.3, pp. 110-114, 2000.

[107] J. FABRE and A. PICHON, "Deterioration Processes and Products of Paper in Oil Application to Transformers", International CIGRE Conference on Large High Voltage Electric System, Paris, France, Paper #137,1960.

[108] T. PREVOST, D. J. WOODCOCK and C. KRAUSE, " The Effects on Winding Clamping Pressure due to Changes in Moisture, Temperature and Insulation Age, Weidmann Technical Services Inc., H. Weidmann Ltd.

[109] F. S. OLIVER, "Doble Power-Factor Valued Oxidation Tests", Minutes of the Annual International Conference of Doble Clients, Doble Engineering Company, Watertown, MA, USA, 1960.

[110] W. J. McNUTT, R. L. PROVOST and R. J. WHEARTY, "Thermal Life Evaluation of High Temperature Insulation Systems and Hybrid Insulation Systems in Mineral Oil", IEEE Transactions on Power Delivery, Volume 11, No.3, pp. 1391-1399, July 1996.

[111] Z. DIANCHUN et al., "Thermal Ageing Behaviour of Oil-Impregnated Paper at 160°C", Proc 5th International Conference on Properties and Applications of Dielectric Materials (ICPADM 1997), Volume: 1, pp. 256-258, 25-30 May 1997.

[112] R. L. PROVOST et al., "High Power Density Transformer for Improved Performance", Proc. Asia Pacific IEEE/PES Transmission and Distribution Conference 2002, Volume: 3, pp. 1814-1819, 6-10 October 2002.

[113] D. F. BINNS, A. B. CROMPTON and A. JABERANSARI, "Effect of Temperature on the Breakdown Voltage of Paper-Covered Conductor Impregnated with Various Liquids", IEEE Transactions on Electrical Insulation, Volume 23, No.3, pp. 475-483, June 1988.

[114] IEEE STANDARD C57.91-1995, "IEEE Guide for Loading Mineral-Oil-Immersed Transformers (ANSI)", 25 April 1996.

[115] R. J. HEYWOOD, A. M. EMSLEY and M. ALI, "Degradation of Cellulosic Insulation in Power Transformers: 1 Factors Affecting the Measurement of the Average Viscometric Degree of Polymerisation of New and Aged Electrical Papers" IEE Proc. Science, Measurement and Technology, Volume 147, No.2, pp. 86-90, 2000.

[116] V. M. MONTSINGER, "Loading Transformer by Temperature", AIEE Transactions, Volume: 49, pp. 776-792, 1930.

[117] T. W. DAKIN, "Electrical Insulation Deterioration Treated as a Chemical Reaction Rate Phenomena", AIEE Transactions, Volume: 66, pp.113-122, 1947.

[118] R. M. MORAIS, and E. ENGELSTEIN, "Thermal Ageing of Oil-Paper Insulation", Conference Record of the 10th International Conference on Conduction and Breakdown in Dielectric Liquids (ICDL1990), pp. 495-499, September 1990.

[119] IEEE STANDARD 99-1980, "IEEE Recommended Practice for the Preparation of Test procedures for the Thermal Evaluation of Insulation Systems for Electric Equipment (ANSI)", 1980.

[120] IEEE STANDARD 1276-1997, "IEEE Trial-Use Guide for the Application of High-Temperature Insulation Materials in Liquid-Immersed Power Transformers (ANSI)", 6 March 1998.

[121] IEEE STANDARD C57.119-2001, "IEEE Recommended Practice for Performing Temperature Rise Tests on Oil-Immersed Power Transformers at Loads Beyond Nameplate Ratings (ANSI)", 2002.

[122] D. R. CULLEN, "Tiny Bubbles, in the Oil", Engineer's Notebook, Electrical World T&D, November/December 2001.

[123] T. V. OOMMEN and S. R. LINDGREN, "Bubble Evolution from Transformer Overload", Transmission and Distribution Conference and Exposition, IEEE/PES, Volume: l, pp. 137-142, October/November 2001.

[124] W. A. FESSLER et al., "A Refined Mathematical Model for Prediction of Bubble Evolution in Transformer", IEEE Transaction on Power Delivery, Volume: 4 Issue: 1, pp. 391-404, January 1989.

[125] K. H. STARK, "Influence of Moisture in Oil-Impregnated Paper Insulation- A Critical Resume", English Electric Company Limited, Stafford, 5 December 1958.

[126] Y. DU et al., "Moisture Equilibrium in the Paper-Oil Systems", Electrical Insulation Magazine, Volume: 15, Issue: 1, pp. 11-20, January/February 1999.

[127] E. B. FRANKLIN, "Distribution of Water in Transformer Insulation: Part 1. Theory and Calculation", Electrical Times, 27 May-3 June 1965.

[128] T. V. OOMMEN, "On-Line Moisture Sensing in Transformers", Proc. 20th Electrical Electronics Insulation Conference, pp. 236-240, 7-10 October 1991.

[129] S. M. ISLAM, P. R. S. JOTA and M. STACE, "Detection of Oil-Paper Equilibrium Moisture Content in Power Transformers Using Hybrid Intelligent Interpretation of Polarisation Spectrums from Recovery Voltage Measurements", Proc. 1998 IEEE Symp. on Electrical Insulation, Volume 1, pp.16-19, June 1998.

[130] H. P. GASSER et al., "Determining the Ageing Parameters of Cellulosic Insulation in a Transformer", 11th International Symposium on High Voltage Engineering 1999, IEE Conference Publication No: 467, Volume: 4, pp. 143-147, 23-27 August 1999.

[131] M. WEBB, "Water in Oils", IEE Colloquium on an Engineering Review of Liquid Insulation, Digest No. 1997/003, pp. 2/1-2/6, 7 January 1997.

[132] L. LEWAND, "Chemist's Perspective: Understanding Water in Transformer Systems: The Relationship Between Relative Saturation and Parts per Million (Double Engineering)", Neta World, Spring 2002.

[133] V. G. DAVYDOV & O. ROLZMANN, "Moisture Assessment in Power Transformers: Lesson Learned", Vaisala News No.160/2002, Australia, pp.18-21, 2002.

[134] B. K. GUPTA, "Direct Determination of Moisture in Solid Oil-Paper Insulation", Conference Record of the 1998 IEEE International Symposium on Electrical Insulation, Volume: 2, pp. 583-586, 7-10 June 1998.

[135] INTERNATIONAL ELECTROTECHNICAL COMMISSION (Draft IEC 60599 Edition 2), "Mineral Oil-Impregnated Electrical Equipment in Service-Interpretation of Dissolved and Free Gas Analysis", 1997.

[136] V. SOKOLOV, V. BULGAKOVA and Z. BERLER, "Assessment of Power Transformer Insulation Condition", Proc. 2001 Electrical Insulation Conference and Electrical Manufacturing & Coil Winding Conference, pp. 605–613, 16-18 Oct. 2001.

[137] FACILITIES INSTRUCTIONS, STANDARDS AND TECHNIQUES (FIST), "Maintenance of Liquid Insulation: Mineral Oils and Askarels", Volume 3-5, United States Department of Interior: Bureau of Reclamation, December 1991.

[138] G. BERG and L. E. LUNDGAARD, "Discharges in Combined Transformer Oil/Paper Insulation", Proc. 13th International Conference on Dielectric Liquids (ICDL 99), Nara, Japan, pp. 144-147, 20-25 July 1999.

[139] V. WASSERBERG et al., "Investigation on Cavities inside Liquid-Immersed Paper and Pressboard Insulation Materials and their Influence on the Electrical Behaviour", Conference Record 2000 IEEE International Symposium on Electrical Insulation, pp. 422-425, 2-5 April 2000.

[140] A. M. EMSLEY R. H. HEYWOOD and G. C. STEVENS, "Ultra Accelerated Thermal Ageing Tests: Slow Thermal Ramp Methods in Predicting Life Expectancy", International Conference on Ageing Studies and Lifetime Extensions of Materials, Oxford, July 1999.

[141] IEEE STANDARD C57.117.1986, "IEEE Guide for Reporting Failure Data for Power Transformers and Shunt Reactors on Electric Utility Power Systems (ANSI)", 1 April 1988.

[142] T. LEIBFRIED, "Online Monitors Keep Transformer in Service", IEEE Computer Application in Power, Volume: 11 Issue: 3, pp. 36-42, July 1998.

[143] F. H. KREUGER, "Partial Discharge Detection in High Voltage Equipment", Butterworth, London, 1989.

[144] FACILITIES INSTRUCTIONS, STANDARDS AND TECHNIQUES (FIST), "Testing Solid Insulation of Electrical Equipment", Volume 3-1, United States Department of Interior: Bureau of Reclamation, December 1991.

[145] M. DARVENIZA et al., "Modern Electrical and Chemical Diagnostic Methods for Assessing Ageing of Transformer Insulation-with Special Reference to Recovery Voltage Analysis", CIGRE Study Committee 15 Symposium "Service Ageing of Materials in HV Equipment", Sydney, Australia, 4 October 1999.

[146] D. A. NATTRASS, "Partial Discharge XVII: The Early History of Partial Discharge Research", IEEE Electrical Insulation Magazine, Volume: 9 Issue: 4, pp. 27-31, July/August 1993.

[147] IEC STANDARD, Publication 60270, "High Voltage Test Techniques-Partial Discharge Measurements", 2000.

[148] ROBINSON ELECTRONIC INSTRUMENTS, "E. R. A. Discharge Detector Model 3: System Manual and Operation Manual", Cheshire, United Kingdom.

[149] R. BARTNIKAS, "Partial Discharges: Their Mechanism, Detection and Measurement", IEEE Transactions on Dielectrics and Electrical Insulation, Volume: 9 Issue: 5, pp. 763-808, October 2002.

[150] H. BORSI and U. SCHRODER, "Initiation and Formation of Partial Discharges in Mineral-Based Insulating Oil", IEEE Transactions on Dielectrics and Electrical Insulation. Volume: 1 Issue: 3, pp. 419-425, June 1994.

[151] N. AHMED and N. SRINIVAS, "PD Types and their Detection Possibilities by PD Test Methods", IEEE: 2001 Annual Report Conference on Electrical Insulation and Dielectric Phenomena, pp. 307-310, 14-17 October 2001.

[152] T. R. BLACKBURN et al., "Advanced Techniques for Characterisation of Partial Discharges in Oil-Impregnated and Gas Insulated Systems", CIGRE 1994 Session, Paris, France, 28 August-3 September 1994.

[153] R. MENON et al., "Correlation of Acoustic Emission Method and Electrical Method for Detection of Partial Discharges in Transformers", IEEE 7th International Conference on Solid Dielectrics, pp. 299-302, 25-29 June 2001.

[154] IEEE STANDARD C57.127-2000, "IEEE Trial-Use Guide for the Detection of Acoustic Emissions from Partial Discharge in Oil-Immersed Power Transformers", 3 December 2000.

[155] P. McMULLAN and E. TRUUPOLD, "Introduction to Partial Discharge Measurement", Electrical Testing Laboratory, ECNSW: Australia, January 1982.

[156] S. K. HALES, "System Monitors Transformer Condition", Electrical World, pp. 63-67, March 1989.

[157] CIGRE SC 12 WG-01, "Measurement of Partial Discharges in Transformer", Electra No. 47, pp. 37-44, 1976.

[158] A. T. THOENG, "Detection and Location of Partial Discharges in Power Transformer", IEEE Conference Publication No: 94, Part: 1, pp. 71-76, 1973.

[159] L. BIN et al., "A Method of Noise Suppression for On-Line Monitoring Partial Discharge in Transformers", Ninth International Symposium on High Voltage Engineering, Graz, Austria, 5587-1, 28th August- 1st September 1995.

[160] A. CAVALLINI et al., "A New Approach to the Diagnosis of Solid Insulation Systems Based on the PD Signal Inferences", IEEE Electrical Insulation Magazine, Volume: 19 Issue: 2, pp. 23-30, March/April 2003.

[161] BROWN BOVERI PUBLICATIONS, "Brown Boveri & Company Switzerland", Publication No: CH-A 064 411E, Switzerland.

[162] C. CHANG and Q. SU, "Analysis of Partial Discharge Patterns from a Rod to Plane Arrangement", Conference Record of the IEEE International Symposium on Electrical Insulation, Anaheim, USA, pp. 439-443, 2-5 April 2000.

[163] R. BARTNIKAS and J. E. McMAHON, "Engineering Dielectrics Volume: 1, Corona Measurement and Interpretation", American Society for Testing and Materials (ASTM), Philadelphia, USA, 1979.

[164] M. RANDOUX and R. WILPUTTE, "Lesson Drawn from the Routine Testing of Insulation Oils Used in Power Transformer on the Belgian Network", CIGRE paper 12-07, CIGRE Paris, 1986.

[165] A. ZARGARI and T. R. BLACKBURN, "Modified Optical Fibre Sensor for PD Detection in High-Voltage Power Equipment", 1996 IEEE International Symposium on Electrical Insulation, Montreal, Canada, pp. 424-427, June 1996.

[166] J. UNSWORTH, "Acoustic Detection of PDs", Electricity Supply Association of Australia (ESAA) Short Course on Insulation Condition Monitoring and Partial Discharge Techniques, Sydney, 18-20 June 2003.

[167] B. HOCHARDT, "Power Transformer Handbook", Butterworth-Heinemann, London, 1987.

[168] J. AUSTIN, R. E. JAMES and P. MARSHALL, "Application of Capacitive Network Winding Representation to the Location of the Partial Discharges in Transformers", EE. Trans. Institution of Engineers Australia, pp. 95-103, 1977.

[169] L. E. LUNGARD and W. HANSEN, "Location of Discharges in Power Transformers Using External Acoustic Sensors", 6th International Symposium on High Voltage Engineering (ISH), paper 15-05, New Orleans, August 1989.

[170] S. L. JONES, "The Detection of Partial Discharges in Transformers Using Computer Aided Acoustic Emission Techniques", Conf. Record: IEEE International Conf. on Electrical Insulation, Toronto, pp. 106-110, June 1990.

[171] P. J. MOORE and H. HOUSE, "Corona Detection Using Image Processing Technique in a High Voltage Environment", Seventh International Symposium on High Voltage Engineering (ISH), Volume: 7, pp. 71-74, 26-30 August 1991.

[172] T. W. DAKIN and J. LIM, "Measurement of Partial Discharge on Transformer by Radio Influence Voltage Meters", Trans. on Power Apparatus and Systems, American Institute of Electrical Engineers, Volume: 76, pp.178-198, Dec. 1957.

[173] H. KAWANDA and M. HONDA, "Partial Discharge Automatic Monitor for Oil-Filled Power Transformers", IEEE Transaction on Power Apparatus and System, Volume: PAS-103 Issue: 2, pp. 422-428, February 1984.

[174] D. KOUADRIA and D. M. RYDER, "On-line Monitoring and Automatic Computer Analysis of Insulating Systems", 1996 IEEE Annual Report-Conference on Electrical Insulation and Dielectric Phenomena, San Francisco, Volume: 2, pp. 533-536, 20-23 October 1996.

[175] M. ZAHN, A. P. WASHABAUGH and J. W. LOU, "Electrical Breakdown in Transformers due to Flow Electrification", Eleventh International Conference (ICDL 93), pp. 322-331, 19-23 July 1993.

[176] E. GULSKI, "Knowledge-Based Rules for PD Diagnosis in Service", CIGRE Study Committee 15 Symposium "Service Ageing of Materials in HV Equipment", Sydney, Australia, October 1999.

[177] M. D. JUDD et al., "Intelligent Condition Monitoring and Asset Management. Partial Discharge Monitoring for Power Transformers", IEE Power Engineering Journal, Volume: 16, Issue: 6, pp. 297-304, December 2002.

[178] J. UNSWORTH, J. KURUSINGAL and R. E. JAMES, "On-Line Partial Discharge Monitor for High Voltage Power Transformers", Proceeding of the 4th International Conference on Properties and Applications of Dielectric Materials 1994, Volume: 2, pp. 729-732, 3-8 July 1994.

[179] D. WENZEL, H. BORSI and E. GOCKENBACH, "Partial Discharge Measurement and Gas Monitoring of Power Transformer On-Site", Proceedings of the 7th International Conference on Dielectric Materials, Measurements and Applications, Publication: 430, pp. 255-258, 23-26 September 1996.

[180] A. M. EMSLEY et al., "Degradation of Cellulosic Insulation in Power Transformers. Part 3: Effects of Oxygen and Water on Ageing in Oil", Proceedings of the IEE Science, Measurement and Technology, Volume: 147 Issue: 3, pp. 115-119, May 2000.

[181] M. S. A. MINHAS, J. P. REYNDERS and P. J. DE'KLERK, "Failures in Power System Transformers and Appropriate Monitoring Techniques", Eleventh International Symposium on High Voltage Engineering (ISH), IEE Publication: 467, Volume: 1, pp.94-97, 23-27 August 1999.

[182] M. D. WILKINSON and P. DYER, "Continuous Moisture Management: Extending Transformer Service Life", Proceedings of the 16th IEE International Conference and Exhibition on Electricity Distribution (2001 CIRED), Part: 1 Contributions Publication: 482, Volume: 1, pp. 5, 18-21 June 2001.

[183] Y. DU et al., "Moisture and Temperature Effects on the Dielectric Spectrum of Transformer Pressboard", Annual Report Conference on Electrical Insulation and Dielectric Phenomena, pp.878-881, 20-24 October 2002.

[184] A. SHKOLNIK, "Determination of Water Content in Transformer Insulation", Proceedings of the 14th IEEE International Conference on Dielectric Liquid (ICDL 2002), pp. 337-340, 7-12 July 2002.

[185] R. E. JAMES, et al., "Challenges for Advanced Diagnostic Techniques Faults Undetectable by Existing Electrical Methods", CIGRÉ Paper 15-306, Paris 2000.

[186] W. G. ARIASTINA, R. H. KHAWAJA and T. R. BLACKBURN, "The Statistical Properties of PD Distribution in Oil-Impregnated Insulation at Elevated Temperature", The 7th International Conference on Properties and Applications of Dielectric Materials (ICPADM), Nagoya, Vol. 3, pp.1116-1119, June 2003.

[187] T. TANAKA AND T. OKAMOTO, "Analysis of q-n and φ-q Characterisation of Partial Discharge in Service Electrode System, IEEE International Symposium on Electrical Insulation, Boston, pp. 190-193, June 1980.

[188] T. OKAMOTO AND T. TANAKA, "Change of Pulse-Mean φ-q Distribution Pattern of Partial Discharges due to Treeing Propagation, Electrical Engineering in Japan, Vol. 102, No. 6, pp. 18-25, 1982.

[189] T. TANAKA, "Partial Discharge Pulse Distribution Pattern Analysis, IEE Proceedings; Science, Measurement and Technology, Vol. 142, pp.46-50, 1995.

[190] A. KRIVIDA, "Recognition of Discharges: Discrimination and Classification, PhD Thesis, Delft University Press, Netherlands, 1995.

[191] IEEE PES TRANSFORMER WORKING GROUP REPORT, "Background Information on High Temperature Insulation for Liquid Immersed Power Transformers", IEEE Trans. Power Delivery, Vol. 9, pp.1892–1906, 1994.

[192] T. K. SAHA, M. DARVENIZA and Z. T. YAO, "Field Experience with Return Voltage Measurements for Assessing Insulation Condition in Transformers and its Comparison with Accelerated Aged Insulation Samples", 11th International Symposium on High Voltage Engineering (ISH), IEE Publication: #467, Volume: 5, pp. 140-143, 23-27 August 1999.

[193] J. P. V. BOLHUIS et al., "Interpretation of RVM Measurements: Beyond the Polarisation Spectrum", IEEE/PES Asia Pacific Transmission and Distribution Conference and Exhibition 2002, Volume: 3, pp. 1829-1833, 6-10 October 2002.

[194] G. CSEPES et al., "Practical Foundations of the RVM (Recovery Voltage Method for Oil/Paper Insulation Diagnosis)", Conference on Electrical Insulation and Dielectric Phenomena, Volume: 1, pp.345-355, 25-28 October 1998.

[195] R. PATSCH and O. KOUZMINE, "The Influence of Climatic Conditions on the Diagnostic Results of Return Voltage Measurements", Conf. Record 2002 IEEE International Symposium on Electrical Insulation, Boston, pp. 191-194, April 2002.

[196] A. KRIVDA and G. RUSSELL, "Assessment of Oil-Impregnated Paper Insulated Transformers Using Recovery Voltage Measurements", Proceedings of the International Conference on Conduction and Breakdown in Solid Dielectrics (ICSD 1998), Vasteras, Sweden, pp. 64-68, 22-25 June 1998.

[197] C. K. TAN and Y. H. LU, "Recovery Voltage Measurement (RVM) Using Lab View", Thesis report, School of Electrical Engineering and Telecommunications, The University of New South Wales, Sydney, June 2002.

[198] T. V. Oommen & T. A. Prevost, "Cellulose Insulation in Oil-filled Power Transformers: Part II – Maintaining Insulation Integrity and Life" Electrical Insulation Magazine, Vol. 22, No. 2 pp5-14, March/April 2006.

[199] C Patrick McShane: "New safety Dielectric Coolants for Distribution and Power Transformers". IEEE Industry Applications Magazine: Vol. 6, No. 3, pp24-32, May/June 2000. [See also: Oommen, T.V: *Vegetable Oils for Liquid-Filled Transformers*. Electrical Insulation Magazine. Vol. 18, #1, pp 6-11 (2002)]

[200] CIGRE Task Force TFD1.01.09 "Dielectric Response Methods for Diagnostics of Power Transformers": CIGRE, Technical Brochure No.254, August 2004.

[201] M. Wang, A. J Vandermaar and K. D Srivastava: "Transformer Winding Movement in Service – Key Factors Affecting FRA Measurements". Electrical Insulation Magazine: Vol. 20, No. 5, pp5-12, September/October 2004.

[202] S. A. Bhumiwat and P. Stattman: "Quality Assurance after Transformer Refurbishment by Means of Polarization Depolarization Currents Analysis". Presented at the 2003 Bologna IEEE Power Tech Conference. IEEE paper 0-7803-7967-5/03. 2003

[203] G. C. Montanari, A. Cavallini & F. Puletti, "A new Approach to Partial Discharge Testing of HV Cable Systems": Electrical Insulation Magazine, Vol. 22, No. 1, pp14-23, Jan. /Feb. 2006.

[204] Standards Australia: Australian Standard AS 2374.7 – 1997: "Loading Guide for Oil-Immersed Power Transformers" [as IEC 354-1991]. (1997).

[205] International Electrotechnical Commission: "Mineral Oil-Impregnated Electrical equipment in service – Guide to the Interpretation of Dissolved and Free Gases Analysis". IEC Standard 60599, 1999. [See also: M Duval: *"New techniques for Dissolved Gas-in-Oil Analysis"*, Electrical Insulation Magazine, Vol. 19, No. 2, pp6-15, 2003.]

[206] W. G. Ariastina: "A Study of the Properties of Partial Discharges in Oil-impregnated Insulation". PhD Thesis, The University of New South Wales, School of Electrical Engineering. 2004.

[207] G. H. Kaufmann: "Gas Bubbles in Distribution Transformers". IEEE Transaction on PAS Vol. No. 5, Sep/Oct. 1977, pp 1596-1603.

Appendix A

Author's Publications

[1] R. H. KHAWAJA, E. S. KIM, W. G. ARIASTINA and T. R. BLACKBURN, "The Effect of High Temperature on Partial Discharges in Oil-Impregnated Insulation", Proceedings of 2002 Australasian Universities Power Engineering Conference (AUPEC 2002), Part: 4 (High Voltage, Condition Monitoring), Melbourne, Australia, 29th September - 2nd October 2002.

[2] W. G. ARIASTINA, R. H. KHAWAJA and T. R. BLACKBURN, "Effects of Elevated Temperature on PD Activity in Oil-Impregnated Insulation: An Experimental Investigation", Proceedings of 2002 Australasian Universities Power Engineering Conference (AUPEC 2002), Part: 4 (High Voltage, Condition Monitoring), Melbourne, Australia, 29th September - 2nd October 2002.

[3] Y. H. LU, C. K. TAN, B. T. PHUNG, R. H. KHAWAJA and T.R. BLACKBURN, "Development of a Computer-Based Data Logger for Recovery Voltage Measurements", Proceedings of 2002 Australasian Universities Power Engineering Conference (AUPEC 2002), Part: 4 (High Voltage, Condition Monitoring), Melbourne, Australia, 29th September - 2nd October 2002.

[4] R. H. KHAWAJA, W. G. ARIASTINA and T. R. BLACKBURN, "Partial Discharge Behavior in Oil-Impregnated Insulation", Proceedings of the 7th International Conference on Properties & Applications of Dielectric Material (ICPADM 2003), Nagoya, Japan, Volume: 3, pp. 1166-1169, 1 - 5 June 2003.

[5] W. G. ARIASTINA, R. H. KHAWAJA and T. R. BLACKBURN, "The Statistical Properties of PD Distribution in Oil-Impregnated Insulation at Elevated Temperature", Proceedings of the 7th International Conference on Properties & Applications of Dielectric Material (ICPADM 2003), Nagoya, Japan, pp. 1116-1119, 1 - 5 June 2003.

[6] R. H. KHAWAJA, T. R. BLACKBURN and B. T. PHUNG, "Partial Discharge Activity at High Temperature", Proceedings of the Xlllth International Symposium on High Voltage Engineering, Delft, The Netherlands, August 2003.

[7] R. H. KHAWAJA, W. G. ARIASTINA and T. R. BLACKBURN, "Investigation of the Statistical Behaviour of PD Patterns in Oil-Impregnated Insulation at Elevated Temperature", Paper #143, Proceedings of the 2003 Australasian Universities Power Engineering Conference (AUPEC 2003), Christchurch, NZ, 28th September - 1st October 2003. ISBN 0-473-09867-9.

[8] W. G. ARIASTINA, R. H. KHAWAJA and T. R. BLACKBURN: "Investigation of Partial Discharge Properties in Oil-Impregnated Insulation". Paper S-3, ICPADM Conference, Bali, August 2006. ICPADM Proceedings, Volume 2, pp714-717, June, 2006.

Appendix B

Software Design of the CDA3 System

B.1 Overview

All the programmes to operate the CDA3 system were written by the author in Pascal language and run within the IBM-DOS environment. The compiler used for the development is Borland Turbo Pascal [1]. For displaying graphics on the colour monitor and generating hard-copy outputs on the printer or plotter, the author utilised the Quinn-Curtis Science and Engineering Tools [2]. These are general-purpose software routines that can be called up in the programme as Procedures or Functions. Also, references [3-4] provide practical guides to Pascal programming and useful background routines (menu management, data entry, string manipulation, screen handling, etc) to create a quality professional application.

The Pascal source codes consist of the following files: GLOBAL.PAS, UTIL1.PAS, UTIL2.PAS, UTIL3.PAS, TESTDMA.PAS, INDI.PAS, DMA.PAS, CALI.PAS, FILES.PAS, SETUP.PAS and CDA3.PAS. Altogether, there are about 5 thousand lines of codes. These programmes were recently given to a third party to produce a commercial version, written in C language and run under the Windows 3.x environment. The Windows version is essentially a direct translation of the DOS version although it is somewhat slower and does not provide all the features available in the DOS version. In this Appendix, the design and operation of the DOS version of the CDA3 software will be discussed in sufficient details to enable others to use the system.

After compilation, there are 4 files generated which are required for running the CDA3 system. These files are stored in the directory CDA3. Two of the files are executable: SETUP.EXE and CDA3.EXE. The SETUP.EXE programme is for altering the parameters of the system configuration such as the type of printer, plotter and discharge detector. Normally, the user runs the SETUP programme once during the initial installation of the hardware to modify the default settings. These parameters are stored

Appendix B: Software Design of the CDA3 System

in the 'PARA.DAT' file for use by the CDA3.EXE programme. There is no need to execute the SETUP programme again unless the configuration has been changed.

CDA3.EXE is the main programme of the system. It has gone through a number of revisions (current version is V3.TP). It is an integrated piece of software which carries out all the necessary functions of PD recording and analysis. The software also requires the EGAVGA.BGI file which is the driver for the colour graphic monitor.

B.2 Programme for configuring the system: 'SETUP.EXE'

To run this programme, go into the 'CDA3' directory then type SETUP. Figure B.1 shows the screen display of the main menu which has 7 different options. Selection can be made by using the Up Arrow (↑) or Down Arrow (↓) key to move to the desired option. The one that is currently selected is highlighted on the display. The 'wrap-around effect' applies at the top or bottom selection. This feature can be utilised to minimise the number of key entries required. For example in Figure B.1, to move from 'Hardcopy Device' to 'Exit', key in ↑ once instead of key in ↓ six times. To go into the sub-menu of the selected option, press the Return key.

CDA3 INSTALLATION AND SETUP [V1.TP-Sept.93]

Main menu: Hardcopy Device.
Printer.
Plotter.
Serial Port.
Organisation Name.
Calibrator Type.
Exit.

Figure B.1: Screen display of the main menu of the SETUP programme.

In each sub-menu, there are a number of options. Selection can be made in a similar manner, i.e. use the ↑ key or ↓ key to move to the desired option and then press the Return key. Each Return key stroke will bring up the next setting on the list for that particular selection. Again, the wrap-around effect applies.

Note that the same format of menu management, entry screen design and data handling is used in the main programme CDA3.EXE and also in the modified version DC.EXE.

If the *'Exit'* function of the main menu is selected, the programme will save all the current settings in a file (PARA.DAT) and then return to DOS. The other functions are described below.

B.2.1 Hardcopy device

```
                CDA3 INSTALLATION AND SETUP [V1.TP-Sept.93]

Main menu:   Hardcopy Device.-------------------> Change
             Printer.                             Exit
             Plotter.
             Serial Port.
             Organisation Name.
             Calibrator Type.
             Exit.

Hardcopy device selected = printer
```

Figure B.2: Screen display of 'Hardcopy Device' sub-menu.

There are two types of hardcopy devices that can be driven by the CDA3 system: printer and plotter. However, only one device is allowed to be active at a time. Upon entering this option, the screen displays the sub-menu as in Figure B.2 and also shows the device currently active. To toggle the hardcopy device, the user selects '*Change*' and presses the Return key.

B.2.2 Printer

This menu is used for selecting the printer type and the port to which the printer is connected (Figure B.3). A variety of printers can be used. The default setting is Epson MX printer type, parallel port 1 (LPT1) connection, quadruple density print mode and (2,1) magnification. The available settings for printer are as follows:

'Printer type':	(a) Epson MX or emulators, e.g. IBM, Okidata. (b) Epson LQ 24-pin or emulators, e.g. Panasonic. (c) Toshiba P 24-pin, (d) HP Laser Jet or emulator and Desk Jet, (e) HP Ink Jet, (f) Epson FX.
'Connection port':	(a) Serial port no.1 (COM1), (b) Serial port no.2 (COM2), (c) Parallel port no.1 (LPT1), (d) Parallel port no.2 (LPT2)
'Mode':	available definitions vary with printer type selected.
'Magnification':	horizontal and vertical scaling multiplers. valid settings are decimal numbers between 1 and 4.


```
                CDA3 INSTALLATION AND SETUP [V1.TP-Sept.93]

Main menu:   Hardcopy Device.
             Printer.------------------------------> Printer type
             Plotter.                                Connection port
             Serial Port.                            Mode
             Organisation Name.                      Magnification
             Calibrator Type.                        Print test pattern
             Exit.                                   Exit

Printer: Epson MX or emulators
Connection: Parallel port no.1 (LPT1)
Mode: quadruple density, normal speed
Magnification (x,y): 2.00, 1.00
```

Figure B.3: Screen display of 'Printer' sub-menu.

The scale and size of the printout depend on the combined settings of *'Mode'* and *'Magnification'*. After making the changes, the function *'Print test pattern'* should be activated for checking the new settings. If the printer fails to respond or the printout is intelligible, further adjustment is necessary. In practice, a number of iterations may be required to find the correct settings for the desired output.

B.2.3 Plotter

This enables the user to specify the configuration for the plotter. When this function is chosen, the screen displays the associated sub-menu selections (Figure B.4). It also shows the current settings for the plotter. The available settings are:

Plotter type:	HP-GL, Postscript
Connection port:	COM1, COM2

The default setting is HPGL plotter type with COM2 as the connection port (300 bauds, no parity, 1 stop bit, 8-bit word). To change the current settings, use a combination of ↑, ↓ and Return keys. Note that connection to the parallel port is not allowed. Also changes to the communication protocols can only be made through the *'Serial Port'* function. After changing to a new setting, the *'Plot test pattern'* function should be activated to check for correct setup. For full colour presentation, the plotter should have at least 4 pens, e.g. Roland DXY-1000 series.

```
              CDA3 INSTALLATION AND SETUP [V1.TP-Sept.93]

Main menu:   Hardcopy Device.
             Printer.
             Plotter. ----------------------> Plotter type
             Serial Port.                     Connection port
             Organisation Name.               Plot test pattern
             Calibrator Type.                 Exit
             Exit.

Plotter type: HP-GL
Connection port: Serial port no.2 (COM2)
Baud rate = 300, no parity, stop bits = 1, word length = 8
```

Figure B.4: Screen display of 'Plotter' sub-menu.

```
              CDA3 INSTALLATION AND SETUP [V1.TP-Sept.93]

Main menu:   Hardcopy Device.
             Printer.
             Plotter.
             Serial Port. ------------------> Port number
             Organisation Name.               Baud rate
             Calibrator Type.                 Parity
             Exit.                            Stop bits
                                              Word length
                                              Exit
Port number = 1
Baud rate = 2400, no parity, stop bits = 1, word length = 8
```

Figure B.5: Screen display of 'Serial port' sub-menu.

B.2.4 Serial port

This function enables the user to specify the communication protocols for the two serial ports COM1 and COM2 of the computer. The screen for this sub-menu is shown in Figure B.5. The available settings are as follows:

Port number:	1, 2
Baud rate:	300, 600, 1200, 2400, 4800, 9600
Parity:	no parity, even parity, odd parity
Stop bits:	1, 2
Word length:	7 bits, 8 bits

B.2.5 Organisation name

This function enables specification of the name of the user or associated organisation which will be displayed as the heading on all graphical outputs. The screen for this sub-menu is shown in Figure B.6. To modify the current entry shown on the screen, select '*Change*' and enter the required name after the prompt. The length of the text entry is limited to 20 characters. Spaces can be embedded within the character string.

```
              CDA3 INSTALLATION AND SETUP [V1.TP-Sept.93]

Main menu:   Hardcopy Device.
             Printer.
             Plotter.
             Serial Port.
             Organisation Name. --------------> Change
             Calibrator Type.                   Exit
             Exit.

Current Name = HV Laboratory - UNSW
Enter name (up to 20 characters) =
```

Figure B.6: Screen display of 'Organisation Name' sub-menu.

B.2.6 Calibrator type

For system calibration, it is necessary to specify which of the two types of calibration is used. With the Robinson Model 3 detectors, the internal calibrator is generated at a fixed phase position and exactly once per ac cycle. The newer models such as the 700 Series generate a pair of internal calibrators of opposite polarity in each cycle and they are 180° apart. The CDA3 programme relies on these special characteristics to carry out automatic calibration.

When this function is chosen, the screen displays the associated sub-menu selections (Figure B.7). It also shows the current selection of the internal calibrator (one per cycle or two per cycle). To alter, select 'Change' and press Return. This will toggle the selection.

```
                CDA3 INSTALLATION AND SETUP [V1.TP-Sept.93]

Main menu:      Hardcopy Device.
                Printer.
                Plotter.
                Serial Port.
                Organisation Name.
                Calibrator Type. ----------------> Change
                Exit.                              Exit

Two internal calibrators per cycle, e.g. 700 Series
```

Figure B.7: Screen display of 'Calibrator Type' sub-menu.

B.3 Main programme for recording and analysis: 'CDA3.EXE'

This is the only programme the user needs to call up in normal operation. To execute this programme, go into the CDA3 directory then type 'CDA3'. The screen will display the main menu as shown in Figure B.8. There are 6 available selections. Their functions are summarised below:

1. *'Parameter setup'*: allow parameters relating to a test to be specified such as PD calibration, signal detection threshold, recording period, recording mode and storage.
2. *'Voltmeter'*: enable calibration of the voltmeter for a particular divider. Also allow specification of the frequency of the test supply and correction of any phase shift.
3. *'Capture and analyse new data'*: this function initiates recording of new data. Analysis follows immediately. Results are shown on the screen in three different presentation formats.
4. *'Replay old records on disk'*: the results from data files recorded previously can be recalled for viewing, printing or plotting. Unwanted records within a file can be edited out to save disk space.
5. *'Examine individual PD'*: capture new data and display numeric values of the recorded pulses. This function is not normally used. It is intended to facilitate manual calibration in very noisy environment.

6. *'Exit'*: quit the CDA3 programme and return to DOS.

```
          COMPUTERISED DISCHARGE ANALYSER CDA3 [V3.TP-Nov95]

Main menu:      Parameter setup.
                Voltmeter.
                Capture and analyse new data.
                Replay old records on disk.
                Examine individual PD.
                Exit.
```

Figure B.8: Screen display of the main menu.

Selection can be made by using the arrow keys to move to the desired option and then press the Return key to go into the sub-menu.

B.3.1 Parameter setup

Upon entering this option, the screen displays the sub-menu as shown in Figure B.9. It also displays the current values of the parameters associated with the various options in the sub-menu. These values can be changed by selecting the appropriate option. When finish, select the 'Exit' function to return to the main menu.

B.3.1.1 Integration time

This function enables the user to specify the time duration T of each recording run. The following message is displayed:

' *Integration period (seconds) =* '

A valid entry is an integer value between 1 and 32767 seconds. A typical setting would be between 5 and 30 seconds. When recording is initiated, the system will continuously capture PD data in real-time for the specified duration. Recording is then stopped. The system analyses the captured data and displays the results on the screen.

Note that data is captured into a memory buffer of limited size (set to 32k words). It requires 2 words to store information for each PD pulse. Also every second, the test voltage is recorded which uses 1 word. During recording, the system constantly checks the buffer. If it is full before T expires, the programme will automatically stop recording and the integration time T will be adjusted accordingly in the analysis.

```
            COMPUTERISED DISCHARGE ANALYSER CDA3 [V3.TP-Nov95]

Main menu:  Parameter setup ---------------------> Integration time
            Voltmeter.                             Detector calibration
            Capture and analyse new data.          Analyser calibration
            Replay old records on disk.            Measurement phase windows
            Examine individual PD.                 Signal threshold
            Exit.                                  File to store results
                                                   Note for identification
                                                   Save new setup
                                                   Exit

Hardcopy device: printer              Integration period: 30s
External cal.: 50pC --> 61dB          Analyser cal.:0.15pC/unit, 614pCmax
Signal threshold: 15 (48pC)           File: Red-1
Notes: Endurance 132kV CT             50Hz phase reference present
Gating windows: none
```

Figure B.9: Screen display of the sub-menu 'Parameter setup'.

B.3.1.2 <u>Detector calibration</u>

The normal procedure for any discharge test is first to calibrate the measurement circuit. Since the PD signal is fed through the Robinson detector and the CDA3 analyser in cascade, calibration of both devices is necessary and must be carried out in the same sequence. Although it is quite possible to calibrate the whole system in one step, the method proposed here is more flexible in that subsequent re-calibration can be carried out on-line.

Detector calibration must be done first. This function enables the operator to enter off-line calibration information based on the use of an external electronic PD simulator such as the Robinson Type 753. Discharges of known magnitude are injected into the test circuit and compared with the internal calibrator of the detector. The attenuation setting of the internal calibrator (in dB unit where 0dB corresponds to a 100V output pulse) is adjusted to achieve the same magnitude on the CRT display. After this has been done, the user enters this menu and types in the pC value of the simulated PD pulse in response to the message:

'*External calibrator magnitude (pC) =* '

Next the user types in the equivalent dB setting of the internal calibrator in response to the message:

'*Equivalent internal calibrator (dB) =* '

The entered calibration data will be confirmed on the screen, e.g.:

'*External cal.: 50.0pC → 46dB* '

This numerical relationship between the dB attenuation (x) and the equivalent pC (y) is valid for all gain settings and from which the software can calculate the conversion factor pC-per-volt (z):

$$z = \frac{y * 10^{(x/20)}}{100} \quad \text{pC/volt}$$

For a given test circuit, it is necessary to calibrate the detector only once.

B.3.1.3 <u>Analyser calibration</u>

To complete the calibration process, this function must be carried out after calibrating the detector. The CDA3 system utilises a 12-bit AD converter for digitising the magnitude of the output pulse from the detector. The conversion will give a number in the range from 0 to 4095 and a scaling factor (pC-per-digitised unit) is required by the software to convert this number into the equivalent pC value. Thus the aim of this function is to establish the correct value for the scaling factor.

Calibration is done either through the use of the internal calibrator or without it. The following message is displayed:

'*Capture internal calibrator (enter dB value, else -1) =* '

B.3.1.3.1 <u>Calibration without using internal calibrator</u>:

If the entry is '-1', the system assumes the user knows the correct pC-per-digitised unit. The following message is prompted:

'*Resolution (pC) =* '

The entered value (e.g. 0.005) will be confirmed on the screen. The programme also calculates and displays the largest measurable pC value (without overloading the AD converter). This is simply the product of the resolution and the maximum number of digitised units (e.g. 0.005 x 4095):

'Analyser cal.: 0.005pC/unit, 20pC max'

This calibration mode is not normally used. If the same test is carried out under the same settings then the user can select this mode to type in the resolution value obtained from the previous test. Another situation is when the user decides to calibrate the whole system in one step. For such a case, the procedure is: (a) inject a known pC source into the circuit, (b) use the 'Examine individual PD' function to read the digitised value of the injected signal, (c) work out the pC-per-digitised value and (d) call this function to key in the value.

B.3.1.3.2 Calibration with internal calibrator:

The normal calibration method is to use the internal calibrator. It should be switched on and the user is required to type in its current attenuation setting. The setting chosen does not have to be the same as that in the 'Detector calibration' step. If the entry is a positive integer (e.g. 43), the system accepts it as a valid dB setting and then requests the user to select the capture mode the programme will use to obtain the digitised value of the calibrator:

'Capture mode [1:auto,largest pulse 2:auto fixed phase 3:manual] ='

Capture modes 1 and 2 are automatic, i.e. the software utilises some intelligent algorithms to recognise the internal calibrator (even in the presence of other live PDs) and to determine its digitised value.

Largest pulse capture mode:

The user has to adjust the internal calibrator so that it is the largest signal seen on the detector CRT. This method will work even if the voltage phase reference input is not present or if it is present but not synchronised with the internal calibrator. The system will record data for one second. Depending on the type of detector used, it will then assume the largest 50 or 100 pulses are associated with the internal calibrator. The average of these pulses will be taken as the digitised value of the internal calibrator. The system will display a message to confirm successful calibration, e.g.

'two internal calibrators per cycle'
'pulse amplitudes (min. ave. max.) = 1772 1796 1825'

Note that the message also shows variation in the pulse magnitudes. Since the calibrator pulses are fairly constant, one should expect a small difference between the minimum and maximum values. Otherwise it means that the calibrator is not large enough and calibration should be repeated. The results shown in the above example are acceptable.

Based on the digitised value of the internal calibrator (x), its dB setting (y) and together with the pC-per-volt (z) obtained from the detector calibration step, the programme then calculates the pC-per-digitised-unit (u):

$$u = \frac{z}{x} * \frac{100}{10^{(y/20)}} \quad \text{pC/digitised unit}$$

A message is displayed which shows this scaling factor together with the maximum measurable pC range, e.g.

'Analyser cal.: 0.375pC/unit, 1535pC max'

If the number of pulses is not sufficient, this capture mode fails and the following message is displayed:

'Calibrator not found. Try manual calibration.'

Fixed phase position capture mode:

The 'fixed phase-position' capture mode assumes that there is a pair of stationary pulses (180° apart) in every cycle. The calibrator pulses are not required to be the largest signal present but they must be synchronised with the voltage phase reference input (a small phase jitter is tolerated). The system will record for one second and the software scans through the data to count the number of PD pairs. Calibration is successful if 50 pairs were found over 50 cycles and at the same phase position. A message will be displayed which shows the digitised value and phase position of the calibrator found in the positive half-cycle, e.g.

'Found calibrator of 2178 at 138 degrees.'

Manual mode:

This method is somewhat tedious and should only be used when both automatic capture modes fail. When this mode is selected, the following message is displayed:

'Enter digitised value of calibrator ='

This value must be obtained prior to running this mode through the 'Examine individual PD' function. This function captures and tabulates all the pulses. By manually observing the list, the user decides which pulses correspond to the calibrator and notes the digitised value. After this value is entered, the programme will follow the same procedure as for the automatic capture modes to calculate the pC-per-digitised-unit.

The 'largest pulse' capture mode is perhaps the easiest and most reliable method to calibrate the analyser. Note that during a test, the amplifier gain of the detector is usually changed a number of times by the operator in order to optimise the signal display on the detector CRT. This, of course, will affect the output signal level from the detector to the analyser. Thus it is necessary to re-calibrate the analyser each time the amplifier gain of the detector is adjusted.

B.3.1.4 Measurement phase windows

In practical environments, the PD measurement circuit is susceptible to noise and interference pickup. Disturbances such as thyristor switching noise are usually synchronised with the power frequency and thus appear as pulses at a fixed phase position. For such a case, this function can be utilised to limit PD measurements over certain sections of the ac cycle. The following message is displayed:

> *' Number of gates (0, 1, 2 or 3) = '*

If the entry is '0', the gating function is disabled, i.e. all the PD data will be taken into account in the analysis. Otherwise, up to 3 separate windows can be specified. The system still records all the pulses but only those occurred inside the gating windows will be processed by the software. For each gating window, the programme will ask the user to provide the phase angles (in degrees) of its start and end positions, e.g. the prompt for gate 1 is:

> *' Start and end degrees of Gate 1 = '*

The entries must be integers within the range [0,359] and separated by a space. Also, the start angle must be smaller than the end angle. Provided the entries for all the gates are valid, they will be confirmed on the screen, e.g.

> *'Gating windows = [0,128] [135,308] [315,359] '*

which specifies 3 gating windows. In this example, the first window extends from 0° to 128 °, the second from 135° to 308°, etc.

Appendix B: Software Design of the CDA3 System

B.3.1.5 Signal threshold

Detection of a PD pulse relies on the input signal exceeding a preset threshold. This option allows the user to change the detection level. The following message is displayed:

> *' Signal threshold can be set between 1 and 255*
> *Typical value should be between 10 and 30*
> *Enter new threshold value = '*

The desired value is then entered by the user. This value (x) will be used by the programme to control an 8-bit digital potentiometer which sets the voltage threshold at ($x/255$) volts. Since the maximum output of the 12-bit AD converter is 4095 which corresponds to an input of 5V and the pC-per-digitised unit (y) is known, the programme can calculate the equivalent minimum detectable pC level (z) :

$$z = \frac{x * y * 4095}{255 * 5} \text{ pC}$$

The entered threshold value will be confirmed on the screen together with the equivalent pC, e.g.

> *' Threshold: 15 (4.583pC) '*

Note that the setting should not be lower than 10 which corresponds to ~40mV. Although this limits the system sensitivity, it is less than 1% of the full scale. In return, this would enable the peak-and-hold circuit to function reliably. Below this level, the system is susceptible to noise pickup from the input and to some extent noise from the electronics on-board.

There are two methods for minimising the effect of the background noise whose level exceeds the threshold. One can reduce the gain of the detector amplifier and do a dummy recording to check whether the system still picks up any pulses (assuming no real PDs or internal calibrator present while doing this adjustment). An alternative is to use this function to increase the threshold value until it is high enough to block out the background noise.

B.3.1.6 File to store results

This function is used to specify whether the new measurement results obtained when running the main selection *'Capture and analyse new data'* will be permanently saved in a file or not. The default setting is no, i.e. new data is still captured and the results are displayed on the screen as usual but that will be overwritten by the arrival of data from the next run.

When this function is selected, the following message is displayed:

> '*File name (no extension):* '

The user is required to enter a standard DOS file name (up to 8 characters), e.g. TEST1. No extension is required as the software will tag its own extension (DAT or RAW). This file will be saved in the current directory. To save the file in a different directory or drive, its full path together with the file name must be specified. Note that if there exists a file with the same name, that file will be overwritten (with no warning given).

After entering the file name, the user is asked to specify the recording mode. The following message is displayed:

> '*Recording mode (0:continuous, 1:periodic, 2:conditional)=* '

If '0' is entered, recording to disk is continuous and the specified file name will be confirmed on the screen as:

> '*File: TEST1.DAT* '

With this mode, the system will capture data, analyse, save the results and then repeat the process immediately. The other two recording modes are useful when the user needs to run the test over a long time and does not want the disk to be quickly filled with all the data captured.

If '1' is entered, recording to disk is made periodically. The system will prompt the following message:

> '*Time interval between recordings (minutes)=* '

The entered time interval (e.g. 30) together with the file name will be confirmed on the screen as:

> '*File: TEST1.DAT* '
> '*Record every 30 minutes* '

The system will capture data for every integration period (e.g. 5 seconds), analyse and display the results on the screen as usual. However, not all the results are saved on disk.

Appendix B: Software Design of the CDA3 System

In this example, the system will save the data from a 5-second record once every 30 minutes. The other records in between will be lost.

If '2' is entered, recording to disk is made only if the discharge activity satisfies some constraints. The system will prompt the following message:

> '*Discharge level (pC) and repetition rate (no./s) =* '

The entered pC value (e.g. 10), repetition rate (e.g. 50) together with the file name will be confirmed on the screen as:

> '*File: TEST1.DAT* '
> '*Record if > 10pC and 50.00 no./s* '

The system will capture data for every integration period, analyse and display the results on the screen as usual. However, not all the records are saved on disk. In this example, the system will save only those records which have more than 50 discharges per second that exceed 10pC.

On completion of this function, the user should immediately go to the *'Capture and analyse new data'* menu and start the recording. New data will be stored in the specified file. This file will be closed when recording is stopped and it can not be re-opened to append new records. To save more data, the user should return to this menu and specify a different file.

B.3.1.7 Note for identification

Additional text may be entered that will be saved along with the recorded data. This can be a brief description of the test object such as its type, part number, serial number or some other reference for the test. Such information is useful for identification purpose when there are many different data records to analyse. The text length is limited to a string of up to 20 alpha-numeric characters.

When this option is selected, the following prompt will appear on the screen:

> '*Enter new information for identification:* '

The text entered, e.g. Endurance 132kV CT, will be confirmed on the screen as:

> '*Notes = Endurance 132kV CT* '

Note that identification can also be made based on the date and time of each test run which are automatically recorded. This information is displayed on the screen when the test records are played back. The CDA3 programme utilises the internal clock of the computer to get the date and time. Thus it is important to check that the clock is accurate prior to the test. If adjustment is necessary, run the two DOS commands: DATE and TIME prior to launching the CDA3 programme.

B.3.1.8 Save new setup

This option allows the user to save the current settings of some of the above parameters: *Integration time*, *Detector calibration* and *Signal threshold*. These are stored in the PARA.DAT file and will be automatically recalled the next time the programme is run. The remaining parameters must be specified if necessary.

B.3.2 Voltmeter

```
COMPUTERISED DISCHARGE ANALYSER CDA3 [V3.TP-Nov95]

Main menu:  Parameter setup.
            Voltmeter. --------------------------> Select
            Capture and analyse new data.          Calibrate
            Replay old records on disk.            Deselect
            Examine individual PD.                 Phase shift
            Exit.                                  Power frequency
                                                   Exit

Test voltage monitored through voltmeter
Last voltage reading = 10kVrms
Phase shift is 0 deg.
Power frequency = 50Hz
```

Figure B.10: Screen display of the sub-menu 'Voltmeter'.

The sinusoidal voltmeter signal is fed into the CDA3 system through the BNC2 socket and from which the hardware generates the phase reference relative to the zero crossing of the test supply. Also the rms value of this signal is digitised and recorded every second. This menu allows the user to control the way these parameters are utilised in the analysis to take into account the effect of different test frequency, phase shift and divider configuration. The screen display is shown in Figure B.10. The available options are: *Select*, *Calibrate*, *Deselect*, *Phase Shift*, *Power Frequency* and *Exit*. The *Exit*

function returns the programme to the main menu. The other functions are described below:

B.3.2.1 Select

The user selects this mode in order to define that the rms value of the test voltage can be obtained directly from the measured value of the voltmeter input signal. The other mode is *'Deselect'* (see below) where the test voltage value is manually entered by the user. In addition, this function will immediately initiate continuous voltage measurement with the result constantly updated and displayed at the bottom of the screen. The system is now simply running as a digital voltmeter until interrupted by the user pressing a key. Note that since the input signal to the voltmeter of the Robinson detector has been diverted to the CDA3, this option can be used in its place to monitor the voltage whenever the user adjusts the HV supply.

B.3.2.2 Calibrate

This option is only applicable when the voltmeter is in the *'Select'* mode, i.e. the value of the test voltage is derived directly from the voltmeter input signal. Normally, this input is connected to the HV supply via the 33MΩ Robinson voltmeter resistor. However, different resistors or other arrangements can also be used as long as the signal that goes into the BNC2 input is linearly proportional to the HV supply. This function enables the user to calibrate the voltage reading so that the correct scaling factor can be established. The following message is displayed:

' Use default calibration setting (y/n) ? '

If the reply is 'y' then no calibration is performed. The CDA3 software will simply apply the default voltage scaling factor that correponds to the use of the standard 33MΩ resistor. Note that internally, the BNC2 input is tied to ground via a 3.3kΩ resistor and thus forms a 10000:1 voltage divider.

If the reply is 'n' then calibration will begin. The system measures the voltmeter input signal and multiplies the reading with the existing voltage scaling factor. The following message is displayed:

' Voltage measuring in progress. Type any key to exit.
15.8kV '

Note that if the input voltage is too small or not present, a warning message of *'no volt'* is displayed instead. The system continues to measure and update the voltage display every second until interrupted by the user pressing a key:

'Measured voltage is 15.8kV. Enter correct voltage value (kV) = '

Based on the measured value and the correct value entered by the user, the software can determine the appropriate voltage scaling factor. This factor will then be applied to all subsequent voltage readings.

B.3.2.3 Deselect

This is the opposite of the *'Select'* mode. When activated, the voltmeter input signal will be used for phase reference only. Although the system still records its magnitude, this will be disregarded by the software in the analysis. Instead, the test voltage will be taken as the value typed in by the user in response to the following prompt:

'Preset voltage value (kVrms) = '

The entered value, e.g. 19.5, will be recorded with the test data and assumed constant during the test. The screen will show a warning message together with another message to confirm the entry:

'Warning: voltmeter reading ignored !!! '
'Voltage value is preset at 19.5kVrms '

This manual mode of voltage setting is applicable when there is no available divider for connection to the CDA3. An example is during on-line site testings where the operating voltage of the test object is already fixed and known.

B.3.2.4 Phase shift

When the voltmeter input signal is not in phase with the actual HV supply, this function can be used to rectify the problem. The user enters a phase shift value in response to the message:

'Phase shift (degrees in integer [0,359]) = '

Only integers between 0 and 359 are accepted. Other types of entries are invalid and ignored by the programme. The default phase shift is zero. A valid entry, e.g. 60, will be confirmed by the following message on the screen:

'Phase shift is 60 deg. '

Note that PD data is always recorded in the data file with the original phase positions. When analysing the data, the recorded phase position of each PD pulse will be shifted in software, i.e.

Calculated phase position = Recorded phase position + *Phase shift*

For a pure resitive voltage divider, there is no phase shift. This is not the case with a capacitive divider since the capacitor in the LV section of the divider *(C)* is now in parallel with the 3.3kΩ input resistor *(R)* of the CDA3. The approximate value of this phase shift (ϕ) can be determined analytically based on the fact that *C* is much larger than the HV capacitance of the divider:

$$\phi \cong \tan^{-1}(1/2\pi fRC)$$

where f is the power frequency. Thus at 50Hz, *C* should be larger than ~55μF in order to limit the phase shift to within 1°. Another configuration with a known phase shift is when the reference is picked up from the mains supply through a step-down transformer (0° if from the same phase, else 120° or 240° in a three-phase system).

Alternatively, a simple calibration method to determine the phase shift empirically is by connecting a piece of wire to the HV. This will generate corona discharges at the protruding end of the wire which, at inception level, occur at 270°. The user then runs the *'Examine individual PD'* function which tabulates the raw discharge data. From the measured value of the phase angle, the phase shift correction factor can be determined.

B.3.2.5 Power Frequency

The default setting for the supply frequency is 50Hz. This can vary, e.g. transformer testing at elevated frequencies. Also in some countries, the standard supply is 60Hz. After activating this function, the user enters the correct value in response to the message:

'Power frequency (Hz) = '

Valid entries should be those within the locking range of the CDA3 phase-locked loop, i.e. from 20Hz to 500Hz.

Independent from the power frequency, the width of each phase window is fixed at 10μs (by hardware). The phase position is recorded as the phase window number relative to the beginning of the half-cycle together with the half-cycle polarity. The CDA3 programme relies on the Power Frequency setting to convert this number into the actual phase angle. For example, window number 100 is 1ms away from the zero crossing of the half-cycle. This corresponds to the relative phase angle of 18° at 50Hz. However, the same window would correspond to 36° at 100Hz. By taken into account the half-cycle polarity, the software can then obtain the actual phase angle over the full cycle, i.e. add 180° if the polarity is negative. The phase resolution of the system is thus inversely proportional with the test frequency.

B.3.3 Capture and analyse new data

COMPUTERISED DISCHARGE ANALYSER CDA3 [V3.TP-Nov95]

Main menu:	Parameter setup.	
	Voltmeter.	
	Capture and analyse new data. ————>	Phase resolved plot
	Replay old records on disk.	IEC quantities plot
	Examine individual PD.	Scatter plot
	Exit.	Exit

Data saved in file Red-1

Figure B.11: Screen display of the sub-menu 'Capture and analyse new data'.

After all the relevant settings have been made using the *'Parameter setup'* and *'Voltmeter'* functions, this sub-menu can then be called to initiate new recordings. The screen display is shown in Figure B.11 which provides the user with three different selections for plotting the results: *Phase resolved plot*, *IEC quantities plot* and *Scatter plot*.

If the user has specified the data to be saved on disk (with the *'File to store results'* function in the *'Parameter setup'* menu), the screen will also show a confirmation message together with the data file name, e.g.

'Data saved in file TEST1'

Note that the internal calibrator should be turned off while this mode is active during a live test. Otherwise, it will be recorded as a real PD pulse and thus invalidate the analysis. An alternative method is to leave the internal calibrator on but the software gating facility is activated to mask out the calibrator.

B.3.3.1 <u>Phase resolved plot</u>

When this function is selected, the system begins recording for a period specified by *'Integration time'*. During this initial period, the screen goes blank as data is still being gathered. On completion, the programme immediately analyses the raw data and displays the results on the screen. The screen remains unchanged as the system starts another session of recording and analysis. When this finishes, the screen is then updated with the new results and the whole process repeats. Thus the screen display is static most of the time but is periodically refreshed as new results become available - a virtual real-time PD monitor.

Monitoring will continue indefinitely unless the user interrupts by pressing a key. The system can be temporarily paused with the 'Space bar'. When this key is pressed, the current display is locked and recording is aborted. Normal operation resumes when the 'Space bar' key is pressed again. This function is useful when changes to the test condition are necessary (e.g. measurements are to be carried out at different specific voltage levels) and the user wants to avoid making unwanted records while the changes are taking place.

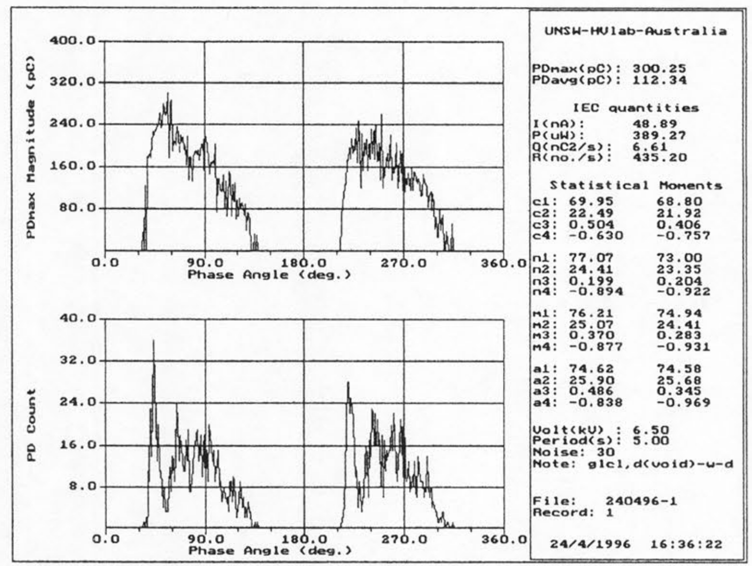

Figure B.12: Screen display of the phase-resolved plot.

If the user has finished and wishes to exit this mode of operation, press the 'x' key. A capital entry 'X' has the same effect, i.e. case insensitive. The system will return the user to the main menu. If data was saved in a file, that file would be closed. Also, the system will complete and exit recording automatically if the size of the data saved in the current file exceeds 10M bytes. This would avoid overflowing the disk space during continuous long-term recording where the system is left unattended.

A typical screen display of the results is shown in Figure B.12. The display consists of three separate boxes: two for plots and an area for presenting numerical data.

Display window 1: Plot of PDmax Magnitude (pC) versus Phase Angle (deg.)

Although the CDA3 system has a phase resolution of 0.18° (at 50Hz), the phase window used for plotting is 1°. This plot shows the maximum discharge magnitude that occurred within each of the 360 phase windows of the ac cycle. If gating is selected, the positions of the measurement phase windows are shown as horizontal bars at the top of the plot.

The software will automatically scale the vertical axis to accommodate changes in the pC values for each screen display. This feature may not be desirable when comparing the results between different screen displays during the same test. The user has the option to lock or unlock the automatic scaling facility while recording is in progress by pressing the 'L' key. When locked, the vertical scale used in the current display will be applied to the subsequent displays until the user presses the 'L' key again to unlock. The character 'L' is displayed at the bottom of the numerical data window to indicate that the vertical scale is locked.

Display window 2: Plot of PD Count versus Phase Angle (deg.)

This plot shows the total number of PD pulses that occurred within each of the 360 phase windows of the ac cycle. Similar to the above, the vertical axis is auto-scaling but can be locked to a fixed scale. There are 2 considerations to be aware of when interpreting this plot. Firstly, the pulse count is obviously dependent on the integration time so this period should be set to the same value to enable comparison between different tests. Secondly, when examining the calibrator pulses the count shown may appear to be smaller than the expected value which is 50 times the integration period (for 50Hz case). This is due to a small phase jitter in the calibrator so that not all the pulses fall within the same phase window. On the plot, it would appear spread out instead of a sharp vertical line.

Appendix B: Software Design of the CDA3 System

Display window 3: Tabulation of results

In this box, the organisation name is shown at the top. This is then followed with the numerical results of the integrated and statistical analysis. Shown after *'PDmax(pC):'* is the magnitude of the largest PD pulse detected over the integration period. If the value is large, it will be presented in the appropriate unit, e.g. nC. Similarly, *'PDavg(pC):'* corresponds to the overall average magnitude of the discharges. *'I(nA):'* denotes the average discharge current, *'P(μW):'* the discharge power, *'Q(nC2/s):'* the quadratic rate and *'R(no./s):'* the repetition rate.

The four sets of statistical moments for the four distributions are also shown on the screen in the following order: current, count, maximum discharge and average discharge versus phase. These are denoted as *'c'*, *'n'*, *'m'* and *'a'* respectively. Each set has 4 rows and consists of 2 subsets: the first column corresponds to the positive half-cycle and the second column to the negative half-cycle. Each subset contains the four statistical moments: average, deviation, skewness and kurtosis. These are denoted as *'1'*, *'2'*, *'3'* and *'4'* respectively. For example, *'n3:'* corresponds to the skewness of the count versus phase distribution. Altogether, there are 32 numbers.

The rest shows various parameters related to the test. Following *'Volt(kV):'* is the value of the applied test voltage as measured at the start of the integration period. Note that if the voltmeter is in the *'Deselect'* mode, the preset value typed in by the user is shown here instead. *'Period(s):'* shows the actual recording time in seconds. There is a small delay - caused by software - before the system can stop the recording. In the worst case, the actual value is only a fraction of a second longer than the preset value. A shorter actual value can occur if the data buffer is full which forces the system to stop recording. The preset value of the signal threshold is shown after the *'Noise:'* heading. If record identification information was specified, this will be shown after *'Note:'*. If data is to be saved in a file, the current file size (number of words) is shown on the next line. If during this integration period, the input signal exceeds the maximum allowable level, a warning message *'Signal Overload !!!'* is displayed. The last line shows the date and time when the record was made.

If the file is played back at a later time in this format, the screen display is identical except that the current file size is now replaced with two lines: *'File:'* which lists the file name and *'Record:'* which lists the record number of the current display.

B.3.3.2 IEC quantity plots

When this mode is selected, the programme captures the data and calculates the integrated quantities only. One set of these quantities is obtained after each integration period. It then plots these quantities as the test progresses so that one can see on the screen how the quantities vary with time. It also tabulates the current, maximum and minimum values for each of these quantities.

If the results are to be saved in a file, only the integrated quantities are stored and the raw data is discarded. This would use less disk space and thus enables recording over a much longer period of time. The trade-off is that when the file is recalled later, it can only be displayed in this format.

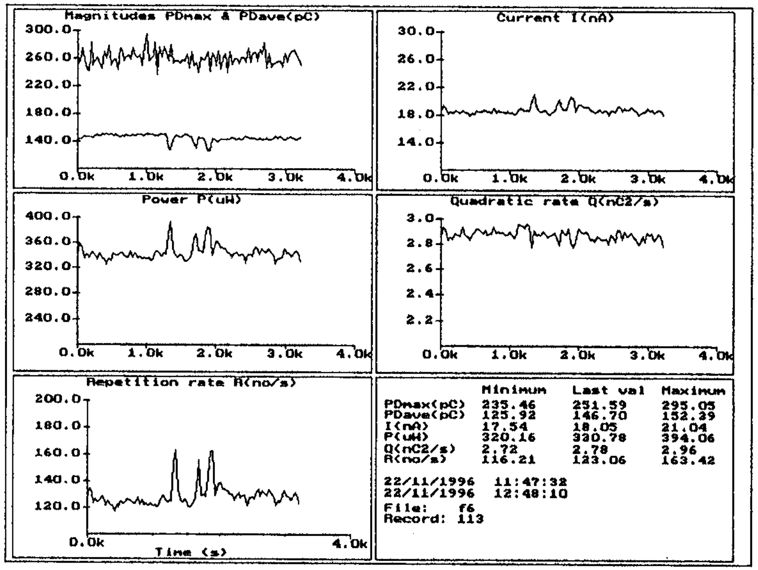

Figure B.13: Screen display of the IEC quantities plot.

A typical screen display of the IEC quantities plot is shown in Figure B.13. The display consists of six distinct windows: five for plots using the same time scale (in seconds) and an area for presenting numerical data.

<u>Display window 1</u>: The upper trace is the maximum discharge PDmax (pC) and the lower trace is the average discharge PDave (pC). Each data point corresponds to one

integration period. If there are more than 100 data points then only the most recent 100 data points are shown on the display.

<u>Display window 2</u>: Plot of the discharge current (nA) versus time.

<u>Display window 3</u>: Plot of the discharge power (μW) versus time.

<u>Display window 4</u>: Plot of the quadratic rate (nC^2/s) versus time.

<u>Display window 5</u>: Plot of the discharge repetition rate (no./s) versus time.

<u>Display window 6</u>: The ranges of variation of the above quantities are tabulated in this window. For each parameter, its minimum, maximum and the current value are shown. Also shown are the date/time when the test began, the date/time when the current record was made.

If the file is played back at a later time in this format, the screen display is identical except that there are two new lines in the last window: *'File:'* which lists the file name and *'Record:'* which lists the current record number.

B.3.3.3 <u>Scatter plot</u>

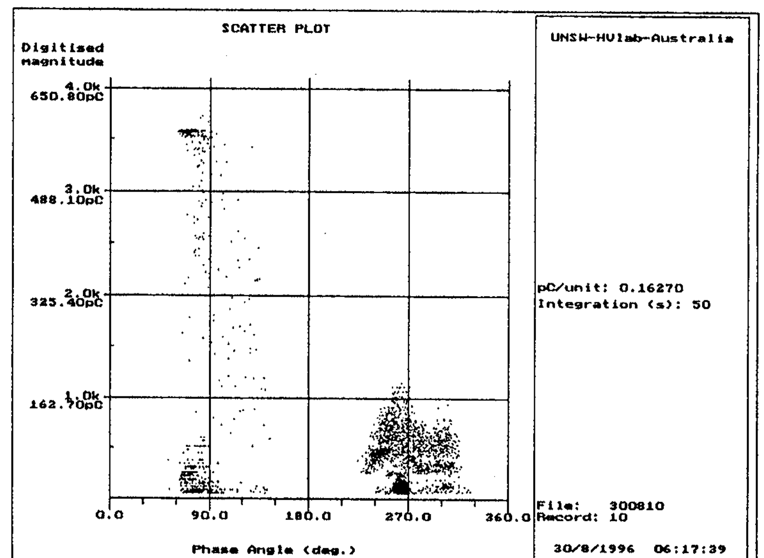

Figure B.14: Screen display of the scatter plot.

When this mode is selected, the programme captures the data and plots the discharge magnitude against the phase position in scatter mode. A typical screen display is shown in Figure B.14. Each individual PD pulse is represented as a single dot on the plot. The scale of the vertical axis is fixed which corresponds to the full range of the 12-bit A/D converter (4095 digitised units). The equivalent pC values are also shown for the 1k, 2k, 3k and 4k markers.

Unless interrupted by the user, the programme will start another integration period and update the scatter plot, i.e. the new dots are added to the existing screen (hence the reason for using fixed scale vertical axis). Thus such a plot provides a cumulative display of all the discharges since the start of the test. The running total of the integration times is also shown on the screen.

B.3.4 Replay old records on disk

```
            COMPUTERISED DISCHARGE ANALYSER CDA3 [V3.TP-Nov95]

Main menu:  Parameter setup.
            Voltmeter.
            Capture and analyse new data.
            Replay old records on disk. ------------> Directory listing
            Examine individual PD.                    Call up a file
            Exit.                                     Edit a file
                                                      Exit
```

Figure B.15: Screen display of the sub-menu 'Replay old records on disk'.

This option can be used to display or process data which was previously recorded on disk. Its sub-menu is shown in Figure B.15 and the available functions are *Directory listing*, *Call up a file*, *Edit a file* and *Exit*.

B.3.4.1 <u>Directory listing</u>

This function enables the user to list the names of the data files. It provides a convenient means of searching for a record without having to exit the program. When selected, the following prompt is displayed:

'Enter file specification: '

If the user simply keys in Return, all the files in the current directory with extension '.DAT' will be listed. Otherwise, the specification should follow the same rules as for the equivalent DOS command 'DIR'.

B.3.4.2 <u>Call up a file</u>

This function enables the user to retrieve previously recorded data from a file for viewing on the display and also for getting its hardcopy if desired. The user is asked to specify the file name:

'Data filename (no extension): '

Its full path must be specified if it is in a different directory. The extension '.DAT' is tagged to the entry by the programme and a file search is carried out. If not found, an error message is displayed:

'File does not exist. Press any key to continue. '

The programme then beeps and returns to the start of this sub-menu. Otherwise, it opens the file, displays the total number of records found in that file (e.g. 20) and requests the user to specify the first record for viewing:

'Total number of records = 20
Select starting record number = '

A valid entry must be an integer not exceeding the total record number. To view all records, enter '1'. If the file contains only the IEC integrated parameters, the results are displayed as an IEC quantity plot (Figure B.13). If the file contains the raw data, the user is asked to specify which of the 3 formats for displaying the results:

'Analysis type (1:phase plot, 2:scatter plot, 3:individual PDs) = '

The *'phase plot'* and the *'scatter plot'* use the same presentation as described earlier and shown in Figures B.12 and B.14. The screen display for *'individual PDs'* is shown in Figure B.16. The basic parameters associated with each PD pulse are tabulated in 5 columns: the ac cycle number, the phase angle of occurrence, the discharge polarity, its magnitude and energy. Up to 40 PD pulses can be listed in each screen.

The program then waits until the user presses a key. If the entry is 'p', the screen will be dumped to the currently active hardcopy device (printer or plotter). An exception is the tabulation of the basic discharge parameters which can be printed only. If the key entry is 'x', it will close the data file and return to the main menu. If any other key is pressed (e.g. space), it will display the next record and the same procedure is repeated until the end of the data file is reached.

BASIC DISCHARGE QUANTITIES

Cycle	Degree	Sign	Magnitude	Energy
0	19	-	231.481pC	1.172uJ
0	60	-	215.699pC	2.906uJ
0	218	+	221.617pC	2.123uJ
1	49	-	227.865pC	2.675uJ
1	220	+	220.960pC	2.209uJ
2	46	-	231.810pC	2.594uJ
2	222	+	217.343pC	2.262uJ
3	46	-	230.495pC	2.579uJ
3	226	+	209.780pC	2.348uJ
4	45	-	251.210pC	2.763uJ
4	228	+	243.647pC	2.817uJ
5	40	-	230.824pC	2.308uJ
5	112	-	198.601pC	2.865uJ
5	198	+	205.506pC	987.901nJ
5	242	+	219.316pC	3.012uJ
6	31	-	232.797pC	1.865uJ
6	87	-	273.240pC	4.245uJ
6	198	+	206.492pC	992.643nJ
6	241	+	238.058pC	3.239uJ
7	31	-	229.509pC	1.839uJ
7	79	-	221.288pC	3.379uJ
7	202	+	205.177pC	1.196uJ
7	249	+	215.699pC	3.133uJ
8	26	-	223.919pC	1.527uJ
8	70	-	214.383pC	3.134uJ
8	213	+	236.085pC	2.000uJ
8	266	+	138.757pC	2.153uJ
9	30	-	212.739pC	1.655uJ
9	76	-	233.783pC	3.529uJ
9	204	+	200.245pC	1.267uJ
9	251	+	227.865pC	3.352uJ
10	28	-	231.810pC	1.693uJ
10	72	-	203.204pC	3.006uJ
10	208	+	216.027pC	1.578uJ
10	259	+	225.563pC	3.444uJ
11	22	-	223.590pC	1.303uJ
11	65	-	239.373pC	3.375uJ
11	210	+	206.492pC	1.606uJ
11	263	+	227.207pC	3.508uJ
12	19	-	225.563pC	1.142uJ
12	61	-	227.865pC	3.100uJ

UNSW-HVlab-Australia

File: f17
Record: 1

19/11/1996 10:23:55

Figure B.16: Screen display of individual PDs.

B.3.4.3 Edit a file

A data file may contain many records. Usually, they correspond to the same test conditions but captured at different times. If the PD pattern does not vary greatly, sometimes it is desirable to edit out some of the redundant records to conserve disk space. This can be done with this option. Only raw data files which correspond to the *'phase resolved plot'* or *'scatter plot'* capture mode can be edited (the *'IEC quantities plot'* does not save raw data). The user is required to specify the original data file name in response to the following prompt:

' Source file (no extension): '

and the new file name in response to the following prompt:

' New filename (no extension): '

The new file name must be different from the original file name. The programme then searches for the original file. If not found, it displays an error message, beeps and returns to the start of this sub-menu. If found, it opens that file and determines the total number of records stored in that file. It then asks the user to enter the starting record number to be replayed. The results of the first selected record will be displayed on the screen in the *'phase resolved plot'* format. If this record is to be copied into the new file, the user presses 'c' (for copy). Otherwise, press Return. The next record will be displayed and the same procedure can be repeated until the final record is processed. However, the user can exit immediately without viewing the remaining records by pressing 'x'. Note that the original data file is intact after using this function. To delete it, use the appropriate DOS command.

B.3.5 Examine individual PD

With this option, the system will capture PDs for a fixed period and display the raw results. This enables the user to preview the discharge activity within each individual cycle and acquire information for use in the *'Parameter setup'* menu. Note that the data recorded with this function will not be saved to disk. For normal recording, the user should use the *'Capture and analyse new data'* option. The sub-menu for this selection is shown in Figure B.17 and it consists of *Tabular display*, *Mixed display* and *Exit*.

COMPUTERISED DISCHARGE ANALYSER CDA3 [V3.TP-Nov95]

Main menu: Parameter setup.
Voltmeter.
Capture and analyse new data.
Replay old records on disk.
Examine individual PD. ——————> Tabular display
Exit. Mixed display
Exit

Figure B.17: Screen display of the 'Examine individual PD' sub-menu.

B.3.5.1 Tabular display

When this selection is made, the CDA3 will start recording for a fixed period of 10 seconds. At the end of this period, the recorded data will be displayed sequentially, cycle by cycle. Each screen summarises the results from 5 consecutive cycles whereby the discharge parameters for each individual PD pulse are shown in tabular format: its phase position (in degree), polarity and digitised magnitude. The digitised magnitude is the raw output of the A/D converter. It must be multiplied with the pC/unit value to convert into pC.

To exit without viewing the remaining of the data, type 'x'. Else, any other key entry will display results of the next 5 cycles and so on until it reaches the end of the record.

B.3.5.2 Mixed display

When this selection is made, the CDA3 will start recording for a fixed period of 10 seconds. At the end of this period, the recorded data will be displayed sequentially. Each screen summarises the results from 2 consecutive cycles using both graphical and tabular formats, the latter is the same as described in B.3.5.1 above. The graphical format shows the amplitude-vs-phase scatter diagram whereby the PD pulses are plotted as crosses in two different colours (to distinguish the two cycles). To exit without viewing the remaining of the data, type 'x'. Else, any other key entry will display results of the next 2 cycles and so on until it reaches the end.

This option is particularly useful when the automatic calibration facility fails, i.e. the system is not able to capture the internal calibrator or it captures the wrong ones. Such a failure is not uncommon and can be caused by stationary interference (e.g. thyristor noise) or if there are so many discharges. By using this option, the user can visually inspect the pulses from 2 cycles to identify the internal calibrator. To qualify as the internal calibrator, the first requirement is that the pulse must occur at the same phase position and with the same amplitude in both cycles, i.e. the user should look for two superimposed crosses of different colours on the scatter plot. Where applicable (e.g. for Model 5 detectors), an additional constraint is the presence of another pair at exactly 180° away. If the user is able to identify the internal calibrator from the plot, its digitised magnitude can be extracted from the accompanied tabular results. This information together with the dB setting of the internal calibrator will enable the user to go back to the Parameter Setup menu and apply Manual Calibration.

B.4 A typical measurement procedure using the CDA3 system

This section describes a typical procedure to carry out PD measurements using the CDA3 analyser together with the Robinson discharge detector.

1. Calibrate the Robinson detector with the external calibrator.

2. Enter 'Parameter setup' option.
3. Select 'Detector calibration' and enter values obtained from Step 1.
4. Turn on the internal calibrator and perform 'Analyser calibration'. The internal calibrator must be switched off after this step.
5. Enter 'Voltmeter' option and choose 'Select' to display the voltage reading. Turn on the HV supply and raise it to the desired level.
6. Enter Option 3 and choose 'Phase-resolved plot'. Measurement results are updated on the screen automatically at the end of each integration period. To freeze the display, type 'space'. To return to the main menu, type 'x'.

B.5 Formats of data files

This section describes how PD data is stored in the files. This information can be used for developing new programmes to analyse the recorded data in a different way than those provided by the existing CDA3 software. In addition, it can be used to convert the recorded data into a different format for importing to other application softwares such as Microsoft Excel, MatLab, etc.

There are two types of data files which can be distinguished from the extension of the filename. The ASCII data file has extension '.DAT' and the raw binary data file has extension '.RAW'.

B.5.1 Format of the ASCII data file (extension '.DAT')

This file is ASCII readable, i.e. a text file which can be listed with DOS command *'type'*. The first 4 lines are defined as follows:

Line 1: type of data file (1 or 2)
Line 2: note for identification (a string up to 20 characters)
Line 3: three numbers separated by a space:
- 'pCpu': the equivalent pC value for each AD unit
- 'kvpu': the equivalent kV value for each AD unit
- 'kvf': if this is non-zero then it is the value of the applied voltage, i.e. voltmeter input reading is ignored.

Line 4: two numbers separated by a space:
- 'shift': the phase shift of the applied test voltage (in degrees)
- 'freq': the frequency of the test voltage (in Hz)

If the file type is 1 then the remaining of the file will contain an integral number of blocks of 3 lines, each block corresponds to one buffer record data in the '.RAW' file. The format for each block of these 3 lines is:

Line 1: [year] [month] [day]
Line 2: [hour] [minute] [second] [hundredth of a second]
Line 3: [integration duration in seconds] [number of words stored]

If the file type is 2 then the remaining of the file will contain an integral number of blocks of 4 lines, each block corresponds to integrated results from one buffer record:

Line 1: [integration duration in seconds]
Line 2: [year] [month] [day]
Line 3: [hour] [minute] [second] [hundredth of a second]
Line 4: seven numbers separated by a space. They are:
Maximum discharge magnitude (in pC)
Average discharge magnitude (in pC)
Discharge current (pA)
Discharge power (pW)
Quadratic rate (pC^2/s)
Repetition rate (number per second)
Actual integration time (second)

B.5.2 Format of the raw data file (extension '.RAW'):

If the file type of a '.DAT' file is 1 then there is another data file associated with it. This file has the same name but with extension '.RAW'. Here, the raw discharge data is saved in binary format. There are two types of data in the '.RAW' file: voltage and PD. Each voltage data requires one word (2 bytes) and each PD data requires two words in sucession (4 bytes). A voltage word is identified by its most significant bit (MSB) set to one. A PD word is identified by its MSB set to zero. The other bits are defined as follows:

Voltage word:	Bit 15:	set to one
	Bits 12-14:	not used
	Bits 0-11:	digitised magnitude of test voltage
PD first word:	Bit 15:	set to zero
	Bits 0-9:	phase position of PD pulse (0 to 999 maximum)
	Bit 10:	half-cycle polarity (1 for positive half-cycle)
	Bits 11-14:	four low bits of relative cycle count

PD second word:	Bit 15:	set to zero
	Bits 0-11:	digitised magnitude of PD pulse
	Bit 12:	PD polarity (1 for positive discharge)
	Bits 13-14:	two high bits of relative cycle count

For dual channel operation, each PD data has 3 consecutive words: the first two words are associated with channel 1 as described above and the last word is associated with channel 2. Note that both channel share the same phase position:

PD third word:	Bit 15:	set to zero
	Bits 0-11:	digitised magnitude of PD pulse (of channel 2)
	Bit 12:	PD polarity (of channel 2)
	Bits 13-14:	not used

For 50Hz testing, the relative cycle count is a 6-bit binary number which increments from 0 to 49 then back to zero, i.e. there are 50 ac cycles in each second. The lower four bits are bits 14-11 of the first PD word. The higher two bits are bits 14-13 of the second PD word. The absolute cycle number is defined as the cycle number with reference to the beginning of the recording. It can be determined from the following formula:

Absolute cycle number = (number of voltage words x50) + relative cycle number

B.5.3 Conversion of raw binary data into ASCII format:

The CDA3.EXE programme does provide a facility to read the raw binary data file and generate a new file which contains the basic discharge parameters in ASCII format. From the *'Replay old records on disk'* menu, the user selects the *'Call up a file'* function and then specifies the file name. After the *'Analysis type'* prompt, key in '99'. The programme will carry out the conversion for all the records up to the record number specified by the user. The results are saved in a file called 'TEMP.DAT'. The parameters for each PD pulse are listed in one line and separated by a space: the absolute cycle number, its phase position (in degrees) and magnitude (in pC).

B.6 DC recording and analysis programme: 'DC.EXE'

Although the CDA3 system is intended mainly for ac testing, it can also be used for PD measurements under dc conditions. The recorded data format remains the same but the phase resolved analysis is no longer relevant. A modified version of the CDA3.EXE programme was written by the author to provide a simple pulse height analysis, i.e.

pulse count (or pulse rate) versus pulse magnitude. This was utilised in a recent study on PDs in SF_6 [5].

The hardware setup is identical. There are no modifications to the CDA3 board. The system still requires a 50Hz reference at the voltmeter input for timing purpose. The value of the dc test voltage is keyed in by the user.

The software requirement consists of the main programme DC.EXE and the on-line manual text file README. These can be installed in the same CDA3 directory. If a separate directory is used, then it also needs the files SETUP.EXE, PARA.DAT and EGAVGA.BGI which can be copied from the CDA3 directory.

```
COMPUTERISED DISCHARGE ANALYSER CDA3 [DC-Oct94]

Main menu:    Parameter setup.
              Set voltage and pulse range.
              Capture and analyse new data.
              Replay old records on disk.
              Miscellaneous functions.
              Exit.
```

Figure B.18: Screen display of the main menu of the DC.EXE programme.

The screen display of the main menu is shown in Figure B.18. There are 6 selections available. The screen presentation and keyboard input handling follow the same format as used in the CDA3.EXE programme.

B.6.1 Parameter setup

Apart from the omission of the *'Measurement phase windows'* function, this menu is identical to that described in Section B.3.1.

B.6.2 Set voltage and pulse range

Set test voltage

This function is used to specify the DC test voltage (in kV unit). When selected, the following message is prompted:

' Enter DC voltage value (kV) = '

Set number of pulse ranges

The range of discharge magnitude is divided into smaller windows. This function is used to specify the total number of pulse ranges. When selected, the following message is prompted:

' Enter total number of allowable pulse ranges = '

A valid entry is an integer between 1 and 10.

Set limits for a pulse range

This function is used to define the minimum and maximum pulse magnitudes for a specified range number. When selected, the screen will prompt:

' Enter range number (1-10) or 0 for linear range division = '
' Enter minimum and maximum pC values = '

Note that if the entered range number is 0 then the magnitude interval defined by the minimum and maximum pC values is divided equally into smaller windows. For example, if the total number of ranges is 10 and the pC values entered are 0 and 400pC then range 1 is from 0 to 40pC, range 2 is from 40 to 80pC, ... , range 10 is from 360 to 400pC. If linear range division is not used then this function must be called again to define the window for the next range number until all the ranges are specified.

Toggle pulse rate (min/sec)

This function is used to select the preferred mode of displaying the pulse rate. Its unit can be either in number of pulses per second (pps) or number of pulses per minute (ppm). To toggle the display mode, select this function so that it is highlighted then press the ENTER key.

Set pulse rate limit

This function is used to set the pulse rate limit for a specified range. When selected, the screen will prompt:

' Enter range number and rate = '

If the range number entered is 0 then the rate entered is applicable to all the ranges. The currently selected pulse rate unit (either pps or ppm) is assumed. When capturing data in the 'Plot current count and rate' mode, the specified maximum permitted levels will be displayed together with the actual values for comparison. This facility is useful in factory proving tests as it enables the operator to compare the measured values against the limits.

Toggle display (rate/count)

This function can be used to select the preferred mode of displaying the results. The data can be tabulated or plotted as either the pulse counts or their equivalent pulse rates against time. To switch the display mode, select this function so that it is highlighted then press the ENTER key.

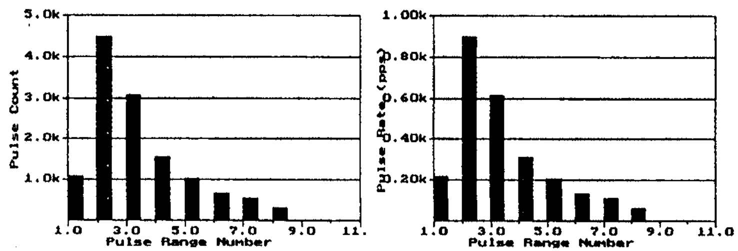

UNSW-HVlab-Australia

Range	pCmin	pCmax	Count	Rate pps	Rate max	Rate limit
1:	0	125	1091	218.20	218.20	
2:	125	250	4501	900.20	900.20	
3:	250	375	3074	614.80	614.80	
4:	375	500	1568	313.60	313.60	
5:	500	625	1036	207.20	207.20	
6:	625	750	684	136.80	136.80	
7:	750	875	572	114.40	114.40	
8:	875	1000	309	61.80	61.80	

Volt(kV) : 5.00
Period(s): 5.00
Noise: 30
Note:

File: test
Record: 1

13/3/1997 10:44:36

Figure B.19: Screen display of 'Plot current count and rate'.

B.6.3 Capture and analyse new data

This menu is used to start the recording. After each record is complete, the data is analysed and the results are shown on the screen. There are 3 different modes of displaying the results:

Plot current count and rate

The screen shows the current record only. A typical example is shown in Figure B.19. Both the plots of the pulse count versus range number and pulse rate versus range number are displayed. Also shown is a table of information associated with each range number: the minimum pC, maximum pC, current pulse count, pulse rate, the maximum pulse rate detected as from the start of the test and the pulse rate limit.

UNSW-HVlab-Australia Tabulate Pulse Rate (pps)

Time \ Range:	1	2	3	4	5	6	7	8
10:44:36	218	900	615	314	207	137	114	62
10:44:45	242	986	554	301	215	137	108	62
10:44:54	225	1040	547	305	217	138	108	63
10:45:03	214	995	565	305	229	128	113	63
10:45:12	200	929	591	306	245	128	98	69
10:45:21	184	883	599	315	262	121	101	67
10:45:30	204	865	554	299	272	142	96	65
10:45:39	195	880	540	298	276	128	100	66
10:45:48	194	876	524	305	274	130	100	67
10:45:57	200	832	542	307	284	130	102	71
10:46:06	202	809	549	283	279	153	94	70
10:46:15	192	725	584	295	260	148	98	62
10:46:24	192	756	572	329	271	138	95	61
10:46:33	189	775	580	316	271	129	92	60
10:46:42	191	723	564	345	252	139	89	61
10:46:51	194	803	536	317	226	141	88	58
10:47:00	199	817	525	311	218	135	82	56
10:47:09	187	807	535	336	238	132	84	52
10:47:18	206	787	492	316	245	145	87	54
10:47:27	209	836	512	318	239	151	85	58

Volt(kV) : 5.00
Period(s): 5.00
Noise: 30
Note:

File: test
Record: 20

13/3/1997 10:47:27

Figure B.20: Screen display of 'Tabulate count/rate against time'.

Tabulate count/rate against time

The pulse count or pulse rate for each pulse range is tabulated against time. A typical screen display is shown in Figure B.20. Only the results from the most recent 20 records are listed. The time shown for each record is the actual time when the record was made. The key entry 'r' can be used to toggle the display between count and rate. To exit recording and return to the main menu, press 'x'. Otherwise, any other key entry will cause the programme to toggle between pause and resume recording.

Plot count/rate against time

The pulse count or pulse rate for each pulse range is plotted against time as a bar chart. A typical screen display is shown in Figure B.21, the format varies slightly depending on the number of graphs. Only the most recent 20 records are plotted. The time unit is second and its value is relative to the beginning of the test. Various key entries as described above can be used for control.

B.6.4 Replay old records on disk

This menu is used to recall data files previously recorded for viewing or printing. The selections available are: *Plot current count and rate*, *Tabulate count/rate against time*, *Plot count/rate against time* and *Exit*. The display formats are identical to that described above.

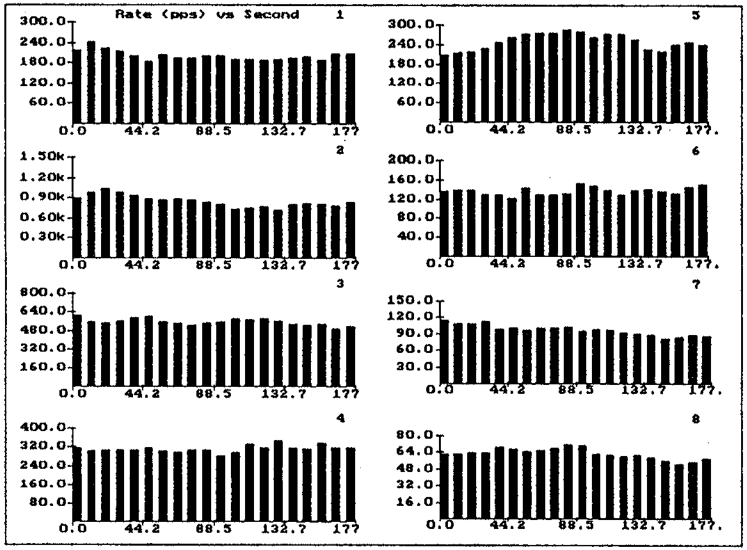

Figure B.21: Screen display of 'Plot count/rate against time'.

B.6.5 Miscellaneous functions

The selections available are: *Directory*, *Manual* and *Exit*. The *Directory* function is identical to that in the CDA3 programme. The *Manual* function provides an on-line facility to display the text file README on the screen. When this function is selected, the PAGE-UP or PAGE-DOWN key can be used to scan through the manual. To exit, press any other key.

B.6.6 Format of data file

The data file is ASCII readable with extension '.DAT'. The format is as follows:

Line 1: 2 (a fixed code)
Line 2: note for identification (a string up to 20 characters)
Line 3: [applied voltage (kV)] [number of pulse ranges 'npr']
Each of the next 'npr' lines has 3 numbers separated by a space:
minimum pC value of the pulse range
maximum pC value of the pulse range
pulse rate limit (in pps unit)

The remaining of the file will contain an integral number of blocks of 4 lines, each block corresponds to integrated results from one buffer record:

Line 1: [integration duration in seconds]
Line 2: [year] [month] [day]
Line 3: [hour] [minute] [second] [hundredth of a second]
Line 4: [range 1 pulse count] [range 2 pulse count] ... [range 'npr' pulse count]

B.7 References

[1] Turbo Pascal Version 5.0, Borland International Inc., 1988.

[2] Quinn-Curtis Science and Engineering Tools for Turbo Pascal 4.0/5.0, Product code IPC-TP-016 Version 6.1.

[3] E.R. Rought and T.D. Hoops, *Turbo Pascal 4.0 Developer's Library*, Howard W. Sams & Company, 1988.

[4] S.D. Palmer, *Mastering Turbo Pascal 6*, Sybex Inc., 1991.

[5] F.S. Abouzakhar and T.R. Blackburn, "Implementations of Computer-Based Data Acquisition (CDA3) to Partial Discharges in SF_6 Stressed by DCHV", Proc. AUPEC'96, Univ. of Melbourne, Australia, pp.365-370, October 2-6, 1996.

Appendix C

Polarisation and Depolarisation Current Test Report #1
Steel Tank Cell

TEST REPORT #1

Polarisation Depolarisation Current Analysis

Test Object:	Steel cell with oil-impregnated paper set-up
Manufacturer:	
Serial number:	
Mfr. Year:	
Rated kVA:	
HV rating (V):	
LV rating (V):	
Test Instrument:	PDC-ANALYSER-1MOD (# PDC010620)
Manufacturer:	ALFF Engineering
Test Temperature:	80°C
Test Date:	30th April 2003
Location:	Electrical Engineering / University of New South Wales
Test Connection:	Connect the V-probe of PDC Analyser to HV electrode Connect the I-probe of PDC Analyser to LV terminals connected together. The steel cell is directly earthed.
Test Voltage:	500V
Test Duration:	3,000 s of Polarisation and 300 s of Depolarisation.
Condition:	Remaining current before polarisation started: -2 pA.
Insulation analysed:	Between the electrodes of the set-up.

STEEL CELL

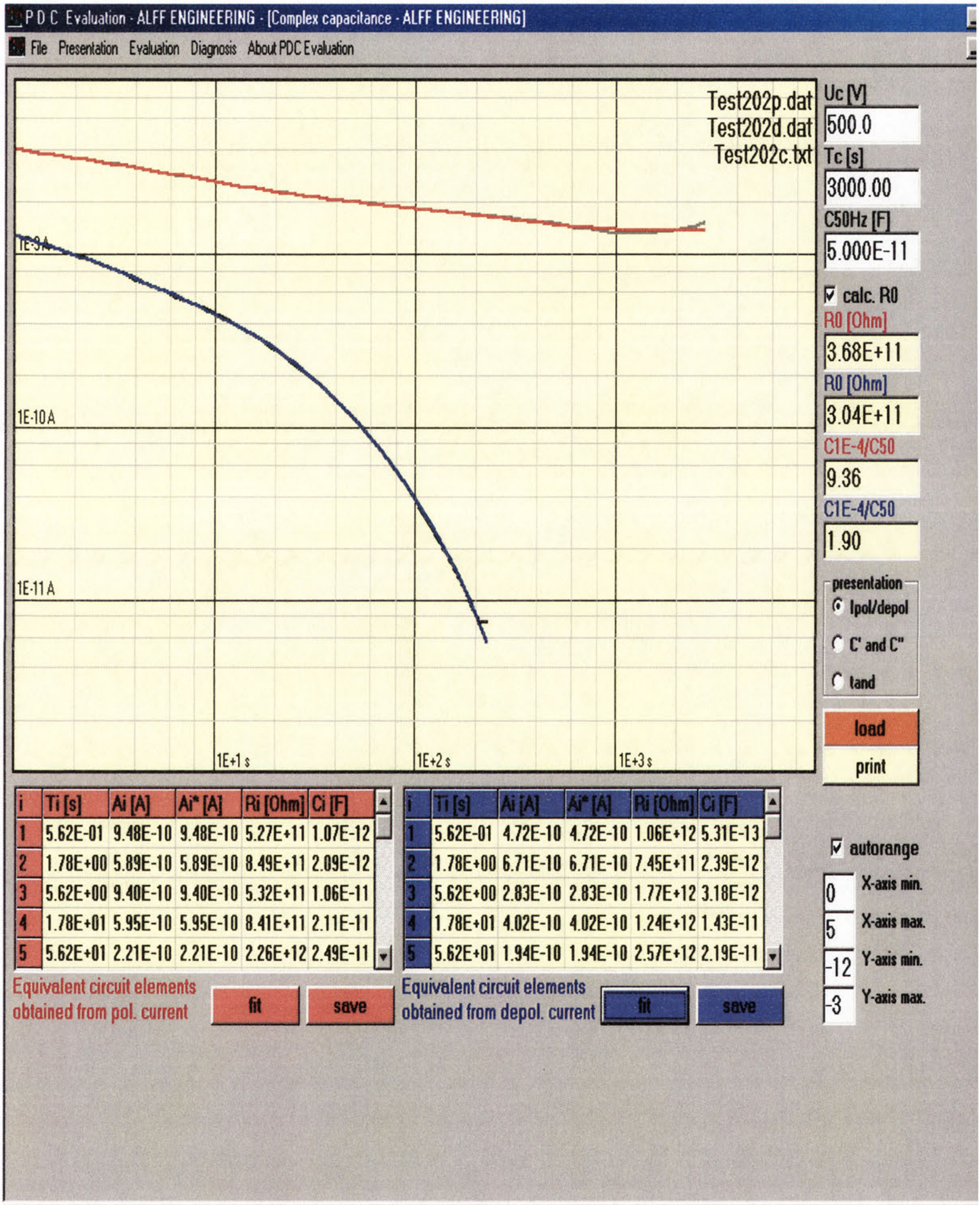

Figure C. 1: The Measured Polarisation Depolarisation Currents

STEEL CELL

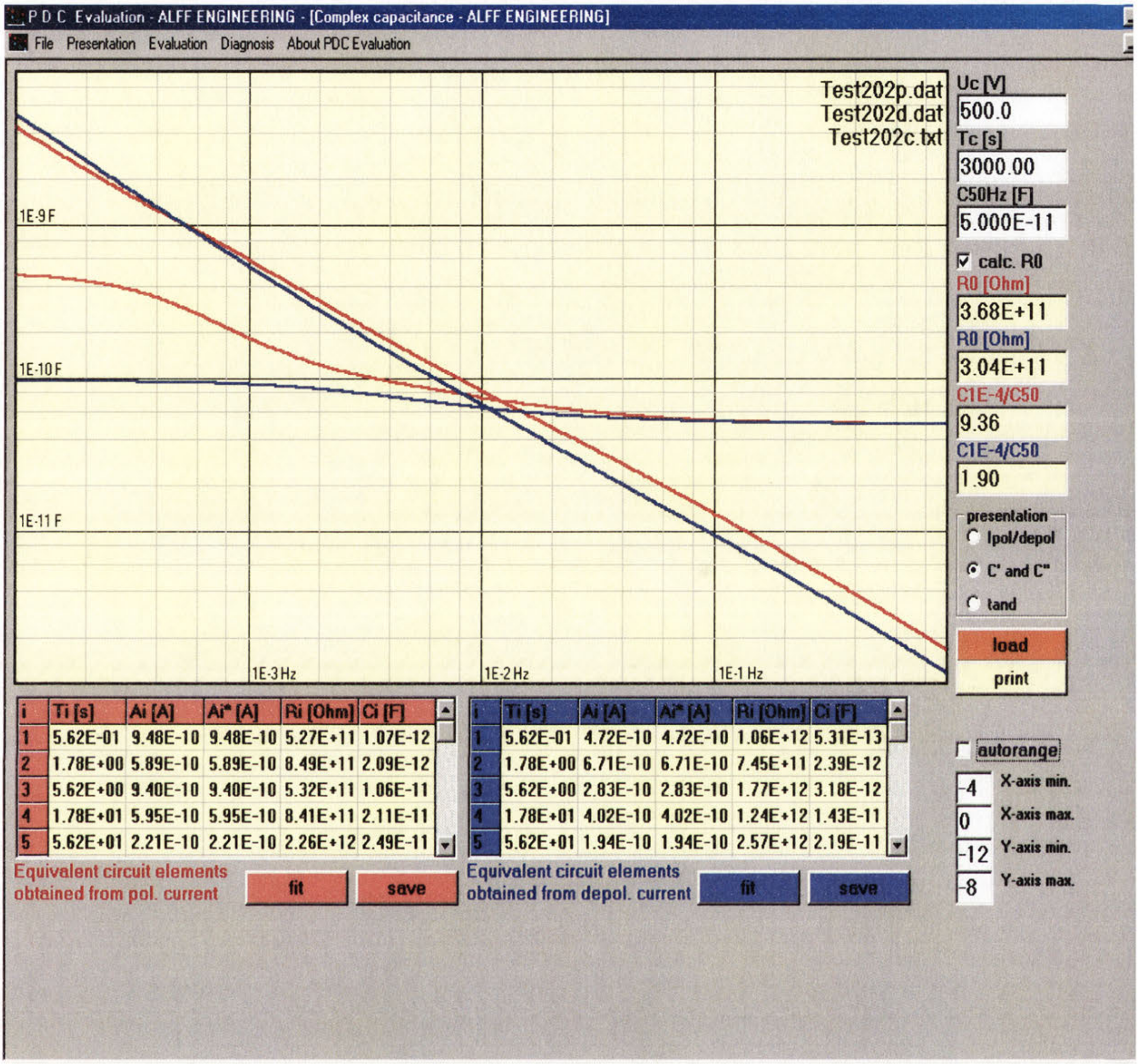

Figure C.2: The Evaluation of Complex Capacitance at the Measured Temperature of 80°C. (Please consider only from 10^{-3} Hz to 1 Hz for polarisation and 10^{-2} Hz to 1 Hz for depolarisation due to the actual measured time frame.)

The capacitance at 50 Hz is 50 pF.

	Polarisation	Depolarisation
C at 10^{-3} Hz (pF)	182.01	-
C at 10^{-2} Hz (pF)	74.724	63.720
C at 10^{-1} Hz (pF)	52.861	51.901
C at 1 Hz (pF)	50.106	50.062

STEEL CELL

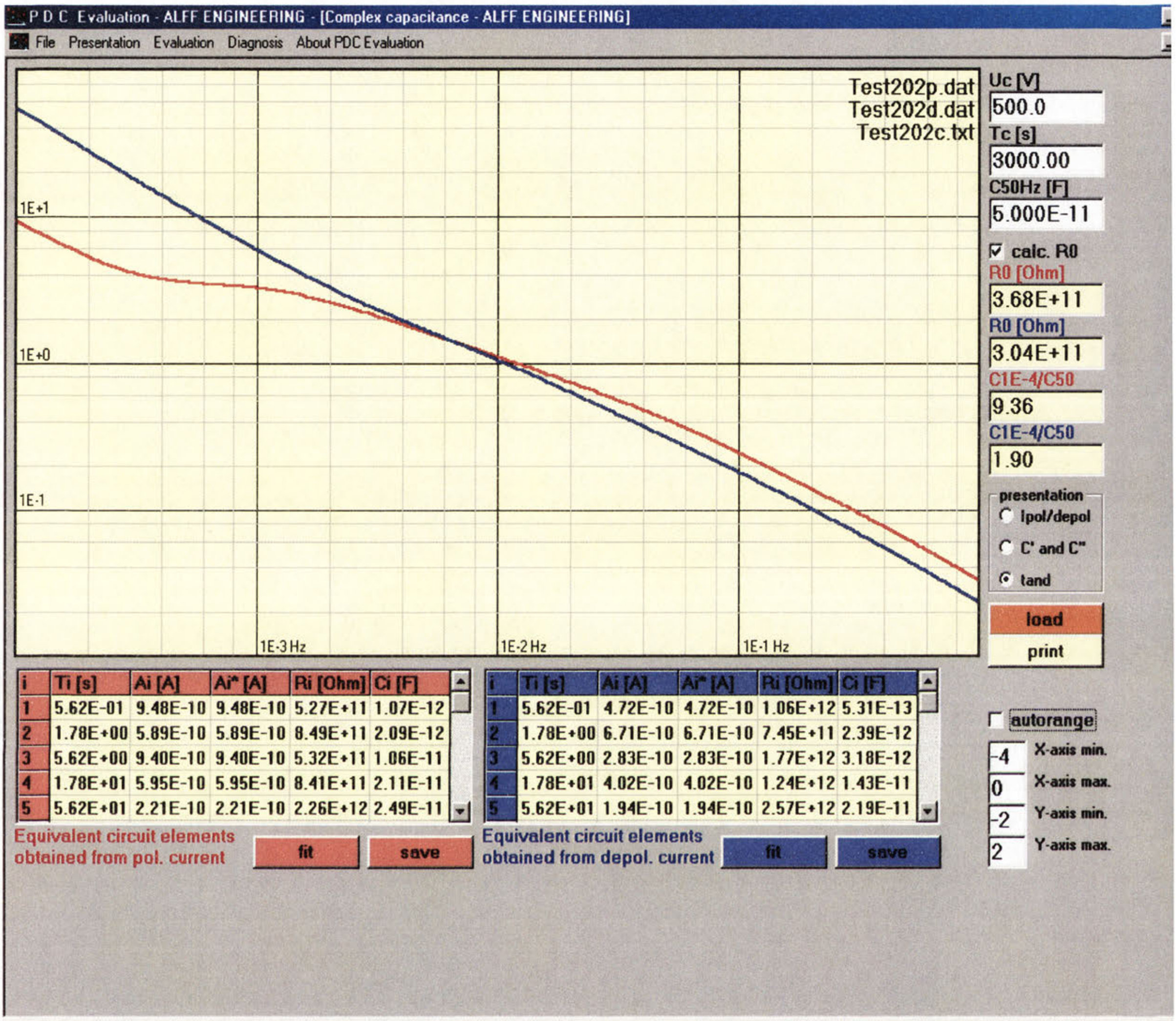

Figure C.3: The Evaluation of Dissipation Factor (tan δ) at the Measured Temperature of 80°C. (Please consider only from 10^{-3} Hz to 1 Hz for polarisation and 10^{-2} Hz to 1 Hz for depolarisation due to the actual measured time frame.)

	Polarisation	Depolarisation
tan δ at 10^{-3} Hz (per unit)	3.2544	-
tan δ at 10^{-2} Hz (per unit)	1.1045	1.0473
tan δ at 10^{-1} Hz (per unit)	2.4449×10^{-1}	1.7990×10^{-1}
tan δ at 1 Hz (per unit)	3.2803×10^{-2}	2.3113×10^{-2}

STEEL CELL

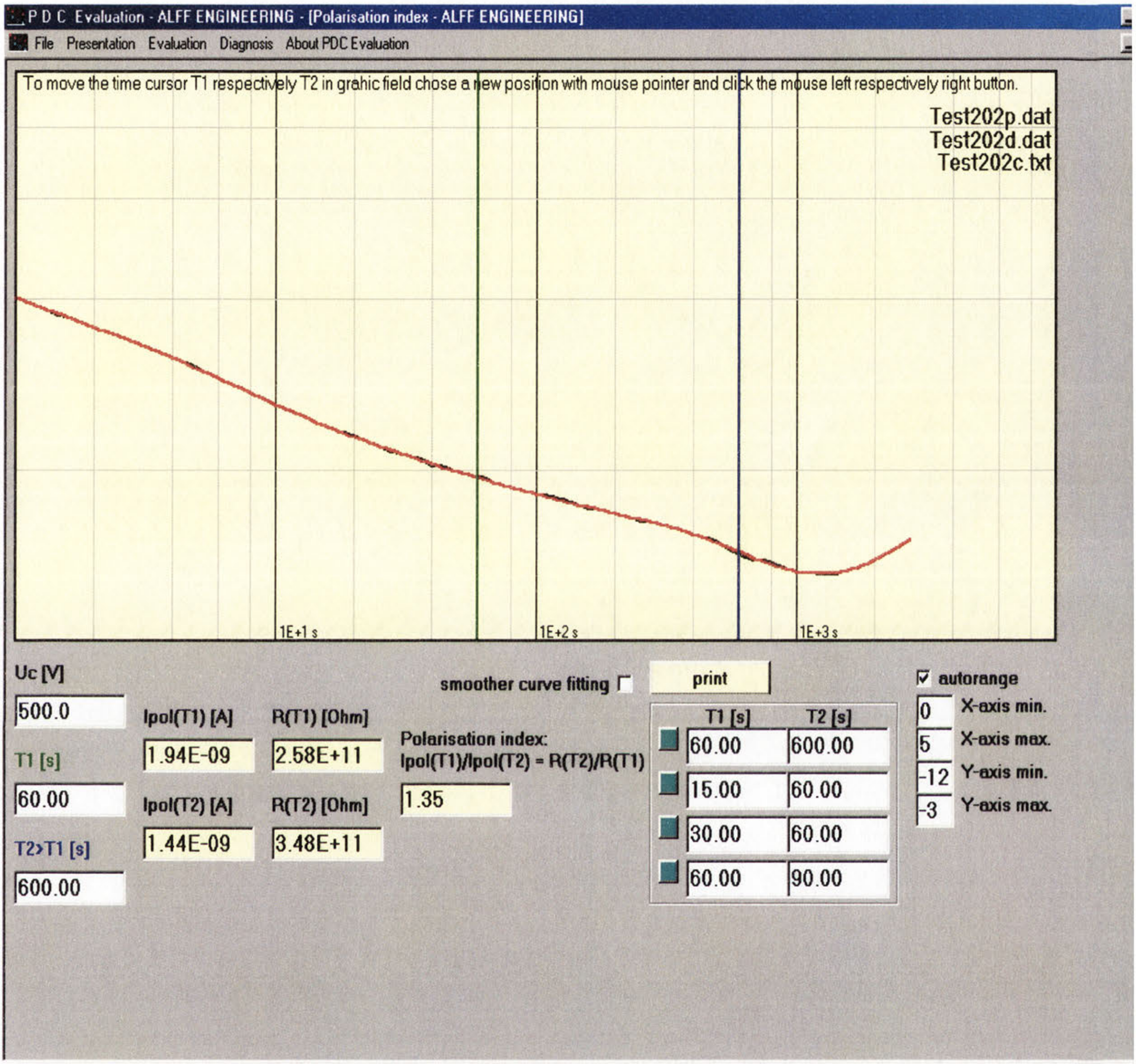

Figure C.4: The Evaluation of Polarisation Index

Result:

Insulation resistance at 15 s (Ω)	2.58×10^{11}
Insulation resistance at 60 s (Ω)	3.48×10^{11}
Polarisation Index (15s and 60s)	1.35

STEEL CELL

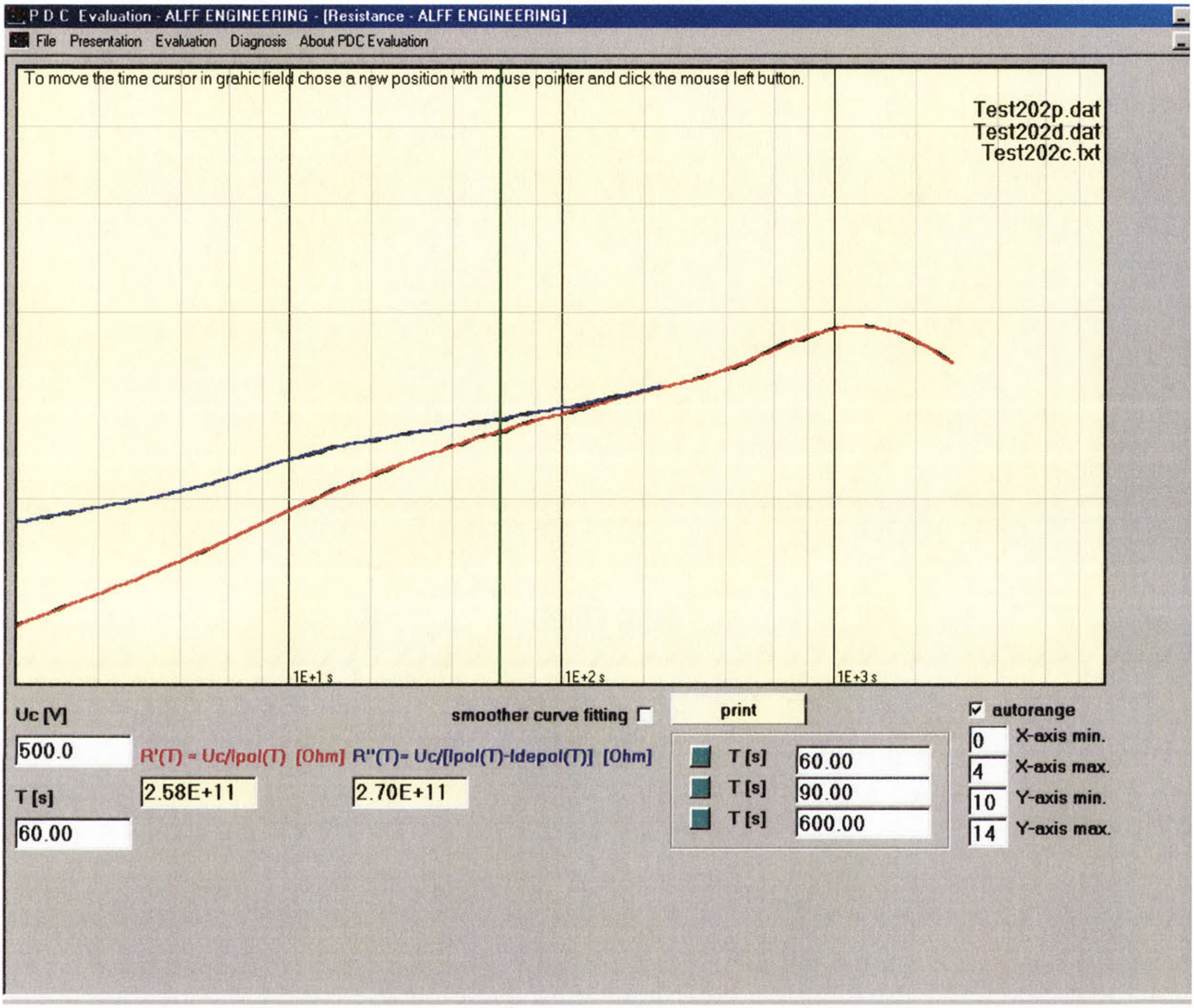

Figure C.5: The Evaluation of Insulation Resistance

From Polarisation current, DC resistance	258 GΩ at 1 min.
From Depolarisation current, DC resistance	270 GΩ at 1 min.

Note:

- If the equivalent circuit is determined from Polarisation current, DC resistance is obtained from a DC component fitting.
- If the equivalent circuit is determined from Depolarisation current, DC resistance is calculated from the difference of polarisation and depolarisation currents for the largest measured polarisation time.

STEEL CELL

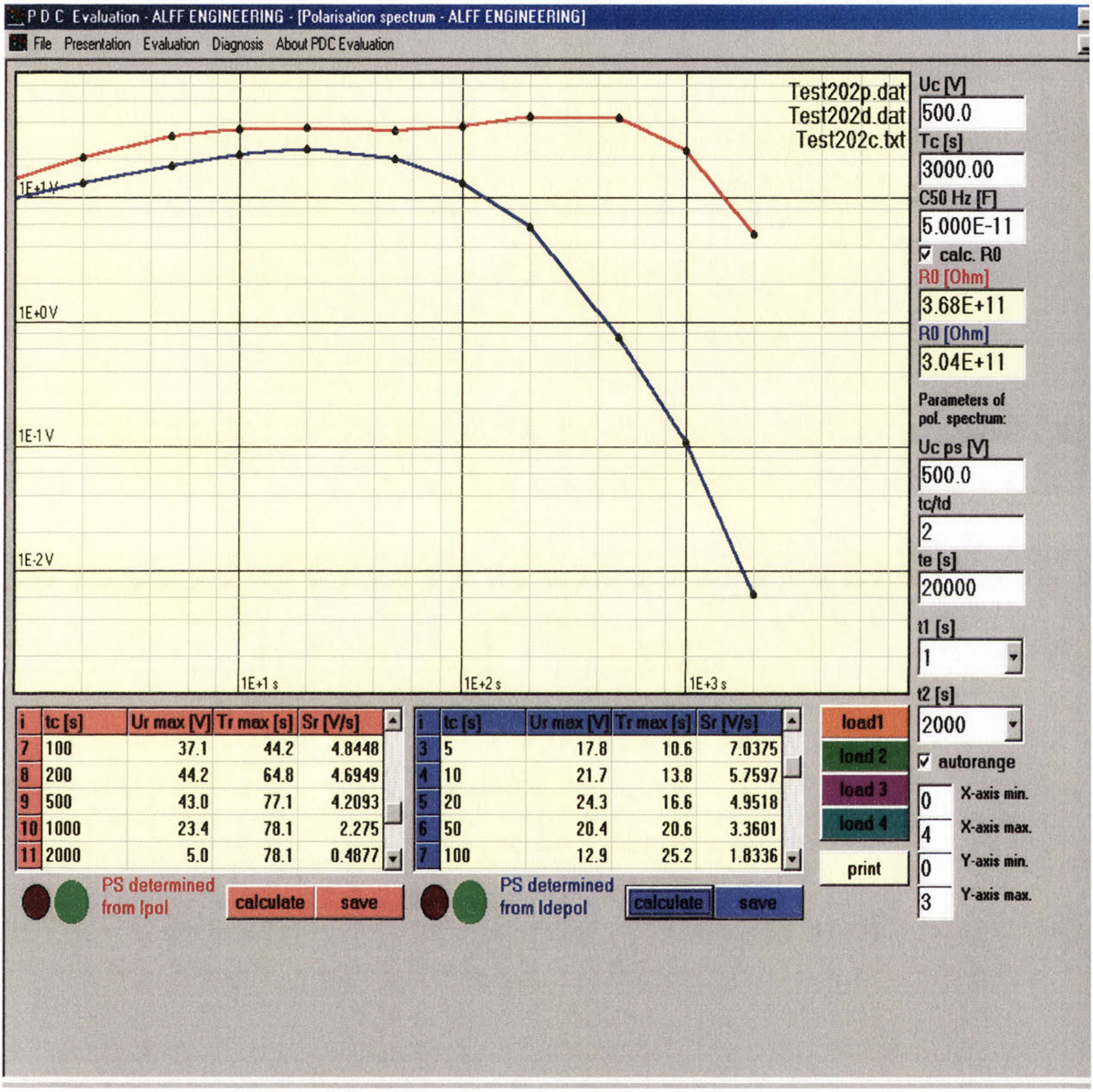

Figure C.6: The Evaluation of Polarisation Spectrum

Charging time at the 1st peak of polarisation spectrum (s)

320 **(Polarisation)**

22 **(Depolarisation)**

STEEL CELL

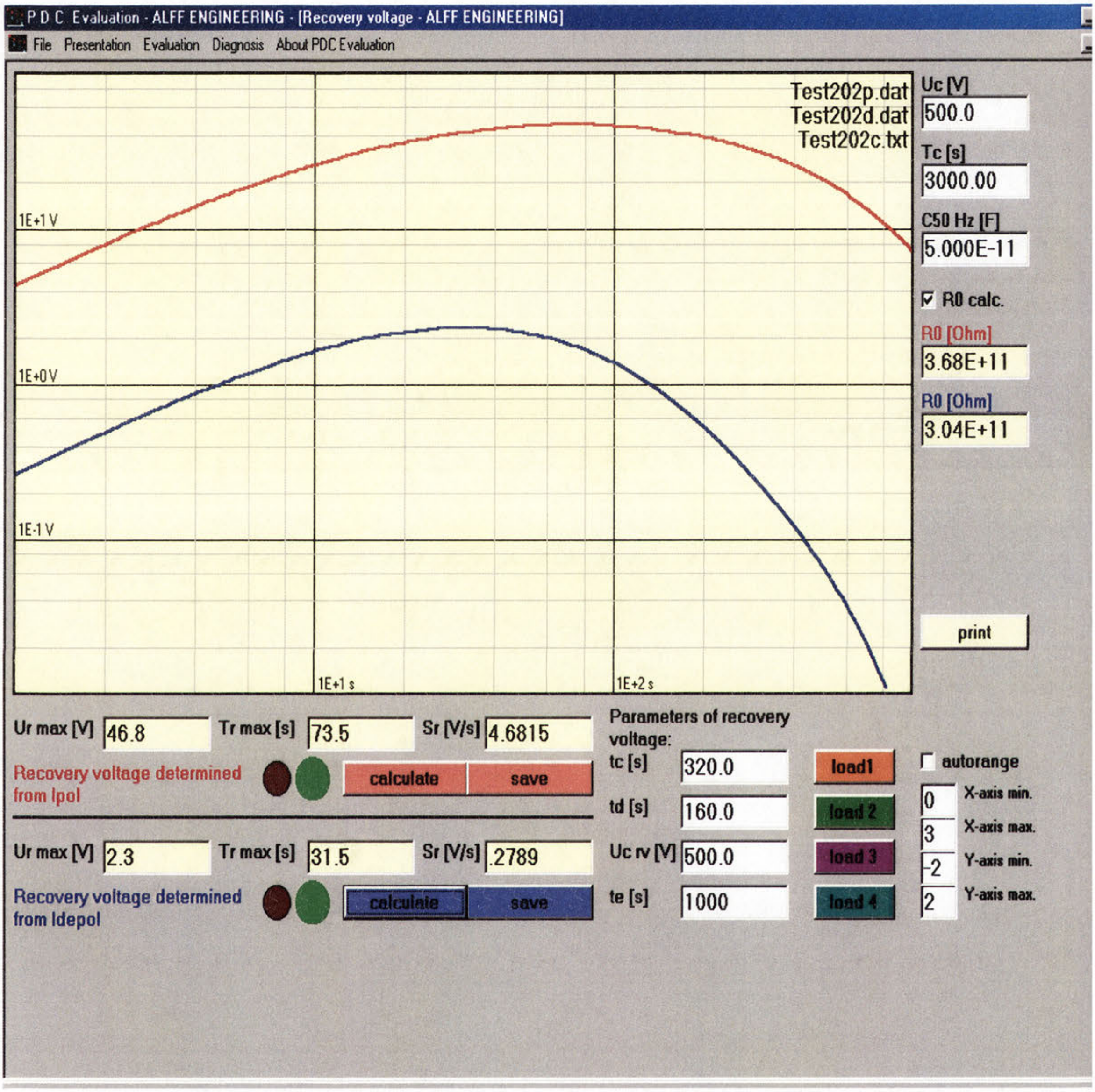

Figure C.7: The Evaluation of Recovery Voltage at the Charging Time of 320 s

Polarisation at 320 s:

The maximum recovery voltage (V)	46.8
The time to peak (s)	73.5
The initial slope (V/s)	4.6815

STEEL CELL

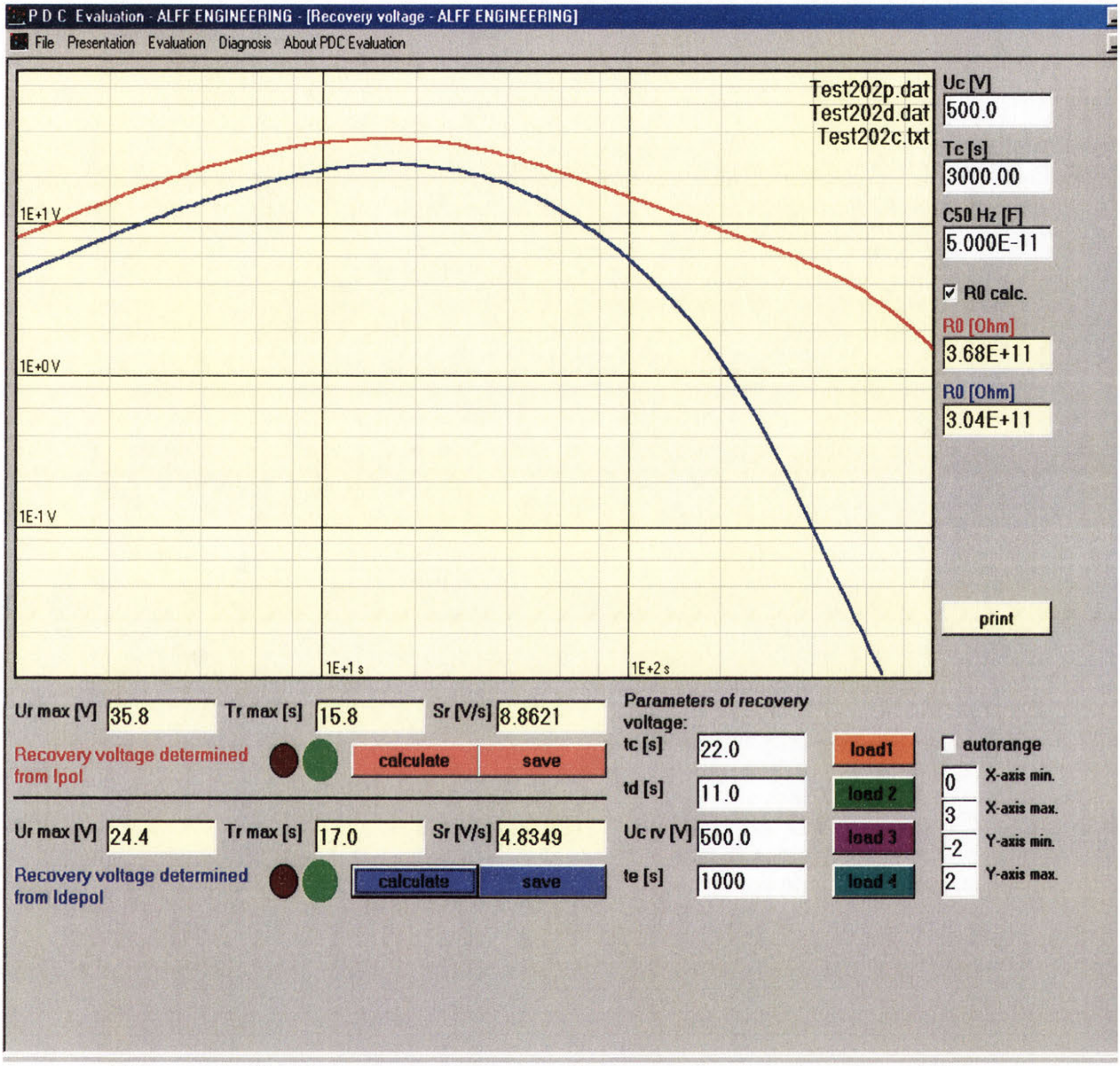

Figure C.8: The Evaluation of Recovery Voltage at the Charging Time of 22 s

Depolarisation at 22 s:

The maximum recovery voltage (V)	24.4
The time to peak (s)	17.0
The initial slope (V/s)	4.8349

STEEL CELL

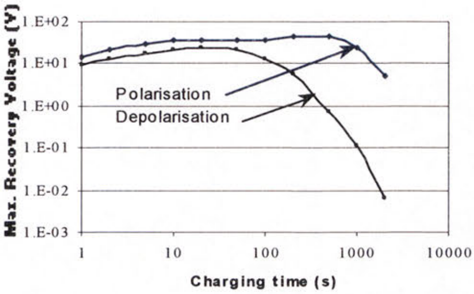

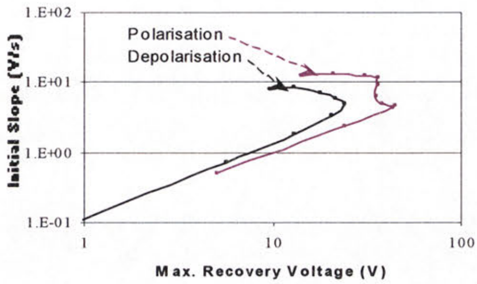

Figure C. 9: Another Presentation form for Polarisation Spectrum (left) and the so-called "Guuinic representation" (right).

Conclusions:

Good oil-paper insulation system will have tangent delta at 1 Hertz less than 1 % or less than 0.01(per unit). Tangent delta at 1 Hertz is normally representative of the quality of oil. The values at other frequencies should be less than 0.1 (per unit) for a good insulation. There is high conduction due to the big difference of polarisation current and depolarisation current. **Polarisation current has more influence in the insulation ageing than conduction**. The first peak of polarisation spectrum occurs in the shorter charging time during depolarisation (22s) than polarisation (320s).

Appendix D

Polarisation and Depolarisation Current Test Report #2
Glass Test Cell

TEST REPORT #2

Polarisation Depolarisation Current Analysis

Test Object: Glass cell with insulating paper in parallel with the transformer oil.

Manufacturer:
Serial number:
Mfr. Year:
Rated kVA:
HV rating (V):
LV rating (V):

Test Instrument: PDC-ANALYSER-1MOD (# PDC010620)

Manufacturer: ALFF Engineering

Test Temperature: 18°C at the end of the test
(Please check the temperature when the test started at 2:08 am of 30-Apr-03)

Test Date: 30th April 2003 (from 2:08 am to 7:41 am)

Location: Electrical Engineering / University of New South Wales

Test Connection: Connect the V-probe of PDC Analyser to HV electrode.
Connect the I-probe of PDC Analyser to LV electrode.
The flange is earthed.

Test Voltage: 500V

Test Duration: 10,000 s of Polarisation and 10,000 s of Depolarisation.

Condition: Remaining current before polarisation started: **2,274** pA.

Insulation Analysed: Between the electrodes of the set-up, in parallel with the oil in the cell. The leakage current along the surface of the glass cell will be included.

GLASS CELL

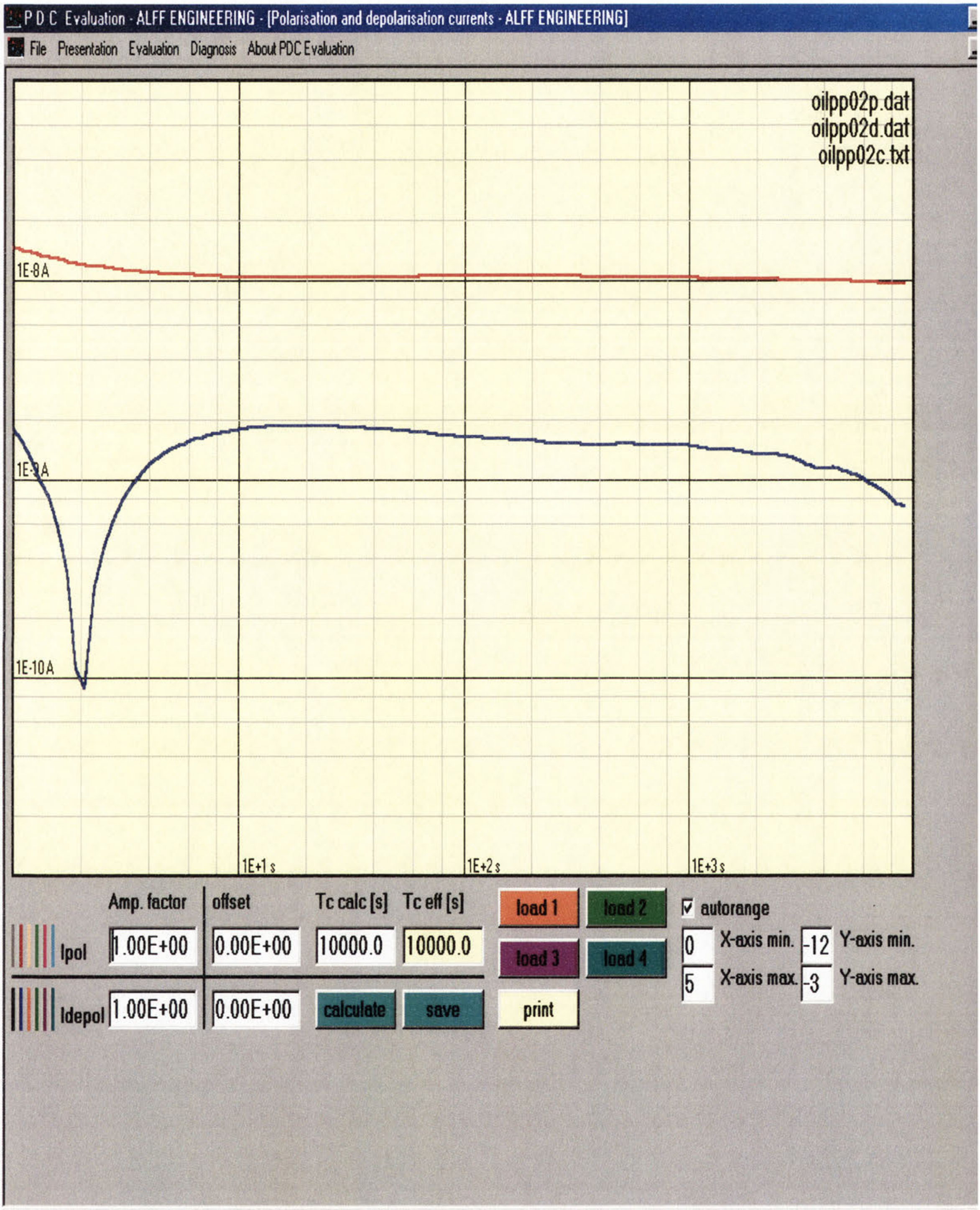

Figure D.1: The Measured Polarisation Depolarisation Currents (before correction due to the remaining current of 2,274 pA).

GLASS CELL

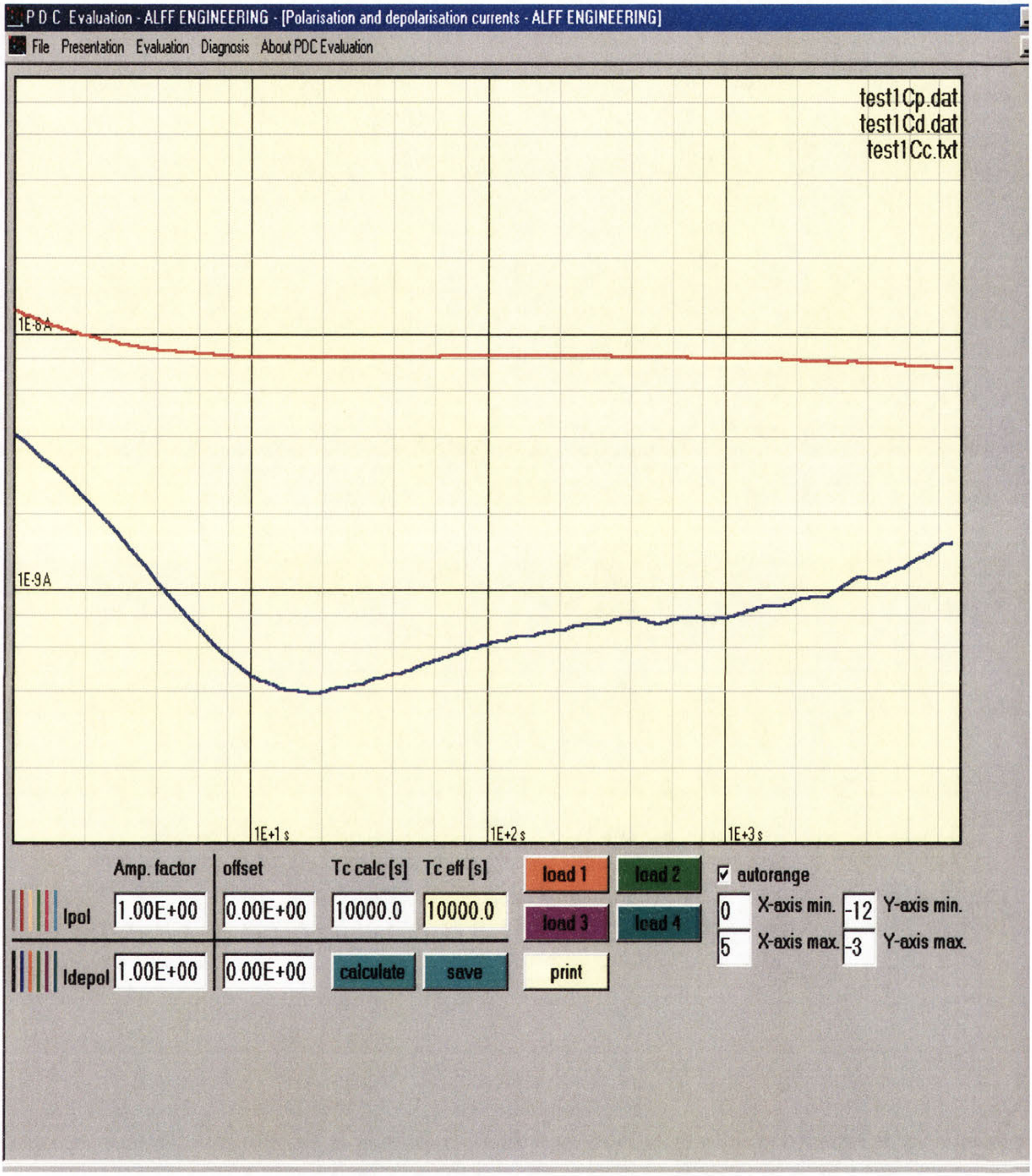

Figure D.2: The Polarisation Depolarisation Currents after Correction due to the Remaining Current of 2,274 pA.

GLASS CELL

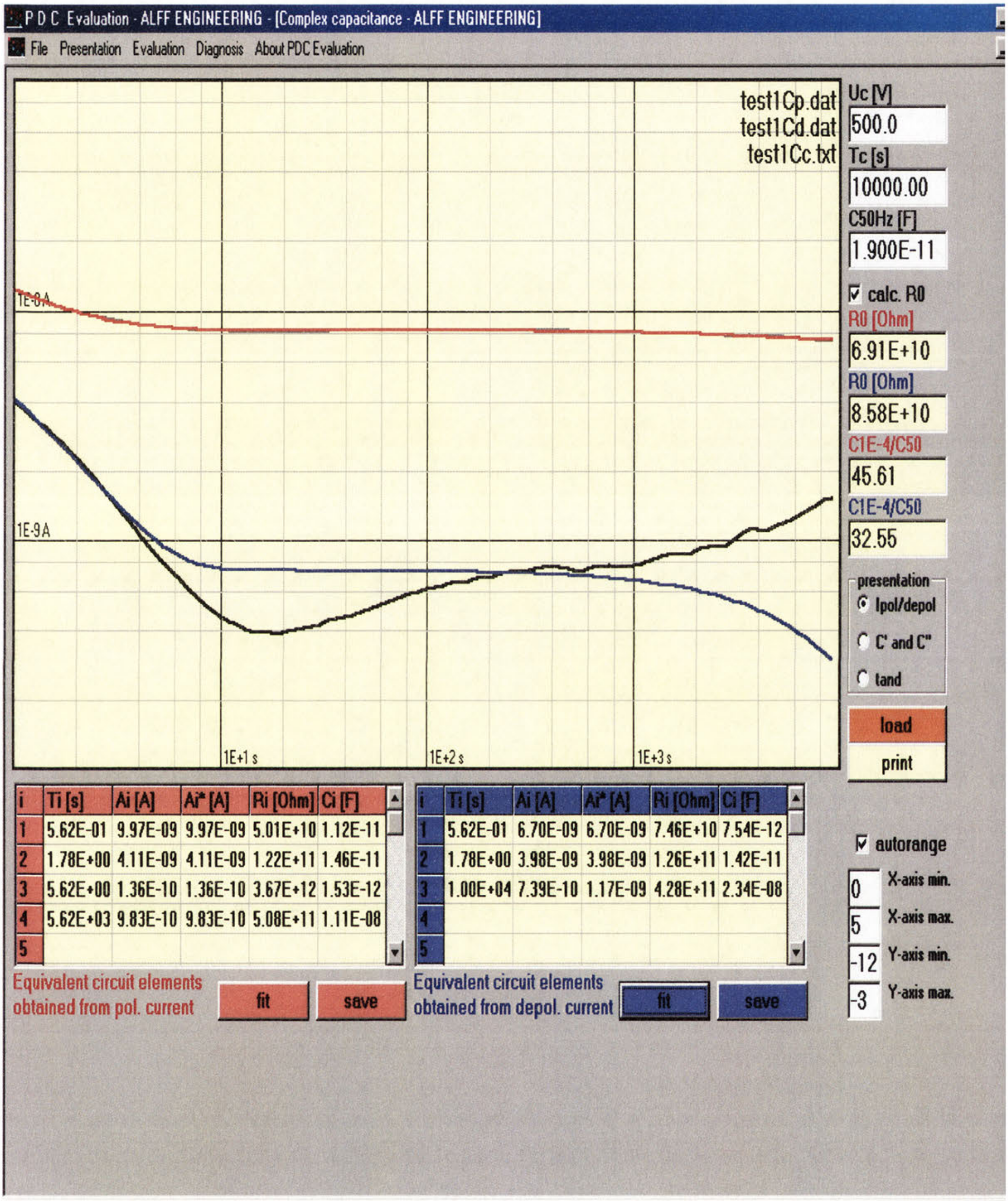

Figure D.3: The Evaluated Polarisation Depolarisation Currents

GLASS CELL

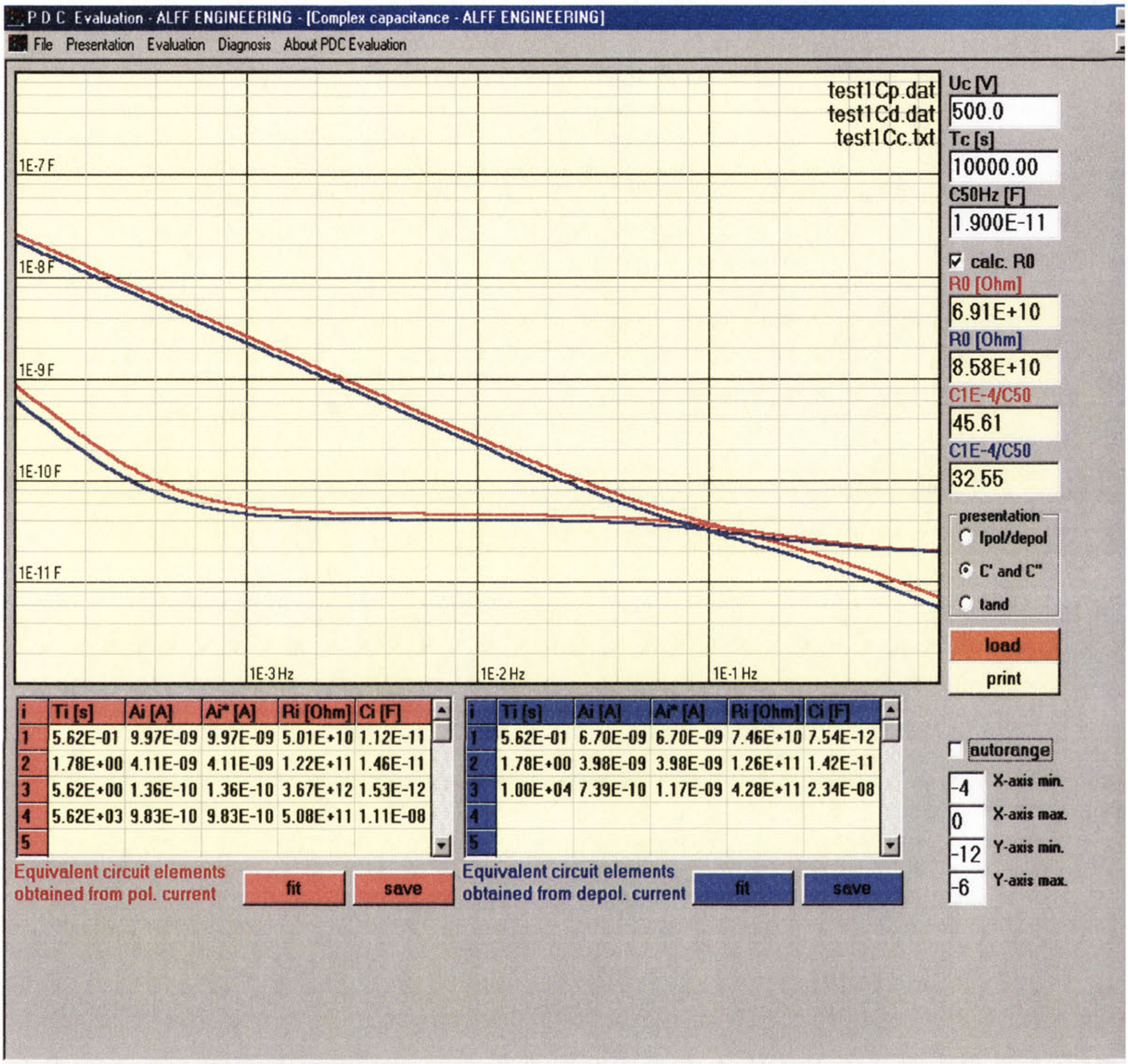

Figure D.4: The Evaluation of Complex Capacitance at the Test Temperature

The capacitance at 50 Hz is 19 pF.

	Polarisation	Depolarisation
C at 10^{-4} Hz (pF)	866.56	618.41
C at 10^{-3} Hz (pF)	55.199	46.610
C at 10^{-2} Hz (pF)	46.076	40.565
C at 10^{-1} Hz (pF)	35.581	31.995
C at 1 Hz (pF)	19.949	19.671

GLASS CELL

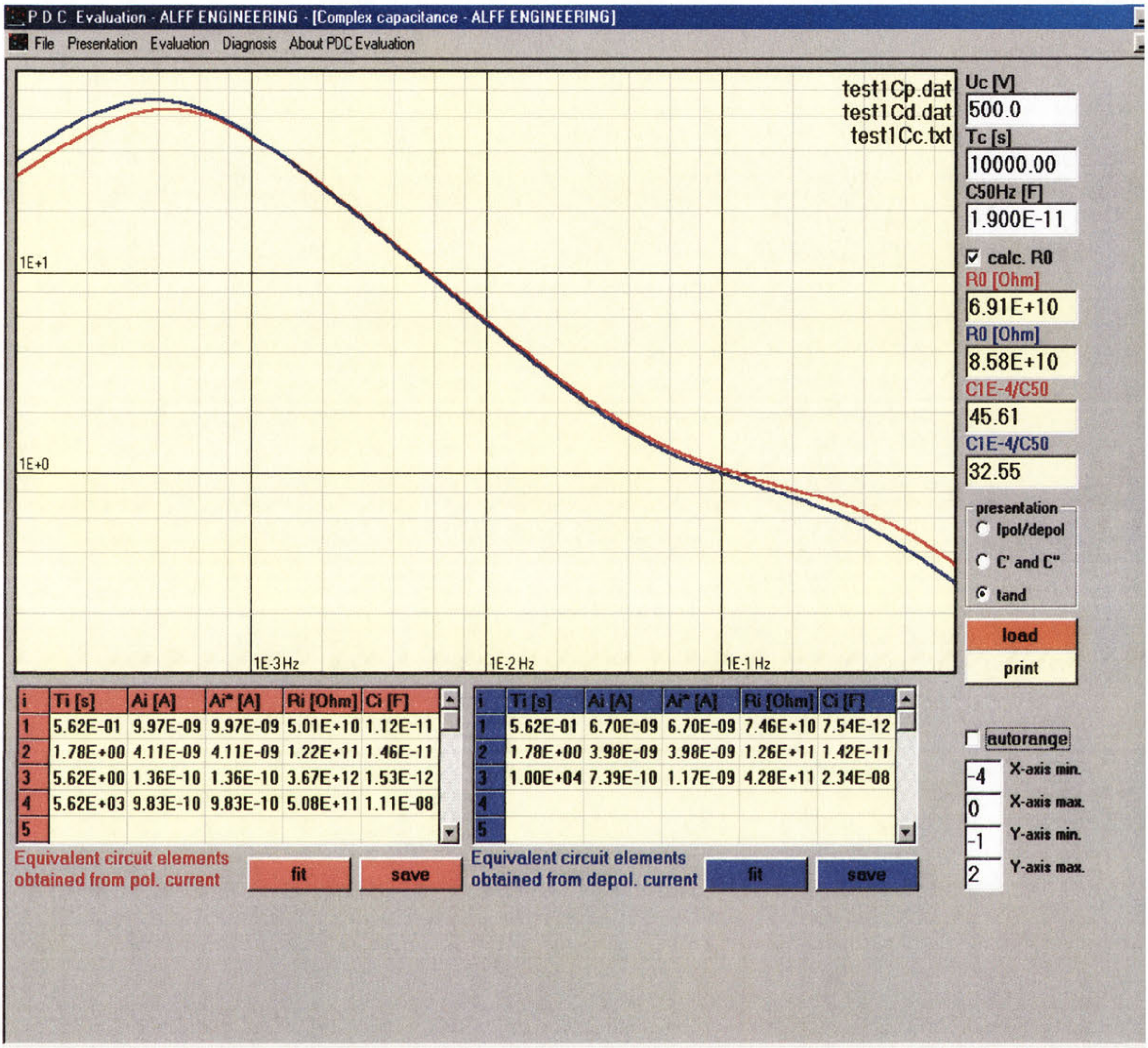

Figure D.5: The Evaluation of Dissipation Factor (tan δ) at the Test Temperature

	Polarisation	Depolarisation
tan δ at 10^{-4} Hz (per unit)	29.926	35.865
tan δ at 10^{-3} Hz (per unit)	47.400	47.784
tan δ at 10^{-2} Hz (per unit)	5.7326	5.5353
tan δ at 10^{-1} Hz (per unit)	1.0496	9.8991×10^{-1}
tan δ at 1 Hz (per unit)	3.4565×10^{-1}	2.7748×10^{-1}

GLASS CELL

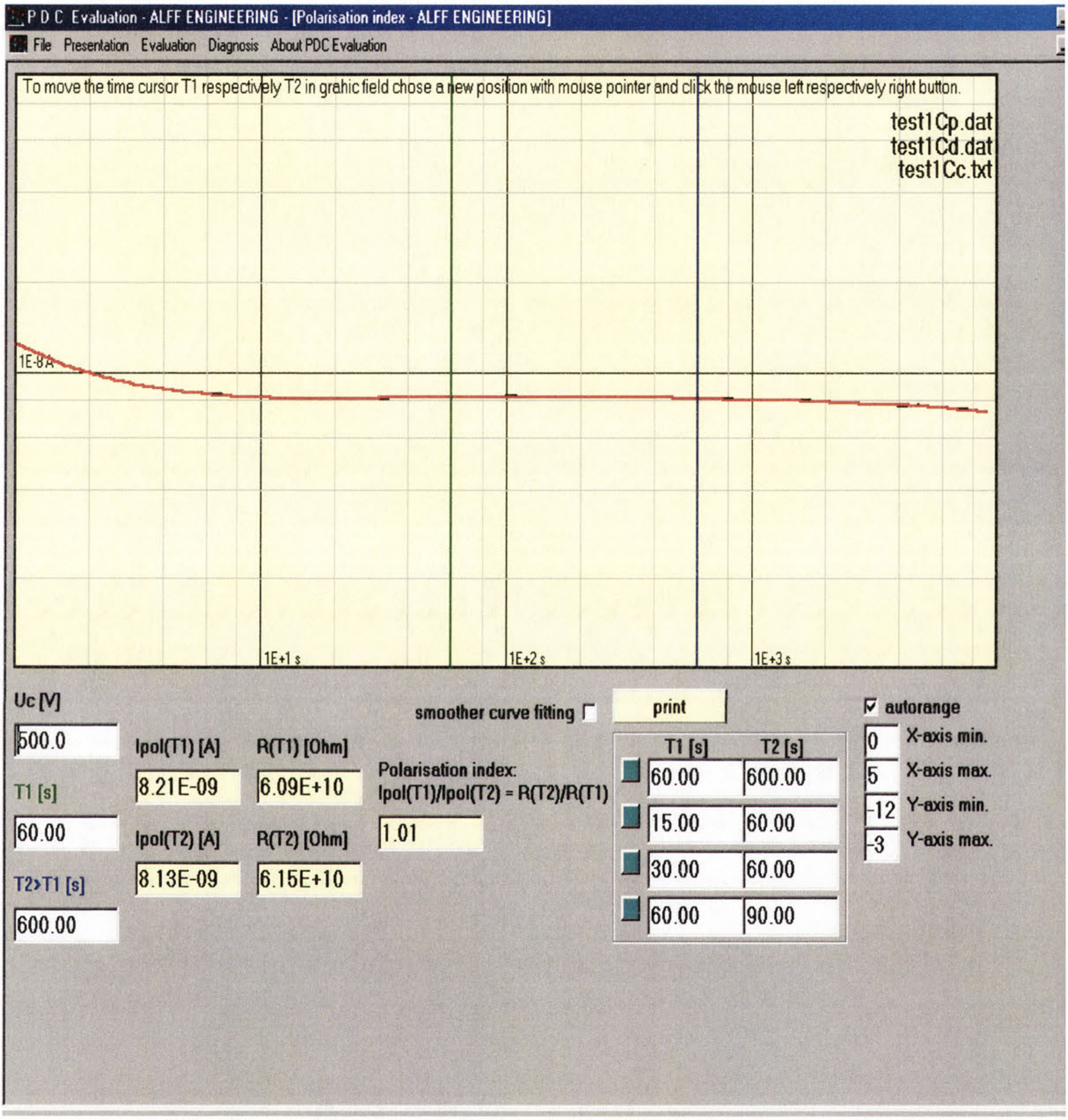

Figure D.6: The Evaluation of Polarisation Index

Result:	Insulation resistance at 15 s (Ω)	6.15×10^{10}
	Insulation resistance at 60 s (Ω)	6.09×10^{10}
	Insulation resistance at 600 s (Ω)	6.15×10^{10}
	Polarisation Index (1 and 10 min.)	1.01

GLASS CELL

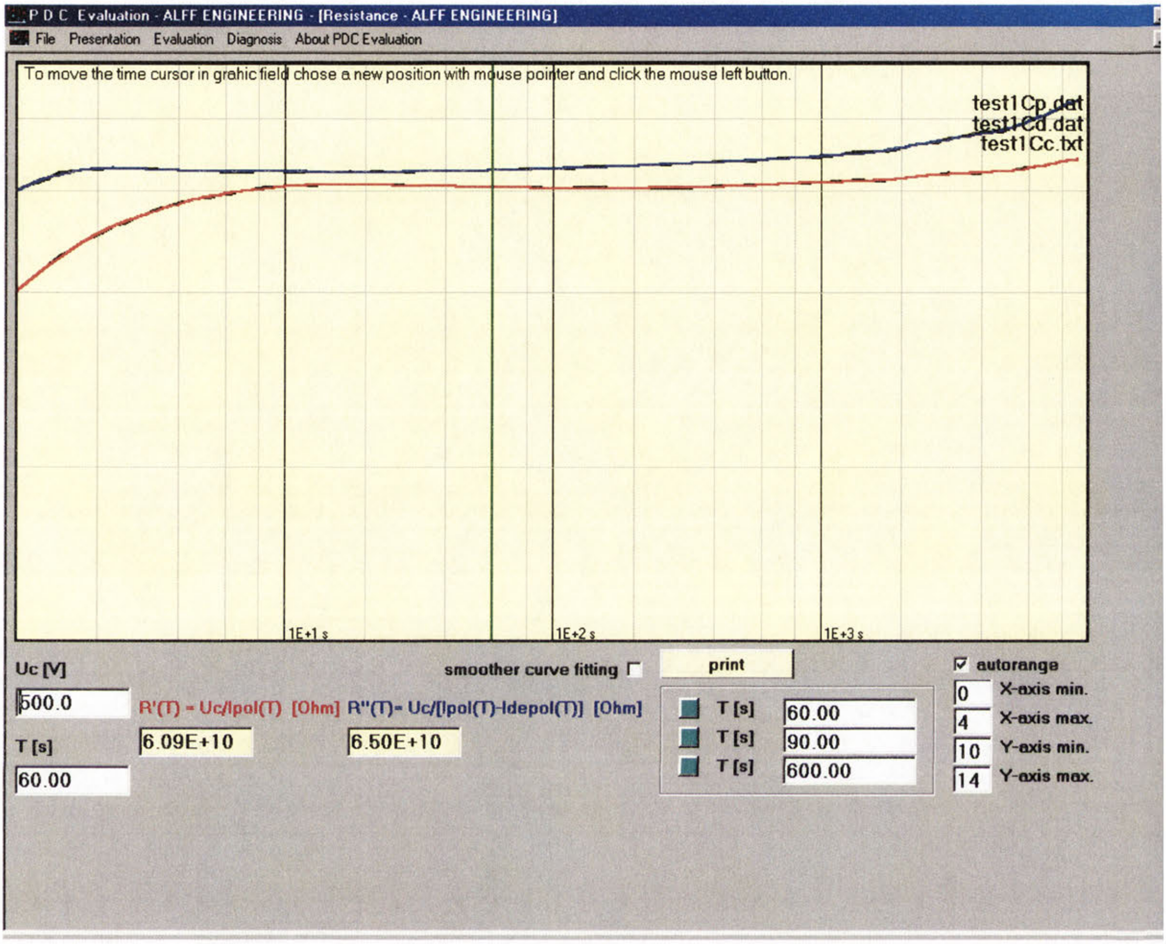

Figure D.7: The Evaluation of Insulation Resistance

From Polarisation current, DC resistance	60.9 GΩ at 1 min.
	61.5 GΩ at 10 min.
From Depolarisation current, DC resistance	65.0 GΩ at 1 min.
	67.8 GΩ at 10 min.

Note:

- If the equivalent circuit is determined from Polarisation current, DC resistance is obtained from a DC component fitting.

- If the equivalent circuit is determined from Depolarisation current, DC resistance is calculated from the difference of polarisation and depolarisation currents for the largest measured polarisation time.

GLASS CELL

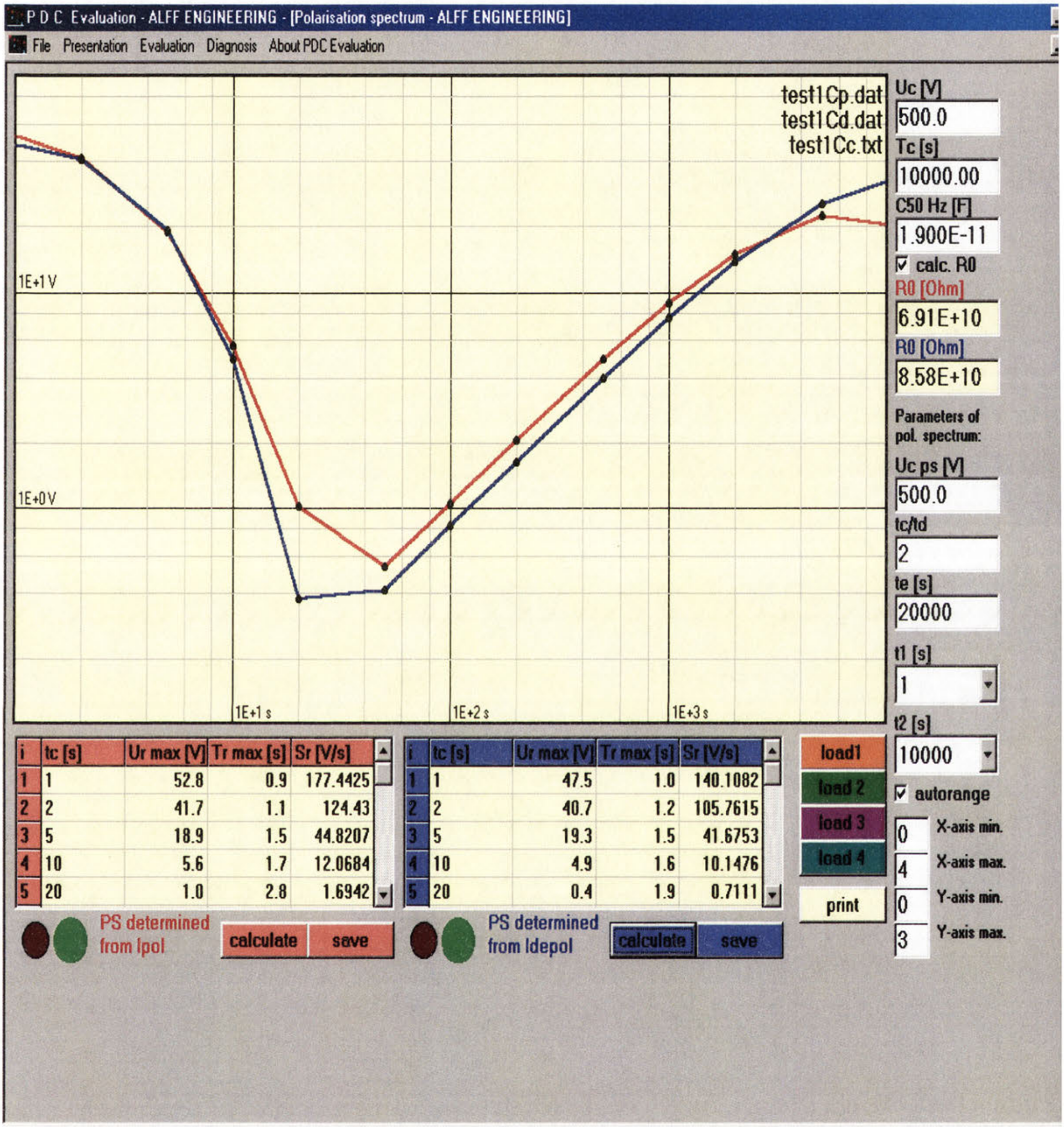

Figure D.8: The Evaluation of Polarisation Spectrum

Charging time at the 1st peak of polarisation spectrum (s)

< 1 (Polarisation)

< 1 (Depolarisation)

GLASS CELL

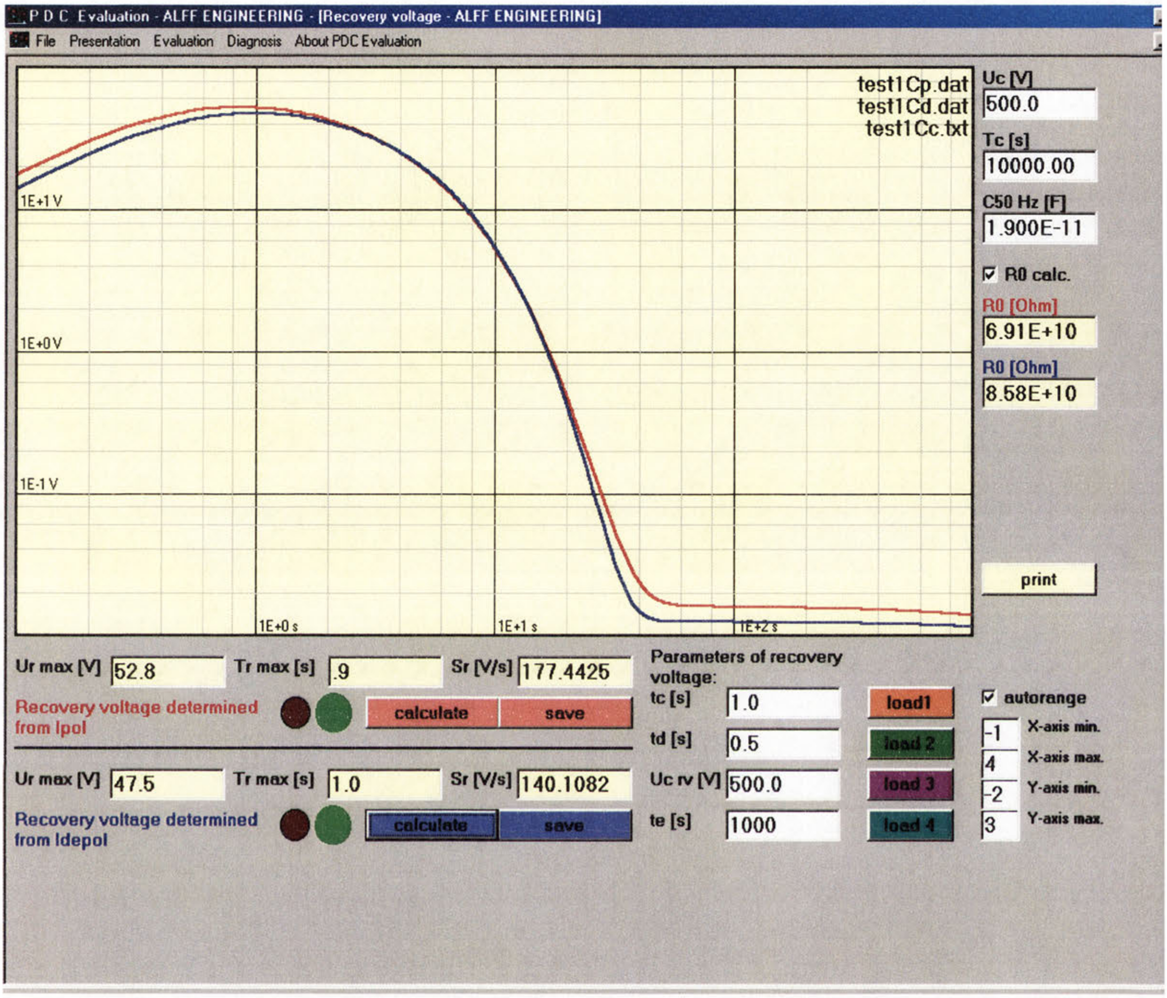

Figure D.9: The Evaluation of Recovery Voltage at the Charging Time of 1 s

Polarisation:

The maximum recovery voltage (V)	52.8
The time to peak (s)	**0.9**
The initial slope (V/s)	177.44

Depolarisation:

The maximum recovery voltage (V)	47.5
The time to peak (s)	1.0
The initial slope (V/s)	140.11

GLASS CELL

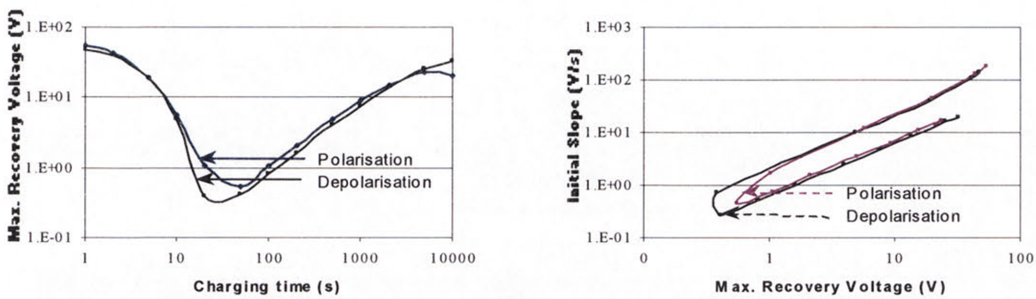

Figure D.10: A Presentation form for Polarisation Spectrum (left) and the so-called "Guuinic Representation" (right).

Conclusions:

Good oil-paper insulation system will have tangent delta at 1 Hertz less than 1 % or less than 0.01(per unit). Tangent delta at 1 Hertz is normally representing the quality of oil. The values at other frequencies should be less than 0.1 (10%) for good insulation. There is no oil duct between the electrodes so the insulation system measured includes the oil in the vessel in parallel. **The overall insulation system is very bad since the first peak of the polarisation spectrum is at less than 1 second**. The paper has bad quality and so the capacitance and the tangent delta at 0.1 mHertz are high. There is high conduction due to the big difference of polarisation current and depolarisation current. The glass cell may have some influence of surface leakage current due to the connection used during the test. The influence of external surface leakage makes it difficult to draw detailed conclusions about the insulation.

Appendix E

Recovery Voltage Measurement Manual

Stage 1: System Checks

Before starting the measurement, the most important thing is to ensure that all the equipment is connected properly. Below is the list of tasks that you need to perform before proceeding to the next stage:

Safety Precaution!!!

The following equipment ***must be switched off***:
- High voltage power supply
- Electrometer
- Switching box
- Computer

Switching Box

1. Two connectors located at the back of the switching box, labelled as ***"Input From Power Supply"*** and ***"Output High Voltage Supply"***, are to be connected to the output of the power supply and to the test object respectively.

2. Another connectors located at the back of the switching box, labelled as ***"Leakage Current Measurement"***, must be shorted together to perform the RVM.

3. The connector located at the front part of the switching box is to be connected to the input of the electrometer.

Data Acquisition Interfacing Card (DAQIC)

1. Three signal lines ***(DIO 0, DIO 1, DIO 2)*** from the DAQ interfacing card are to be connected to the 3 red connectors ***(Charging, Discharging, Measurement)***, locate at the back of the switching box, respectively.

2. Two digital ground lines ***(DGND)*** from the DAQ interfacing card are to be connected to the 3 green connectors ***(Charging, Discharging, Measurement)***, located at the back of the switching box, respectively. *

*Note: Since the DAQ card offers only 2 digital ground lines, we can tap any of these 2 digital ground lines to the third green connector of the switching box.

Electrometer

The output of the electrometer can be connected to perform the followings:

1. Manual Recording

   To record the peak recovery voltage for each RVM test cycle, you need to connect the output of the electrometer to a digital multi-meter. During the measurement phase, the maximum recovery voltage for a particular charging time is to be recorded manually from the digital-multi-meter.

OR

2. Digital Acquisition Using Computer

   To record the peak recovery voltage using the computer, you need to connect the output of the electrometer to the DAQ interfacing card. The following connections must be made:

- Red output line from the electrometer is to be connected to ACH 0 (pin 3) of the DAQ interfacing card.
- Black output line from the electrometer is to be connected to ACH 8 (pin 4) of the DAQ interfacing card.

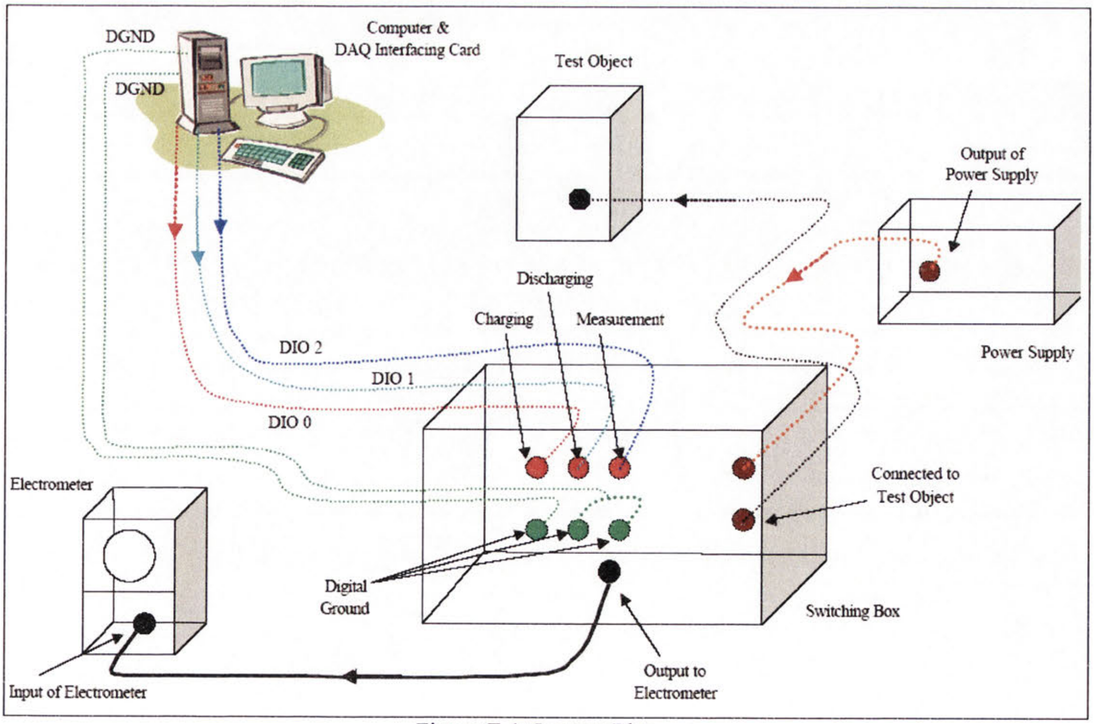

Figure E.1: Layout Plan

Stage 2: Initial Preparation

Once you have performed the system checks, you may proceed on to perform the followings:

1. Switch on the following equipment:

- ➢ Computer
- ➢ Switching box
- ➢ Power supply
- ➢ Electrometer (from ***power off*** to ***off***)

2. Once the computer is ready, click on the icon to launch LabVIEW, as seen in Figure E.1:

Figure E.1: Shortcut icon to LabVIEW

3. You will be able to see the following pop up menu. Click on the "Open VI" icon.

Figure E.2: Pop up menu of LabVIEW

4. Next, you will be able to see another window, as seen in Figure E.3. Click on the folder "RVM". After that, you need to look for "RVM.vi". Once you have located it, just double click on it and you will be able to open the program of RVM.

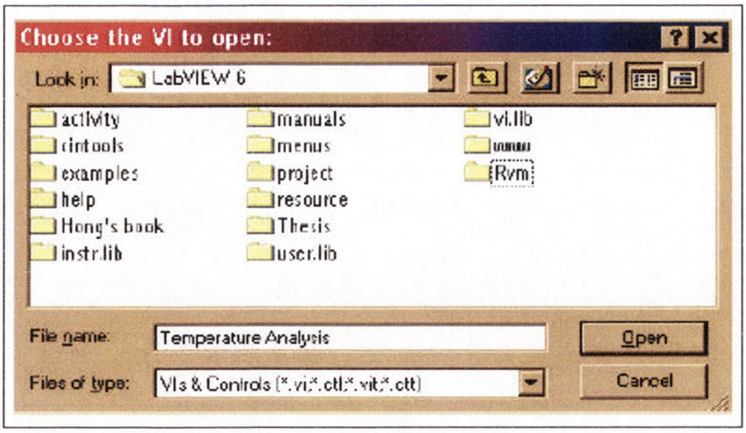

Figure E.3: Locating the RVM folder

5. The RVM program will then appear as seen in Figure E.4:

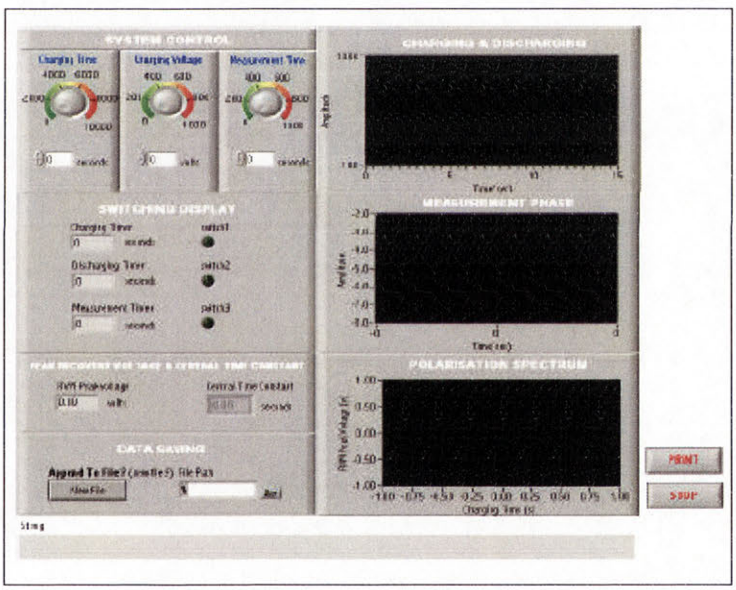

Figure E.4: View of the RVM program

6. Once all the equipment and the LabVIEW program are ready, you can then proceed to the next stage of the experiment – ***Operating Procedure.***

<u>Stage 3a: Operating Procedure (Manual Recording)</u>

If you are doing the manual recording, you must ensure that the output of the electrometer is connected to a digital multi-meter as described in Page 2 of the operating manual. If you have not done so, please refer to page 2 for details.

The operating procedure is as follows:

1. You need to enter the following data: (a) charging time, (b) charging voltage, and (c) measurement duration, as seen in Figure E.5:

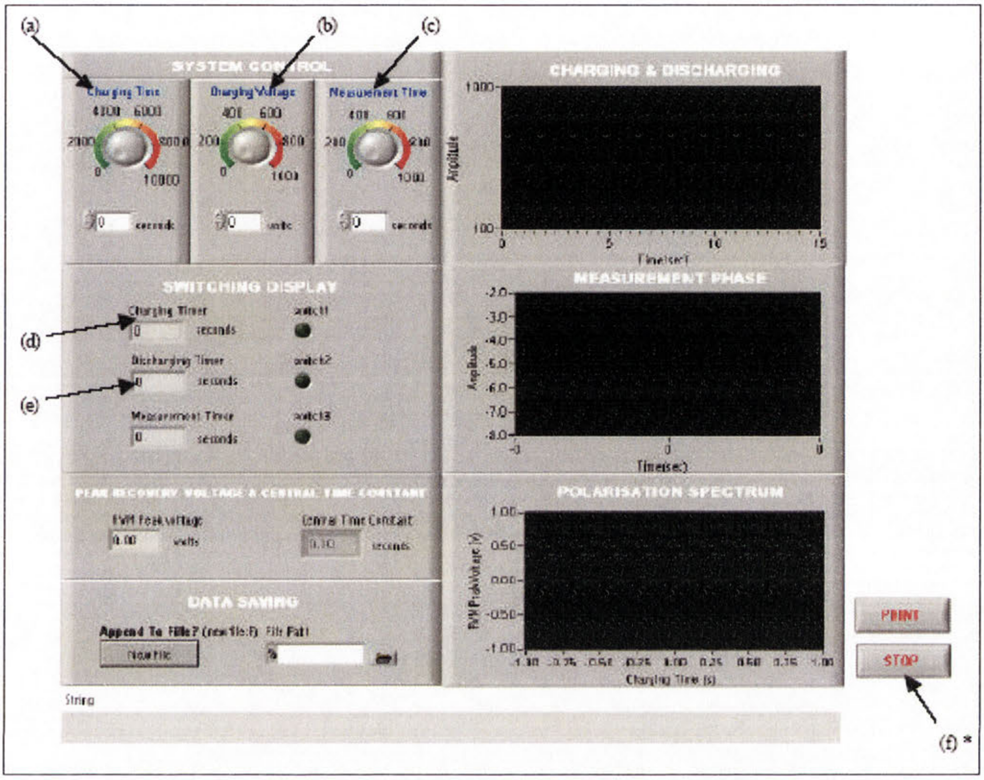

Figure E.5: View of RVM program

Note: The "STOP" button, labelled as (f), is used if you want to terminate the program mid way through the execution of the program.

2. After performing step (1), you may set the desire charging voltage on the power supply. However, you must ensure that the power supply is switched to the ***standby mode***.

3. Once the power supply is ready, the orange LED will light up. You will then need to switch the power supply to ***power mode***, and wait for the power mode LED to turn red.

4. Now, you are ready to perform the recovery voltage measurement. Click on the arrow button locates at the top left corner of the LabVIEW program, as seen in Figure E.6, to start the measurement process.

Figure E.6: Program starts button

5. When the charging timer (d), as seen in Figure E.5, reaches the charging time (a) you have keyed in, switch the power supply to ***standby mode immediately***.

6. When the discharging timer (e), as seen in Figure 5, reaches half the charging time (a) you have keyed in, start observing the recovery voltage from the digital multi-meter.

7. Record the maximum recovery voltage observed from the digital multi-meter. This is the recovered voltage corresponding to the charging time you have keyed in earlier.

8. Step 1 to step 7 is repeated by varying the charging time, tc. Each test cycle is repeated every ***10 minutes interval.*** This is necessary to remove the residual voltage within the test object.

9. When you have collected sufficient results, you may plot the polarisation spectrum, which is a graph of charging time against the corresponding maximum recovered voltage.

Stage 3b: Operating Procedure (Data Acquisition Using Computer)

If you are doing data acquisition using the computer, you must ensure that the output of the electrometer is connected to the DAQ interfacing card as described in Page 2 of the operating manual. If you have not done so, please refer to page 2 for details.

The operating procedure is as follows:

1. You need to enter the following data: (a) charging time, (b) charging voltage, and (c) measurement duration, as seen in Figure E.7.

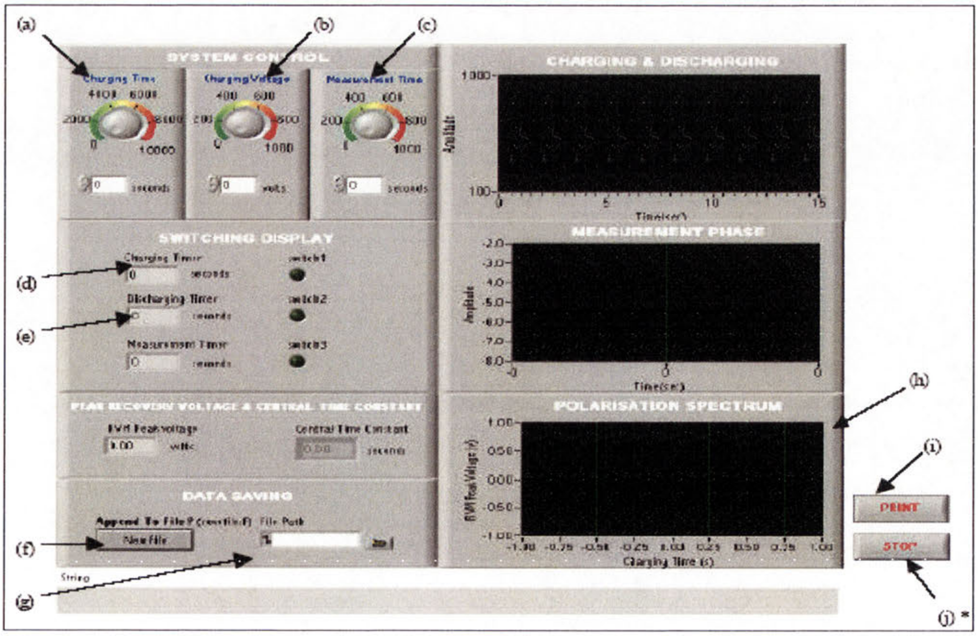

Figure E.7: View of RVM program

Note: The "STOP" button, labelled as (j), is used if you want to terminate the program mid way through the execution of the program.

2. Enter the file name (g) in the space provided. You may either create a new file or append to the existing file (f), to store the value of the maximum recovery voltage and central time constant.

3. After you have performed step (2), you may set the desire charging voltage on the power supply. However, you must ensure that the power supply is switched to the ***standby mode***.

4. Once the power supply is ready, the orange LED will light up. You will then need to switch the power supply to ***power mode***, and wait for the power mode LED to turn red.

5. Now, you are ready to perform the recovery voltage measurement. Click on the arrow button located at the top left corner of the LabVIEW program, as seen in Figure E.8, to start the measurement process.

Figure E.8: Program starts button

6. When the charging timer (d), as seen in Figure E.7, reaches the charging time (a) you have keyed in, switch the power supply to ***standby mode immediately***.

7. When the discharging timer (e), as seen in Figure E.7, reaches half the charging time (a) you have keyed in, the computer will record the maximum recovery voltage and the time to peak automatically.

8. Similarly, step 1 to step 7 is repeated by varying the charging time, tc. Each test cycle is repeated every ***10 minutes interval.*** This is necessary to remove the residual voltage in the test object.

9. The polarisation spectrum (h) is plotted automatically and you may print this out by clicking the ***PRINT*** button (i), as seen in Figure E.7. However, you may choose to plot the polarisation spectrum using Excel, as the recovered voltages and central time constant have already stored in the file you have created in step (2).

Brief Idea Of RVM Using The RVM Set UP

1. The test object is charged (S1 is closed, S2 and S3 are opened) for the selected charging time, tc.

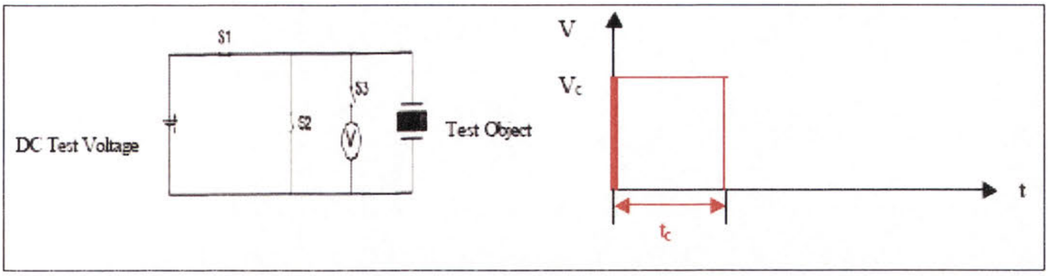

2. The test object is then short-circuited (S1 and S3 are opened, S2 is closed) for a discharging time, t_d, which is half of the charging time ($t_d = t_c/2$).

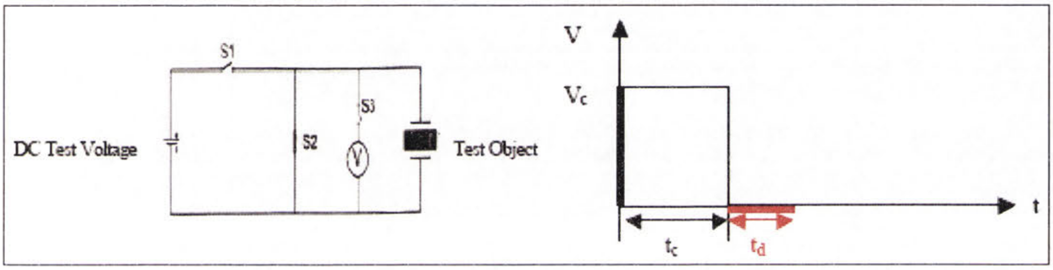

3. The test object is then open circuited (S1 and S2 are opened, S3 is closed). The peak value of the recovery voltage and time to peak (central time constant) are measured.

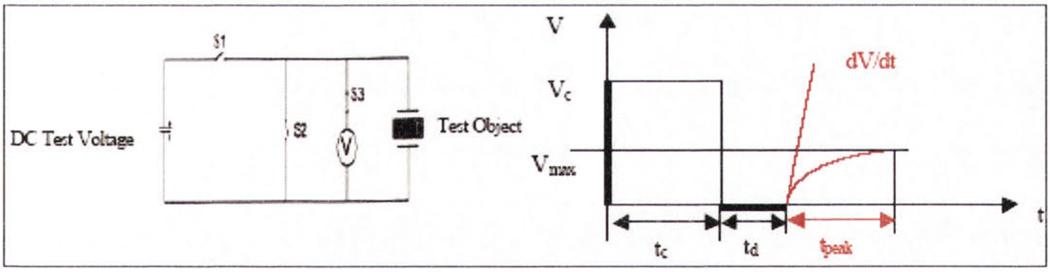

4. At the completion of the measurement phase, the test object is short-circuited to neutralize the stray charge within the test object before repeating the next test cycle.